Freezing and freeze-drying highly concentrated carbohydrate systems

by

RUI WANG

A thesis submitted to the University of Birmingham for the degree of DOCTOR OF PHILOSOPHY

School of Chemical Engineering

University of Birmingham

November 2016

UNIVERSITY OF
BIRMINGHAM

University of Birmingham Research Archive

e-theses repository

This unpublished thesis/dissertation is copyright of the author and/or third parties. The intellectual property rights of the author or third parties in respect of this work are as defined by The Copyright Designs and Patents Act 1988 or as modified by any successor legislation.

Any use made of information contained in this thesis/dissertation must be in accordance with that legislation and must be properly acknowledged. Further distribution or reproduction in any format is prohibited without the permission of the copyright holder.

ABSTRACT

Freeze drying is a widely-used dehydration technique in food and pharmaceutical industry, involves water crystallisation (freezing) and ice sublimation during the process. The purpose of the study is to enable the initial concentration of solutions that are used in freezing and freeze drying processes to be increased, as an approach to reduce the energy consumption of the process.

Spontaneous crystallisation from both sucrose solutions and coffee solutions was studied by DSC, XRD and cryo-SEM, and results showed that increasing solid concentration (up to 70%) significantly delayed the water crystallisation, shown as lower crystallisation temperature and less or even no ice crystal formation.

A method was developed to induce water crystallisation by adding already formed ice seeds to water, which allowed the study of ice crystal growth rate at controllable conditions. The method combined the use of a temperature controlled stage and an optical microscope, and the effects of solid concentration (up to 60%), temperature, viscosity, solute type, and air bubbles on crystal growth were investigated.

Freeze drying high concentration sucrose (up to 60%) showed significant volume expansion (collapse), and methods to reduce the collapse were tried by modifying the formulation (adding high molecular weight gum Arabic) or freeze drying cycles (reducing heating rate between primary and secondary drying). Results showed that the up to 30% concentration of sucrose solution can be dried without volume expansion with modified freeze drying process.

Acknowledgement

I gratefully acknowledge my supervisors; Prof. Peter J. Fryer and Prof. Serafim Bakalis for their supervision. I am grateful for their guidance in the research, for checking my thesis, and for always being very encouraging.

I would like to express my gratitude to Dr Ourania Gouseti, for not only giving me help in experimental work and writing, but being a great friend as well. Also, Dr Estefania Lopez Quiroga, thanks for her help, discussion, support and delicious cakes. Assistance provided by Mrs Tamsin Jackson is greatly appreciated.

I would like to express my gratitude to Food Group and staff in School of Chemical Engineering, especially Mrs Lynn Draper and Dr Taghi Miri, for giving me help throughout my PhD.

I would like to thank all my friends here in UK and home in China, for the good time we spent together and their encouragement. I am very thankful to Martin for standing next to me and supporting me in those difficult days.

Finally, I would like to thank my family, for their unlimited support and love.

INDEX

LIST OF FIGURES

LIST OF TABLES

Nomenclature

Abbreviations

Cmc	Carboxymethyl Cellulose
Cryo-ESEM	Low temperature Environmental scanning electron microscopy
DSC	Differential scanning calorimetry
ESEM	Environmental scanning electron microscopy
SEM	Scanning electron microscopy
XRD	X-ray diffraction

Symbols

A	Pre-exponential factor, see equation 4-4
a	Coefficients, see equation 4-3
b	Coefficients, see equation 4-3
C'_g	Maximum freeze concentration
C_p	Heat capacity,J K^{-1}
E_d	Activation energy, J mol^{-1}
h	Height of freeze dried sample, cm
ΔH	Enthalpy change of water crystallisation, J g^{-1} solution
ΔH_s	Enthalpy change of ice sublimation, J g^{-1} solution
ΔH_w	Enthalpy change of freezing pure water into ice, J g^{-1} solution
K_v	Heat transfer coefficient, J $^oC^{-1}$
m	mass of solid, g
Q_{in}	Heat transferred into the system, J
Q_{out}	Heat transferred out of the system, J
R	Gas constant, J $mol^{-1}K^{-1}$
r	Radius, mm
R_p	Resistance from dry layer, µbar hour g^{-1}
R_s	Resistance from vial stopper, µbar hour g^{-1}
S	Area, mm^2
T	Temperature, ^oC or K
ΔT	Supercooling, ^oC
T_g	Glass transition temperature, ^oC
T'_g	Glass transition temperature at maximum freeze concentration, ^oC
T_m (T_f)	Equilibrium freezing temperature, ^oC
T'_m	Melting temperature at maximum freeze concentration, ^oC
T_p	Product temperature, ^oC
T_s	Shelf temperature, ^oC
P_c	Chamber pressure, µbar
P_{ice}	Equilibrium vapour pressure of ice at the interface temperature, µbar

ρ	Density, g mL^{-1}
v	Growth velocity, cm min^{-1}
V	Volume, mL
w_s	Concentration

Chapter 1 Introduction

This chapter explains the background of the project, the objectives of the research, the choice of the material in the research, and the outline of the thesis structure. Finally, a list of publications and presentations based on the findings of this work is displayed.

1.1 Background of the research

Instant coffee, or soluble coffee, is the most popular instant beverage among millions of people because of its convenience and long shelf life, as well as the flavour and stimulating effects (Ramalakshmi, Rao *et al*. 2009, Huang and Zhang 2013). The importance of instant coffee as a consumer product and traded commodity has promoted a lot of research work on the field, as processing conditions are known to have a significant impact on the final quality of the instant coffee product (Pardo, Suess *et al*. 2002, Hindmarsh, Russell *et al*. 2007, Huang and Zhang 2013).

Manufacturing of instant coffee starts from raw coffee beans. Coffee beans are dried after harvest either naturally (sun-dried) or in a manufacturing unit (Clarke 1987). Dried coffee beans then undergo the processes of roasting, grinding and extraction (Vincze and Vatai 2004, Farah 2012, Pan, Yan *et al*. 2013). During roasting the flavour and aroma compounds of the coffee are developed, while grinding facilitates extraction of the soluble content and flavour. The extract is then filtrated, concentrated, and dehydrated into instant coffee powder before packing (Clarke 1987).

There are two conventional drying methods for instant coffee production: freeze drying and spray drying (Padma Ishwarya and Anandharamakrishnan 2015).

Spray drying is a technique in which solutions are sprayed as droplets into hot air, and this is a widely used technique especially in the manufacture of milk powder (Huang and Zhang 2013). The temperature of the sample surface can be maintained low drying spray drying

due to the evaporation of water even if the drying air temperature is high (Ho, Truong *et al*. 2017). However instant coffee manufactured by spray drying is still considered by consumers as low quality when compared with freeze dried instant coffee (Hartel and Heldman 1997).

Freeze drying (lyophilisation) is a method based on sublimation of ice crystals in a frozen sample (Pikal, Roy *et al*. 1984, Ratti 2001). Before freeze drying, coffee extracts are often aerated to create a foam with a density of 450 to 750 g/L (Suwelack and Kunke 2002). Heat-sensitive or oxidative components are more likely to be preserved during freeze drying (Franks 1998, Ratti 2013), and it makes freeze drying a widely used drying method in the food/pharmaceutical industries for systems such as coffee. The low temperature involved in freeze drying reduces the chance of deterioration or reaction, and the vacuum avoids long-time contact between the sample and oxygen. As an example, freeze drying resulted in 20% more volatile retention than spray drying in instant coffee processing (Padma Ishwarya and Anandharamakrishnan 2015). In addition, freeze dried products maintained the structure without significant reduction of product volume (Franks 1998, Ratti 2001). Porous structure is typically obtained after freeze drying, resulting in good rehydration properties of freeze dried products (Ratti 2001).

Despite the good product quality, the use of freeze drying technique in manufacturing has disadvantages, due to the significant amount of energy consumed to maintain the low temperature (-40, -50°C) and vacuum (0.3 to 0.4 mbar) throughout the process (Ratti 2001, Suwelack and Kunke 2002, Padma Ishwarya and Anandharamakrishnan 2015). The heat required for water removal in spray drying is 4000 to 6000 kJ/kg of water removed, but can be up to 100,000 kJ/kg in freeze drying (Marcotte and Grabowski 2008). To produce same

amount of products, freeze drying is much more expansive than spray drying (Ratti 2013). Due to the high cost, freeze drying techniques are only used for high-value commercial products manufacturing, e.g. baby food, herbs, and instant coffee (Ratti 2013).

In general, drying is energy-intensive and costly (Marcotte and Grabowski 2008), and industrial drying accounts for 12% of the total energy used in manufacturing processes on average (Strumillo, Jones *et al*. 2014). There is a growing concern over sustainable manufacturing in the food and beverage industry worldwide (Marcotte and Grabowski 2008), and reducing the energy/cost in freeze drying coffee extract is of great importance for the instant coffee manufacturer.

Energy consumed during processing could be saved by better understanding and improving the processes (e.g. freeze drying) and systems (Roos, Fryer *et al*. 2016). One of the possibly methods to save the energy during instant coffee manufacturing is to reduce the amount of water, that is, to increase the solid concentration in the process (Palzer, Dubois *et al*. 2012, Moreno, Raventós *et al*. 2014). As mentioned in previous context, instant coffee manufacturing involves both addition and sublimation of water (in extraction and drying), thus reducing the water in the process will be beneficial in energy and cost saving (Roos, Fryer *et al*. 2016). In industrial manufacturing, concentration is a common treatment before drying the coffee extract, to reduce the cost of drying (Berk 2009).

There has been an increasing interest in the freezing and freeze drying of high solid content food systems due to the consideration of energy reduction in freeze dried food production. Freeze drying has been widely used in food and pharmaceutical industry since 1950, and is intensively studied by researchers, as an example, in year 2000 about 600 publications were

produced in the field (Franks 2007). However, the systems used in freeze drying are often diluted solutions (less than 40% solute concentration).

Understanding the water crystallisation (first step of freeze drying) and freeze drying is important for the design of freezing or freeze-drying processes, aiming to identify optimal working conditions such as temperature or concentration. In particular, processing highly solid concentrated systems has been associated with manufacturing at reduced energy and waste usage. However, these systems are difficult to crystallise/freeze-dry and detailed studies on water crystallisation and freeze-drying at low water content are needed. In this study, the aim is to develop understanding of freezing and freeze drying processes for high solid content solutions (>50%). Concentrated sucrose solutions (up to 70% solute) will be used as the main model system.

1.2 Objectives

As explained in section 1.1, the main purpose of this research is to understand and improve freezing and freeze drying processes, to freeze dry high solid content systems in order to save the energy and cost. Two steps: water crystallisation (during freezing) and ice sublimation (freeze drying) were studied in this thesis.

The objectives of this research are as follow:

1) to develop and apply methods to study phase transitions (water crystallisation in particular) involved during freezing and freeze-drying solutions;

Information about phase transitions is of great importance both to understand the process, and then to subsequently modify the process to fit the high concentration systems. For example, information should include the crystallisation temperature of water, the amount

of water available to crystallise during freezing, the growth rate of ice crystals, the crystal form of the crystals, and the morphology of the ice crystals.

Methods need to be developed to investigate these aspects. Due to their nature, ice crystals are very fragile and sensitive to temperature change. Thermal history or any change in the environment may cause the ice melting or sample structure change. Characterisation methods that will not damage the structure (ice) are preferred. Ideally, samples should be examined in real-time and at the same place as they are prepared. If this is not possible, the storage and transfer of the sample between preparation and further examination need extra care.

2) To examine the parameters that will affect crystal growth kinetics and freeze drying, especially in high concentration systems;

Based on the methods developed, the behaviour of solutions with a certain range of concentrations (low to high) can be investigated during freezing and freeze drying, to find out the difficulties to process high concentration systems and the highest concentration that can be used.

Effect of formulation (e.g. concentration, viscosity, solute with different molecular weight) and effect of processing conditions (e.g. freezing rate, heating rate, annealing or nucleus addition) can be studied to identify the factors that can promote water crystallisation or reduce the chance of collapse in freeze drying.

3) To advise on new processing conditions to suit the increased concentration.

Freezing and freeze-drying processes can be modified, based on the previous findings about the factors that promote water crystallisation and freeze drying. Samples produced from

modified process need to be examined and compared with traditional processed samples to validate the modification.

1.3 The choice of the material in this thesis

1.3.1 Sucrose

Sucrose is common table sugar, which is usually manufactured from sugar beets and sugar cane (Featherstone 2015). Sucrose (α-glucopyranosyl-β-D-fructofuranoside) is a disaccharide, and each sucrose molecule is composed of dextrose(d-glucose) and levulose (d-fructose). The structure of sucrose is shown in Figure 2-1.

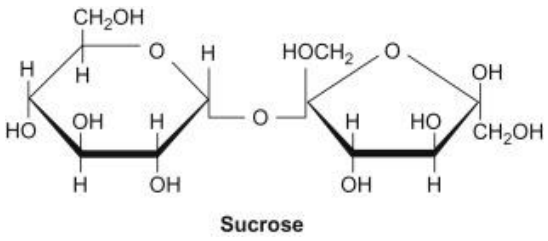

Figure 2-1 Structure of sucrose (Pontis 2017)

1.3.2 Coffee

Coffee brew is a worldwide popular beverage, mostly produced from two coffee species: Coffee Arabica (Arabica) and Coffee canephora (Robusta) (Esquivel and Jiménez 2012). There is a large number of chemical components identified in coffee beverage (Esquivel and Jiménez 2012). The components of coffee brew vary, depending on many factors including brewing conditions such as water temperature, water pressure, brewing time etc., as well as the composition of the roast and ground coffee. Coffee brew are complex in components

but main components are chlorogenic acids, caffeine, trigonelline, soluble fibre, protein, lipids, minerals, niacin, melanoidins, and volatiles (Farah 2012).

1.3.3 Gum arabic

Gum arabic is a natural gum exudate from certain species of acacia tree, that contains a mixture of different composition which are mainly carbohydrate (galactose, arabinose, rhamnose, and glucuronic acid) and a small proportion of proteins (Islam, Phillips *et al*. 1997, Montenegro, Boiero *et al*. 2012). The molecular weight of gum Arabic depends on the source, but typically in the range of 10^5 to 10^6 (Mothé and Rao 1999, Mahendran, Williams *et al*. 2008). It is often used as emulsifier, stabilizer or thickener, or to avoid sugar or water crystallisation (Mothé and Rao 1999).

1.4 Structure of the thesis

This thesis is presented in seven chapters and the contents of each chapter are summarised as follow:

Chapter 1 combines the introduction of the research project, the objectives of the study, the choice of the material used in thesis, and the outline of the thesis.

Chapter 2 reviews the literature that is relevant in the study, including (i) knowledge of phase transitions and phase diagrams, (ii) the control of the freezing process and the factors that affect water crystallisation, and (iii) principles of freeze drying process.

Chapter 3 displays the materials, experimental equipment and characteristic methods used in this study. There are six sections in this chapter. Section 3.1 discusses the formulation of the investigation systems, and section 3.2 shows their preparation. The samples processing methods are then displayed in section 3.3, including aeration and freezing. Section 3.4 shows the freeze drying study, including the equipment, the container used in the

experiment, the freeze drying cycles, and characteristic methods for freeze dried samples. The methods to study spontaneous crystallisation are displayed in section 3.5: DSC, XRD and SEM. Section 3.6 reports the development of a method to study crystallisation with nuclei addition, both in microscope scale and larger scale.

Chapter 4 provides the experimental results about water crystallisation from highly concentrated carbohydrate systems. Two parts of work are displayed here: (i) spontaneous crystallisation studied by DSC, XRD and cryo-ESEM; (ii) crystal growth kinetic of induced crystallisation. Parameters that affect water crystallisation are investigated, e.g. concentration, cooling rate, viscosity.

Chapter 5 further discusses water crystallisation from highly concentration solutions containing air bubbles. Air bubbles are either added on purpose or from sample preparation (in the case of gum arabic or coffee). Section 5.1 investigates spontaneous water crystallisation in coffee solutions using DSC, XRD and cryo-ESEM. Section 5.2 displays the study carried out under microscope to understand crystal growth kinetics of systems which contains air. Section 5.3 shows the scale up study of induced crystallisation in coffee system. Section 5.4 reveals the characteristic methods for freeze dried coffee samples.

Chapter 6 investigates freeze drying process in highly concentration carbohydrate solutions. Volume increase in freeze dried sucrose is first studied, and effect of concentration, drying temperature and heating rate are investigated. Then it moves to another system, gum arabic. Finally a mixture of gum arabic and sucrose is used in freeze drying.

Chapter 7 summarises of conclusions of experimental studies and some recommendations for future work.

1.5 Publications and presentations

Journal articles have been prepared/published based on this research, and some of the findings has been presented in international conferences as posters and oral presentations, as shown below:

Journal publications:

- Modelling freezing processes of high concentrated systems (2015). Lopez-Quiroga, E., **Wang, R.**, Gouseti, O., Fryer, P.J., Bakalis, S. IFAC Proceedings Volumes (IFAC-PapersOnline), 48 (1), pp. 749-754.
- Crystallisation in high concentrated systems: a modeling approach (2016). Lopez-Quiroga, E., **Wang, R.**, Gouseti, O., Fryer, P.J., Bakalis, S. *Food and Bioproducts Processing.* Vol. 100, pp. 525-534 (2016).
- Kinetic of seeding-induced ice crystallisation from high solid content system. **Wang, R.**, Gouseti, O., Fryer, P.J., Bakalis, S. (In preparation)

Oral presentations:

- A study of water crystallisation in highly concentrated food systems. **R. Wang**, E. Lopez-Quiroga, O. Gouseti, P.J. Fryer, S. Bakalis. 1st International Conference on Sustainable energy and Resource Use in Food Chains. (Windsor, UK). 19-21 April 2017.
- Modelling of ice crystal formation and morphology in highly concentrated systems. E. López-Quiroga, O. Gouseti, **R. Wang**, S. Bakalis , P.J. Fryer. TFMST II IFAC Workshop on Thermodynamic Foundations of Mathematical Systems Theory. (Vigo, Spain) 28-30 September 2016.

- Seeding-induced crystallisation in highly concentrated system. **R. Wang**, O. Gouseti, E. Lopez-Quiroga, P.J. Fryer, S. Bakalis. 29th EFFoST Conference (Athens, Greece). 10-12 November 2015.
- Water crystallisation in concentrated systems for reduced energy consumption in freeze-drying. **R. Wang**, O. Gouseti, E. Lopez-Quiroga, P.J. Fryer, S. Bakalis* 10th European Congress of Chemical Engineering (ECCE). Nice (France), Sept 27-Oct 1, 2015.
- Kinetics of ice crystallisation in supercooled high concentration sugar solution. **R. Wang**, O. Gouseti, E. Lopez-Quiroga, P.J. Fryer, S. Bakalis* 12th International Congress on Engineering and Food (ICEF). Quebec city (Canada), June 14-18, 2015.
- Crystallisation of highly concentrated sucrose systems. **R. Wang**, O. Gouseti, E. Lopez-Quiroga, P.J. Fryer, S. Bakalis*. 1st Congress On Food Structure Design. Porto (Portugal), 15-17 October, 2014.

Poster presentations:

- A study on crystal growth kinetics in high concentrated food systems. **R. Wang**, O. Gouseti, E. Lopez-Quiroga, P.J. Fryer, S. Bakalis. Conference of Food Engineering COFE 2016. (Columbus, US). 12-14 September 2016.
- Water crystallisation during freezing in highly concentrated systems (ePoster). **R. Wang**, O. Gouseti, E. Lopez-Quiroga, P.J. Fryer, S. Bakalis. IFT 2016. Chicago (US). 16-19 July 2016.

- Freezing of low water systems for reduced energy. **R. Wang**, T. Jackson, S. Fox, O. Gouseti, P.J. Fryer, S. Industrial Technologies conference (Amsterdam, The Netherlands). 22-24 June 2016.

- Structuring through crystallisation at high solids content. **R. Wang**, E. Lopez-Quiroga, O. Gouseti, P.J. Fryer, S. Bakalis. DOF Conference, Paris (France) 14-17 July 2015.

- Assessment of energy consumption in thermal phase transitions: freezing and freeze-drying. E. Lopez-Quiroga, **R. Wang**, O. Gouseti, P.J. Fryer, S. Bakalis. ICEF12 (Quebec, Canada) 14-18 June 2015.

- A first approach to the modelling of freezing in high solid content systems. E. Lopez-Quiroga, **R. Wang**, O. Gouseti, P.J. Fryer, S. Bakalis. ICEF12 (Quebec, Canada) 14-18 June 2015.

- Modelling of crystallisation processes: application to high concentrated systems. E. Lopez-Quiroga, **R. Wang**, O. Gouseti, P.J. Fryer, S. Bakalis. 28th EFFoST International Conference. Uppsala (Sweden), 25-28 November, 2014.

Chapter 2 Literature review

This chapter discusses the processes of freezing and freeze-drying of foods, including ways to control the microstructure formation and performance of freeze-dried products. Specific focus is given in sugar-based systems, as well as gum arabic and coffee, as these have been used during the work.

2.1 Phase/state transitions during freezing and freeze drying foods

The homogenous part of a system is defined as a phase (Mullin 2001). Compounds in foods may exist in different physical states, and the three simple states are gas, liquid and solid (Roos 1995). Phase transition takes place when the physical state of a material changes (Roos 1995). The transitions usually result from temperature, pressure or/and concentration change, and may have a significant effect on the physical properties of the material (e.g. heat capacity, viscosity, density, heat and mass diffusivity etc.) (Mullin 2001, Icoz and Kokini 2008). When a phase transition occurs, heat transfer takes place between the system and the environment (Mullin 2001). The enthalpy change of the system during the phase transition is often regarded as the latent heat (Mullin 2001). The transition of water into ice during freezing is probably one of the most well-known examples of phase transitions in food manufacturing (Roos 1995).

The components in the food may go through one or more phase transitions during processing and storage (Hartel, Ergun *et al*. 2011). Understanding and controlling phase transitions of food components is key to the manufacturing of food products, as the physical states of food materials determines the processing conditions and the quality of the final food product (e.g. texture, appearance and shelf life) (Icoz and Kokini 2008, Hartel, Ergun *et al*. 2011). As an example, by controlling sugar crystallisation in confectionary

manufacturing, different textures can be obtained to fit customers' expectations varying from a chewy marshmallow to a brittle hard candy (Hartel, Ergun *et al*. 2011).

Phase transitions can be classified into two types:

(i) first-order transitions;

First-order transitions are indicated by a change in enthalpy, entropy and volume, and the transitions between solids, liquids and gases are first-order transitions, including crystallisation and melting (Roos 1995).

(ii) second-order transitions.

During second-order transitions, there is no change in the enthalpy but a difference in heat capacity can be seen between the two phases (Roos 1995).

Phase transitions of carbohydrate-water systems during freezing have been extensively investigated due to their importance in freezing and freeze-drying applications, including foods and pharmaceuticals (Levine and Slade 1988, Hartel, Ergun *et al*. 2011). They will be briefly reviewed in this chapter.

2.1.1 Crystallisation

This section discusses crystallisation (especially water crystallisation), one of the most important phase transitions during freezing of carbohydrate systems, also the first step of freeze drying.

Crystallisation is the organisation of molecules into a solid phase from the liquid phase (a melt or a solution) in equilibrium (Cook and Hartel 2010). The process of crystallisation can be divided into three main steps: supercooling, nucleation, and crystal growth (Cook and

Hartel 2010). Sometimes the maturation or recrystallisation of crystals (especially during storage) is considered to be the final step of crystallisation (Hagiwara and Hartel 1996)

The steps of crystallisation are illustrated in a temperature-time profile in Figure 2-1.

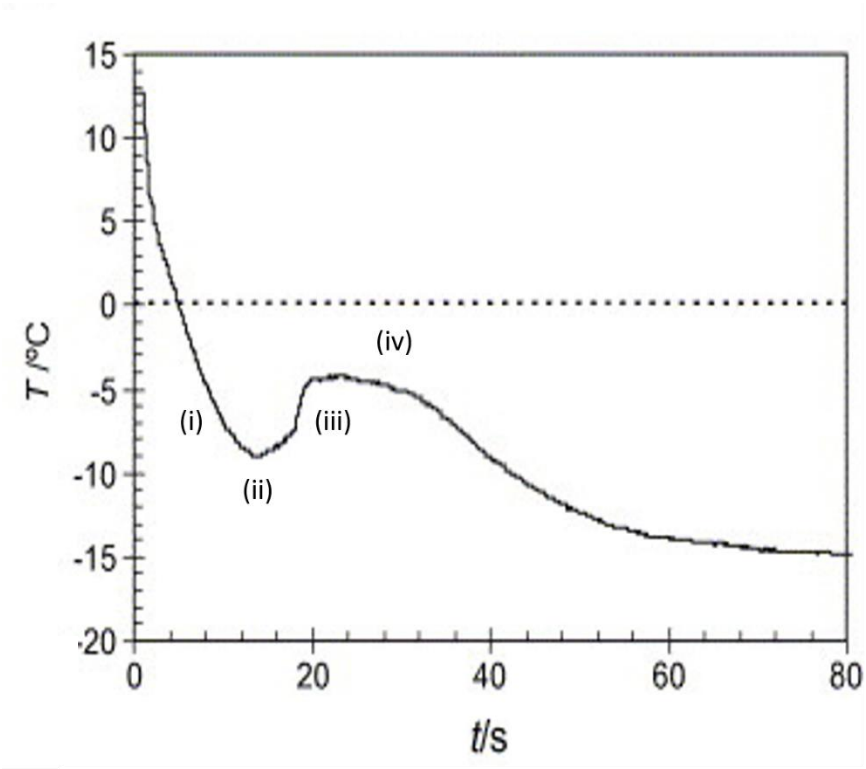

Figure 2-1 A temperature-time profile during freezing (MacLeod, McKittrick et al. 2006). Steps of i, ii, iii, and iv are indicated.

In the Figure 2-1, each step of crystallisation is identified by the change in the temperature.

(i) Supercooling: the temperature of the sample keeps decreasing below the equilibrium freezing temperature;

(ii) Nucleation: the lowest temperature that the sample reaches during freezing is regarded as the nucleation point;

(iii) Crystal growth: sample temperature increases after nucleation and reaches a plateau as crystal growth occurs with latent heat release. The plateau

temperature is often the same as the equilibrium freezing temperature (Hindmarsh, Buckley *et al*. 2004);

(iv) Further freezing: temperature decreases again with further cooling.

Detailed discussion of each step is given in the following section.

Supercooling

A system is supercooled when it is cooled to below equilibrium freezing temperature, in which state water molecules may cluster into ordered structures, but these clusters may not be stable enough to induce crystallisation in the whole system and they melt (Ayel, Lottin *et al*. 2006). A certain level of supercooling is necessary before spontaneous nucleation can occur to overcome the energy barrier of surface forming (the energy difference between the solute in solution and the solid particle of solute) (Ayel, Lottin *et al*. 2006, Hartel 2008, Patel, Bhugra *et al*. 2009).

Nucleation

Nucleation is the birth of a crystal, and it is classified into three types:

(i) Primary homogeneous nucleation: nucleation takes place spontaneously in a clean, homogenous solution. It is not common, as it is very difficult to have a solution without any foreign bodies (Mullin 2001)

(ii) Primary heterogeneous nucleation, in which nucleation is facilitated by the presence of foreign particles, including dust, impurities or surfaces (Hartel and Chung 1993, Garside, Mersmann *et al*. 2002).

(iii) Secondary nucleation, which occurs when small crystal fragments of the crystallising material are present in the solution, acting as a seed to form stable nuclei.

It is difficult to have a nucleus formed in supercooled liquid, as the formation of clusters is often not energetically favourable (Petzold and Aguilera 2009). The nuclei formed in the

solution must exceed the critical size to lead to further crystal growth, otherwise the crystalline structure is not stable and will dissolve into the liquid phase as the system always prefer to reduce its free energy (Mullin 2001).

Nucleation sites, as well as supercooling, are essential to form a crystal. (Mullin 2001). Primary homogeneous nucleation can be delayed due to lack of nucleation sites (e.g. foreign surface, dust particles or impurities) (Garside, Mersmann et al. 2002, MacLeod, McKittrick *et al*. 2006, Hartel, Ergun *et al*. 2011). Nucleation is a stochastic event (Hartel and Chung 1993), and variable primary nucleation results can result from slightly different nucleation sites (Hartel, Ergun *et al*. 2011).

Crystal growth

After the formation of stable nuclei, crystal growth takes place, with molecules added to the crystal interface (Mullin 2001). During water crystallisation in a solution, solute molecules diffuse away from the crystal and water molecules diffuse towards the crystal and organise into the crystal matrix (Roos 1995), and latent heat must be removed (Cook and Hartel 2010).

Recrystallisation

Recrystallisation, or Ostwald ripening , is a process in which the larger ice crystals grow at the expanse of small crystal (Searles, Carpenter *et al*. 2001). The mechanism of recrystallisation is the different chemical potentials between small and large ice crystals. Smaller ice crystals have higher chemical potentials, and melt faster than the large ones (Searles, Carpenter *et al*. 2001). During temperature fluctuations, the smaller ice crystals will melt during heating, and during refreezing the large ones are preferred to grow as they have lower chemical potentials. And there are no more new small ice crystals formed from

nucleation during freezing, as the big ice crystals will serve as crystal growth sites (Searles, Carpenter *et al*. 2001, Hartel 2008).

Recrystallisation can be undesirable, for example during storage of ice cream. As the temperature fluctuates in the freezer, ice may melt, regrow and ripen, which results in a product with fewer number, and larger in size ice crystals (Hagiwara and Hartel 1996). The texture of ice cream strongly depends on the size of the ice crystals, and small ice crystals are preferred to create a smooth and creamy texture (Hagiwara and Hartel 1996). Thus, recrystallization is not desirable in ice cream manufacturing and storage, as the increased size of ice crystals gives a coarse and icy taste which will fail customer's expectations (Roos 1995).

Recrystallisation can sometimes be desirable as well, for example in the freezing step of freeze drying process, the recrystallization of ice crystal may result in large ice crystals, which will facilitate sublimation during freeze drying.

2.1.2 Glass transition

Apart from equilibrium crystalline state, food material can also be in an amorphous, glassy state (White and Cakebread 1966, Roos 1995). A glass (or vitreous) material is not a crystalline, but is an amorphous solid (Sperling 2005), usually brittle and transparent. Glassy state has similar mechanical properties as solids (e.g. high viscosity of 10^{12} Pa.s or above) but the molecules are not ordered as in equilibrium crystalline materials (White and Cakebread 1966, Franks 1998).

The transition between rubbery liquid state and glassy (solid but not crystal) state is the *glass transition*, which is a reversible second-order type transition (White and Cakebread

1966). After glass transition, the system can be below equilibrium melting temperature, but it is not in a thermodynamically equilibrium state., i.e. the structure is kinetically trapped.

Cooing rate plays an important role in determining which phase transition (crystallisation or glass transition) will take place. If two transitions are both thermodynamically possible, it is the one which takes places faster that will occur, not necessarily the most thermodynamically preferred one (Mullin 2001). The non-equilibrium state is obtained from rapid change as the time is not long enough for the material to transit from one phase to equilibrium (Roos 1995). Water in a supercooled solution might crystallise into ice, but the crystallisation process takes time. If the cooling rate is rapid enough, it does not allow enough time for crystallisation to occur, i.e. cooling rate is faster than nucleation rate. The viscosity of the fluid keeps increasing and it reaches a rigid state without any crystalline formation (Rey 1960). As a result, the solution turns into a very high viscous glass with rapid freezing.

Glass, especially sugar glass, is very common in foods, e.g. spray dried milk powder or freeze dried juice (White and Cakebread 1966). Methods to produce foods in glassy states include removing the solvent or cooling the sample rapidly, so that the formation of crystalline equilibrium state is kinetically inhibited. High viscosity and complex molecular structures may also help in the formation of glass, again by kinetically obstructing the formation of crystals (White and Cakebread 1966).

Sugar glass is very unstable to the presence of moisture (White and Cakebread 1966). Water decreases the glass transition temperature significantly even if there is only a small change in the moisture content. In general, for a single component system, the glass transition temperature depends on its molecular weight. Components with higher molecular weights

usually have a higher glass transition temperature than components with lower molecular weights (White and Cakebread 1966). As water has a small molecular weight (18 g/mol) compared with most of the food materials (e.g. 342 g/mol for sucrose), the glass transition temperature of pure water (-150~-125°C) (Pryde and Jones 1952) is much lower than that of food material (e.g.67°C for pure sucrose)(Kauzmann 1948). As a result, water often takes the function of a plasticizer, that is, as the water content increases, glass transition temperature of the food material decreases.

When the rapidly frozen glass is reheated, the reverse process (glass-rubber transition) takes place. The viscosity of the solid glass decreases and the system gradually returns into liquid state (Rey 1960). After glass-rubber transition, there is a significant change in the mechanical properties, and the solid material is softened into a highly viscous liquid. As a result of the viscosity drop, the molecular mobility will increase dramatically after the glass-rubber transition, which makes it possible for the amorphous material to crystallise if it is held above its glass transition (and below its melting) temperature for enough time, and this will be discussed in the following section.

2.1.3 Devitrification

Rapid freezing results in the formation of a glass (see section 2.1.2). The glassy state is a metastable state, in which the thermodynamic driving force always exists to transfer it into a more stable, lower energy and equilibrium state. As an example, water can crystallise into ice from amorphous by heating the glass, as the glass has a higher system energy than ice crystals (Roos 1995). This is defined as devitrification.

The temperature at which the structure of the system transfers from vitreous to crystalline is the devitrification temperature (Luyet 1939, Rey 1960). It is closely linked to the glass

transition temperature. The high viscosity of the glassy state below glass transition temperature limits molecular motion, thus crystal formation is kinetically forbidden. Above glass transition temperature, molecules gain enough mobility to move and organize into crystals (Roos 1995).

Devitrification is sometimes not desirable in food manufacturing. For example, the amorphous lactose in milk powder might crystallise during storage if the temperature is above glass transition temperature, bringing caking or lumpiness into the product (White and Cakebread 1966).

However, it could be very useful on other occasions, for example in freeze drying operations, as it results in the creation of more ice crystals that can then be sublimated.

2.1.4 Techniques to study and compare crystallisation and glass transition

Differential scanning calorimetry is a popular technique used to study phase transitions (e.g. melting, crystallisation, glass transition and devitrification) in food or polymer systems (Roos 1995). The technique measures the heat flow changes as the sample's temperature changes. Crystallisation and glass transition are the two most important phase transitions occurring during freezing of carbohydrate-water systems, and both involve changes from liquid state to solid state. While crystallisation is the transition that takes place between two equilibrium states, glass transition involves non-equilibrium states. As a transition involving enthalpy change, crystallisation is classified as a first-order transition, and results in a peak in a DSC heat flow-temperature thermogram as shown in Figure 2-2.

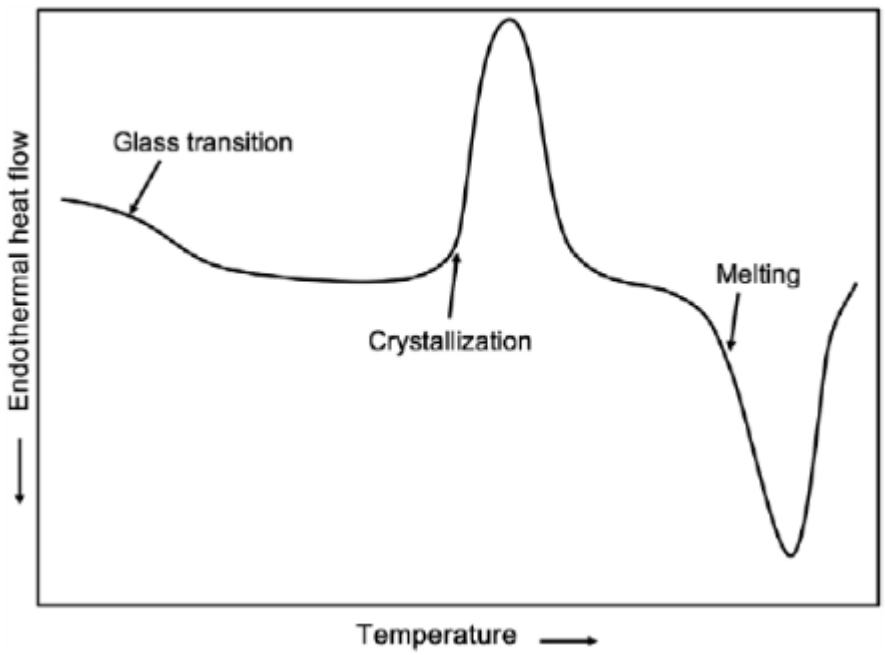

Figure 2-2 An example of DSC thermograph typical of freeze-dried amorphous sugar, which shows glass transition, crystallisation peak and melting peak. Exothermic peaks are plotted upwards (Roos 1995).

Crystallisation temperature can be obtained from the thermogram, and by integrating the peak area, the latent heat released during the transition can be calculated (Roos 1995).

Glass transition is a second-order transition, which only involves changes in heat capacity. It shows as a step change in a DSC cooling curve and it is often difficult to detect (see Figure 2-2), as it could: (i) overlap with the onset temperature of the melting peak; (ii) take place over a temperature range (could be 20°C) instead of at a certain temperature (White and Cakebread 1966), in which case care should be taken when interpreting data from the literature, as the stated Tg may refer to the onset, the middle, or the end of the glass transition (Searles, Carpenter *et al*. 2001); (iii) reflect only a small ΔCp and therefore difficult to identify.

Table 2-1 summarises characteristics of crystallisation and glass transition.

Table 2-1 Comparison between crystallisation and glass transition

Phase transitions	Thermodynamic status	Order of transition	Change during transition	Detected by DSC as
Crystallisation	equilibrium	First-order	enthalpy change	peak
Glass transition	non-equilibrium	Second-order	heat capacity change	step change

2.1.5 Phase/state diagram

A phase diagram describes equilibrium states of a system under different conditions, which is vital in controlling phase transitions in food manufacturing (Roos 1995, Hartel, Ergun *et al*. 2011). A phase diagram of a single material describes the physical state of the material as a function of temperature, pressure and concentration in equilibrium (Roos and Karel 1991, Roos 1997). In two-phase systems, the equilibrium state indicates that all molecules in the system have the same chemical potential (Hartel, Ergun *et al*. 2011).

However, kinetic limitations often prevent food components from reaching phase equilibrium, and metastable states are attained during food manufacturing or storage (Roos 1995, Hartel, Ergun *et al*. 2011), e.g. in the freezing of foods, ice formation is usually not in equilibrium (Roos 1995). A state diagram is similar to a phase diagram, but display non-equilibrium states, as well as equilibrium states.

Phase/state diagrams provide a way to predict the state of food materials and are thus important in improving the quality of current food products, developing novel products, and

understanding storage stability (Icoz and Kokini 2008). For example, during freezing of foods, a phase diagram can be used to state the crystalline yield of the material, or predict which crystal form the product will be in (Hartel 2008).

2.1.5.1 Phase diagram for a single-component system

As water is one of the most important components in foods, controlling phase transitions of water is critical in food processing and in determining the final texture and quality of many food products (Roos 1995). Understanding the phase transitions of water is critical in controlling and optimising freezing and freeze-drying operations, as ice crystal formation (during freezing) and sublimation (during freeze-drying) are central to those two processes (Ratti 2013). A simplified temperature-pressure phase diagram for water is displayed in Figure 2-3 and shows the three simple states (gas, liquid and solid) and the transitions between each other.

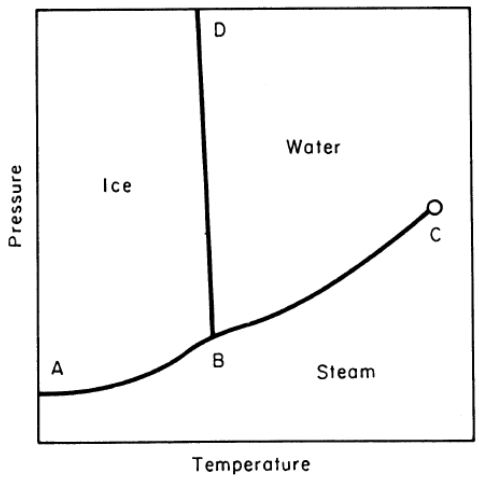

Figure 2-3 Phase diagram for water, showing relationships between equilibrium states and their dependence on temperature and pressure (Mullin 2001).

The phase diagram of water (Figure 2-3) describes the equilibrium states of solid ice, liquid water and gaseous water vapour at given temperatures and pressures. It can be used to predict the phase behaviour of water and high water content foods.

(i) Water vapour curve (BC) indicates the equilibrium temperature and pressure at which both liquid water and water vapour could coexists, and at higher temperature, water vapour pressure increases.

(ii) Freezing curve (BD) illustrates the effect of pressure on the freezing point of the water. At a given pressure (often atmospheric pressure), water could only crystallise into ice when temperature is lower than equilibrium freezing temperature.

(iii) Sublimation curve (AB) shows the increasing ice vapour pressure as the temperature increases. By crossing this curve (e.g. dropping the pressure at a given temperature), solid ice will sublimate into water vapour, as in the process of freeze drying (Mullin 2001).

The evaporation, sublimation, and freezing curves divide the diagram into three areas: water, ice and vapour. At a given temperature and pressure, the equilibrium phase of water can be predicted via this diagram. Three phases of water may only coexist in equilibrium at the triple point (point B), which has a temperature of 0.01˚C and pressure of 6.1mbar. Below this pressure water will not exist in its liquid form. Freeze drying must be conducted below this region as it allows the phase transition of water from ice to vapour without transferring into liquid water.

2.1.5.2 Phase diagram of two-component systems

To understand the freezing process of a solution, a phase diagram of a two-component system (solute and solvent) is needed. A state diagram of sucrose-water is displayed in Figure 2-4. In a two-component system, temperature, pressure and concentration are the variables that can affect the equilibrium of phase. Typically in food applications, the phase transition is simplified as a temperature-concentration diagram when the pressure is atmospheric pressure (Rey 1960, Mullin 2001).

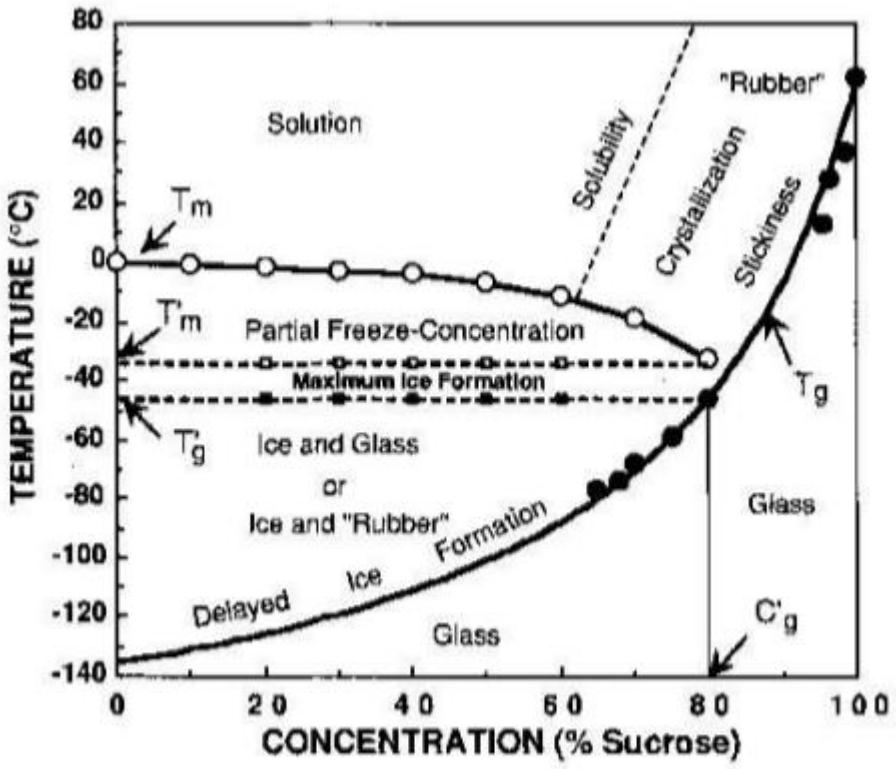

Figure 2-4 State diagram of amorphous sucrose-water system (Roos and Karel 1991).

There are two solid lines in this graph. One is the equilibrium freezing curve (labelled as Tm), and the other is the glass transition curve (labelled as Tg). Several regions are divided by

these curves, in which the physical state and stability of the sucrose-water system is predicted at a given temperature and concentration (Hartel, Ergun *et al*. 2011).

The equilibrium freezing curve shows the equilibrium temperature (Tm) at which the liquid water coexists with the ice in equilibrium. Above Tm, the liquid water exists, while below Tm water crystallisation may occur (Hartel 2008). Freezing temperature decreases as concentration increases, resulting from the decreased vapour pressure of water (Mullin 2001). As more ice is formed in the system, the remaining material in the system becomes more concentrated, thus its freezing point further decreases (Roos 1995). When the concentration reaches its maximum (C'g), maximum amount of ice has been formed in the system and the melting temperature is T'm. No more ice will form and the concentration of the system will not change further even if the system was cooled to lower temperatures.

The glass transition line represents the metastable boundary between liquid-like rubber and solid-like glass. Below this line the system will be in glassy state, and crystallisation is impossible due to the high viscosity of the system. Glass transition temperature increases as concentration increases. With the maximum ice formed in a system, the concentration reaches C'g, and the glass transition temperature at this concentration is T'g (Roos 1995).

Maximum freeze concentration can be created by keeping the system below its melting point but above its glass transition temperatures (a process called annealing, which will be discussed in more detail in section 2.2.2). The maximum amount of ice formation is obtained in the temperature range between T'g and T'm (as shown in Figure 2-4).

During freezing of some systems, some of the material (e.g. sodium chloride or other mineral salts) can form a eutectic crystal with the solvent (water). Eutectic means that solvent and solute both crystallise. Below the eutectic temperature, the solution is

separated into ice crystals and solid eutectic mixture (Rey 1960, Mullin 2001). However, food is rarely considered as a eutectic system. In many situations like sucrose-water solution, eutectic crystallisation is unlikely to happen, instead, the concentrated solution will turn into a glass (Roos 1995, Franks 1998). After freezing is completed, the system is separated into two phases: ice crystals and frozen concentrated matrix.

2.2 Controlling the freezing process, and factors affecting crystallisation

Freezing is a technique that removes water from food materials in the form of ice crystals. Freezing is widely used in the food manufacturing industry. For example, meats, vegetables and fruits are frozen to extend the shelf life, while frozen desserts (e.g. ice cream or sorbet) are manufactured to meet customers' needs (Hartel, Ergun *et al*. 2011). Freezing is also the first step of freeze drying to produce dehydrated food stuffs (will be discussed in section 2.3.2).

Controlling freezing process is of great importance, as it determines the ice crystal formation and morphology (size and shape), which dominates the texture, quality and storage stability of the frozen or subsequently freeze dried food (Hindmarsh, Russell *et al*. 2005, Cook and Hartel 2010). As an example, large ice crystals formed during slow freezing will result in big pore sizes in the freeze dried cake and short primary drying time (Rambhatla, Ramot *et al*. 2004; Ratti, 2013)

In order to improve process conditions, it is important to understand the mechanisms of water crystallisation and the parameters that affect crystallisation. There are several factors that determines crystallisation and they often influence each other (Hagiwara and Hartel 1996).

2.2.1 Freezing rates

Freezing rate is important in determining (i) the amount of ice crystals formed before the system gets into a glassy state; and (ii) the morphology of the ice crystals.

At high freezing rates, the amount of crystallised water in the system decreases, that is, the unfrozen water (glassy water) increases. In a DSC study, when the cooling rate increased from 1°C/min to 20°C/min, the amount of unfrozen water increased from 14% to 19.5% (Zasypkin and Lee 1999). As discussed in section 2.1.2, if the cooling rate is sufficiently high, no water crystallisation but only glass transition takes place, as the freezing rate is faster than nucleation rate.

Freezing rate also determines the size of the resulting ice crystals (Roos 1995). Fast freezing leads to small in size but large in number ice crystals and slow freezing results in large and less ice crystals, subsequently a slower primary drying rate during freeze drying (Cook and Hartel 2010). As mentioned in 2.1.1, crystallisation involves the remove of latent heat, so fast freezing, which provides fast transport of latent heat, results in more nuclei to form and the space for each crystal to grow is reduced and thus a large number of small ice crystals are obtained (Cook and Hartel 2010).

2.2.2 Temperature (supercooling)

The nucleation rate determines the number of crystals that can be formed, and as a result, the size of the crystals that can be formed (Cook and Hartel 2010). Supercooling, as the driving force for ice nucleation, is the most pronounced factor for ice nucleation took place. More supercooling (lower temperature) provides more driving force to increase nucleation rate (rapid and massive nucleation) (Hartel 1996) , however, when the temperature is too

low, the mobility of molecular decreased to slow down nucleation rate (Cook and Hartel 2010).

The effect of temperature on nucleation rate and crystal growth rate is displayed in Figure 2-5.

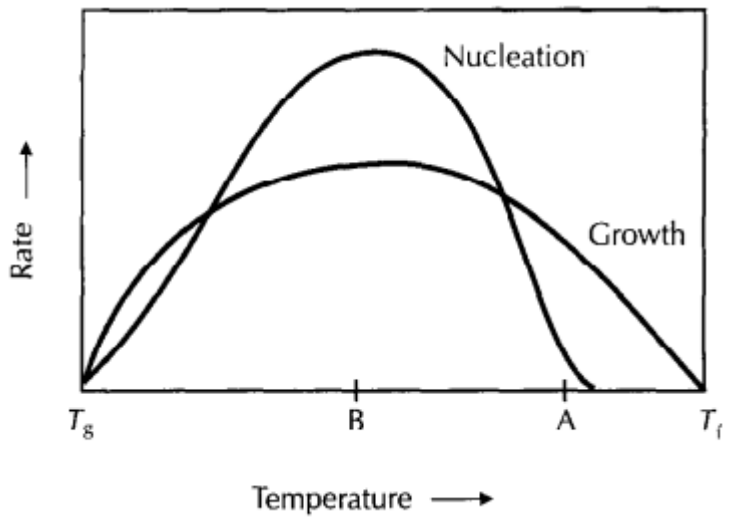

Figure 2-5 Rate of nucleation and crystal growth as a function of temperature (Hartel 1996).

Crystallisation only occurs within the temperature range between the equilibrium freezing temperature (T_f) and glass transition temperature (Tg). Above T_f, crystallisation is not thermodynamically possible; and below T_g, glass transition restricts crystal growth kinetically (Mullin 2001).

Within the temperature range, as temperature decreases both nucleation and crystal growth rate first increases due to the increase in driving force, then decreases when the temperature further decreases, as the very low temperature causes a limited molecular mobility (Hartel 2008).

Freezing temperature may also affect rate of water crystallisation by its influence on freezing rate. As freezing temperature decreases, the freezing rate increased, resulting in large number of small ice crystals (Searles, Carpenter *et al*. 2001).

2.2.3 Annealing

Annealing describes a thermal process in which a frozen solution is rewarmed to a certain temperature level (above its Tg and below its Tm) and it is held at that temperature for a certain length of time before being cooled again (Roos 1995). The thermal treatment (heating, cooling and holding) involved in annealing may promote recrystallization (see section 2.1.1) (Rambhatla, Ramot *et al*. 2004) and devitrification (see section 2.1.3), and it is used in this thesis to promote water crystallisation (see section 4.1.1.4, 5.1.3.3).

Annealing is often used in freeze drying to:

(i) promote the formation of ice crystals.

As mentioned in section 2.1.2, the formation of glassy ice is common with rapid freezing, but it is not desired in freeze drying as the glassy water will not sublimate during primary drying. To avoid this, annealing can be applied to transfer water from glassy state to crystals (devitrification, see section 2.1.3) (Rey 1960)

(ii) create large size ice crystals, and thus larger pores in the eventual freeze dried cake, which will facilitate sublimation, reduce primary drying time by reducing the product resistance to water vapour (Tang and Pikal 2004, Ratti 2013).

Searles (2001) have published SEM image of freeze dried hydroxyethyl starch (HES) cakes with/without annealing, and annealing increase the spacing from around 5 to 100 micrometers.

(iii) homogeneous ice crystals after freezing, which is critical to freeze drying efficiently (Ratti 2001, Rambhatla, Ramot *et al*. 2004).

(iv) promote the crystallisation of crystalline components such as bulking agents

The selection of temperature and time is of great importance for annealing. Molecular mobility increases significantly when the system is heated above Tg, so annealing should be conducted above Tg (Searles, Carpenter *et al*. 2001). Ice formation is also time-dependant. Increasing annealing time will result in more amount of ice formation until the solution reaches the maximum freeze concentration (Roos 1995).

2.2.4 Seeding

As mentioned in section 2.1.1, primary nucleation might be delayed due to lack of nucleation sites, and variable primary nucleation results can result from slightly different nucleation sites. Adding seed crystals (nucleation sites) can avoid this variability so that secondary nucleation takes place (Hartel, Ergun *et al*. 2011). In addition, much lower supersaturation/supercooling is needed for secondary nucleation to take place than for primary nucleation (Hartel and Chung 1993, Garside, Mersmann *et al*. 2002).

Seeding is one method, which seeds (small particles of the crystalline material) are introduced into a supersaturated solution to create nucleation sites (Mullin 2001). It is a widely used method (Hartel 2002), based on secondary nucleation. The material of the seed crystal could also be a different substance than the material to be crystallised (based on primary heterogeneous nucleation), for example, silver iodide is generally used to crystallise water in artificial rain. The choice of AgI to aid water crystallisation is based on the fact that it has similar crystal lattice with ice crystals. (Mullin 2001).

Seeding is sometimes conducted on purpose to control the crystal size distribution in the sample, however it could also take place unintentionally. In a lab or factory, some dust of the crystalline material will be distributed in the air inevitably, and this dust might act as a seed to induce the supersaturated liquid to crystallise (Mullin 2001).

2.2.5 Solid concentration

The solid concentration (or the water content) plays an important role in ice crystals forming. Increasing solid content in the system results in freezing point depression and glass transition temperature increases (see section 2.1.5.2). As a colligative property, freezing point depression depends on the moles of solute rather than the mass of the solute in the solution (Cook and Hartel 2010).

As solid concentration increases, the amount of water that does not crystallise on freezing also increases. For example, it was shown that when the sucrose concentration increased from 5% to 40%, the amount of the unfrozen water increased from 7.5% to 40.9% (Zasypkin and Lee 1999). The uncrystallised water will not be able to be removed by sublimation during primary drying but have to be desorbed during secondary drying (Kasper and Friess 2011)

2.2.6 Viscosity

Viscosity of the solution can be increased by adding stabilizer, such as locust bean gum, guar gum and sodium carboxymethyl cellulose (Goff, Caldwell *et al*. 1993). Addition of stabilizer does not have significant impact on ice melting temperature or amount of ice, but viscosity increases especially at subzero temperatures, result in a decrease in molecular diffusion rate. As a result, both water molecular moving to the existing ice crystals and solid

molecular diffusion away from the growing crystal surface are limited, and crystal growth rate is decreased (Goff, Caldwell *et al*. 1993, Bolliger, Wildmoser *et al*. 2000)

2.3 Freeze drying

In this section, the principles of the freeze drying process will be briefly reviewed, including the different stages during freeze drying, the collapse phenomena that could happen in freeze drying, the freeze-drying condition setup and finally the effect of molecular weight on freeze drying.

Freeze drying usually results in products with porous structure that will facilitate rehydration (Brennan 2011), and an example of typical microstructure of freeze dried food product can be seen in Figure 2-6.

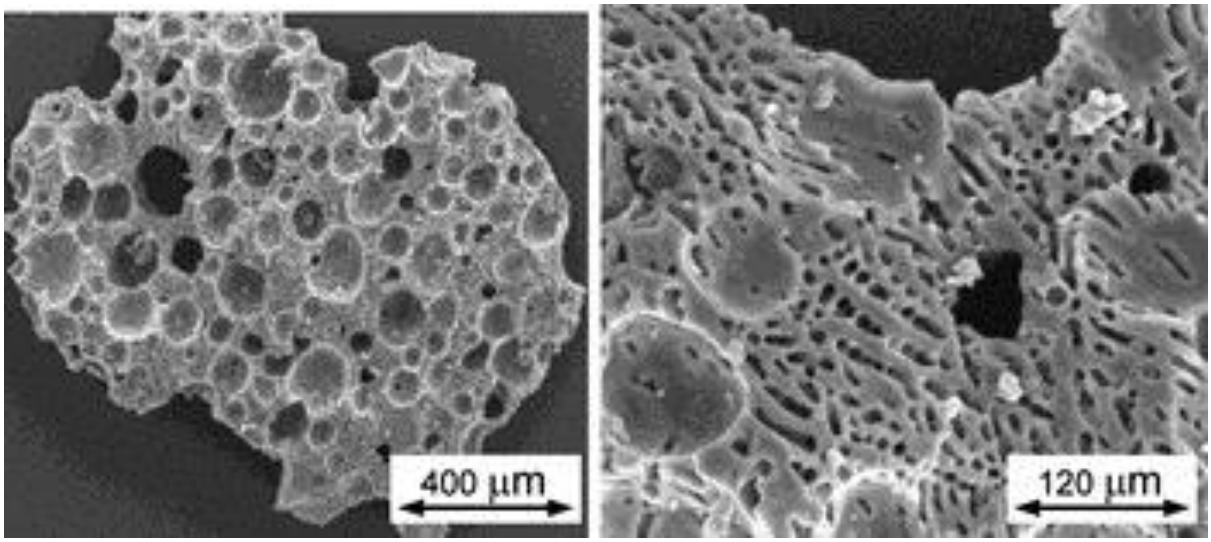

Figure 2-6 SEM image of a freeze dried food powder (Palzer, Dubois et al. 2012).

Figure 2-6 displays a SEM image of freeze dried food powder, showing the typical porous structure obtained from freeze drying. Pores of two sizes existed in the sample: the big

round pores in the structure resulted from air bubbles in the solution, and the small pores were created by ice crystal sublimation.

2.3.1 Three steps of freeze drying

Freeze drying can be divided into three steps (Tang and Pikal 2004, Ratti 2013):

(i) Freezing: Sample solidifies as temperature decreases below freezing curve, and ice crystals are formed during this step. This process usually takes several hours to allow the sample to be completely frozen.

(ii) Primary drying: Ice crystals in the frozen sample sublimate under vacuum (usually in the range of 4 to 27 Pa) (Ratti 2013). Pore spaces are created in the solid matrix which were occupied by ice crystals. Water vapour produced during drying travels to the surface of the material before getting expelled (Franks 1998).

(iii) Secondary drying: Bound water in solid matrix are desorbed with shelf temperature increases.

In order to understand the freeze drying process, a phase diagram (Figure 2-9 a) is used to show the phase transition of water; and a temperature profile (Figure 2-9 b) illustrates the sample temperature change during a freeze drying cycle.

The sample starts from ambient temperature and pressure (point A in Figure 2-7 a). During freezing, the sample temperature decreases and crosses the freezing curve (point B in Figure 2-7 a), and the water solidified into ice (point C in Figure 2-7 a). During primary drying, the pressure decreases (between 100 and 150mTorr in Figure 2-7 b, that is, 133 to 200mbar), and ice sublimates into water vapour by crossing sublimation curve (point D in Figure 2-7 a). Evidence of the end of the primary drying phase (i.e. that the majority of the

ice has been sublimated) can be indicated from the sharp increase and then that the sample temperature approaches shelf temperature (Tang and Pikal 2004, Patel, Doen *et al*. 2010).

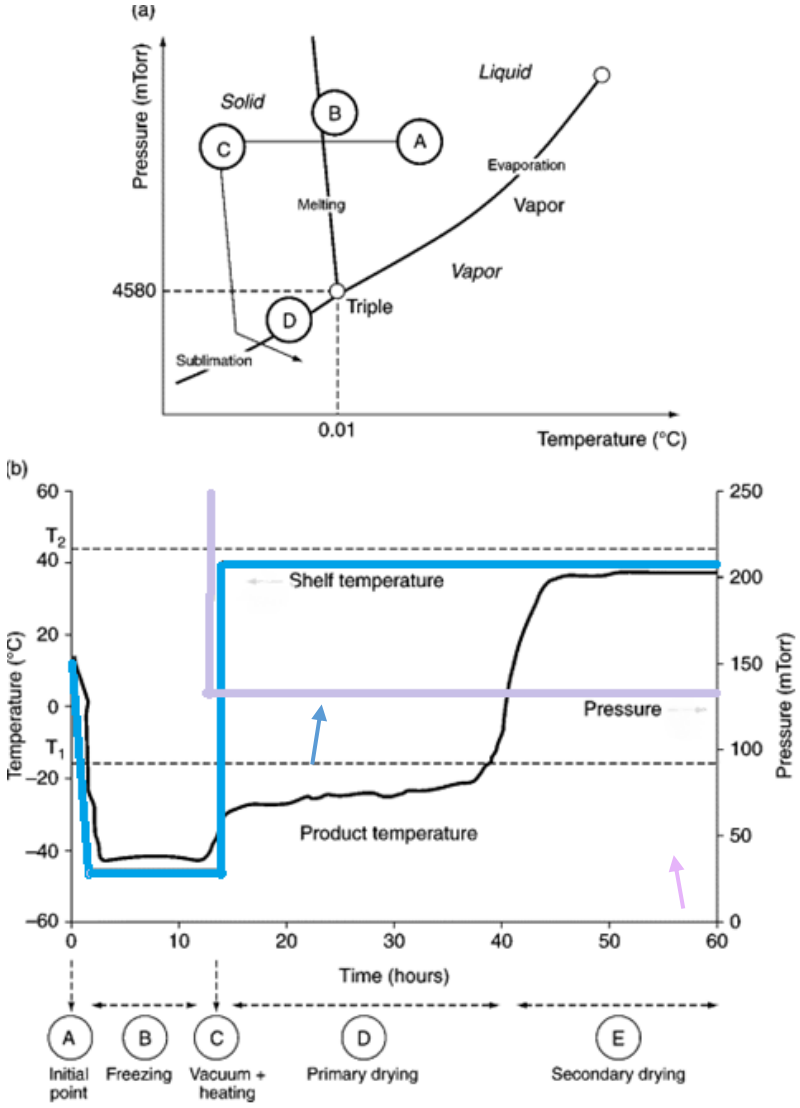

Figure 2-7 (a) freeze drying process illustrated in a phase diagram of water, (b) sample temperature profile during a freeze drying cycle (Ratti 2013)

Freezing

The process of freezing has been reviewed in section 2.2. After freezing, the solution has separated into two phases: the ice crystals and the freeze concentrated amorphous phase

(Franks 1998, Tang and Pikal 2004). It has been estimated that on average there is about 20% unfrozen water in the freeze concentrate at the end of freezing (Tang and Pikal 2004).

Controlling the freezing step has a remarkable impact on the freeze drying process and final product quality, as the sublimation rate in freeze drying strongly depends on the morphology of ice (Searles, Carpenter *et al*. 2001). Larger ice crystals, which typically result from slow cooling, promote easier sublimation during primary drying, and accelerate primary drying (Ratti 2013). Fast freezing/low temperature was found to result in small ice crystals (Quast and Karel 1968), higher product resistance and longer primary drying time (Esfandiary, Gattu *et al*. 2016).

During water crystallisation, the distribution of solids and water changes. During freezing of a sucrose-water droplet, the sucrose molecules redistribute towards outside of the droplet, the amount of the sucrose was found to increase in the surface of the droplet in a cryo-SEM study (Hindmarsh, Buckley *et al*. 2004). Before freeze drying, an impermeable surface film might form due to the same reason, which would slow down ice sublimation rate by increasing the resistance to mass flow of water vapour to the surface of the material (Quast and Karel 1968). Slush freezing (freezing with manual agitation) is possibly a way to avoid the surface layer forming during freezing and thus give the sample with best permeability (Quast and Karel 1968)

Annealing

As discussed before in section 2.1.1, nucleation can be random and not controlled directly. The randomness in nucleation created heterogeneity in ice crystal size, which may cause the sublimation rate change unpredictably during freeze drying, resulting in the difficulties in

primary drying process control and even loss of quality (Searles, Carpenter *et al*. 2001, Rambhatla, Ramot *et al*. 2004)

The variation in the sublimation rate and the total drying time can be reduced by conducting annealing before primary drying. The increase of sublimation rate will reduce primary drying time. After annealing, the drying rate is independent of nucleation temperature, and the drying rate is increased up to 3.5 fold compared with rate in unannealed samples (Searles, Carpenter *et al*. 2001).

Primary drying

After the product is completely solidified during the freezing process, vacuum is applied in the freeze-drying chamber and primary drying starts. The heat and mass transfer in a product in a glass vial is illustrated in Figure 2-8.

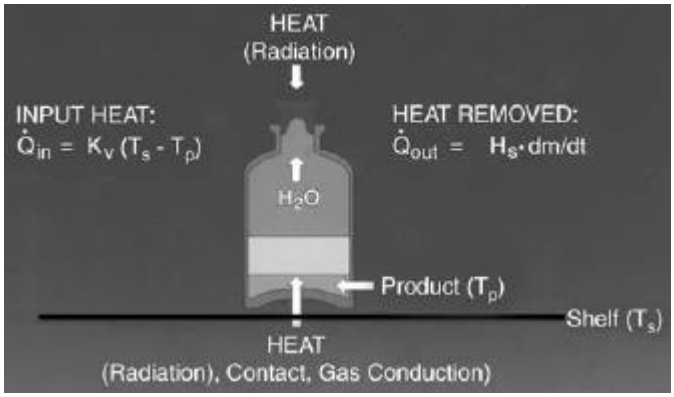

Figure 2-8 Heat and mass transfer in a glass vial during primary drying (Franks 1998)

During primary drying, there are several types of the heat transfer into the product (Q_{in}); mainly from conduction from the shelf and radiation from chamber wall (Franks 1998).

The heat transferred into the system Q_{in} can be described by equation 2-1:

$$Q_{in} = Kv(Ts - Tp) \quad (2\text{-}1)$$

Where Q_{in} is the heat transferred into the system,

K_v is heat transfer coefficient,

T_s is shelf temperature,

T_p is product temperature,

Meanwhile, heat is also transferred out of the system as the ice sublimates.

$$Q_{out} = \Delta Hs(dm/dt) \quad (2\text{-}2)$$

Where Q_{out} is the heat transferred out of the system

ΔH_s is enthalpy change during ice sublimation,

And dm/dt is sublimation rate of ice (Franks and Auffret 2007).

During freeze drying, ice starts to sublimate from the surface of the sample. There will be a moving front between the frozen layer (high water content) and the dry layer (low water content) (Franks and Auffret 2007). The plane of sublimation, often called sublimation surface or sublimation front, starts at the outer surface of the sample and then moves inwards. Above the sublimation front there is porous dried material, and below it there is the frozen material (Bruttini and Liapis 2006). Sublimated water vapour generated at the sublimation front is transported through the dried (porous) layer to the surface and out of the sample. The schematic graph in Figure 2-9 displays the dried layer (indicated as dry solids), sublimation front, and frozen layer (indicated as ice) during primary drying. The position of the sublimation layer moves from the top (at the beginning of primary drying) to the bottom of the sample.

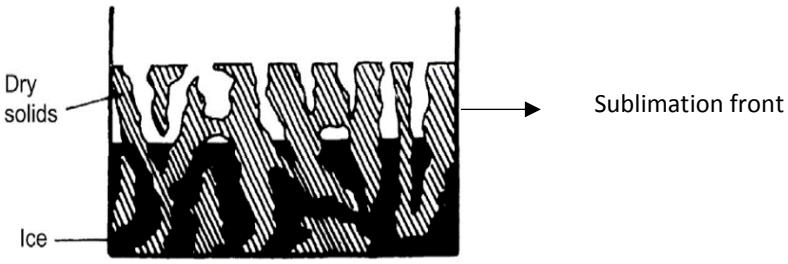

Figure 2-9 Schematic of material during freeze drying. Above the sublimation front, sample is dried; and below the sublimation front, sample is still frozen (Fellows 2009).

There is significant difference in moisture content in frozen and dried layers, as shown in the schematic in Figure 2-10.

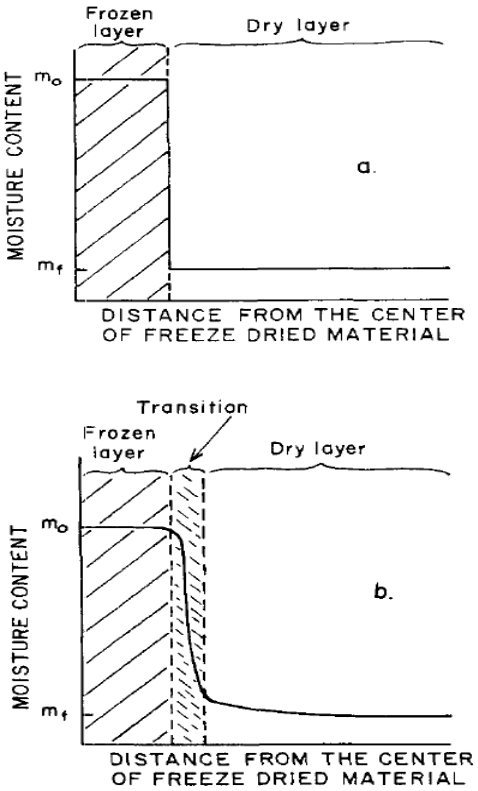

Figure 2-10 Moisture profiles in freeze drying materials (a) ideal (b) actual (Karel and Flink 1973).

In theory, the moisture content is high in the frozen layer and drops discontinuously to a very low value in the dried layer (Figure 2-10 a). In reality, the sublimation front is a transition layer, where moisture drops sharply but continuously to low value in the dried layer (Figure 2-10 b).

Primary drying is the longest step in freeze drying (Tang and Pikal 2004), and accounts for half of the total energy consumption (Ratti 2001). Optimising primary drying to reduce sublimation time is one approach to reduce the energy cost during freeze drying.

During primary drying, as the moisture content in the sample decreases, the matrix becomes more stable and can maintain the structure at higher temperature without transferring into liquid state (Tsourouflis, Flink *et al*. 1976). Shelf temperature can be increased to accelerate sublimation as increasing temperature will increase water vapour pressure (driving force for water removal) logarithmically (Franks 1998). However, if the sample temperature increased faster than the collapse temperature, the sample collapses. Therefore slow heating rate from primary to secondary drying is preferred (Tang and Pikal 2004). A slow rate of heating (e.g. 5-9°C/hour) is reported to reduce the chance of structure collapse (Shalaev and Franks 1996, Patel, Doen *et al*. 2010).

Secondary drying

During secondary drying, uncrystallised water desorbs as the shelf temperature increases. Secondary drying and primary drying might overlap, and secondary drying is only dominating the drying process once the primary drying finished (Tang and Pikal 2004).

2.3.2 Collapse

Collapse, loss of structure, can occur during freeze drying if the sample temperature exceeds a certain level, which is called the collapse temperature (Tsourouflis, Flink *et al*.

1976), or maximum allowable temperature (Pikal, Roy *et al*. 1984). Once sample exceeds this temperature, structure loss may take place as the decreased viscosity fails to maintain the structure under vacuum (Franks 1998).

The quality of freeze dried material (collapse or not) can be assessed directly by visual observation of its cake appearance, as shown in Figure 2-11.

Figure 2-11 Freeze dried cake with (a)no collapse and (b) severe collapse (Stärtzel, Gieseler et al. 2015).

Figure 2-11 (a) shows freeze dried sample with retention of cake structure, while Figure 2-11 b shows a severely collapsed freeze dried cake with loss of original structure, shrinkage and a foamy appearance.

Collapse temperature is usually measured by observation of trial-and-error results, but it is often linked with some measurable thermal properties of the material (Ratti 2013).

When the freeze drying formulation is crystallised materials (e.g. lactose or mannitol) (Franks 1998), the collapse temperature is the eutectic temperature (Tang and Pikal 2004).

However most of the freeze drying formulations, including sucrose (main material in this thesis, see section 3.1), does not crystallise but stays in amorphous state throughout freezing and freeze drying (Franks 1998), even after annealing (Searles, Carpenter *et al*. 2001). In this case, collapse temperature corresponds to the glass transition temperature of the maximum concentration T'g (Franks 1998, Ratti 2013) or T'm (Roos 1995). It is widely believed that T'g or T'm can be used as a theoretic indication of maximal allowable temperature during primary drying. Below this temperature, significantly high viscosity of sucrose-water glass maintains its structure and behaves like a solid, but it is not thermodynamically stable (Franks 1998). Once it exceeds this temperature, the significant viscosity drop drives it to a liquid-like system, without being able to support its own weight (Roos 1995).

There are two types of collapse in the freeze drying process: one is the collapse during primary drying, which is more relevant to the present work. The other is the collapse during secondary drying or after freeze drying. In this case, the collapse temperature is the glass transition temperature of the dry solids. Take freeze drying sucrose solution as example: primary drying sucrose should be conducted under T'm or T'g of sucrose solutions (-34 and -46°C, respectively)(Roos and Karel 1991), otherwise collapse may take place during primary drying. After primary drying finishes, the moisture content of the matrix is significantly decreased ($\leqslant$10%), and the collapse temperature changes to the glass transition temperature of solid sucrose (56°C). Sample temperature during secondary drying and storage should be lower than this value (Tg of solid material) to avoid collapse (Ratti 2013).

As mentioned in section 2.1, product temperature/moisture content determines the phase of the system, and any change in them could lead to a phase transition, which may cause an

undesired loss in product quality. Increasing temperature/moisture content leads to the transition from stable glass state to viscous liquid state, which results in loss of structure of the freeze dried product. Collapse can also occur in other than freeze-drying process, for example it may cause stickiness or caking of spray dried particles (Tsourouflis, Flink *et al*. 1976).

2.3.3 Freeze drying conditions setup

Although trial-and –error is always used in the industry, freeze drying technique is based on knowledge and techniques from physical, chemistry and engineering principles. Thus a stable, acceptable product can be achieved from the design of successful freeze drying conditions (Franks 1998). The design of freeze drying cycles (parameters setup) will be introduced in this section.

Control of sample temperature is vital. As discussed in previous section (2.3.3), sample temperature should be lower than collapse temperature to avoid any ice melting/collapse. However, it should also be as high as possible to maintain a high sublimation rate (Rey 1960). The pressure difference of water between the subliming surface and the condenser is the driving force of mass transfer through the dry layer (ice sublimation) (Quast and Karel 1968, Franks 1998, Tang and Pikal 2004, Franks and Auffret 2007).

As water vapour pressure is inversely proportional to the temperature, the driving force can be in thought of as the difference between the ice front temperature and the temperature of the condenser (Franks and Auffret 2007). High shelf temperature can significantly reduce drying time thus reducing energy requirements (Ratti 2013). The ideal product temperature during freeze drying should be set at just below collapse temperature. Design of a successful

freeze drying cycle requires therefore knowledge of the collapse temperature of the formulation.

However, control of the sample temperature cannot be controlled directly. Sample temperature depends on the formulation, shelf temperature, chamber pressure and heat transfer between shelf and sample (Tang and Pikal 2004, Tang, Nail *et al*. 2005). The sample absorbs heat from the shelf and chamber, and then consumes it during ice sublimation. At steady state, heat transferred to the sample is equal to the heat removed from the sample during sublimation, as described by equation 2-3.

$$Q_{in} = Q_{out} \tag{2-3}$$

Using the equation 1 and 2, equation 3 can be written as:

$$Kv(Ts - Tp) = \Delta Hs(dm/dt) \tag{2- 4}$$

And dm/dt is sublimation rate of ice (Franks 2007, Franks and Auffret 2007).

If the energy transferred into the sample is greater than the energy that gets out, the sample will overheat.

Sublimation rate depends on the sublimation area, the thickness of the drying sample and the porosity of the dried matrix. Generally, large surface area and thin sample thickness leads to better sublimation (Franks 1998). The relationship between chamber pressure and sublimation rate can be defined as shown in equation 5

$$\frac{dm}{dt} = \frac{P_{ice} - P_c}{R_p + R_s} \tag{2-5}$$

Where dm/dt is ice sublimation rate,

P_{ice} is the equilibrium vapor pressure of ice at the sublimation interface temperature,

P_c is the chamber pressure,

R_p is resistance from dry layer,

and R_s is the resistance from vial stopper (Tang and Pikal 2004). Mostly, product resistance is the major resistance, so sublimation rate mainly depends on the product resistance, which results from the dimension of the pores in the sample (Rambhatla, Ramot *et al*. 2004).

The sublimation front moves towards the bottom of the sample, as the freeze drying continues. The resistance to the water vapour increases, due to the longer distance required for vapour to escape from the freeze dried matrix.

2.3.4 Effect of molecular weight of the material on freeze drying

Formulation affects the quality of freeze drying. Systems with low glass transition temperatures are generally more difficult to freeze dry, e.g. juice or sucrose solutions. The glass transition temperature of a pure material depends on its molecular weight (see section 2.1.2). Typically, high molecular weight materials have high collapse temperature, which makes it easier to freeze dry (Ratti 2013). These high molecular weight materials (excipient or bulking agent) can be added into a freeze drying formulation to improve the thermal stability of the product during drying to avoid collapse (Franks 1998). As an example, high sugar content systems may be freeze dried with some addition of microcrystalline cellulose and heated potato starch to stabilise the structure (Quast and Karel 1968).

2.4 Conclusions

Section 1.1 discusses the importance of freeze drying highly concentrated systems, as an approach of reducing energy consumption during manufacturing. Processes of freezing and freeze drying has been reviewed in Chapter 2, however, majority of the published work is for low concentration systems and is for pharmaceutical systems. The aim of this work is to freeze dry high solid content systems in order to save the energy/cost of the freeze drying process.

However, processing high solid content systems is challenging due to (i) limited ice crystal formation, as there is little amount of water to crystallise, (ii) low freezing temperature due to freezing temperature depression at increasing solids concentration, and (iii) low porosity of the dried material due to the decreased amount of water, causing high resistance to the vapour transportation towards the surface for the material, which might result in limited sublimation rate and overheating of the sample.

Meanwhile, the quality of the freeze dried product should remain acceptable for the customers, which means fast rehydration and a porous cake structure without collapse. To reach this aim, a suitable freezing and freeze drying process is required, to create as many ice crystals as possible during freezing, and to sublimate all the ice without losing the structure during freeze drying.

Chapter 3 Materials and Methods

Chapter 1 and 2 discussed the aim of the thesis, to investigate the freezing and freeze drying processes of highly concentrated system. Chapter 3 explains the systems investigated in the present work and the methods /equipment involved to make this study possible. It starts from the formulation of the systems then moves to preparation of the sample. The main processes in this research, freezing and freeze-drying, are displayed as well as the characteristic methods for crystallisation and for freeze-dried sample.

3.1 Materials

Material selection was based on the requirement for high solubility, as focus of the present work was on studying processing (freezing and freeze-drying) of high solids content systems. Sucrose, maltose, and gum arabic are carbohydrate systems often found in foods with low (sucrose, maltose) and high (gum arabic) molecular weight. They all exhibit high solubility (≥ 60%).

Sucrose, also known as table sugar, is a disaccharide (α-glucopyranosyl-β-D-fructofuranoside) commonly used in foods. It is a well-studied system with a well reported phase diagram and solubility of 67% at room temperature. Sucrose solutions were used in crystallisation and freeze-drying experiments (Zasypkin and Lee 1999, Zumbé, Lee *et al*. 2001, Hindmarsh, Buckley *et al*. 2004).

The effect of viscosity on crystallisation kinetics was studied by addition of Carboxymethyl Cellulose (CMC) to sucrose solutions, while maintaining the same amount of total moisture content (water concentration) in the system. CMC is a food thickener and was used here to increase the viscosity of the system.

Maltose is another type of disaccharide (contains two glucose molecules), which was used in calorimetric experiments to compare with sucrose and study the effect of different solute material (similar molecular weight) on water crystallisation during freezing.

Gum Arabic is a natural gum with high molecular weight (10^5 to 10^6, see section 2.4). Systems of up to 60% solids were prepared and compared with the sucrose systems (with/without CMC) in crystal growth rate and freeze drying studies.

A mixture of sucrose and gum Arabic solution was also prepared to study the effect of adding high molecular weight component on freeze dried product quality.

Coffee is a complex, multi-component system and freeze dried coffee is a real product in manufacturing. Coffee solutions of concentrations up to 70% were used in crystallisation and freeze drying studies in this research.

Sucrose used in the experiments was purchased from local supermarket. Freeze dried coffee granules were obtained from a company. Both sucrose and coffee were stored in an air tight container to reduce exposure to the humidity from the atmosphere. All other chemicals used, i.e. CMC, maltose and gum arabic, were purchased from Sigma-Aldrich.

3.2 Sample preparation

3.2.1 Sucrose solutions

Sucrose solutions of 10, 20, 30, 40, 50, and 60% solids were prepared. Concentration here refers to mass fraction.

The required amount of sucrose was added into a beaker containing distilled water. The mixture was covered with parafilm to reduce vapour loss during dissolution and was mixed

under magnetic stirring (Stuart CB162 hotplate stirrer) at room temperature until the solution was clear.

3.2.2 Maltose solutions

Maltose solutions of 5, 10, 15, 20, 40, 60 and 70% solids were prepared.

The required amount of maltose was added into a beaker containing distilled water. The mixture was covered with parafilm to reduce vapour loss during dissolution and was mixed under magnetic stirring (Stuart CB162 hotplate stirrer) in room temperature until the solution was clear.

3.2.3 Sucrose and cmc (carboxymethyl cellulose) solutions

Two sucrose/CMC solution were prepared with a fixed amount of water content of 40% (w/w); one with 59% sucrose and 1% cmc and the other with 59.5% sucrose and 0.5% cmc. To prepare those solutions, sucrose was first dissolved into distilled water and the required amount of cmc was then added gradually into the system and was mixed at room temperature until fully dissolved.

3.2.4 Gum Arabic solution

Gum Arabic solutions of 50% and 60% solids were prepared.

Gum Arabic was added slowly into a glass jar with distilled water under vigorous stirring. The jar was covered and mixing was maintained until the carbohydrate was fully dissolved (this required 24-36 hours). Foam formed during dissolution was discarded.

3.2.5 Sucrose and gum Arabic solutions

Six sucrose/gum arabic solutions (with 10, 20, 30, 40, 50, and 60% total solids) were prepared with a fixed amount of gum arabic at 1% (w/w). To prepare those solutions,

sucrose was first dissolved into distilled water and the required amount of gum arabic was then added gradually into the system and was mixed at room temperature until fully dissolved.

3.2.6 Coffee

Coffee solutions with 30%, 50%, 60% and 70% solids were prepared. Freeze dried coffee granules were gradually added into a beaker with distilled water under vigorous overhead stirring (Radleys RS100 control plus). Continued mixing was needed until the coffee and water was well mixed. Freeze dried coffee granules were used to prepare solution as the solid concentration can be controlled.

3.3 Sample pre-treatment

This section explains sample pre-treatment before further studying of crystallisation and freeze drying.

3.3.1 Aeration

Aeration was conducted to study the effect of air bubbles on water crystallisation in different systems. The methods to aerate the samples are displayed as below.

Aeration of sucrose-cmc

The 59% sucrose+1% cmc solution was selected in the aeration study, for it is viscous enough to hold the air bubbles during freezing. In the case of 60% sucrose, air bubbles disappeared within 2min after aeration. A hand mixer (Andrew James HJ2105) was used to aerate the sample. 100g of the sucrose/CMC solution was poured into a beaker then mixed at mode 1 for 1 minute, until the volume of the solution increased from 80mL to 100mL. The volume was read from label of glass beaker. This process resulted in systems in which the air

bubbles could be clearly seen and were stable under the microscope until the crystallisation experiment was completed (see for example Figure 5-17).

Aeration of gum Arabic

Gum arabic solution of 50% concentration was aerated in the same way as sucrose-cmc system, and example images taken under the microscope before before/after aeration are displayed in Figure 5-20.

Aeration of coffee solution

Coffee samples were aerated such as to reach a target density. For the 50% systems the target density was approximately 70g/mL, whereas for the 60% coffee the target density was approximately 60%.

To reach the target density, 50% coffee was aerated by hand mixer (Andrew James HJ2105) at mode 1 for 30 seconds. 60% coffee was too viscous and hand mixer failed to aerate it, so a blender (Kenwood CH180A) was used instead. The blender was half filled with 60% coffee and operated at mode 1 for 1 minute to reach the desired density.

3.3.2 Freezing

Two different methods and equipment were used during freezing experiments and they are displayed as below.

Peltier stage

A peltier stage (Linkam, LTS 120) was used to provide accurate temperature control of the sample. The stage offered a different cooling rates ranging from 0.1°C /min to 30°C /min. A lowest working temperature of -24°C was achieved with the help of recirculating water from a refrigerated water bath (Grant). The stage allowed direct visualisation of its entire cooling surface (4cmX4cm square) by using a 4mm thick transparent cover. The cover served to

isolate the sample from the environment and reduce the interfering effects of moisture and temperature from the atmosphere on the freezing sample.

Rapid freezer

A CO_2 Eliminator low temperature rapid freezer (Bright Clini-RF) was used to freeze the sample prior to freeze-drying. The lowest temperature that the rapid freezer can reach is -80°C. Temperature-time profile of the sample can be recorded during freezing via data logger (Pico Technology, TC-08) and thermocouples (Omega).

3.4 Freeze drying

3.4.1 Freeze drier

A VirTis adVantage freeze drier was used for freeze drying. Freeze drying cycles can be set up through Wizard 2.0 data centre. Shelf temperature, chamber temperature/pressure, and duration of each freeze drying stage can be programmed before running the freeze drying cycle. Measurements of the sample temperature were carried out through thermocouples and built-in data logger. Temperature-time profile can be exported into excel spreadsheet through wizard 2 software.

3.4.2 Container used during freeze drying

Freeze drying sucrose experiments (see chapter 6) were carried out in freeze drying glass vials (SCHOTT, VCDIN10R), which has an inner diameter of 24mm and a volume of 10mL. This type of glass vials was widely used in freeze drying studies and they allow direct observation of the sample during and after freeze drying.

Freeze drying coffee experiments (chapter 5) were carried out in cake tins (purchased from local supermarket). The cake tins are made of metal and the inner diameter is 8.5 cm. Cake

tins were used due to their good heat conductivity and similarity of the metallic freezing tray used in manufacturing.

3.4.3 Freeze drying cycles

There are three steps in freeze drying: freezing, primary drying and secondary drying. Freezing was carried out in the rapid freezer. Freeze drier was not preferred for freezing step, because the chamber door was sealed thus it was impossible to have any treatment or direct observation on the sample. And two other steps, primary drying (ice crystal sublimation) and secondary drying (bound water desorption) were carried out in the freeze drier.

Before transferring the frozen sample from freezer to freeze drier, the freeze drier shelf was pre-cooled below -40˚C to reduce the chance of ice melting in the sample before freeze-drying commenced. After sample was transferred into the freeze drier, the door of the chamber was sealed and a pre-programmed freeze drying cycle was started.

Different cycles were operated during the work (shown in table 3-1), and the difference was mainly in primary drying. The effect of primary drying temperature on the quality of the dried product was studied by drying at -20°C and at -40 ˚C. Primary drying time was set at 12 hours. After primary drying, the shelf was heated up to 20˚C for secondary drying. Three heating rates were used: a fast (set at the fastest rate that the shelf can reach, >100 ˚C/hour), a medium rate (10 ˚C/hour) and a slow rate (2 ˚C/hour). After the shelf reached 20 ˚C, it remained at that temperature for six hours during secondary drying. During the two drying steps, the pressure kept constant at 100 µbar, below the water vapour pressure at these temperatures.

Table 3-1 Freeze drying processes

	Freezing (rapid freezer)	Primary drying	Heating rate between primary and secondary drying	Secondary drying
	1 atm, 6 hours	100 µbar, 12 hour	100 µbar	100 µbar, 6 hours
Cycle i	-40 ˚C	-40 ˚C	180 ˚C /hour	20 ˚C
Cycle ii		-20 ˚C	180 ˚C/hour	
Cycle iii		-40 ˚C	10˚C/hour	
Cycle iv		-40 ˚C	5˚C/hour	

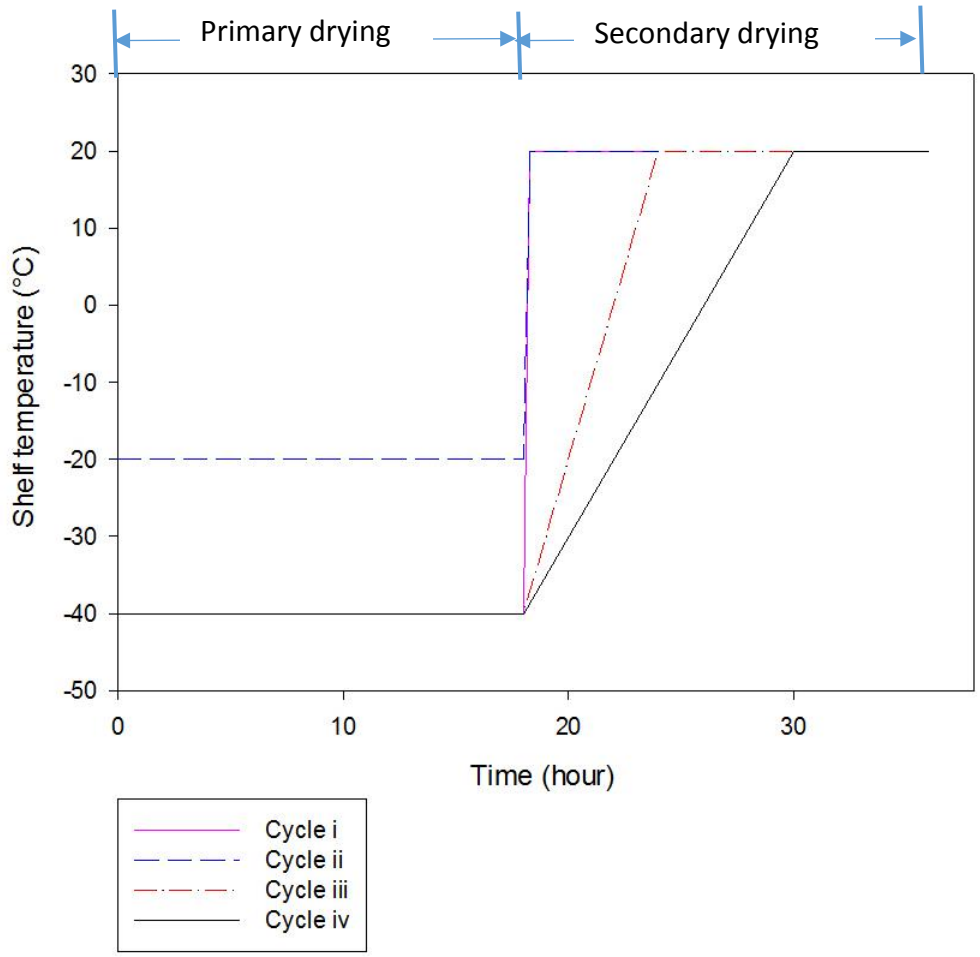

Figure 3-1 Temperature profile of the four freeze drying cycles used in this work

3.4.4 Freeze dried sample characterisation

Moisture content

Moisture content of the freeze-dried samples was estimated using two methods:

Method i

Freeze-dried samples were placed in an oven (60°C) until the weight of the sample (measured in a balance) was constant.

Each sample was weighed after freeze drying (m_{after}) and after oven drying (m_{final}). The final mass of the sample after oven drying was regarded as the solid amount of the sample. The

moisture amount in the sample was calculated from the difference between mass of the freeze dried sample and mass of the sample after oven drying.

$$m_{solid} = m_{final} \tag{3-1}$$

$$m_{water} = m_{after} - m_{final} \tag{3-2}$$

$$moisture \cdot content = \frac{m_{water}}{m_{after}} \tag{3-3}$$

This method proved very useful in characterising moisture content in freeze dried gum Arabic samples. However, the high temperature during oven drying might overheat the sucrose. In some cases, the weight of sample after oven drying was less than its initial solids amount. Thus the oven method was only used to measure moisture content in freeze dried gum Arabic.

Method ii

The residual moisture content in freeze dried sucrose was measured as following:

Each sample was weighed before (m_{before}) and after (m_{after}) freeze drying. The solids amount in the sample was calculated from concentration and weight of the sample before freeze drying:

$$m_{solids} = m_{before} \times c\% \times (1 - 0.5\%) \tag{3-4}$$

where m_{solids} is solids mass in the sample

m_{before} is the total sample mass before freeze drying

$c\%$ is sample concentration before freeze drying, and 0.5% moisture accounted for the original moisture in sucrose (measured by method i).

The amount of solids was considered to be constant during freezing and freeze drying, thus, amount of residual water in dried sample can be calculate from:

$$m_{water} = m_{after} - m_{solids} \quad (3\text{-}5)$$

m_{water} is mass of residual water

m_{after} is the sample mass after freeze drying

Moisture content can be calculated as

$$moisture \cdot content = \frac{m_{water}}{m_{after}} \quad (3\text{-}6)$$

Volume and density

The relation between liquid volume and sample height in the freeze drying vial were calibrated by filling accurate amount of distilled water (from 1 to 12mL) into vial by automatic pipette (Eppendorf). The sample volume is plotted as a function of sample height in Figure 3-2.

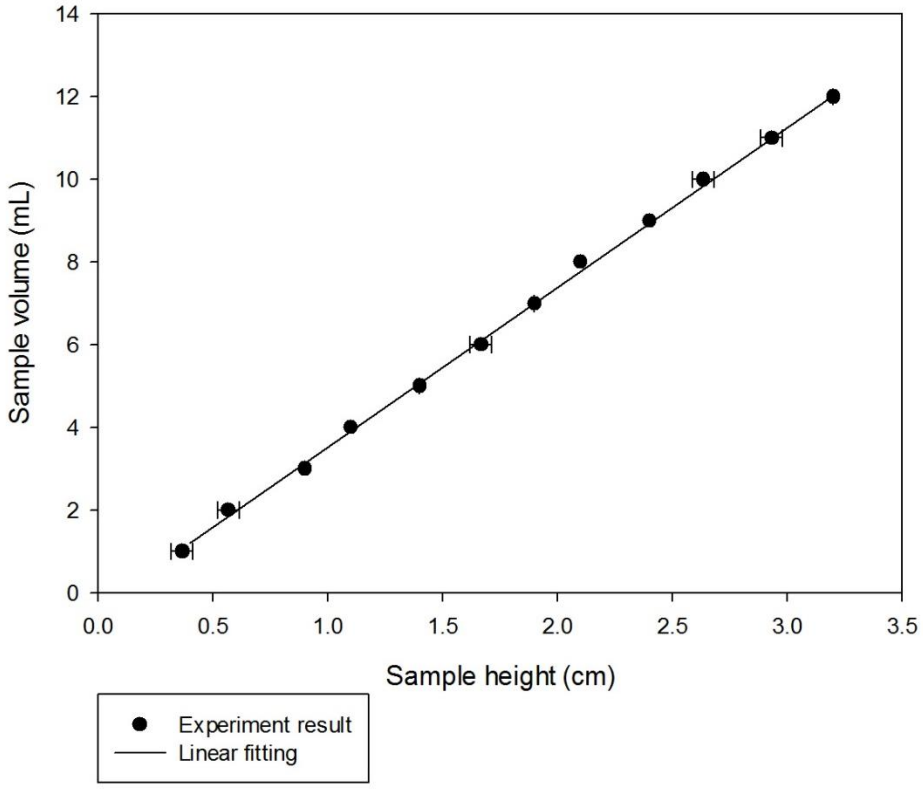

Figure 3-2 Sample volume in the vial as a function of sample height. Measurements were triplicated, and error bars represent one standard deviation of uncertainty.

A linear fitting was shown between volume and height:

$$V = 3.8909h - 0.3631, R^2 = 0.999 \quad (3\text{-}7)$$

where V is volume of freeze dried sample, and

h is height of freeze dried sample.

Equation 3-7 should go through the origin, but for the purpose of this work, this equation is only used within the range of values that were determined experimentally.

After freeze drying, the height of the sample in the vial was measured. So the volume and density of freeze dried sample can be determined:

$$\rho = \frac{m_{after}}{V} \tag{3-8}$$

m_{after} is weight of freeze dried sample.

The desktop SEM

Morphology of freeze dried samples was examined using a desktop SEM (Hitachi TM3030). Samples were cut into small cubes (1mm^3) and were subsequently glued to the SEM sample stand, with fracture plane exposed on top. The sample was then transferred into the SEM chamber and the chamber was vacuumed. Visualisation was accomplished using 15kV voltage electronic beams.

Dissolution

A dissolution rig was used to test the dissolution kinetics of freeze dried coffee samples, by measuring the conductivity value change as the sample was dissolving in water. The rig (shown in figure 3-3) combined a water bath (to control dissolution temperature), a glass vessel (where dissolution took place) and a conductivity probe connected to a computer (to measure and record the conductivity in real time).

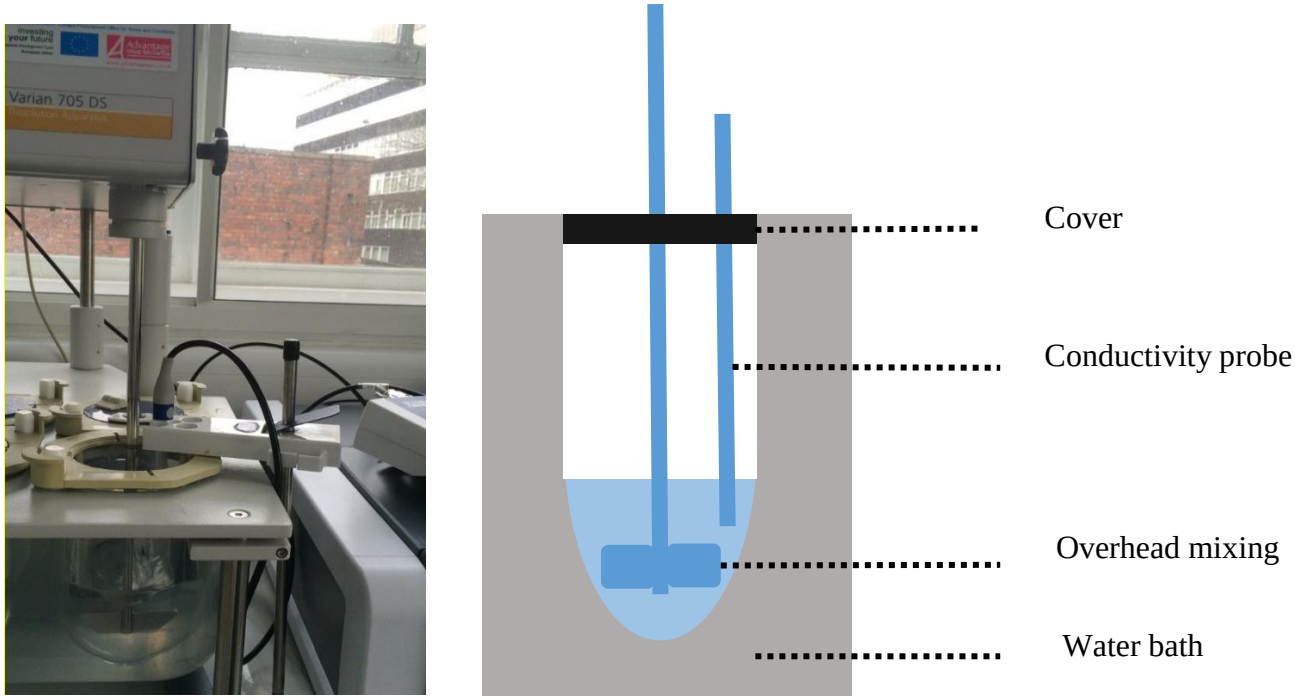

Figure 3-3 Experimental apparatus: (a) photograph (b) schematic diagram

During the experiments, 400mL distilled water was added into the glass vessel, and water was heated up by the water bath to the set temperature. After the water temperature was stable, overhead mixing was maintained at 250rpm to mix the water vigorously, and 8g sample was added into the water. Conductivity was recorded from before addition of the sample into the water until it reached a constant, maximum value.

Two water bath temperatures were used in the experiments, 40 ˚C and 55 ˚C (highest working temperature of the water bath).

3.5 Methods to characterise crystallisation

3.5.1 Differential Scanning Calorimetry (DSC)

DSC was used to study the thermal behaviour of sucrose, maltose and coffee solutions during crystallisation over a range of concentrations (10-70% solids). Two DSC instruments

have been used in the study: one is Perkin Elmer DSC 7, and the other one is Mettler Toledo DSC 2. Around 5mg (20mg in the case of Mettler Toledo DSC 2) of the investigated solution was weighed (the exact weight was recorded) and sealed into a 40μL aluminium pan, then placed into the DSC. A sealed empty pan was used as reference. Various temperature cycles were used in DSC study; they will be mentioned in the result and discussion (chapters 5 and 6 for the sucrose/maltose and coffee samples, respectively).

3.5.2 cryo-X-Ray Diffraction (cryo-XRD)

Cryo-XRD was used to characterise the crystals during water crystallisation in concentrated sucrose/coffee solutions. Approximately 0.01mL of the investigated system was injected by syringe and needle into a 1mm diameter borosilicate glass capillary tube (Capillary Tube Supplies Ltd). The capillary was fixed on sample stand vertically by blue tack, centred by goniometer with great care and then transferred into the powder diffractometer (Siemens D5000) equipped with an Oxford low temperature cryostream.

Scanning angle was set to 20-50^{o} in all experiments (except when otherwise stated) to cover the identical peaks for ice crystals. Three different cooling/heating rates, ranging from 0.1^{o}C/min to 6^{o}C/min, were used in the XRD experiments to study the effect of thermal treatment (cooling rate) on water crystallisation, as discussed below.

Fast rate 6˚C/min

Cooling rate of 6˚C/min is the fastest cooling rate that the D5000 diffractometer with cryostream can reach. It was used in experiments with sucrose (20%, 50% and 70%) and coffee (50 % and 70%). The scanning temperatures were selected based on phase transition temperature of the sample according to previous DSC studies and the literature.

For 20% sucrose, the sample was cooled from room temperature to -50˚C then heated back to room temperature at a constant rate of 6˚C/min. Scans were carried out at -30 ˚C / -40 ˚C / -50˚C during cooling and heating.

Similar experiments were carried out for 50% sucrose. The system was cooled to a lower temperature of -70˚C to match with the DSC experiments. Scans were obtained at -35 ˚C /-50 ˚C /-70˚C during cooling.

For 70% sucrose, there showed no crystallisation peak in DSC when the cooling was carried out at 6 ˚C/min to -100 ˚C. Scans were obtained during heating at -80 ˚C /-60 ˚C /-35 ˚C /-30˚C.

Coffee samples were cooled to -100˚C, then heated to room temperature at 6˚C/min. 50% coffee was scanned at -100˚C/-80 ˚C /-60 ˚C /-40 ˚C /-30 ˚C during heating, while 70% coffee was scanned at -100 ˚C /-55 ˚C /-50 ˚C /-40 ˚C /-35 ˚C /-30 ˚C /-20 ˚C during heating.

Medium rate 1˚C/min

The sample (60% sucrose) was cooled from room temperature to -70°C and then reheated to 20°C at a constant rate of 1°C/min, matching the DSC experimental conditions. Three identical experiments were conducted and in each one the sample was scanned (scanning angle 2θ of 20-50°) at different temperatures (-20°C, -30°C, -40°C, respectively) during the cooling and heating processes, and also at -70°C.

Slow rate 0.5˚C/min (small angle scaning)

A heating rate of 0.5°C/min was used in one XRD experiment for 70% coffee as the slowest heating rate. The details of this experiment displayed with the result and discussion in section 5.1.2.

3.5.3 Cryo-Environment Scanning Electron Microscope (ESEM)

SEM is a widely used technique for sample microstructure characterisation. However it cannot be used to examine samples containing water/ice because of possible damage from water evaporating at such low pressure (10^4 Pa) in the SEM chamber (Ong, Dagastine *et al*. 2011). Etching, removing ice on the surface of sample by sublimation at higher temperature (e.g.-95°C), is usually conducted during sample preparation for SEM (Hindmarsh, Russell *et al*. 2007, Ong, Dagastine *et al*. 2011). Metal coating (e.g. gold) is then applied to improve the contrast and resolution of microscopic image (Ong, Dagastine *et al*. 2011). Then the pores created by ice sublimation is regarded the same size of the ice crystals formed in frozen sample (Flores and Goff 1999, Hindmarsh, Russell *et al*. 2007, Mousavi, Miri *et al*. 2007). This is a way of studying ice crystals indirectly. However, in this work, efforts have been made to visualise ice crystals directly to minimise the structure change during ice sublimation.

Images were obtained via ESEM, a slightly different technique, which provides a way to observe highly hydrated samples. Cryo ESEM (Philips XL30 ESEM-FEG) was used to observe ice crystals in frozen sample. Frozen sucrose and coffee samples were prepared and kept frozen in the lab for one day before the SEM experiment. Then the sample was placed into an insulated bag (Sofribag) which was filled with dry ice and transferred to the electronic microscope lab. Due to the good insulation and cold temperature provided by dry ice sublimation, melting of sample was not observed during the transfer.

Sample preparation for SEM study was done with great care, and the time that samples were exposed to the environment was minimised to have less ice crystals melting in the

sample. Before sample preparation, all the tools (including hammer, blade, and tweezer) were immersed into liquid nitrogen to maintain low temperature.

A frozen sample was taken out from insulated bag and smashed by the hammer to break into small pieces. Small cubes of smashed sample (1mm^3 in volume approximately) were immediately immersed into liquid nitrogen. During the crushing, fracture planes were created in each sample. One cubic sample was selected and glued onto the SEM stud, with the fracture plane on the top. It was then transferred into SEM chamber.

Operating temperature of the chamber was lower than -170^{o}C, but before sample examination, it was increased to -95^{o}C and held for 5 minutes to etch the sample, in order to remove the frosted ice. The selection of etching time and temperature was based on experience and trial-and-error, to remove most of the frost formed on the surface during crushing and gluing of the sample to the SEM stud, without losing all the ice crystals formed during freezing.

The sample was then examined by SEM at -170^{o}C with 3kV electron beam. The small voltage, relative to other SEM studies, of the electron beams was chosen to reduce overheating the sample and prevent sample being charged. This process allowed acquisition of at least 20 clear images at different magnifications before evident sample charging was observed.

In one experiment of 50% frozen coffee sample (see section 5.1.3.2), further etching was carried out at -70^{o}C for 30 minutes. The sample was then sputter coated with gold to have a better conductivity and then studied under electronic microscope again. Using extended etching, all the ice crystals in the sample were sublimated and it was therefore possible to see the structure of sample without ice crystals.

3.6 Crystallisation with nucleus addition

Crystallisation was further studied under induced water crystallisation conditions by adding ice nuclei in the freezing system. Experiments were conducted in two scales. At small scale (0.1mL droplets), experiments were conducted under a microscope for in-situ crystallisation observations At bigger scale (2mL sample) the samples were left to crystallise at different temperatures and the final freeze-dried system was examined.

3.6.1 Drop scale

The small scale experiments of induced crystallisation were carried out in sucrose, gum Arabic and coffee systems. Experimental setup and data analysis details are as below.

3.6.1.1 Method

An optical method was developed to study crystal growth kinetics of induced crystallisation under a microscope. The apparatus, shown in Figure 3-4, combined a temperature control stage with an optical microscope and camera, to visualise changes in the sample during crystallisation. A Peltier stage (Linkam, LTS 120) was used to provide accurate temperature control. A Leica optical microscope provided detail look at the sample, and a camera was connected with the microscope to record images during experiments at 1 frame per second.

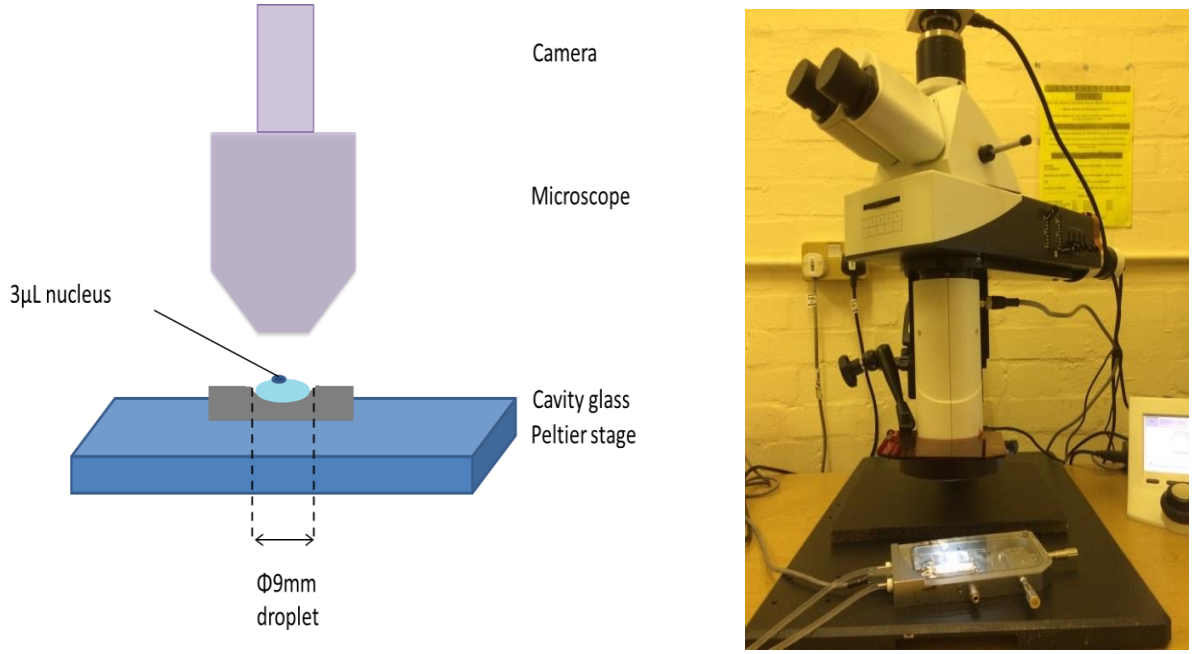

Figure 3-4 Experimental apparatus (a) schematic diagram (b) photograph

Experiments were designed to study growth rates of ice crystals in concentrated systems at different degrees of supercooling, where nucleation was not spontaneous, by adding already formed ice nuclei into supercooled solutions.

One droplet (0.1 mL) of the concentrated sample was placed on a cavity glass slide (with a diameter of 9mm) and onto the peltier stage. The droplet filled the cavity on the glass slide, the surface thus having minimal curvature compared to the case if the drop had been placed on a flat slide, thus enhancing image quality. Droplet volume was chosen by trial-and-error to give optimal quality images. Larger drops resulted in blurred, out-of-focus images due to increased drop curvature or even overfilling glass cave, while smaller drops were too small for measuring crystal growth. A small droplet (3µL) of the nucleating solution was placed next to the glass slide onto the cooling stage (the size of the nuclei was chosen for convenience, see section 3.6.1.3). The peltier chamber was then closed with the cover,

and the stage cooled at 1°C/min to a set temperature to produce the required supercooling. Cooling rate was set at 1°C/min to match with previous DSC and XRD experiments. When the temperature reached the chosen set value, the nucleating droplet was frozen into the ice granule, forming the nucleus, while the mother solution was in the form of a supercooled liquid. The nucleus was then added into the centre of the supercooled droplet using tweezers, and crystal growth was recorded (1fps) using the camera and software (μ-manager). Recorded images were subsequently analysed (see section 3.6.1.2) to obtain crystal growth rates (mm min-1).

Sucrose (40, 50 and 60%), and gum Arabic (50, 60%), and sucrose/cmc (0.5 and 1% cmc) solutions were used as systems in which crystallisation took place. Cmc is a thickener and was added to study the effect of viscosity on crystal growth kinetics. Ice nuclei were formed either from a 10% sucrose solution (for experiments with sucrose) or from distilled water (for experiments with gum arabic).

3.6.1.2 Data processing

A typical microscope image is shown in fig 3-5. The light area in the centre represents the crystallised region, which grows with time. The darker area that surrounds the crystal is the supercooled liquid, and it gets smaller with time as the crystal grows. The bright circle is the reflection of the microscope's lighting and was ignored in image processing.

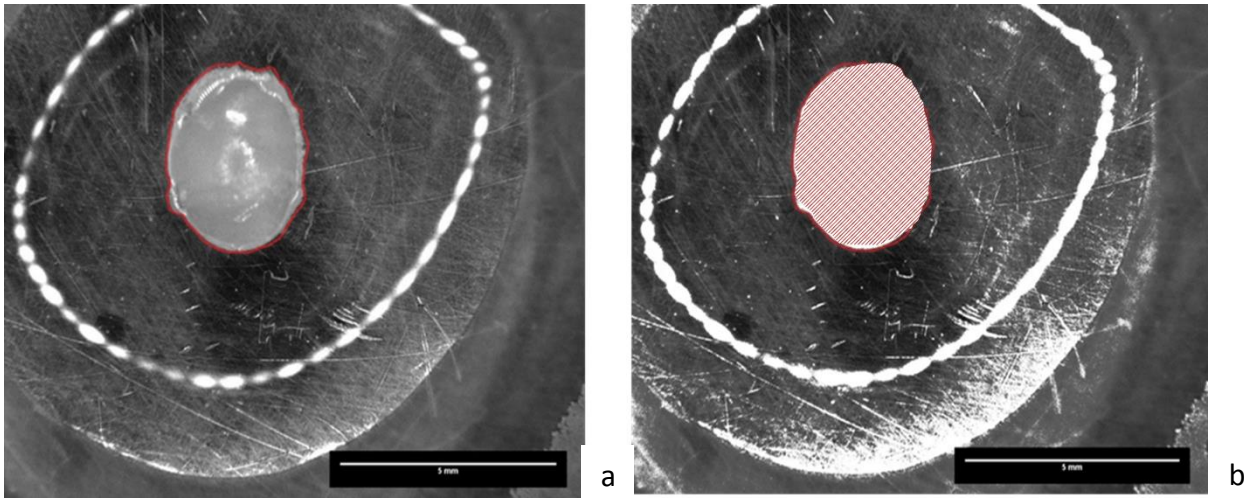

Figure 3-5 Example of image processing (scale bar 5 mm); (a) image of ice crystal with its edge enclosed, (b) same crystal with its area highlighted.

To estimate crystal growth rate, the boundary of the light region was identified and drawn (digitally, through the software Image J) circling the solid part (fig. 3-5 a). The area S of the solid part was then measured (Image J, fig. 3-5 b) and plotted as a function of time in (Fig. 3-6 a). The area S was used to calculate the radius r of an area-equivalent circle using:

$$r = \sqrt{\frac{S}{\pi}} \tag{3-9}$$

The radius was plotted as a function of time (see Fig. 3-6 b) and growth rate was determined as the slope of a linear fitting of the resulting plot. Estimated growth rates were compared between different systems and conditions.

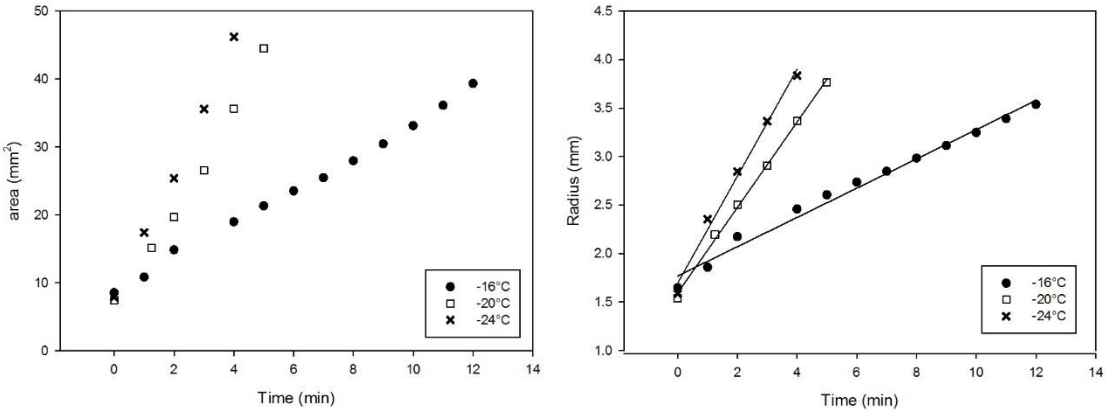

a b

Figure 3-6 Representative example of growth rate calculation (a) area of crystallised region as a function of time; (b) radius of the equivalent area, calculated from equation (3-9); Both are plotted as a function of time.

3.6.1.3 Effect of nucleus size on crystal growth kinetics

Preliminary experiments were conducted to test the effect of nucleus size on ice crystal growth rate. Three different nucleus volumes were tested (1, 3, and 5µL) and results for the 60% sucrose solution crystallising at -20°C are showed in Fig 3-7. Results showed marginal effect on crystal growth kinetics. In the following experiments, a seed size of 3 µL was used because the smaller seed (1µL) was difficult to transfer into the liquid and the bigger one (5µL) had large initial size compared to the droplet.

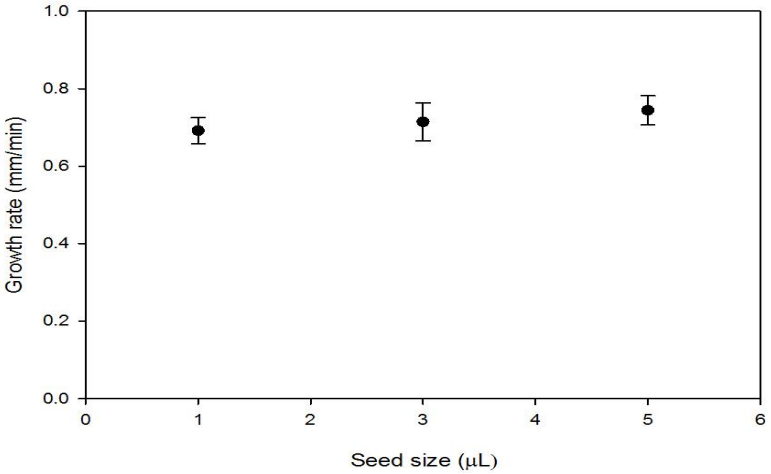

Figure 3-7 Effect of seed size on growth rate for 60% sucrose at -20°C. Experiments were triplicated, and error bar represents ± one standard deviation.

3.6.2 Larger scale

A method was further developed to study the effect of crystallisation kinetics on the microstructure of the freeze-dried systems. 50, 60% coffee samples were used in these experiments.

3.6.2.1 Method

Figure 3-8 Photograph of experiment apparatus of crystallisation with nuclei addition in larger scale

Figure 3-8 shows the experimental setup of the large scale experiments. A 2mL plastic tube was cut from a syringe tube and the bottom was covered with parafilm to use as sample container in this experiment. Parafilm was selected to seal the container because it prevented sample leaking, and the thin layer made good conduct with the cooling surface. Peltier stage was used here to control the sample temperature.

Ice nuclei were made in the rapid freezer by pipetting 5μL droplets of distilled water onto the cold surface. These served as ice nuclei once they were fully frozen.

A 2 mL sample was placed into the container, covered with plastic insulator and cooled to -5^{o}C at 1^{o}C/min on the Peltier stage. When the sample reached the -5^{o}C, 6 ice nuclei were added into the coffee and slightly mixed. In this experiment, ice nuclei addition accounts for 1.5w/w % of the total sample mass.

-5^{o}C was selected as the temperature to add nuclei because at this temperature the ice nuclei did not melt in the sample, while the 60% coffee did not nucleate spontaneously. The mixture was then covered with insulator and cooled down to the set temperature.

The sample was held at the crystallisation temperature for 30 minutes to allow crystal growth before it was transferred into rapid freezer for 6 hours extra solidification. Samples were then freeze dried and further examined as described in section 3.6.3.2. The freeze drying cycle used in this set of experiments was as following: The samples went through primary drying at -40 ^{o}C for 12 hours and secondary drying at 20 ^{o}C for 6 hours. The chamber pressure was constant at 100µbar during drying steps.

Aerated coffee samples with 50% and 60% concentration were used in these experiments (preparation of sample see section 3.2.5 and 3.3.1).

3.6.3.2 Sample characterisation

Freeze dried samples are examined by dissolution test and desktop SEM as mentioned before in section 3.4.4.

3.7 Conclusions

Materials and methods used in this research has been introduced in this chapter. The following chapters, Chapter 4, 5, and 6 will display the results and discussions about the work carried out using these materials and methods.

Chapter 4 Water crystallisation from high concentration sugar solution

The main aim of the study is to understand and modify freezing and freeze drying processes to enable the manufacturing of freeze-dried product from initially highly concentrated solutions. First step of freeze drying, freezing process is studied in this chapter to investigate water crystallisation from highly concentrated carbohydrate solutions. Maximum amount of ice crystals formation is ideal for a subsequent successful freeze drying process.

Methods were applied and developed to study phase transitions (especially water crystallisation) during freezing high concentration sugar solutions, and the methods will be also applied in the further studies in the following chapter, to investigate more complex systems.

This chapter investigated:

The factors (both formulation and processing conditions) that affect water crystallisation;

The difficulties in water crystallisation in high concentration system and the highest concentration at which water crystallisation could take place;

Method to induce water crystallisation and crystal growth rate in induced crystallisation.

This chapter uses carbohydrate solutions as investigated material, studies the two types of crystallisations: spontaneous and induced crystallisation.

4.1 Spontaneous crystallisation

This section starts from the study of spontaneous crystallisation. Techniques of DSC, XRD and SEM were involved. Effect of concentration, cooling rate, annealing on spontaneous crystallisation were investigated.

Experiments were first carried out in DSC, measuring phase transition temperatures and enthalpy change. Effect of concentration, cooling rate, annealing, and solute were studied.

Then XRD and DSC were used together to study water crystallisation under same thermal conditions to compare the results, to see if those two methods work or not.

Efforts were also made to visualise ice crystals directly in frozen 30% sucrose solutions using cryo-ESEM.

4.1.1 Enthalpy measurement using DSC

4.1.1.1 Effect of concentration

DSC measurements have been carried out for 20, 30, 40, 50 and 60% sucrose solutions. Samples were tested by cooling from 20°C to -70°C and then heating up to 20°C at a constant rate of 1°C/min. Cooling curves are shown in Figure 4-1.

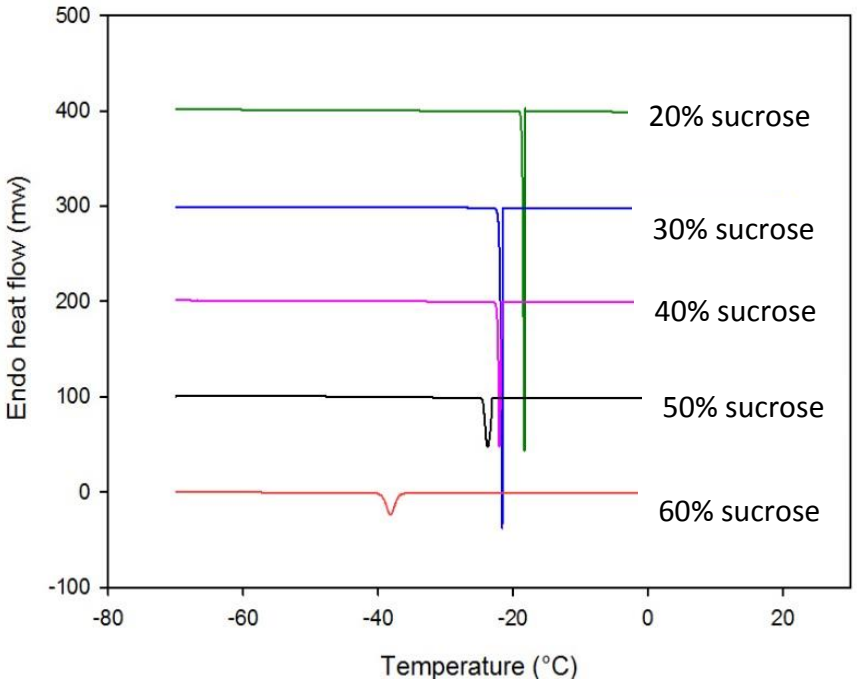

Figure 4-1 Differential scanning calorimetry thermograms of sucrose solutions (20, 30, 40, 50, 60% solids) with a cooling rate of 1°C/min to -70°C. Experiments were triplicated, and only one plot for each concentration is shown here.

All samples showed an exothermal peak during cooling, which corresponds to the water crystallisation. As sucrose concentration increased from 20 to 50%, the onset temperature of crystallisation declined gradually from -19°C to -25°C. Further increase to 60% concentration resulted in a sharp decrease in crystallisation temperature to -37°C. The observed crystallisation temperatures are much lower than the equilibrium freezing temperature, which is reported to be at -11°C for 60% sucrose (Roos 1995).

A system is supercooled when it is cooled to below equilibrium freezing temperature, in which state water molecules may cluster into ordered structures, but the clusters may not be stable enough to induce crystallisation in the whole system and they melt (Ayel, Lottin *et al*. 2006). The required supercooling for stable nuclei formation, the difference between nucleation and equilibrium freezing temperatures, increases as concentration increases (26°C difference for the 60% solids system), which is possibly due to the increase in viscosity (Roos 1997, Goff, Verespej *et al*. 2003, Ayel, Lottin *et al*. 2006).

At increasing solid content, the area under the crystallisation peak also decreased. By integrating the ice crystallisation peak per sample mass, the enthalpy change (ΔH) can be calculated, and this gives information about how much water turns into ice during freezing. Assuming the latent heat of freezing does not change, the fraction of ice formation in each sample can be calculated (Levine and Slade 1986):

$$Ice \cdot fraction = \frac{\Delta H}{\Delta H_w} \qquad (4\text{-}1)$$

Where ΔH (J/g) is the enthalpy change of water crystallisation of each sample, estimated from the DSC curve and ΔH_w (J/g) is the latent heat of freezing pure water into ice (334 J/g) (Roos and Karel 1991). Calculated values of crystallisation enthalpy and ice fraction from 20

to 60% sucrose are displayed in table 1 and plotted in fig. 4-2 as a function of solid concentration, together with the data expected if all the water solidified. (i.e. ΔH_{ideal}=(1-solid fraction)×ΔH_w).

Concentration (%)	ΔH (J/g)	Ice fraction (%)	Unfrozen water (%)	$T_{crystallisation}$(°C)
20	-253.8±1.1	76.5	3.5	-19.2±0.9
30	-200.4±0.7	60.2	9.8	-19.9±1.1
40	-155.2±4.8	45.5	14.5	-21.7±0.8
50	-111.2±0.9	33.6	16.4	-24.7±1.6
60	-74.9±2.2	22.0	18	-36.9±0.1

Table 4-1 details of crystallisation peak during cooling 20 to 60% sucrose solutions

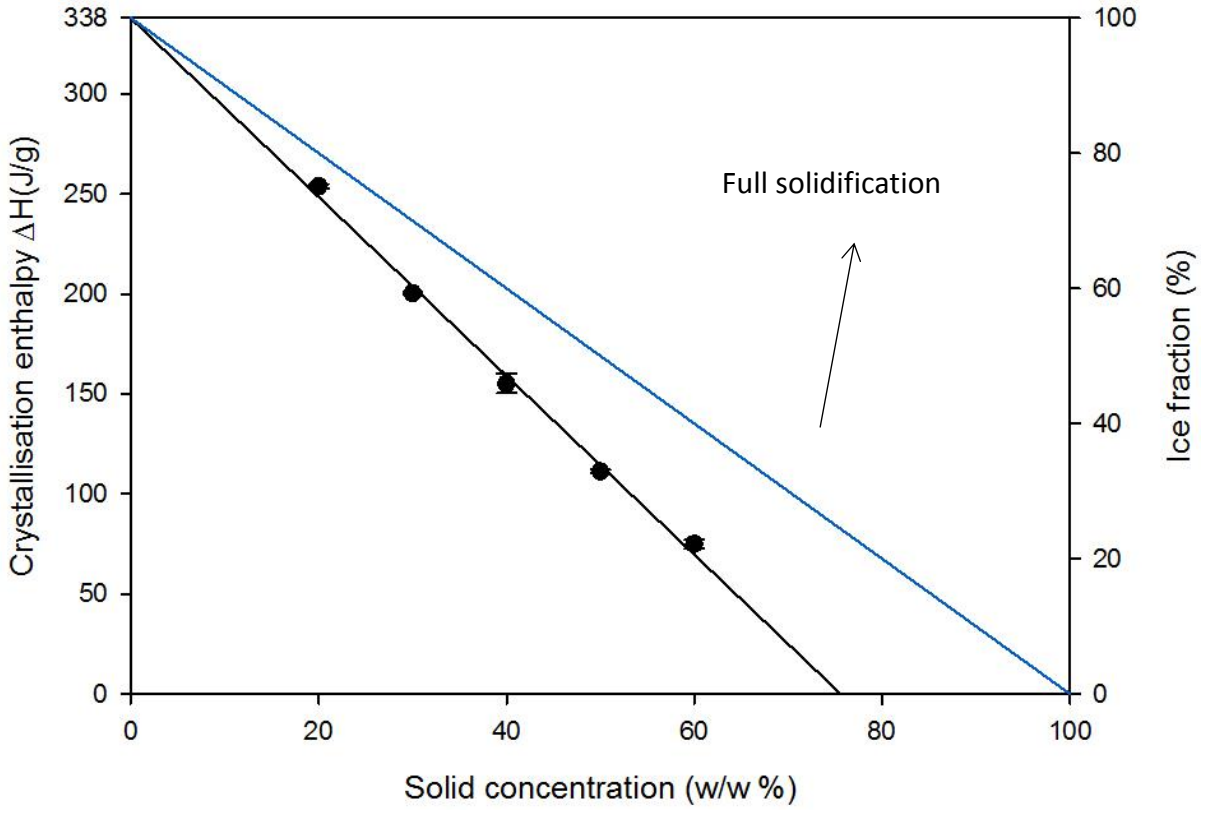

Figure 4-2 Absolute value of enthalpy change of water crystallisation at different sucrose concentration (dots: experimental data; line: linear fitting). Experiments were triplicated and error bars (represent ± one standard deviation of uncertainty) are not distinct as they are smaller than the size of the dots. The figure includes the ideal crystallisation line, i.e. at 60% solids, full crystallisation would give 40% ice. The actual values are less than this, showing that full amount of water crystallisation is not achieved.

When the concentration of the system increased from 20% to 60%, the enthalpy change decreased about 70%, from over 250 (J/g solution) to 74 (J/g solution), indicating reduced amount of ice formation from 76% of the total system to 22%. Meanwhile the unfrozen water in the system increased from 3.5% to 18%. The decrease in the calculated enthalpy change at increasing content fits well to the linear model (Roos and Karel 1991, Schawe 2006):

$$\Delta H = A - Bw_s \qquad (4\text{-}2)$$

Where ΔH (J/g) is the enthalpy change during crystallisation; w_s (wt. %) is sugar concentration;

As water continues to crystallise in the sample, the remaining solution becomes gradually more concentrated in sucrose until it reaches a maximum concentration above which no further crystallisation is possible. This critical concentration can be estimated by linear extrapolation of equation 4.2 to ΔH=0 J/g (Roos and Karel 1991, Furuki 2002, Schawe 2006).

Fitting the data of Table 4-1 into Equation 4.2 gives A=338 J/g, and B=4.5J/g and maximum concentration of solid at 76%. This is in agreement with values reported in the literature (Roos and Karel 1991, Furuki 2002, Schawe 2006), ranging between 69% and 78% (Furuki 2002, Schawe 2006). It should be noted that the exact number highly depends on selection of cooling rate and determination of the peak's baseline.

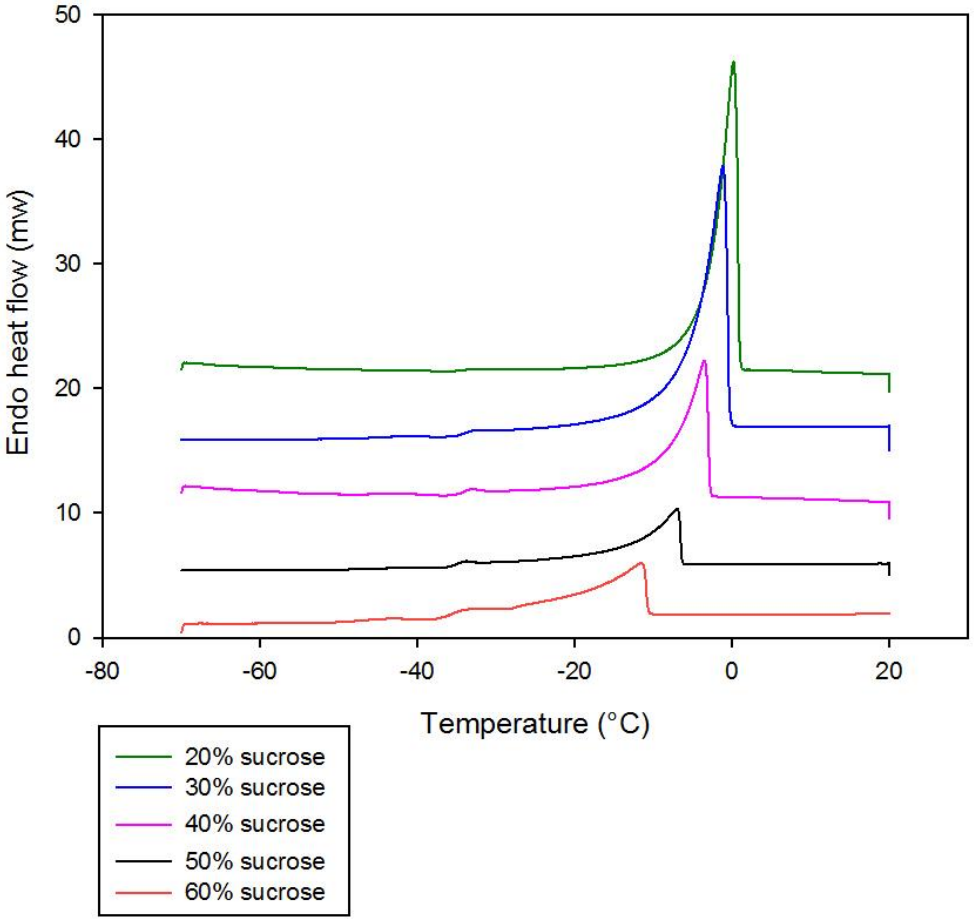

Figure 4-3 Differential scanning calorimetry thermogram of sucrose solutions (20, 30, 40, 50, 60% solids) with a heating rate of 1°C/min to 20°C. Experiments were triplicated, and only one plot for each concentration is shown here.

After cooling, samples were heated to 20°C at 1°C/min, and heating curves of the 20, 30, 40, 50 and 60% sucrose are displayed in Fig. 4-3. Endothermic peaks can be seen in each curve, corresponding to ice crystal melting during heating. As solid concentration increases from 20% to 60%, the onset of melting temperature decreases from -3.4 to -20.6 °C. The onset of melting temperatures is estimated by the software of the DSC, using the intersection point of the baseline before transition and the inflectional tangent. The melting temperature in

each sample is always higher than crystallisation temperature as supercooling is needed during crystallisation but not during melting.

The enthalpy change also decreases from 246 J/g to 75 J/g when concentration increases, matching well with the enthalpy change during freezing. The energy needed for ice to melt is the same amount of energy that water releases during crystallisation.

4.1.1.2 Effect of cooling rate

This section displays the work about the effect of cooling rate on water crystallisation in three sucrose solutions with different concentrations (20, 40 and 60%).

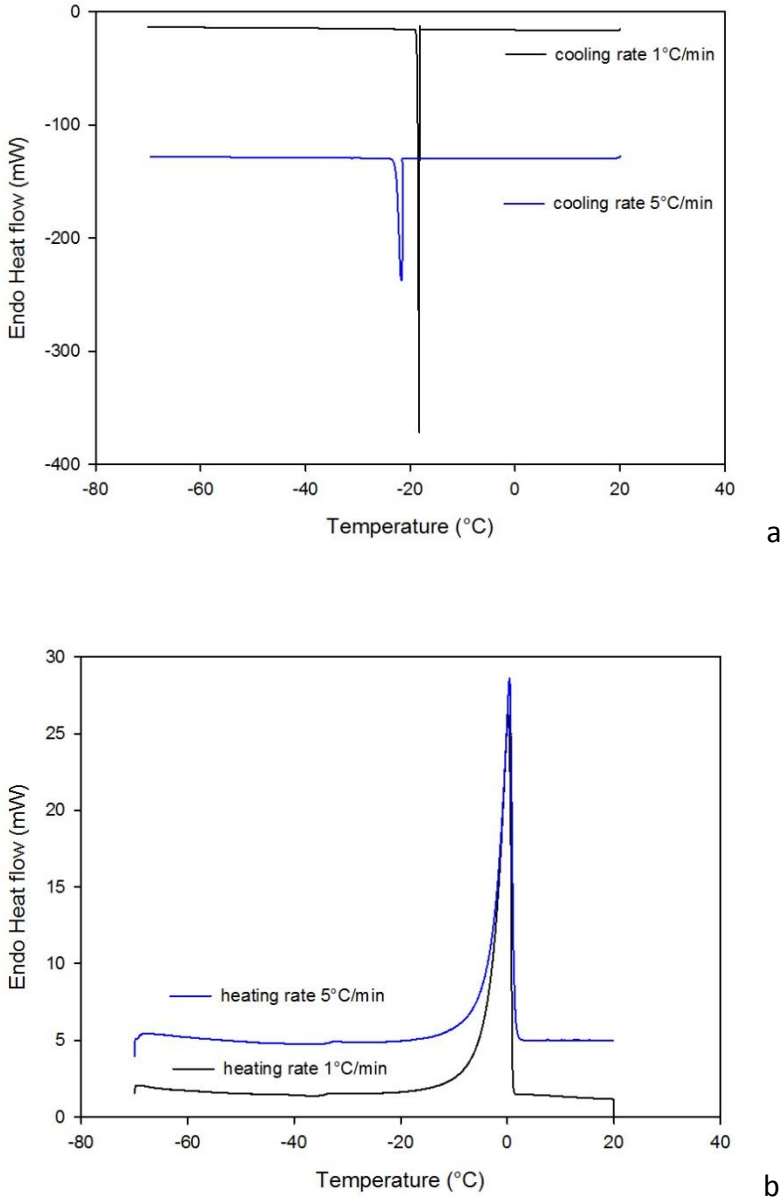

Figure 4-4 different scanning calorimetry scans of 20% sucrose at 1 and 5°C/min, (a): cooling from 20 °C to -70°C; (b): following heating from -70°C to 20°C.

Fig. 4-4 display the cooling (a) and heating (b) curves of 20% sucrose solutions scanned at 1˚C/min and 5˚C/min. Exothermal crystallisation peaks occurred during cooling at each both cooling rates, however the higher cooling rate resulted in both a lower onset crystallisation temperature and a wider peak. A shift from –19°C to -21°C in the onset crystallisation

temperature can be noticed when the cooling rate increased from 1°C/min to 5°C/min. Similar trend of crystallisation temperature shift towards lower temperatures and widening of the crystallisation peak has been reported on increasing of the temperature rate in high concentration system via DSC study (Thanatuksorn, Kajiwara *et al*. 2008). DSC detects phase transitions by recording heat flow change when the sample and the reference are kept at the same temperature during a constant temperature ramping. Water crystallisation is observed as an exothermic peak in a DSC scan, and a higher scanning rate might lead to a broader freezing peak due to damping of heat transfer (Marcolli, Gedamke *et al*. 2007).

DSC results of 40% and 60% sucrose at different cooling rate were displayed in Figure 4-5.

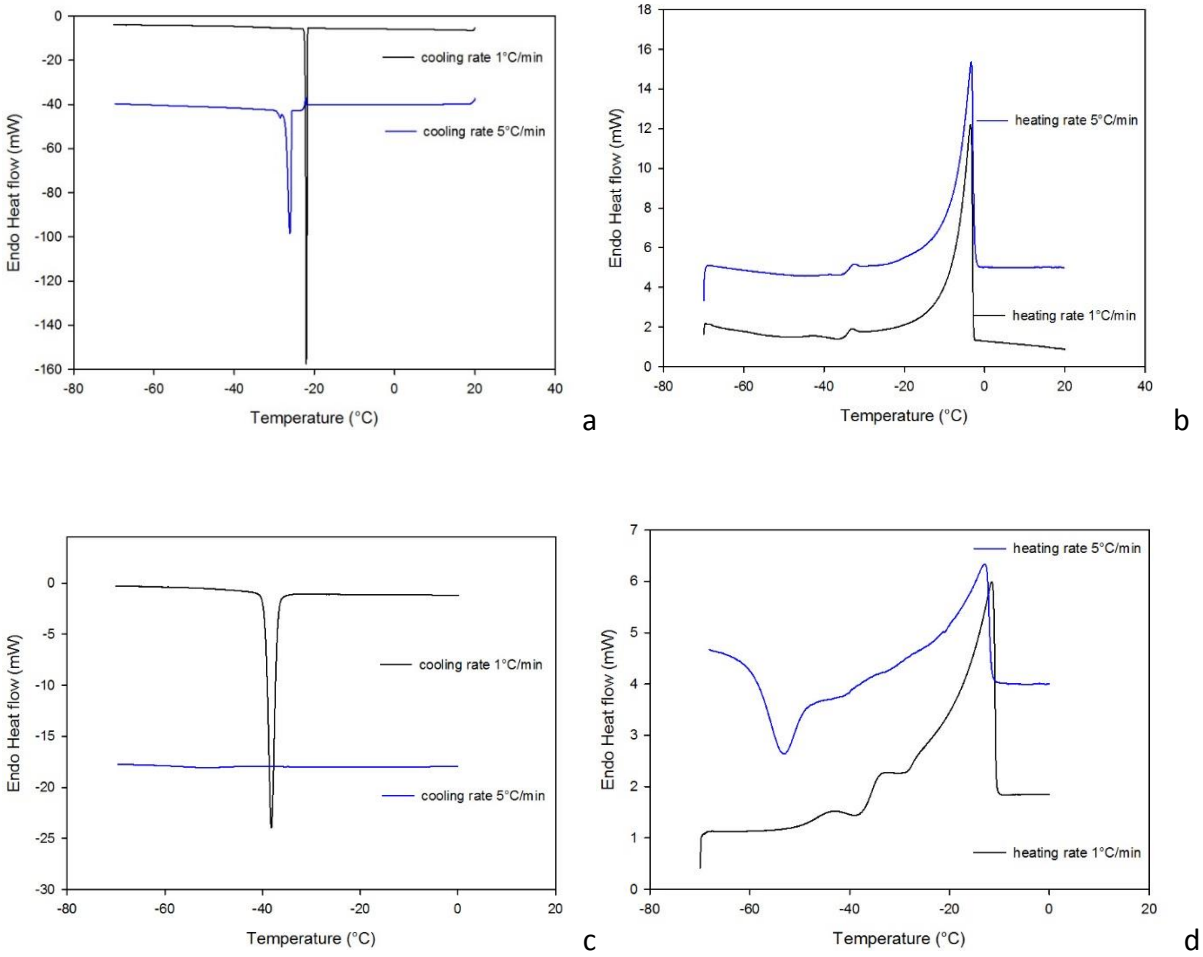

Figure 4-5 different scanning calorimetry scan of sucrose at 1 and 5°C/min, (a): 40% sucrose cooling from 20 °C to -70°C; (b): following heating from -70°C to 20°C (c): 60% sucrose cooling from 20 °C to -70°C; (d): following heating from -70°C to 20°C.

The same trend of delayed crystallisation onset temperature and a broader crystallisation peak can be seen in 40% sucrose system at higher cooling rate (Fig. 4-5 a). The heating curves are shown in Figure 4-5b.

DSC freezing and melting curves for 60% sucrose are displayed in Fig. 4-5 (c and d). When the sample was cooled at 1˚C/min, a crystallisation peak can be seen at -37˚C, and the

following heating resulted in step change in heat flow at -36˚C, indicating the onset of melting.

When the cooling rate increased to 5˚C/min, there was no crystallisation taking place during cooling. However, as shown in Figure 4-5 (d), heating the rapidly frozen 60% sucrose resulted in (i) an exothermic peak at -60˚C due to water crystallisation, and (ii) an endothermal peak for melting occurred after crystallisation. The same phenomenon, crystallisation during heating a rapidly frozen solution, is devitrification (see section 2.1.3). It was noticed in 66.4% sucrose solution in DSC; the author concluded that water did not crystallise after fast cooling because the sucrose and water are well mixed in an amorphous glassy phase (Schawe 2006). Heating provides the system with more mobility as viscosity drops, so that the molecules are able to move and form into crystal matrix (Roos and Karel 1991).

Even under slow cooling, the presence of carbohydrate hinders water crystallisation (Schawe 2006). The cooling rate affects the amount of ice that can be formed during cooling, i.e. increasing cooling rate leads to less ice formation (Roos and Karel 1991). When the cooling rate is fast enough, no water crystallisation will take place (Schawe 2006).

4.1.1.3 Crystallisation in high concentrations at extreme rapid freezing rate

Previous study (sections 4.1.1.1 and 4.1.1.2) has demonstrated that increasing solid content or/and increasing cooling rate will delay water crystallisation. In this section, a very rapid cooling rate of 30˚C/min and a heating rate of 5˚C/min were used. This setting has been reported in glass transition temperature investigation (Roos and Karel 1991). This setting was used in literature to measure glass transition temperature, as the high cooling rate reduce the chance of water crystallisation and promote formation of glass. Here this cooling

rate was used to see if water crystallisation is still possible from high solid concentration solutions.

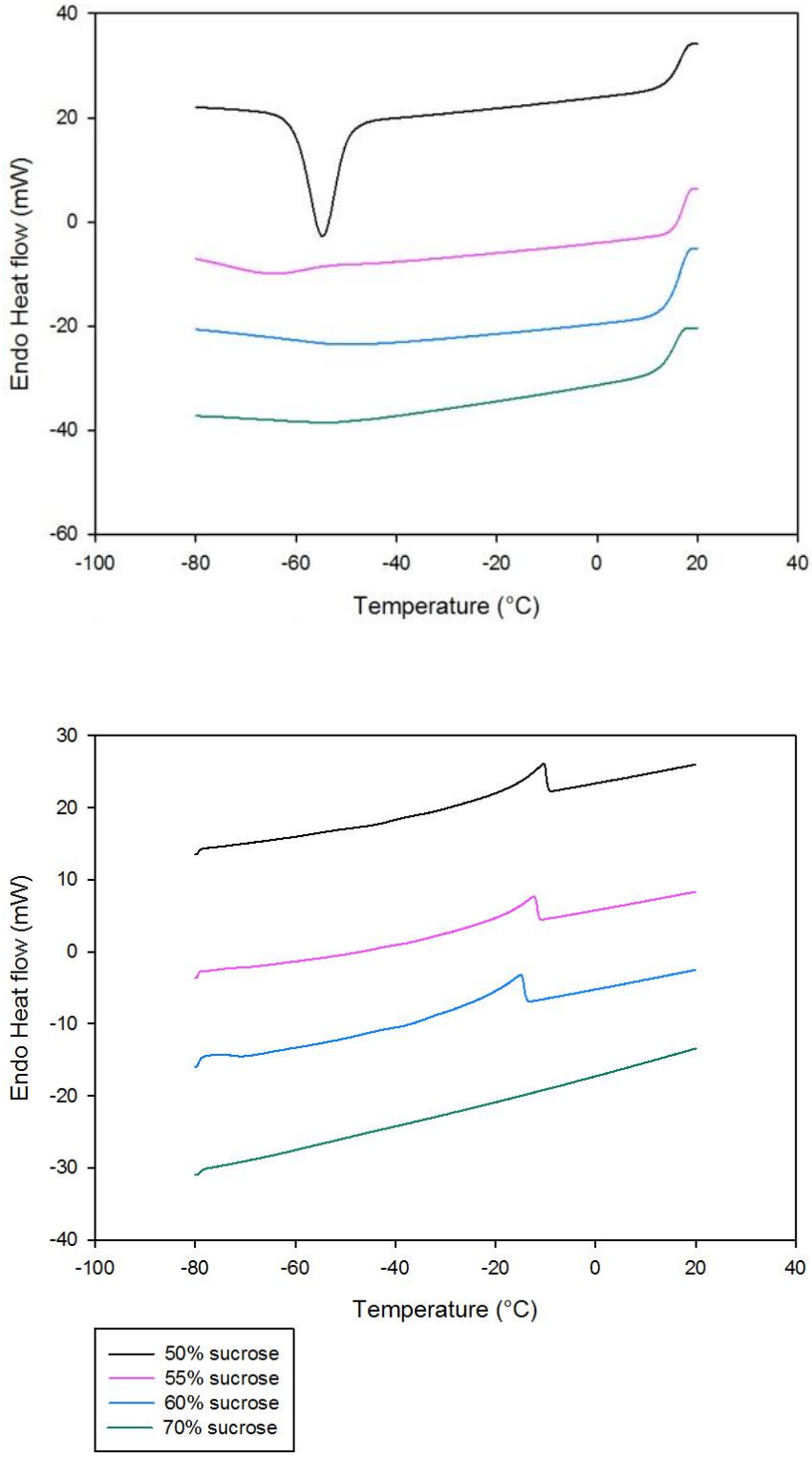

Figure 4-6 DSC thermograms of sucrose solutions with 50%, 55%, 60%, and 70% concentration. Samples are (a) cooled at 30°C/min from 20°C to -80°C and then (b) reheated to 20°C at 5°C/min.

Cooling curves of fast freezing 50-70% sucrose solutions are plotted in Fig. 4-6.

There is an exothermal peak in the 50% sucrose cooling curve, which refers to water crystallisation. Water in 50% sucrose solution crystallises during cooling even at such a fast cooling rate. Ice melting, indicated by endothermal peak, was observed during the following heating.

For 55% and 60% sucrose, no distinct crystallisation peak can be noticed when cooling, but a gradual decrease and increase can be seen in the heat flow. Endothermal peaks (corresponding to ice melting) exist in the heating curves although the peak area is very small.

The phenomenon of ice melting but not water crystallisation that can be observed in 55% and 60% might result from (i) only a limited amount of crystallised water due to fast cooling, so the amount of ice is not big enough to be detected as a peak in DSC scan (ii) the fast freezing rate broadening the crystallisation peak (see section 4.1.1.2), making it difficult to identify.

For 70% sucrose solutions, no crystallisation peak or melting peak can be spotted during the rapid freezing and melting cycles. Under such fast freezing and at this concentration, no water crystallisation occurred.

4.1.1.4 Effect of annealing

In this section, the effect of annealing on water crystallisation is studied. Annealing (see section 2.2.3) is found to be an essential process to create maximum ice formation, and it is time dependant, which means longer annealing time results in larger ice melting peaks (Roos and Karel 1991). The temperature profile of the annealing DSC scans is displayed in Fig. 4-7.

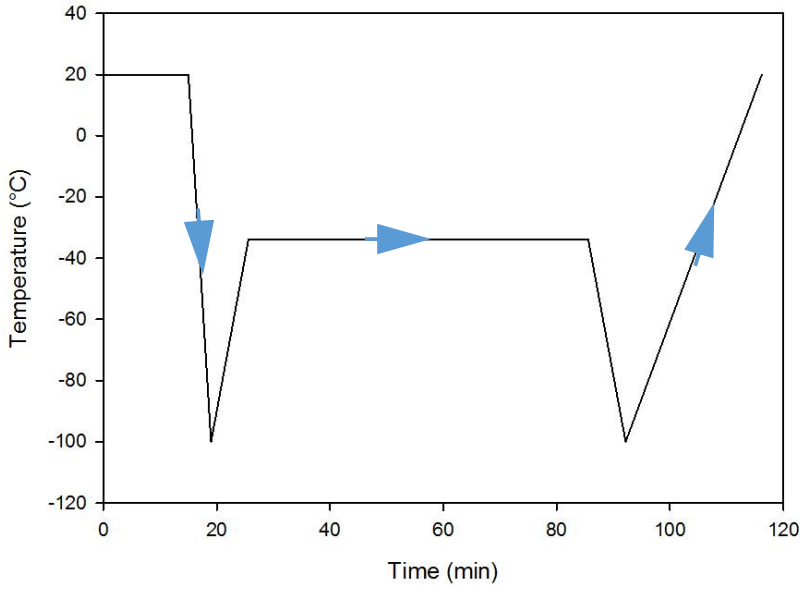

Figure 4-7 Temperature profile of annealing DSC scan

After the sample was placed into the DSC, it was kept at 20°C for 15 minutes to stabilise the sample temperature. The sample was then cooled down rapidly at 30°C/min to -100°C, heated up to -35°C at 10°C/min. Then it was held at -35°C for one hour for annealing. After annealing, the sample was cooled back to -100°C (10°C/min) and then heated to 20°C at 5°C/min. The annealing temperature was set at -35°C because this is slightly below the onset of melting temperature (T'_m=-34°C) and above the glass transition temperature (T'g= -46), and therefore in the temperature range that allows maximum ice formation (see section 2-4). Both T'm and T'g are obtained from literature (Roos and Karel 1991).

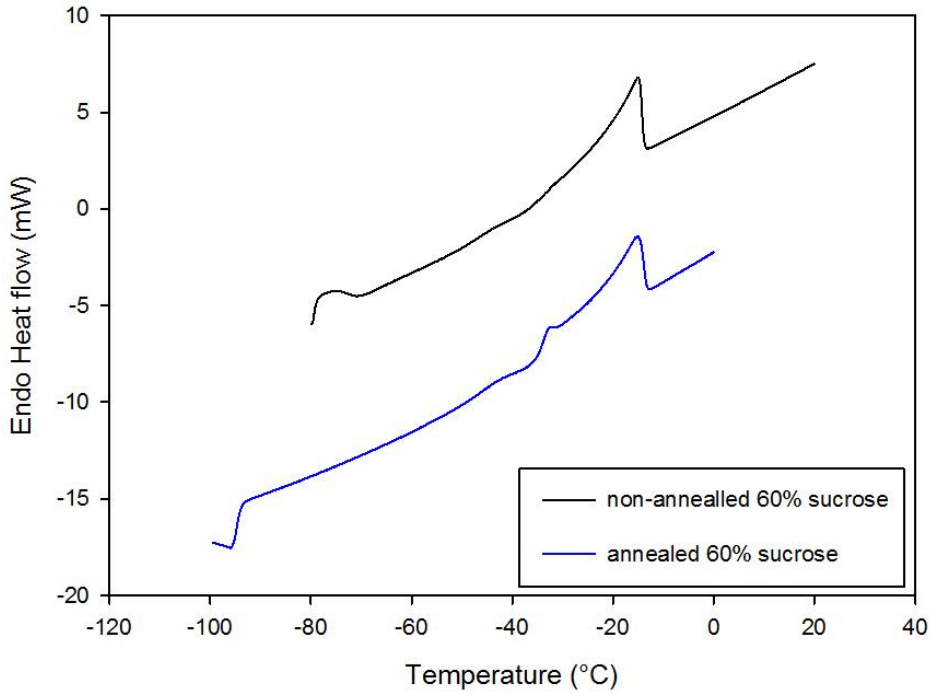

Figure 4-8 DSC heating curves for 60% sucrose solution with and without annealing (profiles from Figure 4-7); arrow indicating glass transitions.

Heating curves for the 60% sucrose are displayed in fig. 4-8. The onset of melting was difficult to estimate due to its overlapping with the glass transition peak.

Glass transition temperature is known to be very sensitive to moisture content, and even very little change in water content will have a dramatic impact (Roos and Karel 1991). The increased glass transition temperature in the annealed sample indicate that more ice crystals are formed than that in non-annealed sample, leaving lower water content in the remaining amorphous system. Once more ice crystals were formed, the amorphous system become more concentrated, so that the glass transition temperature increases. However, it is difficult to compare the enthalpy change of melting between the annealed and non-annealed samples.

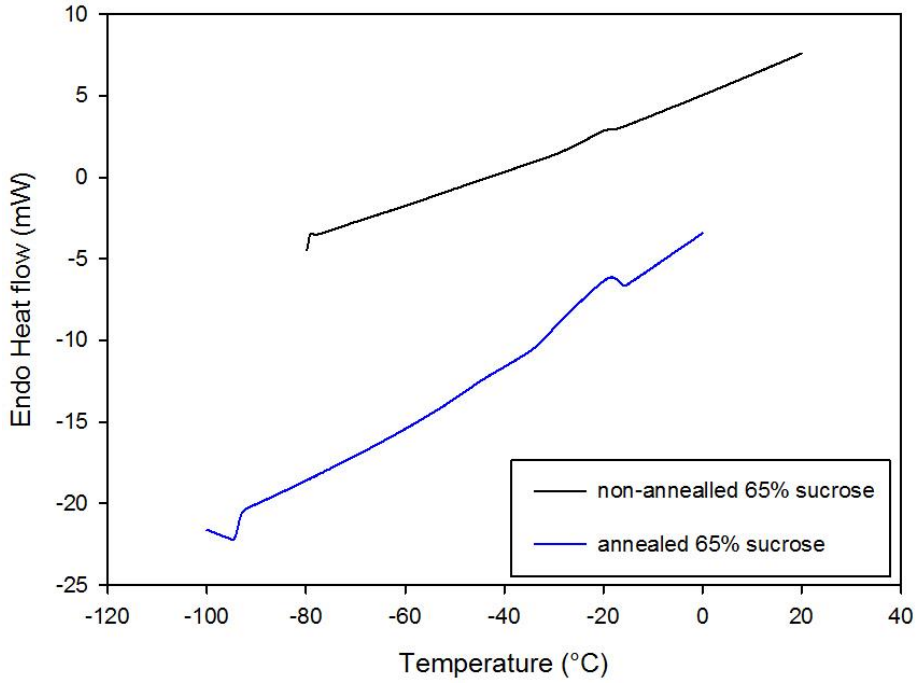

Figure 4-9 DSC heating curves for 65% sucrose with/without annealing (profiles from Figure 4-7).

A small endothermic melting peak can be seen during heating of the 65% sucrose solutions both with and without the annealing treatment (Figure 4-9). Not unexpectedly, the size of the melting peak was larger in the annealed sample and the enthalpy change increased slightly from 1.5 J/g to 2.4 J/g, indicating a larger amount of ice crystal formation when the 65% sucrose solution was annealed.

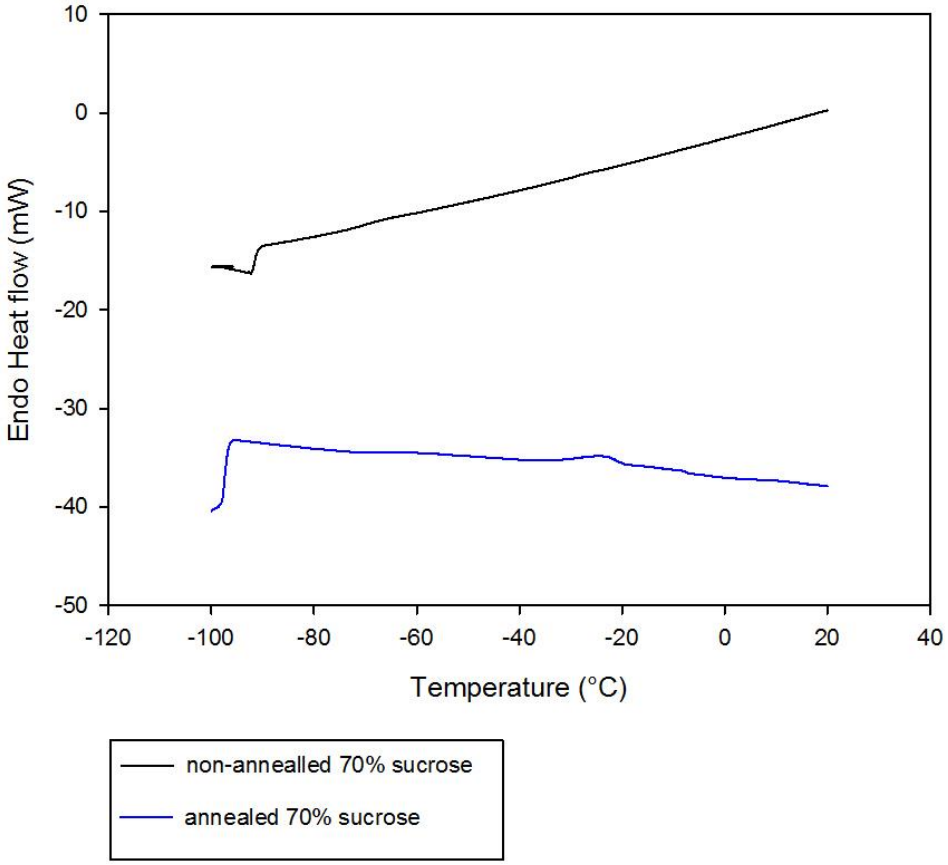

Figure 4-10 Heating curves for 70% sucrose with/without annealing.

Figure 4-10 shows heating curves of 70% sucrose with/without annealing. For non-annealed sample, no evident phase transition can be identified. For the annealed sample, a small endothermal peak appeared during heating at around -20°C, which indicates that traces of water crystallised during annealing. However, the size of the peak is too small to calculate enthalpy change accurately.

Overall, more ice formation were achieved after annealing, and that was noticed in different ways: increased glass transition temperature (in 60% sucrose, Figure 4-8); increased enthalpy change (65% sucrose, Figure 4-9); and the appearance of melting peak (70% sucrose, Figure 4-10).

4.1.1.5 Effect of different solutes

In this section, DSC enthalpy measurement in maltose solutions (another type of disaccharide) is displayed, to investigate effect of solute on water crystallisation during freezing.

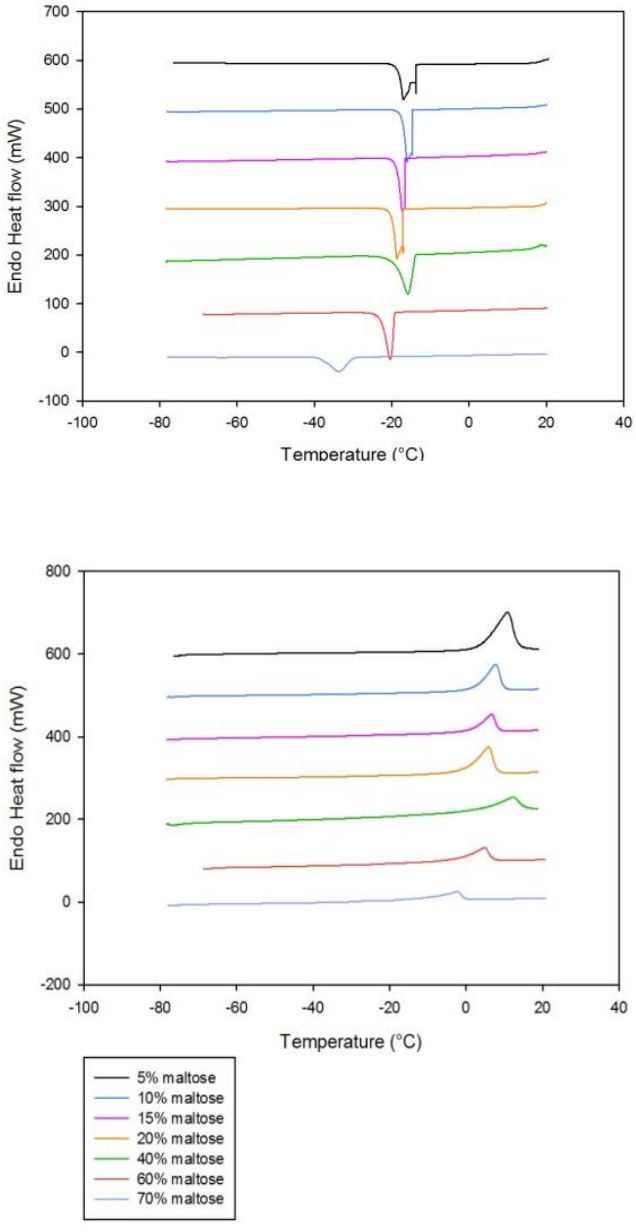

Figure 4-11 Thermograms of maltose solutions with concentration ranging from 5% to 70%. The samples were (a) cooled at 10°C/min to -80°C and then (b) heated at 10°C/min to 20°C.

Maltose solutions (5, 10, 15, 20, 40, 60 and 70%) were used. The samples were scanned at a constant rate of 10°C/min during freezing and melting cycle (Figure 4-11). Crystallisation/melting peak can be seen in each cooling/heating curve at all concentrations up to 70%. Enthalpy change and ice fraction calculated from DSC is displayed in Table 4-2.

Table 4-2 Crystallisation information in freezing maltose solutions

Solid concentration (w/w %)	**Crystallisation enthalpy ΔH(J/g)**	**Ice fraction (%)**
5%	225.155	67.4
10%	184.498	55.2
15%	185.478	55.5
20%	169.364	50.7
40%	106.152	31.8
60%	99.564	29.8
70%	59.325	17.8

The onset crystallisation temperature/melting temperature decreased as concentration increased. The only exception is 40% maltose, which has the highest crystallising/melting temperature. As the scanning rate is comparatively high and these set of experiments were conducted only once, the abnormal behaviour of 40% sucrose might result from experimental error or a delay in heat transfer into the DSC sample capsule.

4.1.2 Characterisation phase transitions using DSC and XRD

4.1.2.1 Combined DSC and XRD to study crystallisation at 1˚C/min

In this section, X-ray diffraction and differential scanning calorimetry were employed together to study water crystallisation under same thermal conditions (cooling and heating at 1°C/min).

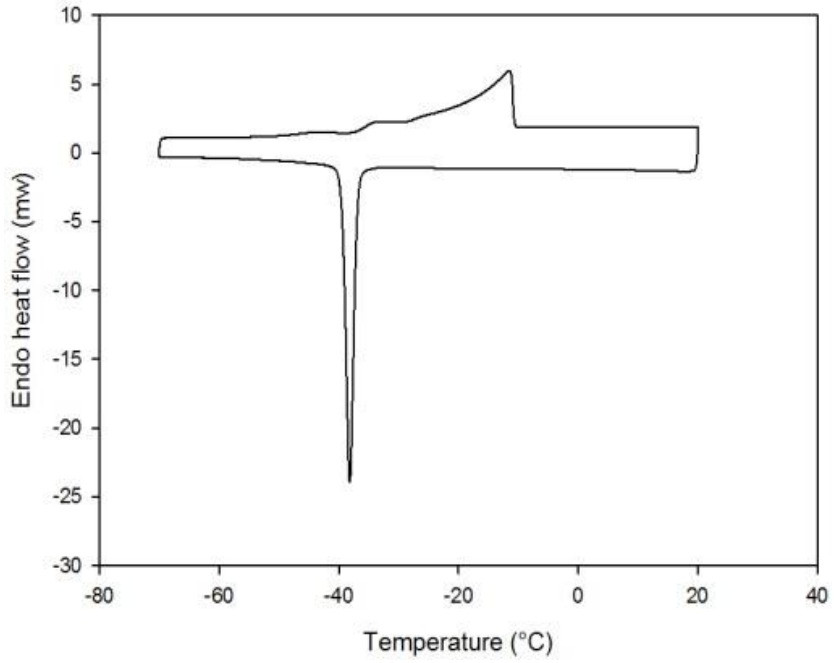
Endo heat flow (mw)
Temperature (°C)
10
5
0
-5
-10
-15
-20
-25
-30
-80
-60
-40
-20
0
20
40

a

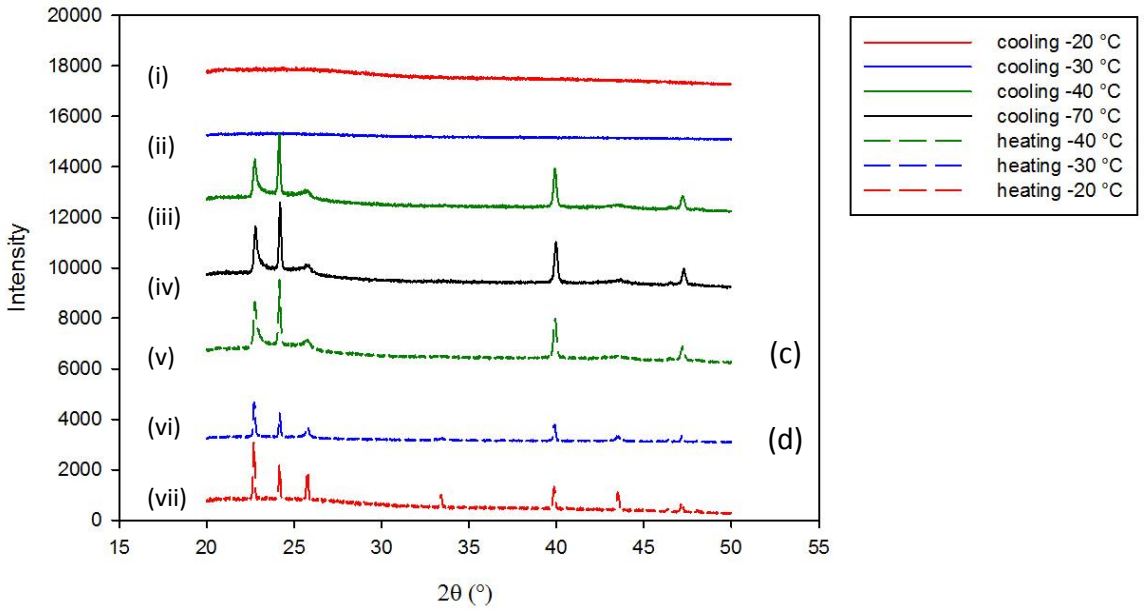
Intensity
2θ (°)
(i)
(ii)
(iii)
(iv)
(v)
(vi)
(vii)
(c)
(d)
cooling -20 °C
cooling -30 °C
cooling -40 °C
cooling -70 °C
heating -40 °C
heating -30 °C
heating -20 °C

b

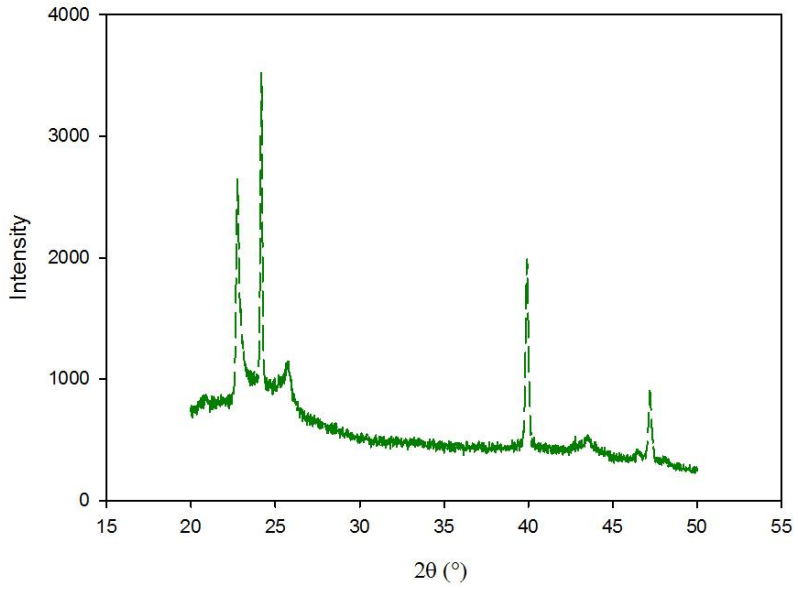

c

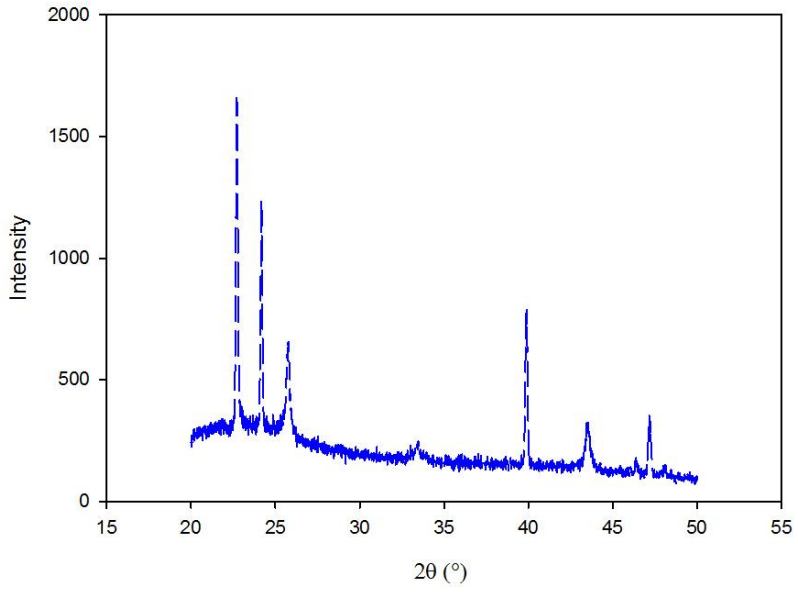

d

Figure 4-12 (a): DSC thermogram for 60% sucrose at same cooling and heating rate of 1°C/min (also shown in figure 4-1 and 4-3); (b):X-ray diffraction patterns of 60% sucrose solutions. Samples were first cooled from room temperature to -70°C and then heated to room temperature at a constant rate of 1°C/min. Scans were conducted at -20°C, -30°C, -40°C and -70°C during cooling, and then -40°C, -30°C and -20°C during heating. To minimise the effect of thermal treatment during scanning time, the scans were obtained in different experiments. Effort has been made to keep all samples the same amount; however the differences between them makes peaks intensities difficult to compare;(c) X-ray diffraction pattern of 60% sucrose solution during heating to -40°C (already shown in b); (d) X-ray diffraction pattern of 60% sucrose solution during heating to -30°C (already shown in b).

A DSC thermogram of 60% sucrose fast cooled to -70°C and then heated to 20°C at a constant rate of 1°C/min is displayed in Figure 4-12 a.

X-ray studies were carried out by:

1. Cooling at 1°C/min from room temperature to the chosen temperature (-20°C/-30°C/-40°C);
2. Holding the temperature constant over the length of an X-ray scan (approximately 15min);
3. Cooling at 1°C/min to -70°C and holding for a scan;
4. Heating at 1°C/min to the chosen temperature and taking a further X-ray scan at same chosen temperature.

Scanning curves from XRD studies are displayed in Fig. 4-12 b. It should be noted that Figure 4-12 b presents results from different experiments, and therefore it is difficult to compare the peak intensities (see chapter 3.5.2, also legend of figure 4-12).

No crystal structure (i.e. no peaks) can be seen in data set (i) and (ii), indicating that no water crystallisation takes places until -30°C.

Further temperature reduction (≤-40°C and up to -70°C) resulted in the appearance of peaks at 22.7°, 24.1°, 25.6°, 39.9°,43.6° and 47.2° (see data set (iii)), which can be identified as ice crystals (Dowell and Rinfret 1960). Water crystallisation takes place between -30°C and -40°C, in agreement with the DSC data in figure 4-12 a, which shows no exothermal peak until -36°C. On heating, the crystal structure persists even at -20°C (i.e. compare (i) and (vii), for example). However, the peak structure is different; the largest peak is at 22.7, rather than at 24.1° (compare (v), (vi) and (vii)). Data set v and vi are plotted in Figure 4-12 (c) and

(d) individually for comparison. The change of crystal patterns indicates transition of ice crystals into different forms, as discussed below.

Three different forms of ice have been described at atmospheric pressure: hexagonal crystal, cubic crystal, and amorphous (Dowell, Moline *et al*. 1962). In XRD scanning, hexagonal ice crystals are indicated by peaks at 22°, 24°, 26°, 34°, 40°,44° and 47°, while cubic ice crystals show peaks at 24°, 40°, and 47° coincidently (Dowell, Moline *et al*. 1962). The diamond structures of those two crystals are closely related, giving them having similar diffraction peaks (Dowell, Moline *et al*. 1962). Cubic ice is a metastable ice crystal form and it is the preferred form to develop during rapid freezing of water to sufficiently cold temperatures (Murphy 2003), which follows the Ostwald's rule that less thermodynamically stable crystal form will take place first. Less activation energy is required during forming a critical cubic embryo than forming a critical hexagonal embryo (Takahashi 1982), thus cubic ice is preferably nucleated at lower temperature. However on increasing temperature, hexagonal ice, which is a more stable ice crystal form, is dominating (Kiefte, Clouter *et al*. 1984). Due to the fact that vapour pressure of cubic ice is larger than that of hexagonal ice, mass transfer from cubic ice to hexagonal ice will take place spontaneously (Murray, Knopf *et al*. 2005). The transformation rate strongly depends on temperature (Murphy 2003).When the temperature is above -80°C, cubic ice will readily transform to hexagonal ice (Fletcher 1970).

The percentage of hexagonal/cubic ice can be calculated from the intensity ratio of the peak at 44° over peak at 40°: I_{44}/I_{40} (Murray, Knopf *et al*. 2005). The minimum value is 0, when all the ice is in cubic form. The value will gradually increase as hexagonal ice increases until a maximum value at 0.8, which indicates that all the ice is in hexagonal form. Value of

0.8 is the intensity ratio of peak 44° and 40° in pure hexagonal ice (Dowell and Rinfret 1960, Dowell, Moline *et al*. 1962). Intensity ratios calculated from Fig 4-12 b is displayed in Fig 4-13.

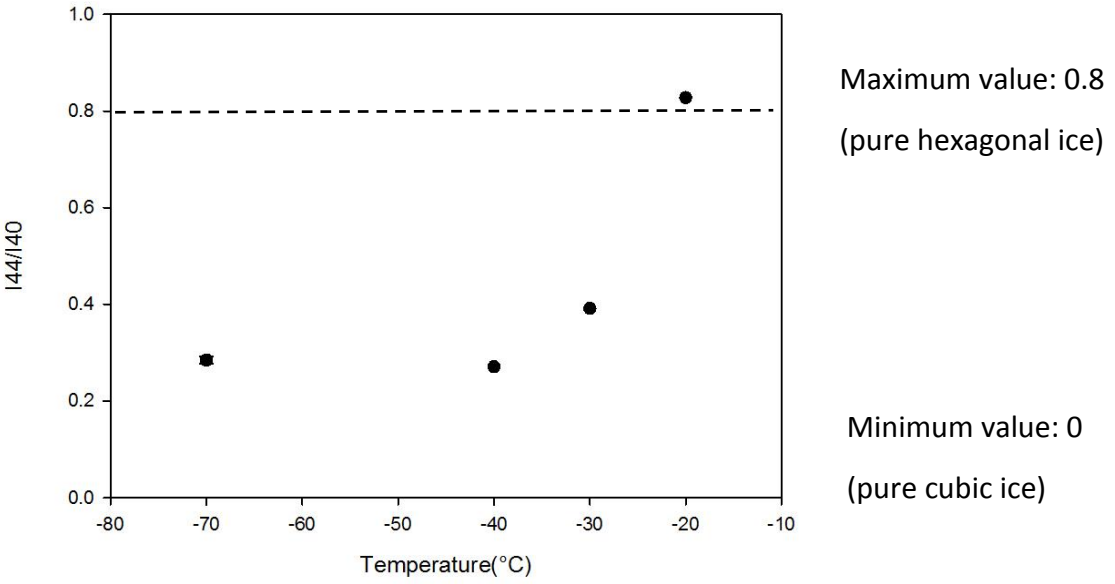

Figure 4-13 Intensity ratio I_{44}/I_{40} calculated from XRD patterns (iv, v, vi and vii in Fig. 4-12 b) as a function of temperature during heating of 60% sucrose. Result of -70°C was triplicated and error bar represents one standard deviation of uncertainty. The rest results were from experiments that were carried out once.

For temperatures ≤ -40°C, the scan patterns indicated a mixture of cubic and hexagonal ice crystals with I_{44}/I_{40} value of 0.28 ± 0.01. It appears that at this temperature range there is insufficient mobility in the structure for water molecules to move and change from cubic crystals into hexagonal over the investigated time scale. When the sample was heated to -30°C, the I_{44}/I_{40} ratio increased to 0.39, indicating a shift from cubic to hexagonal ice. When temperature increased further to -20°C, the ratio reached its maximum of 0.82 (this should theoretically be 0.8), which means that all the ice in the sample has changed into

hexagonal form. The result is in agreement with XRD patterns of ice crystals in highly concentrated systems. The authors reported that cubic ice crystals would transform into hexagonal form during heating in high concentration glucose solution (Thanatuksorn, Kajiwara *et al*. 2008), various disaccharide solutions (Uchida and Takeya 2010) and gelatine gels (Dowell, Moline *et al*. 1962).

The crystal form transition usually takes place after glass transition because molecules in the system will then have more mobility (Uchida and Takeya 2010). The transition temperature from cubic to hexagonal ice is reported to be between -40°C and -30°C in sucrose and maltose solutions (Uchida and Takeya 2010), which is in good agreement of results in figure 4-13.

4.1.2.2 Combination of DSC and XRD to study crystallisation at 6°C/min

In this section, the study of water crystallisation in 20, 50, and 70% sucrose systems using XRD and DSC is displayed at a higher scanning rate of 6°C/min.

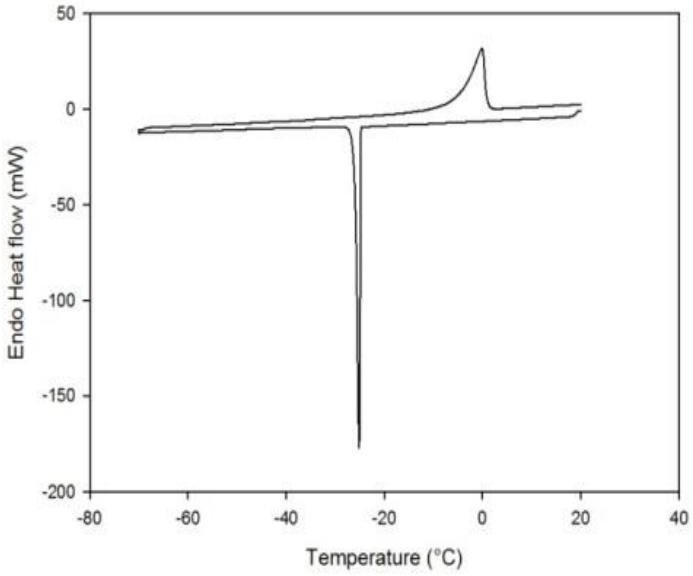

a

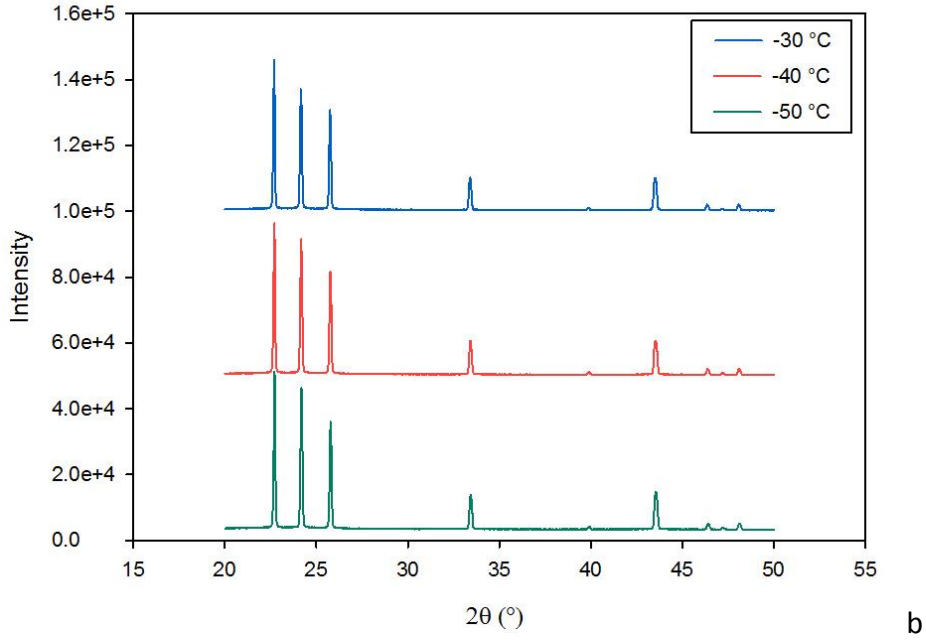

b

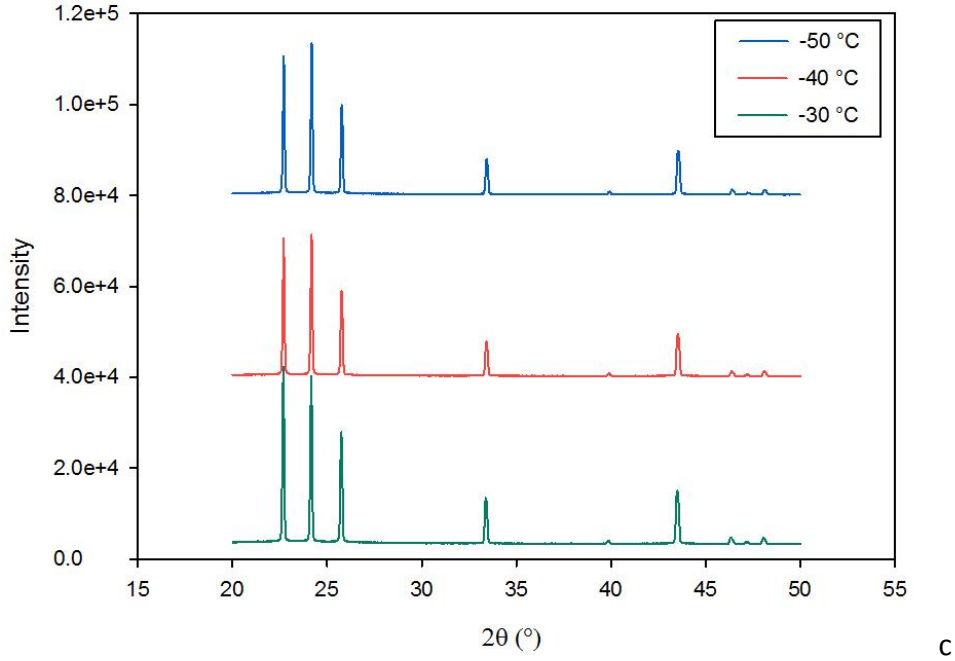

c

Figure 4-14 (a): DSC thermogram of 20% sucrose with cooling and heating rate at 6°C/min. (b) X-ray diffraction patterns of 20% sucrose solution. The sample was cooled from room temperature to -50°C at 6°C/min. Three scans were conducted at -30°C, -40°C and -50°C. (c): X-ray diffraction patterns of 20% sucrose solution carried out during re-heating. The sample was cooled from room temperature to -50°C at 6°C/min then heating back to 20°C at 6°C/min. Three scans were carried out at -50°C, -40°C and -30°C. Experiment was carried out once.

DSC scan of 20% sucrose at 6°C/min is displayed in figure 4-14 a. The onset of exothermal peak (water crystallisation) took place at -25 °C during cooling and endothermal peak (ice melting) occurred at -5°C.

Figure 4-14 b shows the X-ray diffraction patterns carried out at -30°C,-40°C and -50°C during cooling. For each curve, similar crystal patterns can be seen, which are characteristic of ice crystals.

Figure 4-14 c shows diffraction carried out during heating at the same temperatures 30, -40 and -50°C). All three curves showed ice crystal patterns but a slight change in the relative intensity of the individual peaks was noticed. Comparing curves obtained at -50°C and -30°C, it could be noticed that highest intensity peak changed from 24° to 22°C. The peak at 24° might originate from both cubic and hexagonal ice, while peak 22° only refers to hexagonal ice, it can be concluded that there are some transform of cubic ice into hexagonal ice during heating from -50°C to -30°C. Cubic ice will form and transform into hexagonal ice even if the concentration of system is not very high (20%).

While the DSC detected the crystallisation and melting of the sample, it was not possible to detect the crystal form transition in the DSC heating curve. This might be due to the latent heat involved being very small (Fletcher 1970): only 12.6-42 J/mol (Hobbs 1974). Considering the small mass of sample in DSC scan (5-20 mg), it is difficult to detect the transition in DSC.

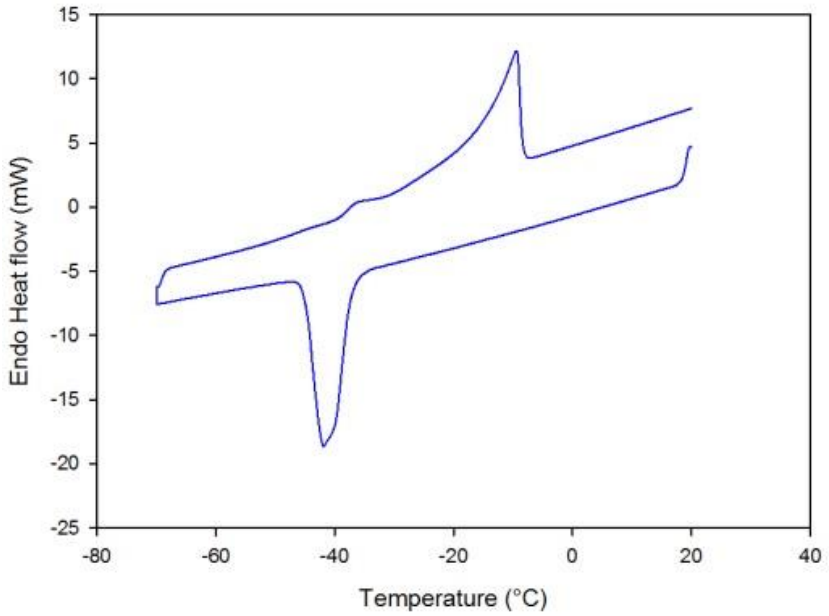

a

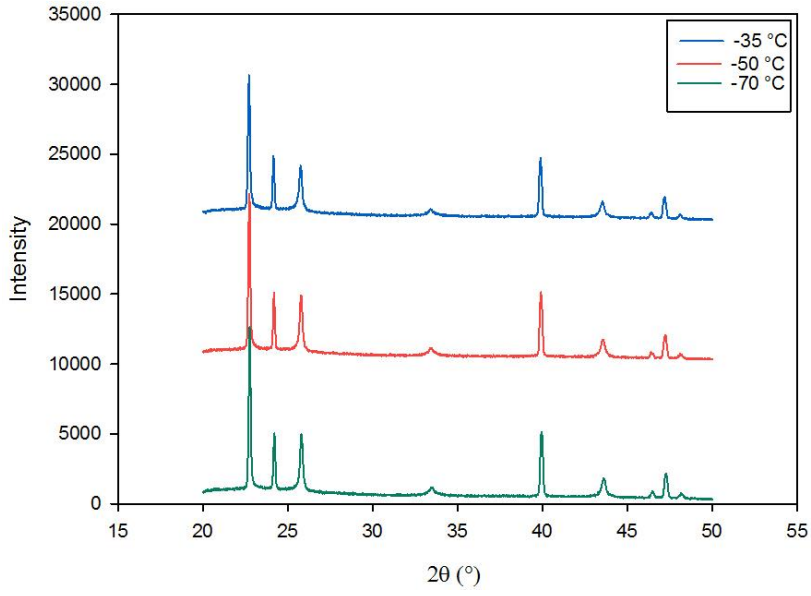

b

Figure 4-15 (a) DSC scanning of 50% sucrose, cooling from 20°C to -70°C then heated back to 20°C at 6°C/min; (b): X-ray diffraction patterns of 50% sucrose. The sample was cooled at 6 °C/min from room temperature to -70°C. Three scans were carried out during cooling at -35°C, -50°C, and -70°C. Experiments were carried out once.

Figure 4-15 (a) shows the thermal behaviour of 50% sucrose when it was cooled to -70°C and then heated to 20°C at 6°C/min. Crystallisation peak can be seen at-37°C during cooling, and glass transition at -39°C and melting at -14°C can be seen during heating.

Three X-ray scans were conducted during cooling at same rate (6°C/min) to -35/-50/-70°C. The same shape of crystal peaks can be seen in each curve, and they are identified as ice crystals.

The calculated I_{44}/I_{40} ratio values are 0.34, 0.34 and 0.35 for the temperatures -35°C, -50°C and -70°C, respectively. This indicates that a mixture of hexagonal ice and cubic ice was formed when the sample was cooled to -35°C, and the ice remained in same crystal from with further cooling.

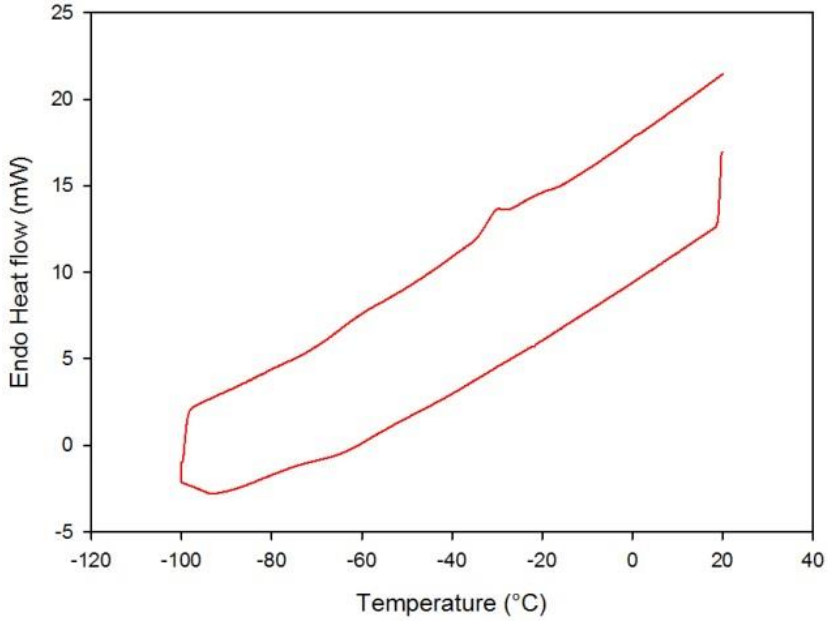

a

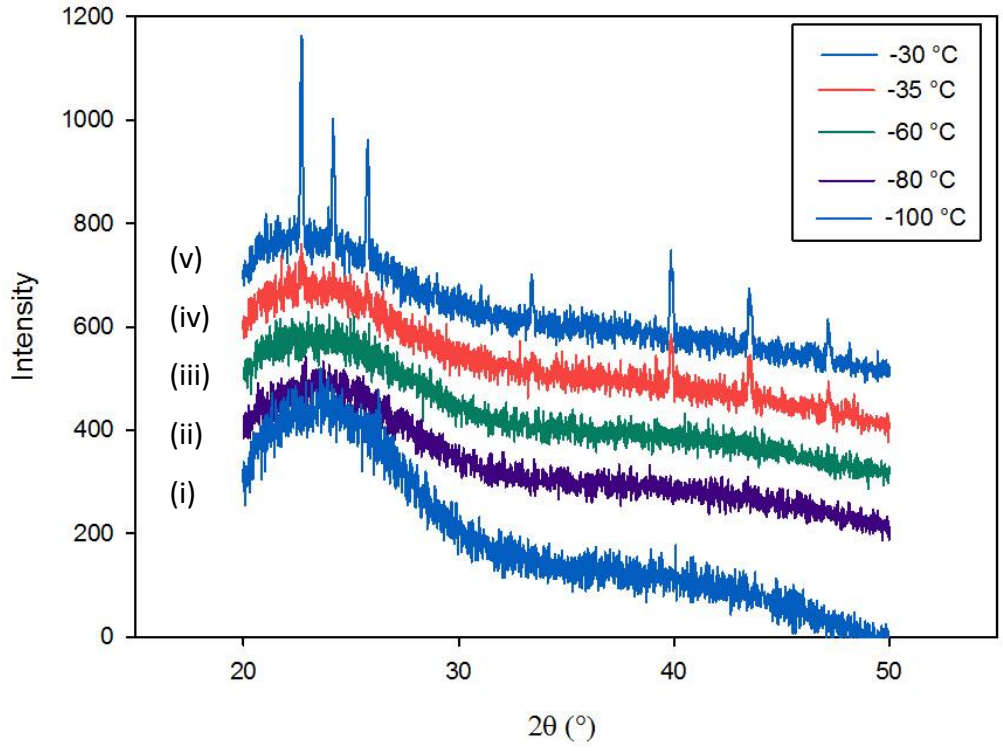

b

Figure 4-16 (a): Differential scanning calorimetry thermogram of 70% sucrose. Sample was cooled from 20 ˚C to -100 ˚C at 6 ˚C/min then heated up back to 20 ˚C at 6 ˚C/min (b) X-ray diffraction patterns of 70% sucrose solution. Same thermal treatment was used as DSC: the sample was cooled from room temperature to -100˚C then heated back to 20 ˚C at a constant rate of 6˚C/min. XRD scans were conducted at -100 ˚C, -80 ˚C, -60 ˚C, -35 ˚C and -30 ˚C during heating. Experiment was carried out once.

Water crystallisation in 70% sucrose solution was investigated in combined XRD and DSC study at fast scanning rate (6°C/min), and results are displayed in figure 4-16. This is the highest concentration used in this chapter, as it approaches the highest concentration (76% according to previous research in section 4.1.1.1) that allows water to crystallise.

The DSC scan of 70% sucrose solution is shown in Figure 4-16 (a). No exothermal peak is observed during cooling to -100 ˚C. The only noticeable change in the cooling curve is a step change at around -70 ˚C, and this might indicate glass transition of the amorphous system. During heating, there is also a slightly slope change at -70 ˚C, which could be the glass-rubber transition. With further heating, DSC detected a small endothermal shift at -34 ˚C, which refers to the situation that water gained enough mobility to transition to crystal form (Thanatuksorn, Kajiwara *et al*. 2008).

The first XRD scan was carried out when the system was cooled to -100 ˚C at 6˚C/min (data set i). A very broad peak area can be seen at 24 ˚, suggesting the existence of amorphous ice (Dowell, Moline *et al*. 1962). This indicates that water in the sample turns into an amorphous glassy state instead of ice crystals. As discussed in section 4.1.1.2 and section 2.1.2, in carbohydrate-water system, water does not crystallise into ice when it is cooled to a sufficiently low temperature at a high cooling rate, as the crystallisation rate is limited (Schawe 2006).

Heating up 70% sucrose to -60 ˚C (data set iii) resulted in a decrease in the peak intensity at 24 ˚, which corresponds to the partial melting of amorphous ice. Further heating to -35 ˚C (data set iv) leads to crystal peaks appearing in the curve at 40 ˚ and 44 ˚, and this can be identified as ice crystal peaks.

Curve (v) shows the X ray scan carried out at -30˚, there are several peaks can be seen at 22˚, 24˚, 26˚, 34˚, 40˚ and 44˚, referring to ice crystals. The I_{44}/I_{40} ratio calculated from the curves gave a number of 0.68, which suggests that the ice in the sample is a mixture of hexagonal and cubic crystals.

It can be seen that curves in Figure 4-16 (b) contained a lot of noise, when compared to other XRD graphs in this chapter. This is attributed to the large amount of non-crystallised material (sucrose, amorphous water and even air bubbles) that exist in the sample during scanning.

When the cooling rate is fast enough, water in high concentration sucrose does not crystallise during cooling but heating (devitrification)(Roos and Karel 1991, Roos 1997). In 70% sucrose solutions, the total water content is 30% and a certain amount of it is bound with solids, leaving only a fraction of the 30% free to crystallise. Also, the viscosity of 70% sucrose is high and will increase at lower temperature; decreasing the mobility of water molecules in the system. So, during fast cooling, the water is solidified into amorphous ice, instead of ice crystals. During rewarming above glass transition temperature, water molecules gain more mobility as viscosity decreases, and form into crystallised ice (Roos and Karel 1991, Goff, Verespej *et al*. 2003).

XRD has been used to study effect of concentration on water crystallisation by Dowell *et al* (Dowell, Moline *et al*. 1962). They investigated gelatine solution with concentration from 10% to 75%. It was found that in diluted system (e.g. up to 50% gelatine), there was enough water to form ice crystals during cooling. When the concentration or cooling rate increased, crystallisation became very difficult to observe, which is also observed in our experiments

(see, for example, Figure 4-16 a). They attributed this observation to the high viscosity of the solution and sparse spatial distribution of water.

Overall, DSC and XRD show good agreement in studying water crystallisation. DSC provides information including phase transition temperatures (crystallisation, melting, and glass transition) and enthalpy change for first-order phase transitions (crystallisation and melting). XRD makes it possible to identify the crystal form and monitor crystal form transition.

4.1.3 Visualising ice crystals in frozen sucrose sample via Cryo-SEM

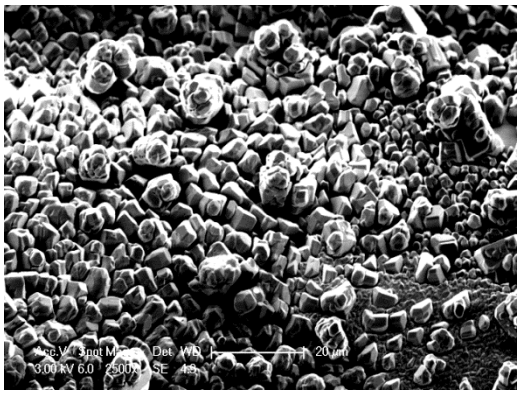

a

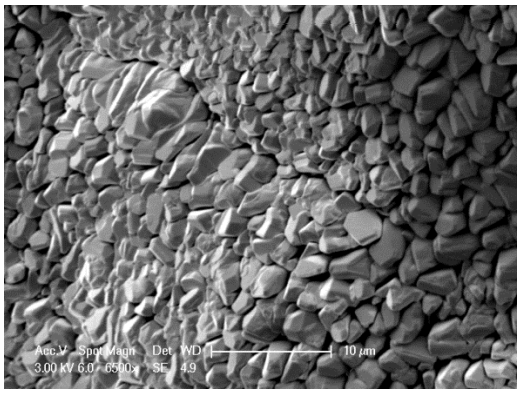

b

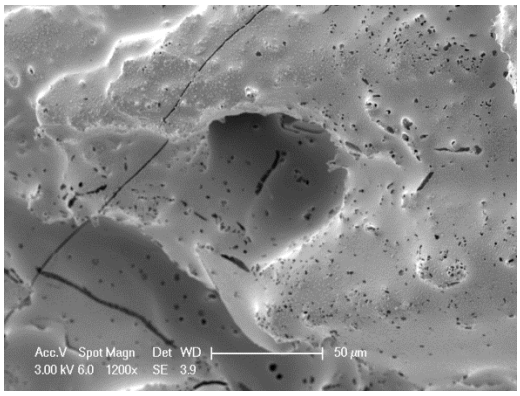

c

Figure 4-17 Cryo-SEM image of frozen 30% sucrose

In this section efforts have been made to visualise ice crystal directly in low temperature Environmental Scanning Electron Microscopy (cryo-ESEM). Only a limited number of cryo-ESEM images have been obtained and three of them for frozen 30% sucrose were shown in Figure 4-17.

During freezing of sucrose solutions, water may crystallise into ice crystals. However, sucrose does not crystallise, and the solution only concentrates as amorphous state (Roos 1997). Thus freezing sugar solution usually leads to ice crystals embedded in freeze concentrated glass (Thanatuksorn, Kajiwara *et al*. 2008).

Different parts in the sample (ice and glass) can be differentiated via different microscope techniques. Uchida and Takeya used field-emission gun type transmission electron microscope(FEG-TEM) to study the phase separation in disaccharide solution including sucrose during rapid freezing, and identified three regions in the frozen disaccharide solution: (i) Some water will form hexagonal ice crystals; (ii) disaccharide solids with hydrated water will form giant clusters, which are unlikely form into crystals (iii) freeze concentrated amorphous material (Uchida and Takeya 2010).

Some crystal shapes can be seen in Fig. 4-17 (a) and (b), and they might refer to ice crystals. The size of crystal is of several micro meters, in good agreement with reported values of Uchida and Takeya (2010). Fig.4-17 (c) shows a more homogeneous structure, which might be the freeze concentrated amorphous glass. Two different types of structure are detected and suggest the existence of dispersed ice crystals and freeze concentrated frozen area, indicating during freezing, water crystallise into ice crystals, and separated from the solutions; while the solution become more concentrated in sucrsose and formed an amorphous structure.

Due to practical difficulties in sample preparation, this was the only frozen sucrose sample examined in cryo-SEM. It is difficult to draw many conclusions from these images. More investigation on frozen sucrose solutions in cryo-SEM is suggested for future studies, for a better understanding of the morphology of frozen sucrose solutions.

4.2 Crystal growth study by adding ice nuclei

Both DSC and XRD results demonstrated that primary nucleation becomes increasingly difficult as sucrose concentration increases, with 26°C supercooling required (temperature of -37°C) for crystallisation to occur spontaneously in a 60% solids system (see from the DSC result in section 4.1.1.1). In this section, microscope images provide direct visualisation of 60% sucrose at low temperatures. The light circles in the images in Figure 4-18 is the reflection from microscope LED light.

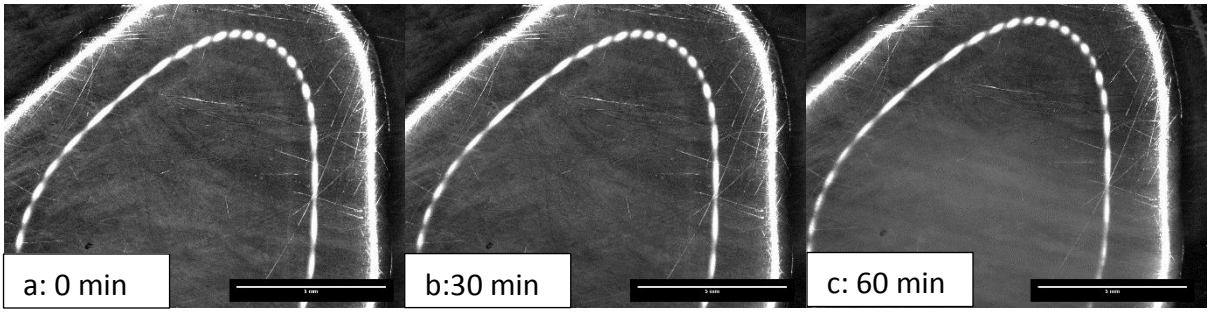

Figure 4-18 Microscope images of 60% sucrose hold at -20°C for (a) 0min, (b) 30min and (c) 60 min after cooling from room temperature to -20°C at 1°C/min. Scale bar =5mm. The light circle in the images is the reflection from microscope LED light.

Images in Figure 4-18 are obtained when the 60% sucrose droplet is hold at -20°C after cooling from room temperature at 1°C/min. There was no crystallisation observed and the sample remained as clear liquid for one hour, which is in agreement with the DSC and XRD results (see Figure 4-12). These results confirm that supercooling to 9°C (i.e. temperature

of -20°C) was insufficient to induce nucleation for 60% system, as no crystal growth was evident after 1 hour of supercooling. As discussed in section 2.1.1, supercooling is needed before crystallisation can take place, and spontaneous crystallisation (primary nucleation) requires more supercooling than induced crystallisation (secondary nucleation). To study crystal growth at higher, industrially more relevant temperatures, an ice nucleus was added to a supercooled solution to induce crystallisation and the system was observed optically. Details of experimental method development is in section 3.6.

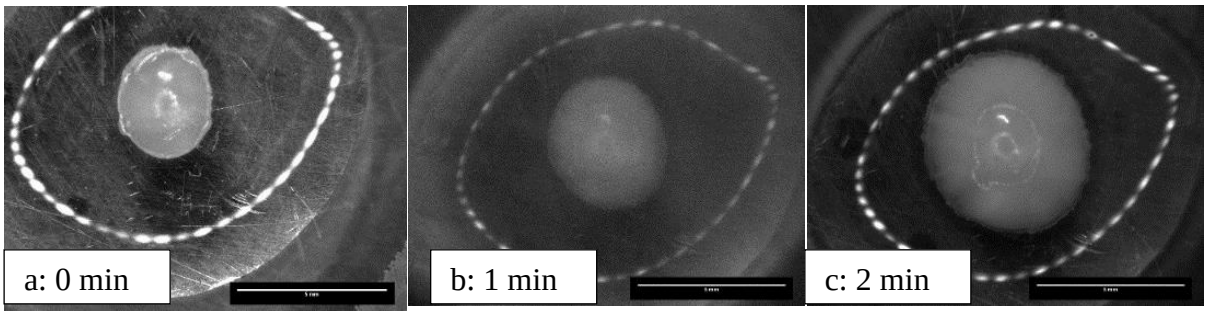

Figure 4-19 Visualisation of 60% sucrose droplet: Microscope images recorded at (a) 0, (b) 1 and (c) 2 minutes after adding ice nucleus into 60% sucrose droplet at -20 °C. Scale bar=5mm.

Figure 4-19 show a sequence of images obtained after adding an ice nucleus into supercooled 60% sucrose at -20°C. Images confirmed that on addition of ice nucleus, crystal growth was evident at a supercooling level as low as 9°C.

Evidence that solidification is from water rather than sucrose crystallisation comes from the XRD results in section 4.1 (Figure 4-12 b). In addition, the temperature range used during the experiments is very low for sucrose to crystallise. However, as water turns into ice, solute molecules might also be trapped into the solid matrix (Worster and Wettlaufer 1997).

It has been reported that higher solids contents and higher ice crystal growth rate will lead to more solute inclusion in the ice crystals (Goff, Verespej *et al*. 2003).

A series of experiments were conducted to study crystal growth kinetics after ice nucleus addition, using this method (see section 3.6.1).

4.2.1 Effect of concentration

In this section, the effect of concentration and temperature on crystal growth rate was studied. Sucrose solutions (40, 50 and 60%) were used in experiments. Different crystallisation temperatures were selected to achieve same range of supercooling between each concentration.

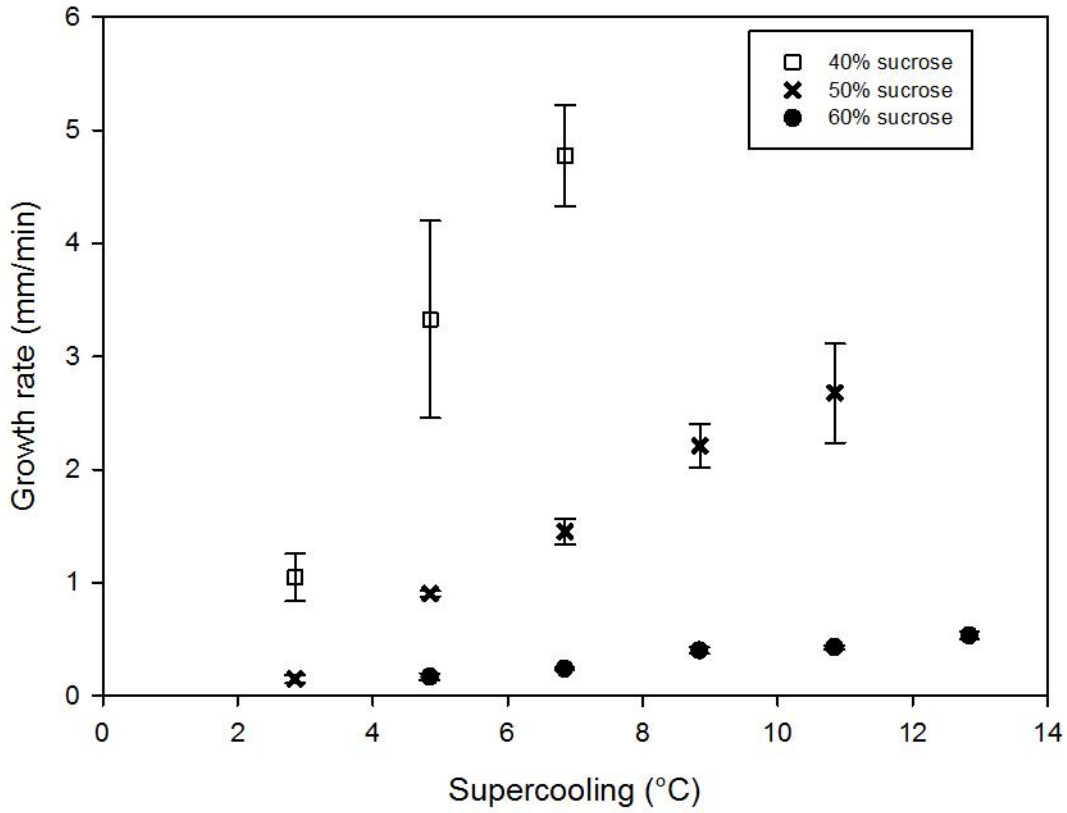

Figure 4-20 Effect of supercooling and concentration on crystal growth rate in sucrose systems. Experiments were triplicated, and error bars represent ± one standard deviation.

Figure 4-20 shows the effect of concentration and supercooling on ice crystal growth rate in sucrose solutions. The supercooling level is calculated from the difference between ice crystallising and equilibrium freezing temperatures, the latter is taken from the literature (T=-4.7°C for 40% sucrose, -7.1°C for 50% sucrose and -11.1°C for 60% sucrose) (Roos 1995). For all concentrations, the growth rate increased with increasing supercooling and significantly decreased with increasing solids concertation.

In water crystallisation, the relationship between crystal growth rate and supercooling can be described by a power law (Teraoka, Saito *et al*. 2002):

$$v = a\Delta T^{b} \qquad (4\text{-}3)$$

Where v is growth velocity, ΔT is supercooling, a and b are coefficients.

The power of the exponent, b has been reported in the range between 1 and 2.4 (Hallett 1964, Kallungal and Barduhn 1977, Teraoka, Saito *et al*. 2002, Hindmarsh, Russell *et al*. 2005, Ayel, Lottin *et al*. 2006). A linear relationship (b=1), has been reported for water crystallisation in 20% sucrose solution (Hindmarsh, Russell *et al*. 2005), or in a 15% MPG-water solution (MPG: Monopropylene glycol, commonly used antifreeze) (Ayel, Lottin *et al*. 2006).

Table 4-3 shows the fit of the line when equation 4-3 is used,

Table 4-3 Data from Figure 4-20 fitting into equation 4-3

	a	b	R^2
40% sucrose	0.1742	1.7698	0.971
50% sucrose	0.0207	2.1422	0.9424
60% sucrose	0.0243	1.2211	0.9704

The b values obtained from fitting is within the reported range from literature.

The growth rate showed a strong dependence on the solids concentration of the system. At a given level of supercooling, the ice growth rate reduced with increasing solids concentration. For example, at supercooling of 7°C, the growth rate was reduced by 70% (from 4.8 to 1.5 mm/min) as the concentration increased from 40% to 50%, and by 95% (to 0.2 mm/min) as the concentration increased further, to 60% sucrose. Adding solids both slows down heat transfer and reduces molecular mobility (Budiaman and Fennema 1987), which causes a significant decrease in crystal growth. As the ice forms from water, sucrose molecules must be displaced from the ice front, and this will become more difficult as the concentration increases.

During crystallisation, molecules must overcome an activation energy (E_d) barrier. The activation energy can be calculated from the Arrhenius equation (Roos 1995, McNaught 1997, Atkins, de Paula *et al*. 2013):

$$\ln k = -\frac{E_d}{RT} + \ln A \qquad (4\text{-}4)$$

Where k is crystal growth rate (m/s),

E_d is activation energy (J mol^{-1}),

R is gas constant 8.314 (J mol^{-1} K^{-1}),

T is Kelvin temperature (K),

A is pre-exponential factor.

Fig. 4-21 shows Arrhenius plots of crystal growth rate as a function of the reciprocal of temperature in 40%, 50% and 60% sucrose solution.

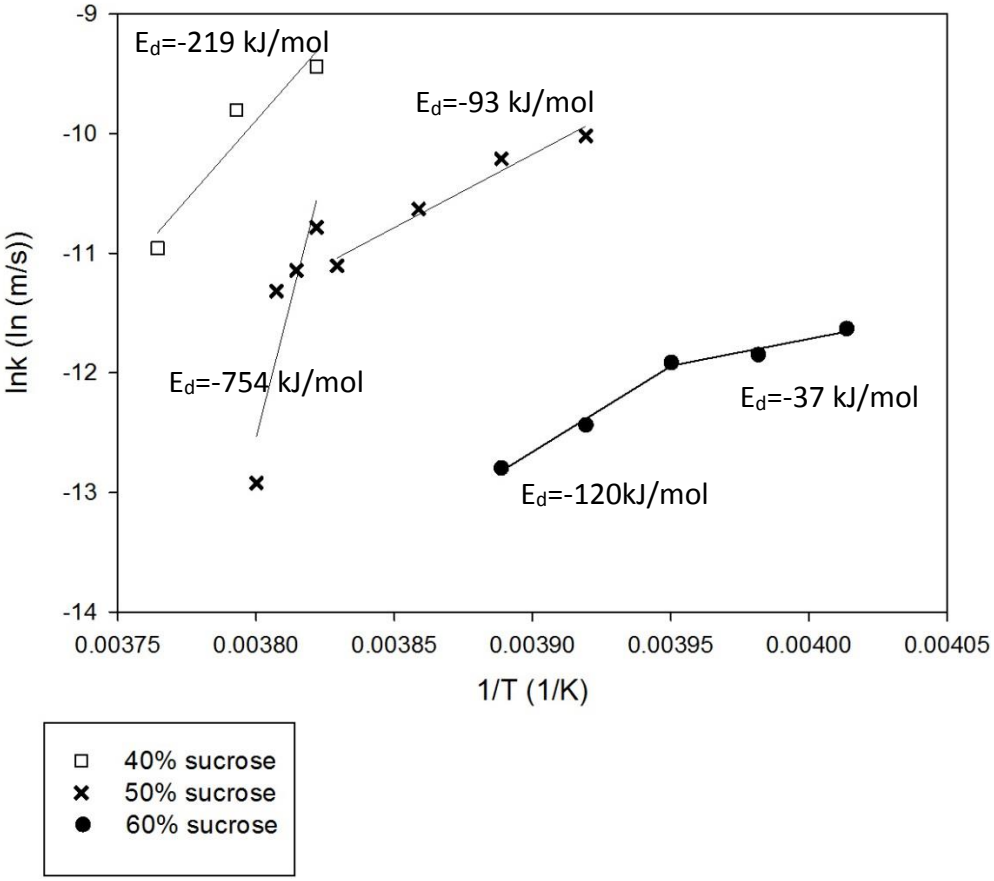

Figure 4-21 Arrhenius plot of nucleus addition crystal growth: logarithm of crystal growth rate as a function of reciprocal of the temperature. Activation energy values are calculated from the slopes of the lines. Results are averages of triplicated results, and error bars represent ± one standard deviation.

In this graph (Figure 4-21), the slope of a linear fit is $-\frac{E_d}{RT}$ (equation 4.4), allowing the activation energy to be calculated. The calculated E_d values are always negative, as the rate of water crystallisation decreases when temperature increases.

Figure 4-21 suggests that for 50% and 60% sucrose solutions, it is possible to fit two straight lines to the plot. The slope of the fitting curves decreases at lower temperatures, indicating

a decrease in activation energy. However for the 50% solution the observation is based on a single point (albeit for triplicated experiments) and more work is required to understand the phenomena.

As there are only three data points in 40% sucrose systems, there is only one straight line fitted to the plot and the activation energy is -219kJ/mol. Detailed discussion of this system is not possible due to the limited amount of the data, and more work is required.

The data for 60% sucrose solution, suggests a 70% decrease in values of the activation energy as temperature decreases below -20°C (from -120 kJ mol^{-1} to -37 kJ mol^{-1}). The decrease of activation energy indicates crystal growth rate is less dependent on temperature (Atkins, de Paula *et al*. 2013), thus the controlling mechanism of crystallisation changes (Levenspiel 1972).

The activation energy for diffusive processes is of the order of 10 to 20 kJ mol^{-1} (Mullin 2001). As all calculated activation energies were larger than that, so it can be concluded that all measured crystallisation kinetics were driven by supercooling (rather than diffusion). However the effect of diffusion becomes more pronounced at lower temperature (Mullin 2001). As temperature decreases, two opposing effects act on the crystal growth rate (Budiaman and Fennema 1987): increased supercooling promotes faster crystal growth, due to a more rapid heat removal, whereas the simultaneous decrease of diffusion rate, due to the lower temperature that limits molecular mobility, reduces growth rate by decreasing mass transfer, for example in the movement of sucrose away from the freezing surface. The relevant importance of these two effects will determine the actual velocity of crystal growth. This is in good agreement in various reported studies e.g. in ethylene glycol (Teraoka, Saito *et al*. 2002) or in pure water (Pruppacher 1967).

In addition, increasing concentration has indicated a possible slope decrease and thus a decrease in activation energy as well. At lower concentration, the growth rate is more sensitive to the crystallisation temperate (Atkins, de Paula *et al*. 2013).

4.3.2 Effect of CMC: viscosity

The effect of temperature and viscosity on ice crystal growth rate was studied. The viscosity of the system was changed by adding cmc while maintaining the water content constant (at 40%, as described in section 3.2.3).

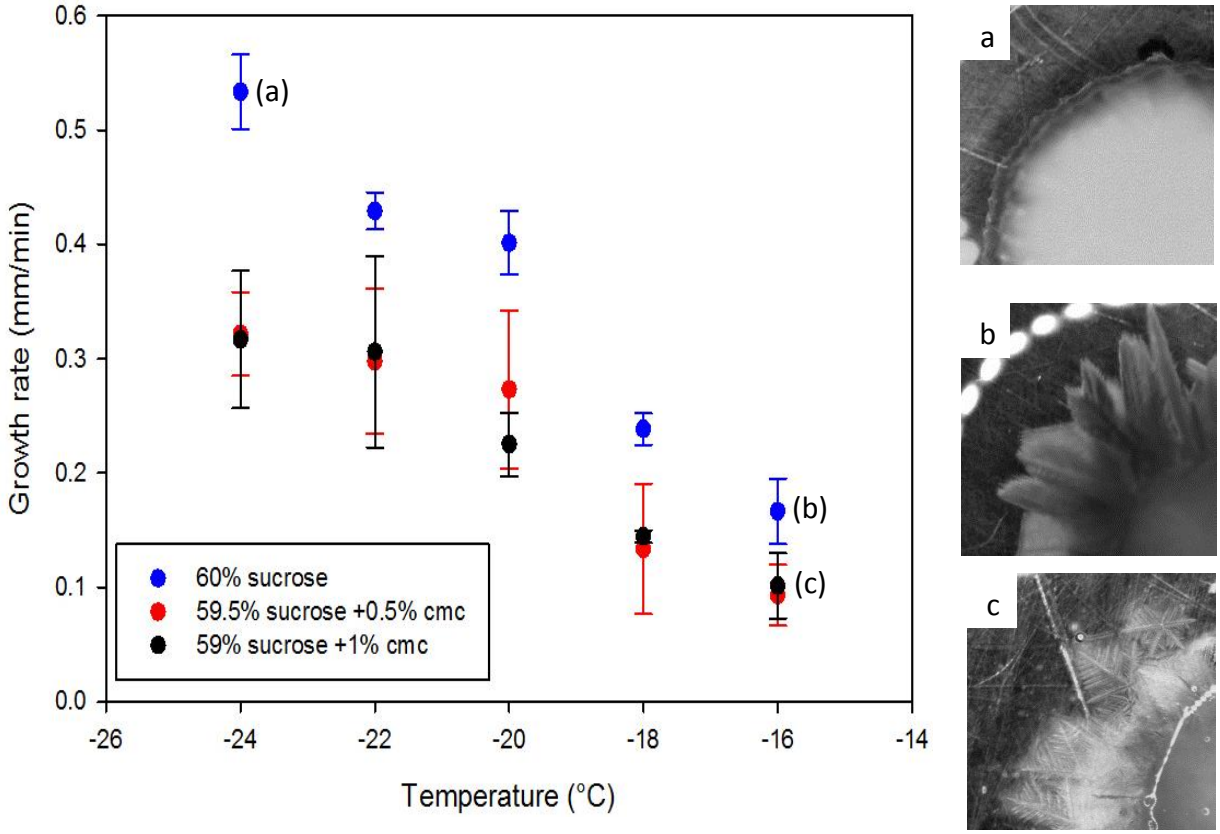

Figure 4-22 Effect of temperature and viscosity (addition of CMC) on growth rate of ice crystals from sucrose solutions of 40% water; image (a): Zoom-in images of ice crystals developed from 60% sucrose solutions at -24°C (13°C supercooling); (b): image of ice crystals developed from 60% sucrose solutions at -16°C (5°C supercooling); (c): image of ice crystals developed from 59.5% sucrose and 0.5% cmc solution at -16°C (5°C supercooling). Image width: 4mm. Results are averages of triplicated results, and error bars represent ± one standard deviation.

Figure 4-22 shows that the growth velocity increases with decreasing temperature for all investigated systems. For the 60% sucrose system, the slope decreased by 50%, from 0.4 mm/min/°C to 0.2 mm/min/°C, as the temperature fell below -20°C, however more work is required to confirm this trend.

At all investigated temperatures there is a decline in the crystal growth rate with CMC addition. Adding 0.5% or 1% CMC did not show a major difference in terms of crystal growth kinetics; the addition of CMC resulted in a 40% decrease of growth rate from 0.4 mm/min to 0.25 mm/min at 20°C.

At different growth rate, different crystal shapes were also observed. Fig. 4-22 shows indicative microscope images of crystal patterns when crystallisation was carried out at different temperatures in the 60% sucrose systems. Figure 4-22 (a) was obtained when crystallisation occurred at high supercooling (low temperature, -24°C), and shows crystals with smooth and round edges. Slower crystallisation (higher temperature, -16°C) resulted in dendritic crystal patterns (Figure 4-22 b), typical of ice crystals (Ablett, Izzard *et al*. 1992). The decreased crystal growth rate in system with CMC addition also resulted in a more dendritic crystal structure (Figure 4-22 c).

Different crystal shapes at different degrees of supercooling has also been reported by Hindmarsh *et al*. (Hindmarsh, Russell *et al*. 2005). The authors observed dendritic crystals in 20% sucrose solutions when the supercooling was 13.5°C while a cellular structure was obtained at 18°C of supercooling.

Similar observations have also been reported for crystallisation of polyethylene polymer from melt, with low temperatures leading to spherilites (smooth rounded structure) and high temperature resulting in axialites (dendritic structure)(Sperling 2005).

4.3.3 Comparison of sucrose solutions with gum arabic solutions

To study the effect of solute on crystal growth kinetic, gum arabic was used as an investigated system, as its high solubility allows 60% solution to compare with sucrose and it has much higher molecular weight (342 g/mol for sucrose and 10^5-10^6g/mol for gum arabic (Renard, Lavenant-Gourgeon *et al*. 2006).

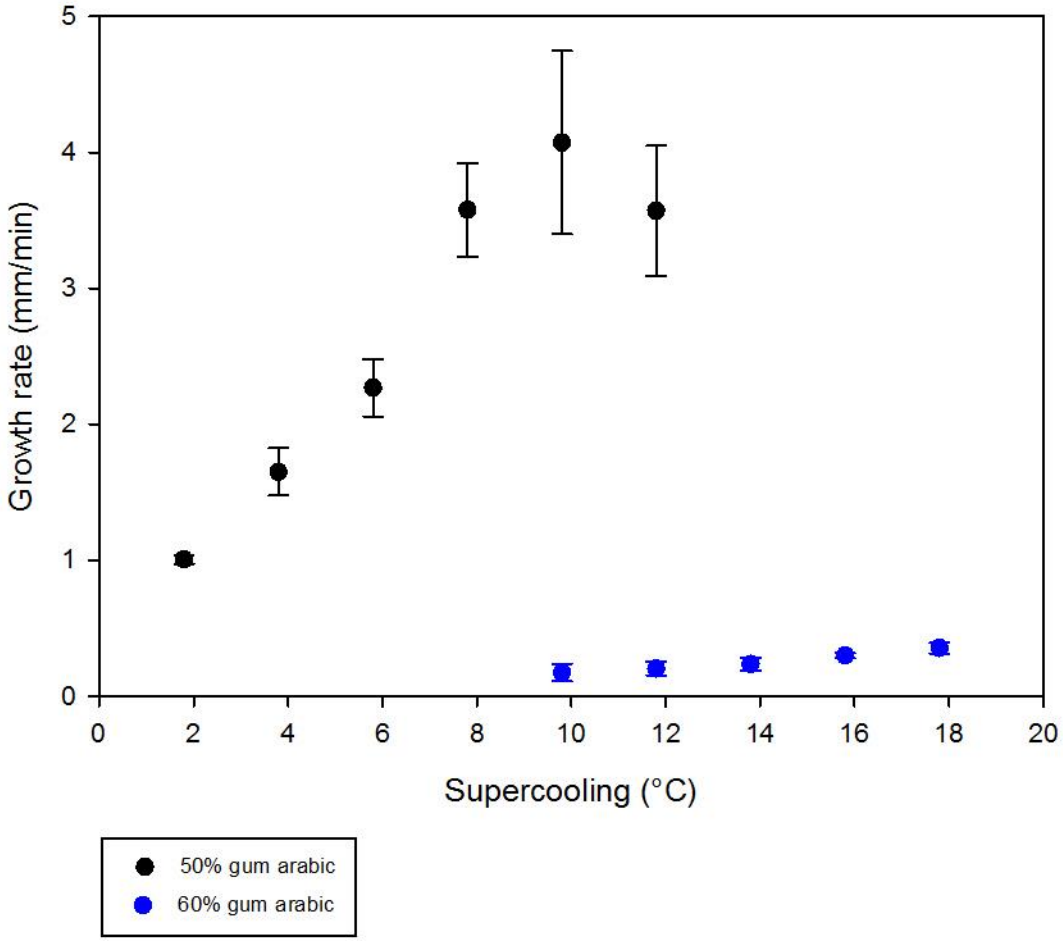

Figure 4-23 effect of concentration on ice crystal growth rate in gum arabic solution. Results are averages of triplicated results, and error bars represent ± one standard deviation.

Using the same method, crystal growth kinetics was studied in gum arabic solutions. Growth rate at different crystallisation temperatures in 50% and 60% gum arabic were shown in Fig.

4-23. The Equilibrium freezing temperature of gum arabic (T_m=-6.2°C) for supercooling calculation was obtained from the literature (Mothé and Rao 2000).

At 50% gum arabic, crystallisation was observed at supercooling of 2°C and crystals grew at a rate of 1mm/min. In 60% systems, the minimum level of supercooling required for ice crystals to grow was 10°C.

For 50% gum arabic solution, when the supercooling level increased from 2°C to 10°C, growth rate increased monotonically, while further temperature decrease appeared to have little effect on the growth rate, albeit within experimental error. This may indicate a change in the limiting step of crystallisation from supercooling-controlled to diffusion-controlled. Growth rate reached the maximum value of 4mm/min at 10°C supercooling.

Increasing solid concentration to 60% slowed down crystal growth significantly to values below 1mm/min. In 60% gum arabic system, when the supercooling level increased from 10°C to 18°C, the growth rate appeared to increase, however maintaining low (<1mm/min) values compared to the 50% solution.

Growth rate in two systems: sucrose and gum arabic were compared at same concentration (50 and 60%) in Figure 4-24.

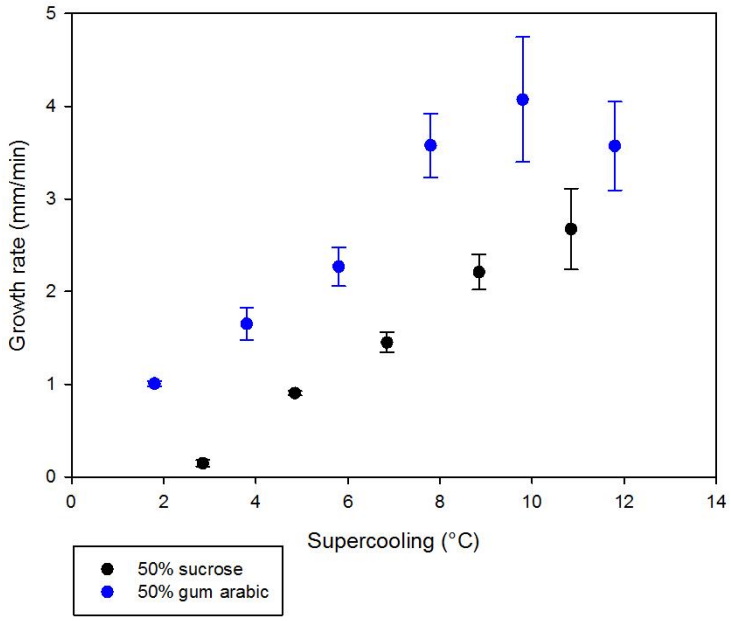

a

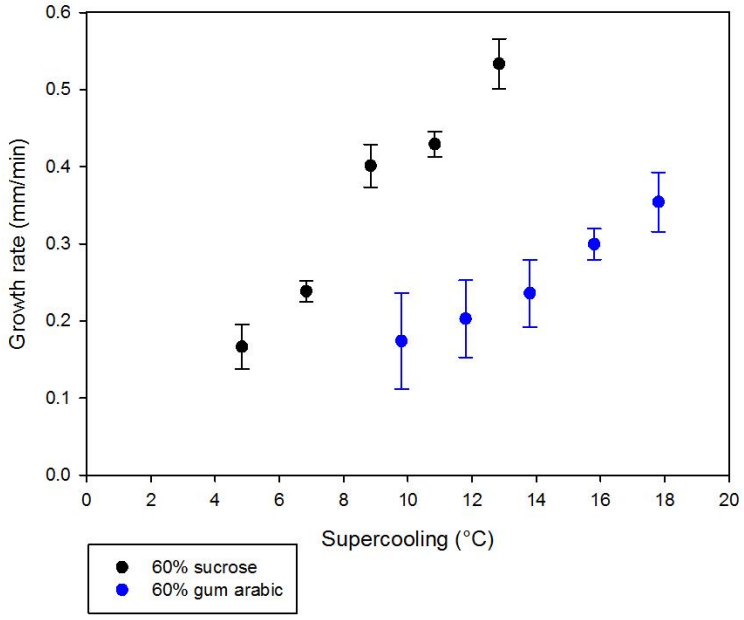

b

Figure 4-24 Effect of different solute (sucrose and gum arabic) on nucleus-induced crystallisation growth rate in (a) 50% and (b) 60% system. Results are averages of triplicated results, and error bars represent ± one standard deviation.

Figure 4-24 compares crystal growth rates of sucrose and gum arabic systems at 50 (Figure 4-24 a) and (Figure 4-24 b) 60% solids system.

For the 50% systems (Fig. 4-24 a), sucrose crystallised slower (by 1mm/min) than gum arabic at same level of supercooling. Sucrose is reported to be more effective in terms of slowing down water crystallisation than other hydrocolloids (Budiaman and Fennema 1987). And as gum arabic has a much higher molecular weight (10^5-10^6g vs 342), at the same concentration, there is a smaller number of gum arabic molecules in the solution.

Interestingly, at 60% concentration, the opposite effect was observed and the growth rate of gum arabic was always slower than that of sucrose with a difference of around 2mm/min.

This might result from the high viscosity of the highly concentrated gum arabic system, and the existence of large number of air bubbles (at this concentration it was impossible to free the system of all air bubbles). Molecular mobility is limited in high viscous systems and thus crystal growth is retarded. Air bubbles, may delay water crystallisation in two ways: (1) air bubbles in the system slows down the rate of heat transfer due to poor thermal conductivity (Sofjan and Hartel 2004); and (2) they will physically take the space in solution which might slow down mass transfer.

4.3.4 Some observations from the microscope experiments

As well as uniform growth as discussed above, a number of different effects were seen in visualisation experiments.

4.3.4.1 Secondary nucleation

Figure 4-25 shows experiments for 60% solutions at -18 ˚C, in which numerous small nuclei formed in the droplet near the added nucleus (in Figure 4-25) and crystal growth followed both from the added nucleus and the from smaller nuclei. This additional nucleation did not occur often, but shows that the solution could form multiple nuclei.

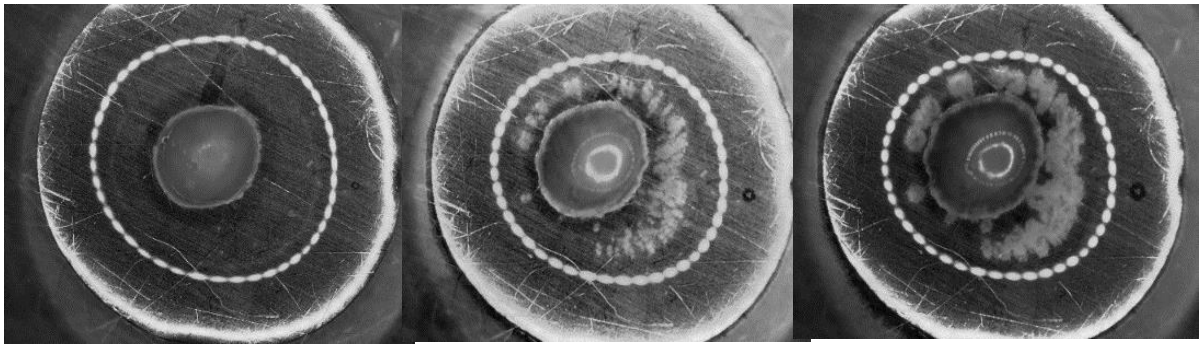

Figure 4-25 microscope images of 60% sucrose solution after adding an ice nucleus at -18˚C

4.3.4.2 Delayed growth on the surface

In Figure 4-26, for 59% sucrose and 1% cmc system, crystal growth was slowed down by the high viscosity as a result of cmc addition. A lower layer of crystal has formed, giving two crystal fronts. Crystal at bottom of droplet grows faster than crystal on the top. This might result from the temperature gradient in the droplet. The bottom sample close to the cooling stage is colder while sample surface is warmer as it contacts the air. This tpe of behaviour was seen in the highest viscosity solutions, of both gum arabic and cmc, and thus suggests that for very slow growth rate, the effect of temperature gradient is significant.

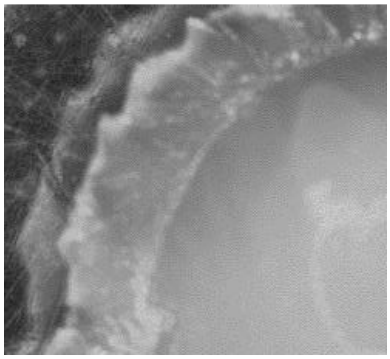

Figure 4-26 image of crystal growth in 59% sucrose and 1% cmc solution at -22˚C. Image width: 4mm.

4.3.4.3 Insufficient supercooling to induce crystal growth

In some cases no crystallisation took place. Figure 4-27 shows 60% sucrose after adding ice nucleus at -15 ˚C. No crystal growth can be seen when the sample was held at -15 ˚C for 7 minutes after adding the ice nucleus. Crystal growth does not take place when the supercooling level is not high enough, even though the crystallising temperature is lower than equilibrium freezing temperature.

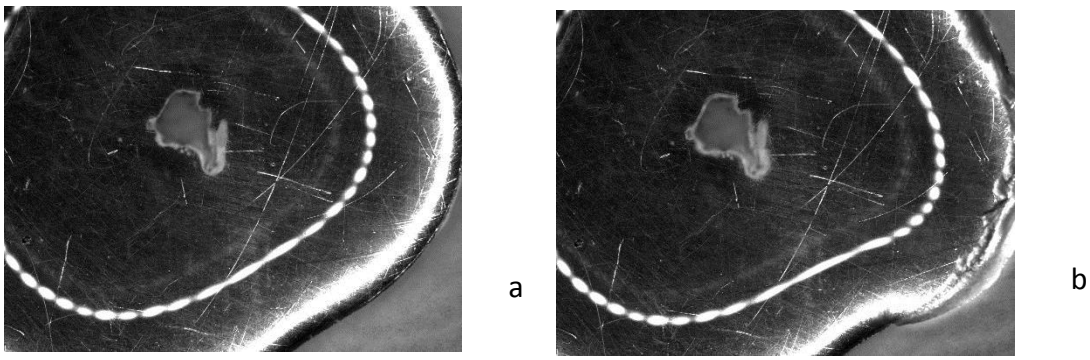

Figure 4-27 microscope images of 60% sucrose at -15 ˚C (a) 0 minute after adding ice nucleus and (b) 7 minutes after adding ice nucleus

4.3.4.4 No crystal growth in 70% sucrose solution

For 70% sucrose solution, crystal growth failed to be observed even with ice nucleus addition at -25 ˚C. The temperature is lower than its equilibrium freezing temperature, but the high concentration limits crystallisation.

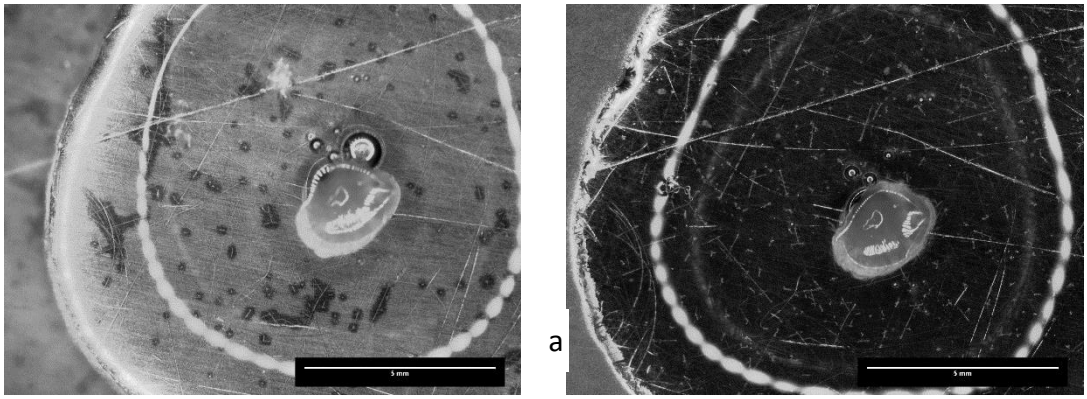

a b

Figure 4-28 microscope image of 70% sucrose at -25˚C (a) 0 minutes after adding ice nucleus and (b) 30 minutes after adding ice nucleus. The colour change (from light to dark) between two images was due to frost condensation between glass slide and peltier surface.

4.3.4.5 Sucrose-induced crystal growth

Sucrose crystal was added into 60% sucrose at -16 ˚C to induce water crystallisation;

however no crystal growth occurred after the addition.

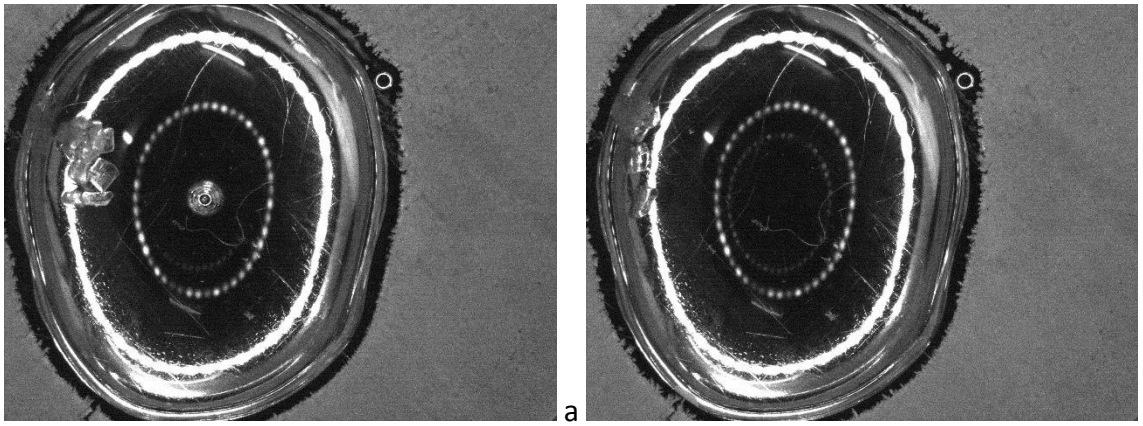

a b

Figure 4-29 microscope image of 60% sucrose solution cooled to -16˚C and (a)0 minute after adding sucrose as nucleating site (b) 3 minutes after adding sucrose.

4.3 Conclusions

DSC was used to measure enthalpy change. Increasing solid content (20% to 60%) resulted in delayed water crystallisation (more supercooling needed) and less enthalpy change (less ice crystal formation). The linear decrease of enthalpy change as solid concentration increases fit well into the reported model. Maximum freeze concentration that estimated from experiments is 76%, in good agreement with literature.

Increasing both in cooling rate and concentration might result in no crystallisation nor devitrification in the sample, as in the experiment of 70% sucrose with a cooling rate of 30˚C/min.

Annealing was conducted for 60, 65, and 70% sucrose. More ice formation was achieved after annealing, and was identified in different ways: increased glass transition temperature (in 60% sucrose); increased enthalpy change (in 65% sucrose); and the appearance of melting peak (in 70% sucrose).

Ice crystals were identified in XRD scan during freezing 60% sucrose solution, and a change in the crystal form (cubic to hexagonal) was seen during reheating.

When cooling rate at 6 ˚C/min, crystal form transition can be seen even at 20% sucrose during reheating.

Overall DSC and XRD show good agreement in studying water crystallisation. DSC provides information including phase transition temperature (crystallisation, devitrification, melting and glass transition), and value of enthalpy change for the first-order phase transitions; while XRD makes it possible to identify the crystal form and monitor crystal form transition.

Cryo-ESEM was used to observe frozen 30% sucrose solution and ice crystals and freeze concentrate were noticed.

Optical microscopy proved that it was difficult for water to crystallise into ice spontaneously even with 9 ˚C supercoolong. However, at the same condition, adding an ice nucleus induced water crystallisation. Crystal growth kinetics were studied using same method, and the effect of concentration, supercooling, viscosity examined.

For 40, 50 and 60% sucrose, crystal growth rate increased as supercooling level increased. At a given level of supercooling, growth rate reduced significantly as concentration increased (e.g. 95% reduce in growth rate when concentration increased from 40% to 60% at 7 ˚C supercooling).

The activation energy for crystal growth was calculated in 40 to 60% sucrose solutions, and the results suggests that the processes was driven by supercooling rather than diffusion.

Amounts of 0.5% to 1% cmc was added into sucrose solution to increase the viscosity of the system, while maintain the same water content at 40% (w/w). For the system with cmc addition, growth velocity increased with decreasing temperature, and each given temperature, addition of cmc resulted in roughly a 40% decrease in growth rate. 0.5% and 1% cmc did not show a major difference in terms of crystal growth kinetics. Different crystal shapes were also observed at different growth rate. Low crystallising temperatures lead to smooth and round crystal resulting from fast growth rates, while high crystallising temperature result in dendritic crystal with slow growth rate.

Gum arabic solutions were also used in crystal growth study. For 50% gum arabic solution, crystal growth rate increased (maximum 4mm/min) with up to 10 ˚C supercooling, and it

remained stable with further increase in supercooling. Growth rate in 60% sucrose was much slower (<1mm/min) and increased slowly.

The growth rate in two different systems (sucrose or gum arabic) were compared at same concentration (50% and 60%). For 50% system, growth rate in sucrose was around 1mm/min slower than that in gum arabic at same level of supercoooling. While at 60% concentration, gum arabic was slower than in sucrose with a difference of 2mm/min.

Chapter 5 Water crystallisation from highly concentrated systems containing air

Water crystallisation from non aerated highly concentrated systems was studied and discussed in Chapter 4, and it was found that increasing concentration resulted in delayed water crystallisation (lower crystallisation temperature and less ice formation).

In chapter 5, work was further conducted to understand how water crystallisation will be affected by air bubbles introduced into the system. The main material used in this chapter is coffee, as freeze drying coffee is of industrial interest, and extra air bubbles are introduced into the coffee extract before freeze drying (see section 1.1).

The effect of introducing additional amount of air to the coffee samples is also presented. In addition, some carbohydrates solutions (sucrose with cmc, and gum arabic) were aerated and used in experiments.

5.1 Spontaneous crystallisation

5.1.1 Water crystallisation studied by combined DSC and XRD

DSC and XRD techniques were used in this section to investigate phase transitions during freezing of coffee solutions. The same thermal conditions were chosen for experimental setup for both techniques to make results comparable.

5.1.1.1 50% coffee with a scanning rate of 6°C/min

Water crystallisation in 50% coffee was first studied in DSC.

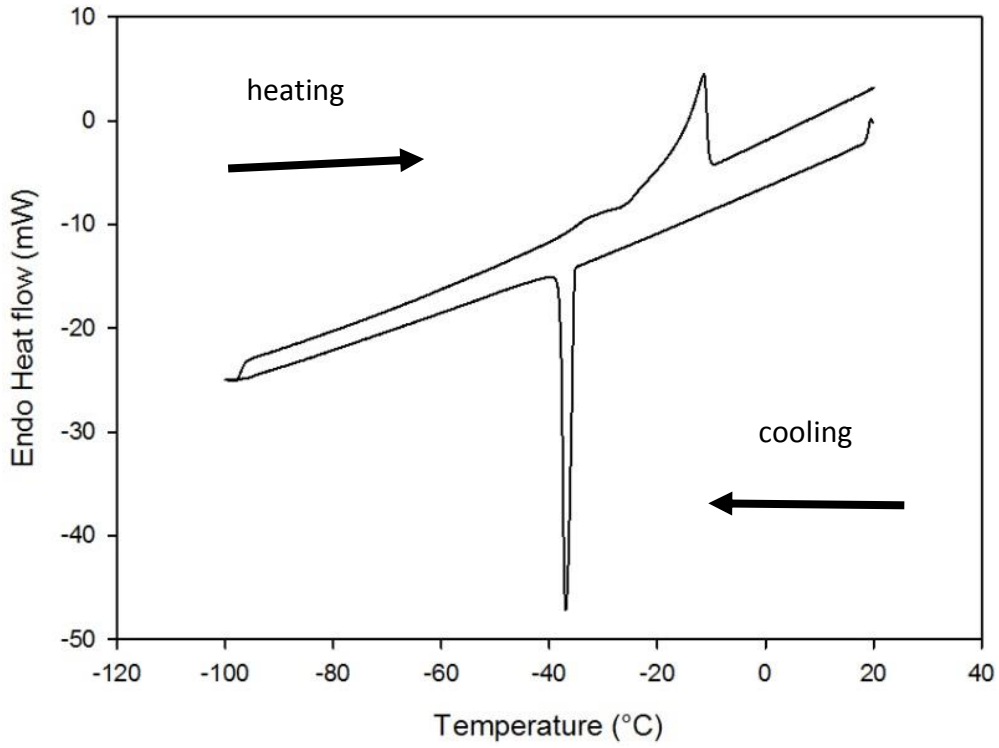

Figure 5-1 DSC thermogram of 50% coffee; sample was cooled from 20°C to -100°C then heated back to 20°C at constant scanning rate of 6°C/min. Circle indicates glass transition.

Figure 5-1 displays thermal behaviour of 50% coffee when it was cooled and heated at 6°C/min during a DSC scan. 6°C/min is the maximum cooling rate that the XRD equipment can reach. In cooling curve, an exothermal peak can be seen at -35.6°C and this refers to water crystallisation with a latent heat of -83 J/g. In section 4.1.1.1 (equation 4-1) a method was used to calculate ice fraction formed in the sample from latent heat value (Levine and Slade 1986):

Fitting the value (-83 J/g) to equation (4-1) gives an ice fraction of 25%, which suggests that 50% of the total water in the sample turned into ice crystals during cooling 50% coffee at 6°C/min.

During heating, an endothermal peak was observed starting at -15.2°C, suggests the melting of ice crystals. The area under the -15°C peak gave an enthalpy change of 80.7 J/g, which is almost the same value as the earlier crystallisation enthalpy change, indicating that the same amount of ice was formed during cooling and melted during heating.

Primary crystallisation in 50% coffee was also studied by X-ray diffraction using the same temperature profile as in DSC. The sample was first cooled to -100°C at 6°C/min then heated up at 6°C/min to 20°C. At the lowest temperature of -100°C, an X-ray scan was conducted. In addition, several more scans were obtained during heating up to -80°C, -60°C, -40°C and -30°C. Results are displayed in Figure 5-2.

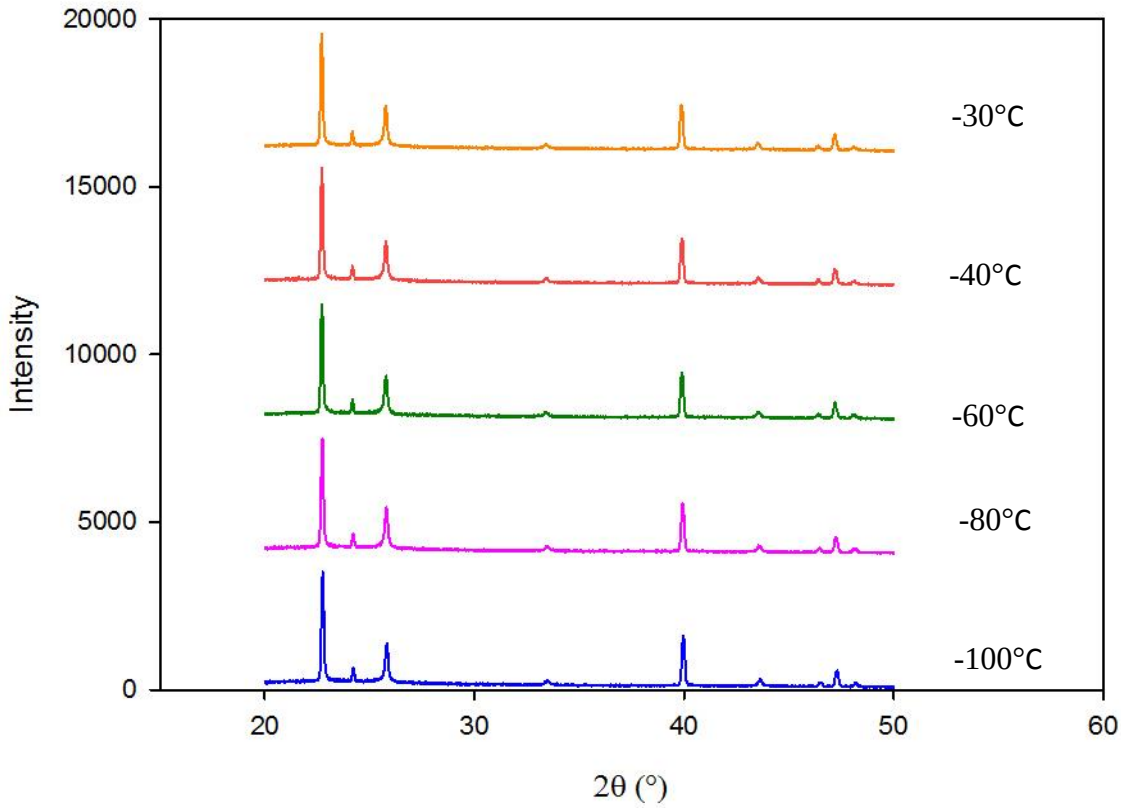

Figure 5-2 X-ray diffraction patterns of 50% coffee solutions. The sample was cooled first from room temperature to -100°C, and then heated up to 20°C at 6°C/min. X ray scans were carried out at lowest temperature -100°C, and at heating to -80°C, -60°C, -40°C and -30°C.

The first curve obtained at -100°C showed crystal peaks at 22.7°, 24.2°, 25.8°, 40.0°, 46.4° and 47.2°, and these crystal patterns match those of ice crystals (Dowell and Rinfret 1960) (see also section 4.1.2.1). The existence of ice crystals at -100°C was in good agreement with DSC data that ice crystals were formed during cooling.

Crystal peaks obtained at higher temperatures showed exactly the same pattern, which means that the same crystal form persisted during heating to -30°C and there was no transformation to more hexagonal ice. As the temperature was lower than its melting temperature (-15.2°C from DSC in Figure 5-1), ice crystals remained in the sample.

5.1.1.2 70% coffee with a scanning rate of 6°C/min

Water crystallisation from 70% coffee was also investigated in DSC and XRD. This was the highest concentration used in this chapter, higher than the highest concentration for sucrose in chapter 4 (60%).

Thermal behaviour of 70% coffee when cooling and heating at 6°C/min was shown in Figure 5-3.

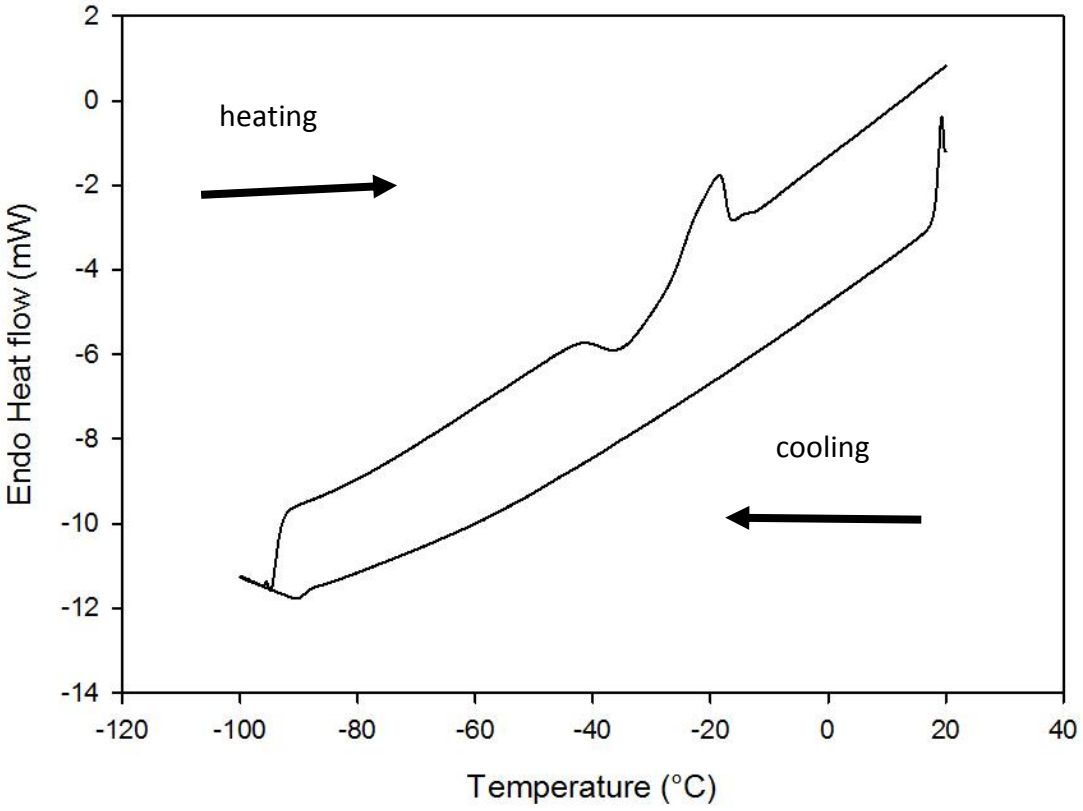

Figure 5-3 DSC thermogram of 70% coffee when it was cooled to -100°C and then heated to 20°C at 6°C/min (again identify curves).

At cooling rate of 6°C/min from 70% coffee solutions, there was no exothermal peak observed during cooling, suggesting that no water crystallised into ice crystals. During heating, there was an exothermal peak at -42°C which refers to water crystallisation, followed immediately by an endothermal peak which corresponds to melting.

The phenomenon where water does not crystallise during cooling but crystallises during heating is called devitrification (Roos 1995). This often takes place in high concentration systems or as a result of a fast cooling rate (see section 2.1.3, also see results of sucrose in section 4.1.1.2).

Primary water crystallisation from 70% coffee was also investigated via X-ray diffraction. A sample of 70% coffee was cooled from room temperature to -100°C and then heated up to 20°C at 6°C/min (same temperature profile as the DSC study in Figure 5-3). Several scans were conducted at lowest temperature at -100°C, and during heating at -55°C, -50°C, -40°C, -35°C, -30°C and -20°C (Figure 5-4).

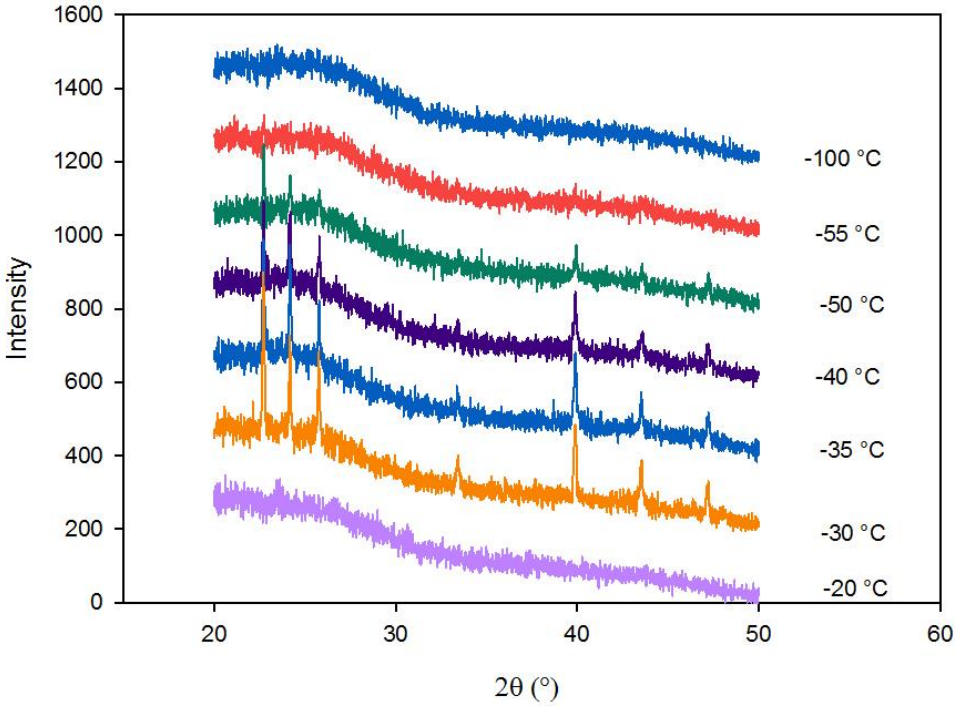

Figure 5-4 X-ray diffraction patterns of 70% coffee during heating the rapid frozen sample at 6°C/min

No crystal patterns can be seen in the curve for -100°C or -55°C, indicating that no water crystallisation was detected by XRD when the 70% coffee was frozen to -100°C and then heated to -55°C. The rapid frozen sample is in an amorphous glassy state, which means water is not crystallised (Roos 1995).

Further heating to -50°C resulted in the appearance of peaks in the pattern of 22.7°, 24.1°, and 39.9°, which can be identified as ice crystals (Dowell and Rinfret 1960). As sample temperature kept increasing till -30°C, more crystal peaks were identified in the curve (identical ice crystal patterns) (Dowell and Rinfret 1960). The peak intensity increased as well; for instance, the peak at 22.7°, with highest intensity, increased from 193 to 448 unit intensity from -50°C to -30°C, suggesting an increase in the amount of ice crystals formed in the sample. It was concluded that water in the amorphous matrix started to crystallise at -50°C, and more crystals were formed as temperature increased to -30°C. The I_{44}/I_{40} value calculated from these four curves (-50°C, -40°C, -35°C, -30°C) gave constant value of 0.57, indicating that no crystal form transitions took place (see section 4.1.2.1 for the discussion about the I_{44}/I_{40} ratio and crystal form transitions). The value is in the range of 0-0.8, suggesting the ice crystals in the sample is a mixture of hexagonal ice and cubic ice (Murray, Knopf *et al*. 2005). There was no crystal patterns on the curve obtained at -20°C, as ice melted to water at this temperature before scanning took place.

The phase transitions monitored by XRD for the 70% coffee system were in good agreement with the DSC study. There was no crystallisation during freezing and devitrification and ice melting occurred during heating.

5.1.2 Small angle scan X-ray diffraction to monitor phase transitions

Phase transition temperature can be detected by monitoring the change of the diffraction intensity at a given angle (Egawa, Yonemochi *et al*. 2005). In this section, effort has been made to monitor ice formation temperature during heating of 70% coffee via X-ray diffraction. Due to limitations of the equipment's software, this could only be achieved by narrowing the scanning angle rather than fixing it. The scanning range was set between

21.5° and 23.5° to include the ice crystal peak with the highest intensity (22.7°) according to results in previous section (Figure 5-4). As a result of the equipment default setting, each scan was carried out in between 20.5° and 24.5°.

The sample of 70% coffee was:

(i) Cooled from room temperature to -100°C at 6°C/min

(ii) Heated from -100° to -63° at 6°C/min

(iii) Heated from -63°C to -30°C at 0.5°C/min, and an X-ray scan (requires 2 minutes) was carried out for every 1 °C

(iv) Once one scan was finished, the sample temperature was increased 1°C, and a new X-ray scan took place

X-ray diffraction patterns were obtained at every 1°C temperature interval, but patterns are presented at every 3°C in Figure 5-5 to demonstrate the intensity change in a clear way.

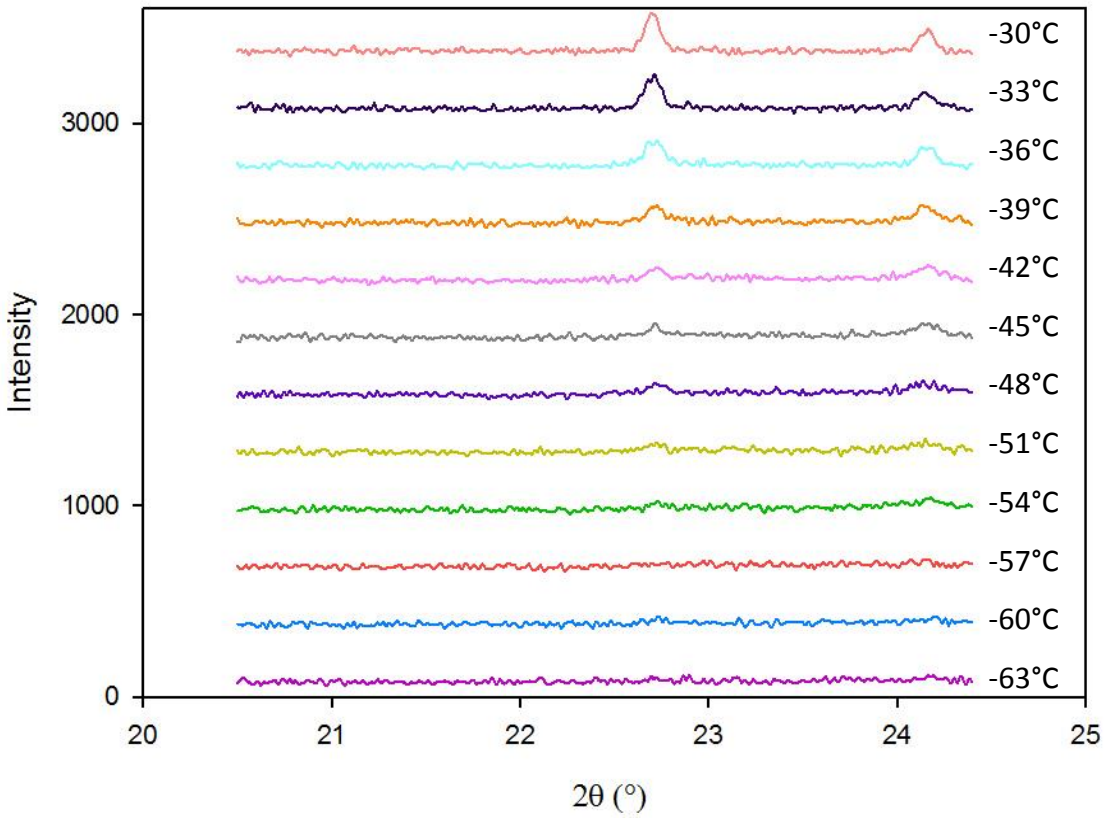

Figure 5-5 X-ray diffraction patterns scanned during heating of rapidly frozen 70% coffee.

No crystal peak patterns can be seen in the curve until the sample was heated to -57°C. Further heating (≥-54°C) resulted in the appearance and intensity increase of peaks at 22.7° and 24.1°, which corresponds to water crystallisation. The peak intensity from diffraction data at each temperature during heating are plotted in Figure 5-6.

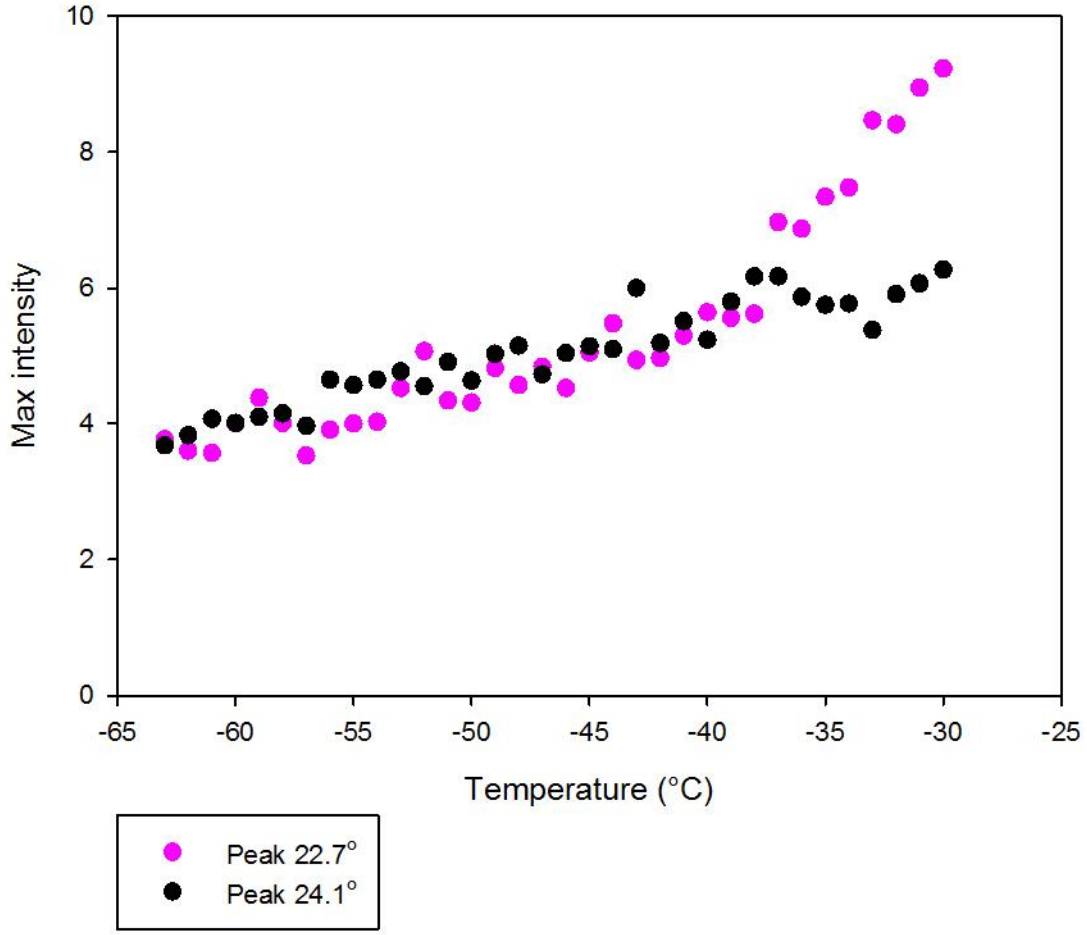

Figure 5-6 Peak intensity extracted from X-ray diffraction at each temperature during rewarming 70% coffee at two selected angle; indicating different water crystal peaks.

Both intensities for peaks 22.7° and 24.1° increased as temperature increased, which indicates that more water crystallised as the sample temperature increased. For the peak at 22.7°, the intensity increase became more significant at temperatures higher than -40°C. From -50°C to -40°C , the intensity increases from 4.5 to 5.5; while from -40°C to -30°C , the intensity increases from 5.5 to 9.Temperature of -40°C is higher than the glass transition temperature thus molecules in the system gain more mobility (Searles, Carpenter *et al*. 2001, Searles, Carpenter *et al*. 2001).

5.1.3 Enthalpy measurement during water crystallisation at different conditions

In this section, the enthalpy change of water crystallisation was measured by DSC at different conditions. The effect of a range of parameters (concentration, scanning rate, annealing temperature and time) on water crystallisation in coffee sample was studied.

5.1.3.1 Effect of concentration

Coffee solutions with 50% and 70% solids concentration were examined to study the effect of high solid concentration on water crystallisation.

A fast freezing rate of 30°C/min was used in DSC for cooling of 50% and 70% coffee (shown in Figure 5-7a) and samples were then heated to 20°C at 5°C/min (Figure 5-7b). The scanning conditions were obtained from literature (Roos and Karel 1991), and also the same as for sucrose (see 4.1.1.3).

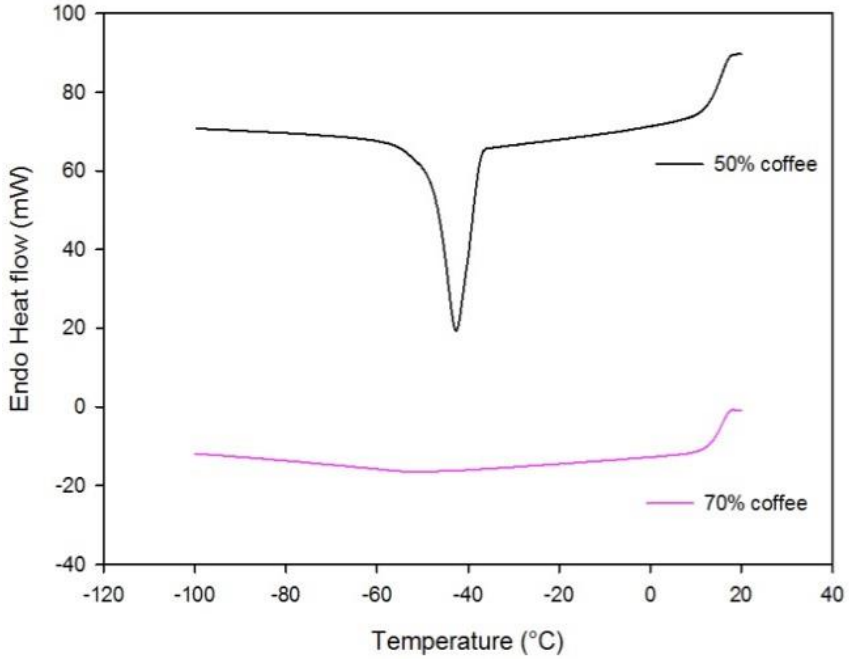

a

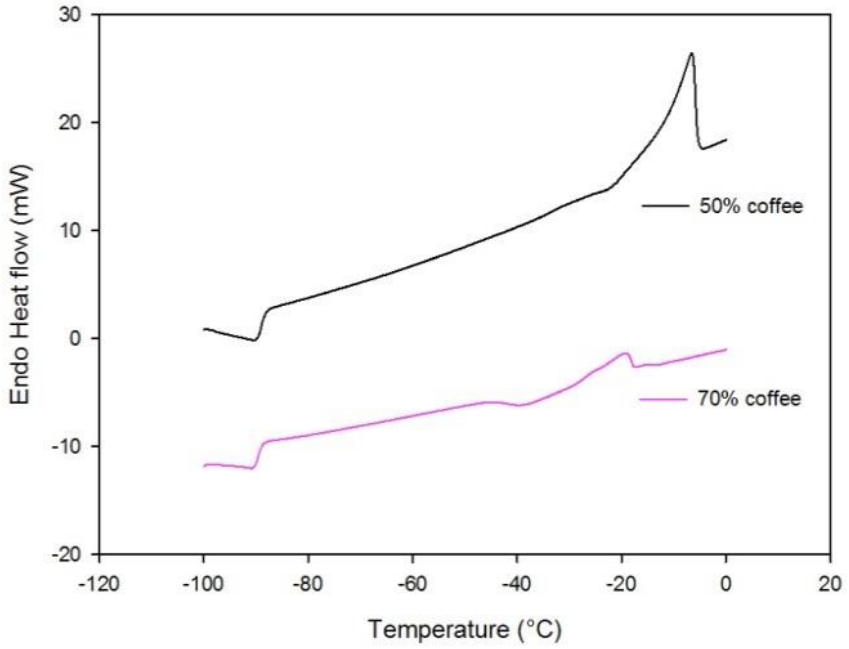

b

Figure 5-7 DSC thermogram of 50% and 70% coffee during (a) cooling at 30°C/min and (b) heating at 5°C/min

In the cooling curve of 50% coffee, there was an exothermal peak appearing at -38°C, indicating water crystallisation with the enthalpy change of -67.3 J/g. Melting took place at -7°C during heating, and latent heat is 64 J/g. Again, the nett enthalpy change of

crystallisation and melting (i.e. the sum of the two) is approximately 0 KJ/mol, which suggests that all the ice formed in the system during freezing melted during the subsequent heating (Schawe 2006).

As concentration increased to 70%, heat flow decreased and then increased gently during cooling without any exothermal peak. When the sample was reheated to above -50°C, a small exothermal peak appeared in the curve, followed by an endothermal peak. This means that devitrification took place: water crystallised into ice during rewarming of the frozen, amorphous sample. The endothermal and exothermal peaks overlapped in the curve, making it difficult to choose the temperature range to calculate enthalpy change for each phase transition.

A slower cooling/heating rate, 6°C/min was also used in DSC scanning 50% and 70% coffee (see Figure 5-8).

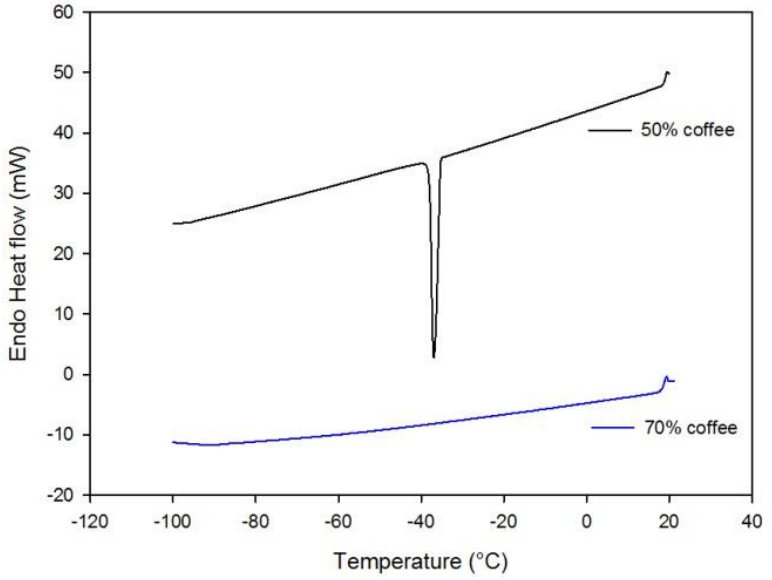

a

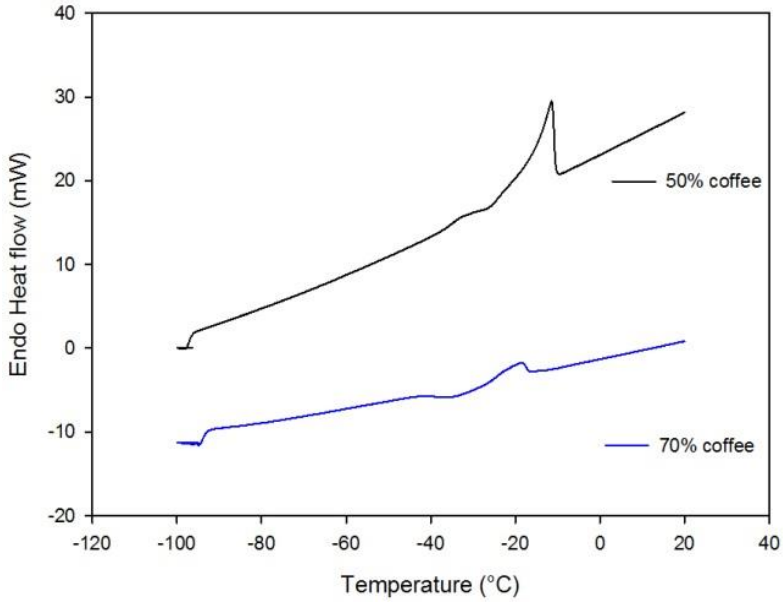

b

Figure 5-8 DSC thermogram of 50% and 70% coffee during (a) cooling at 6°C/min and (b) heating at 6°C/min

Water in 50% coffee crystallised during freezing and melted during heating (see section 5.1.1.1). Increasing solid content to 70% resulted in no crystallisation occurring during freezing. During heating to temperature above -40°C, a small exothermic peak appeared in

the curve, and followed by an endothermic peak, indicating the water crystallisation during heating of the frozen sample and then the melting of ice.

5.1.2.2 Effect of cooling rate

In this section, the effect of cooling rate (30˚C/min and 6˚C/min) was investigated. DSC cooling and heating curves for 50% coffee at different scanning rates are displayed in figure 5-9.

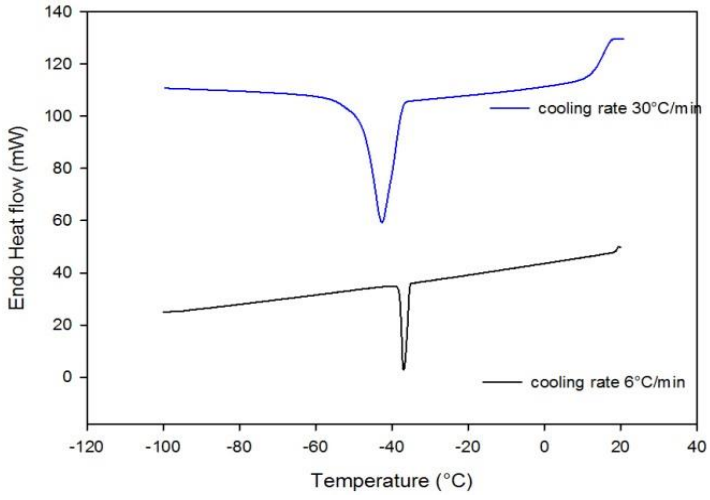

a

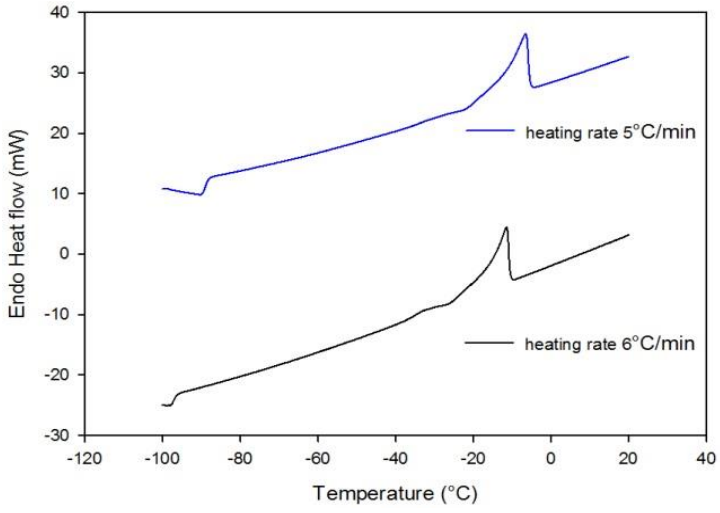

b

Figure 5-9 DSC thermograms of 50% coffee (a): cooling curves of 30°C/min and 6°C/min; (b): heating curves of 5°C/min and 6°C/min

Water in 50% coffee crystallised at each freezing rate, but the onset temperature of crystallisation decreased from -35°C to -38°C when cooling rate increased from 6 °C/min to 30°C/min. Fast scanning rate also broadened the crystallisation peak, and resulted in a smaller amount of ice crystald formed (enthalpy change decreased from -83 to -67 J/g).

Figure 5-10 displays the thermal behaviour of 70% coffee at different scanning rates.

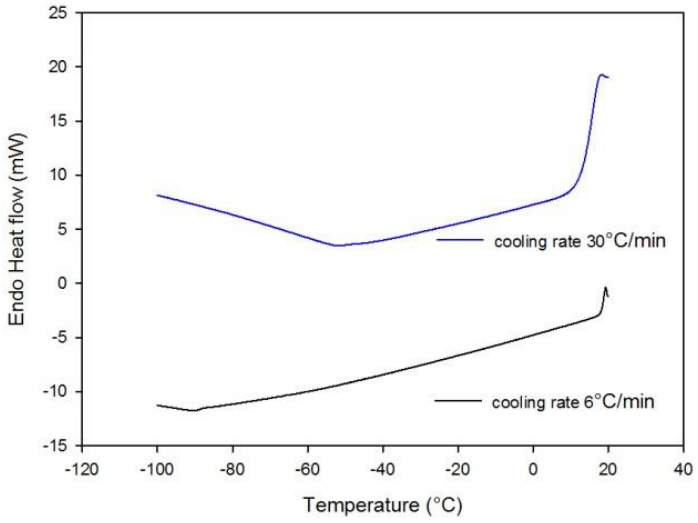

a

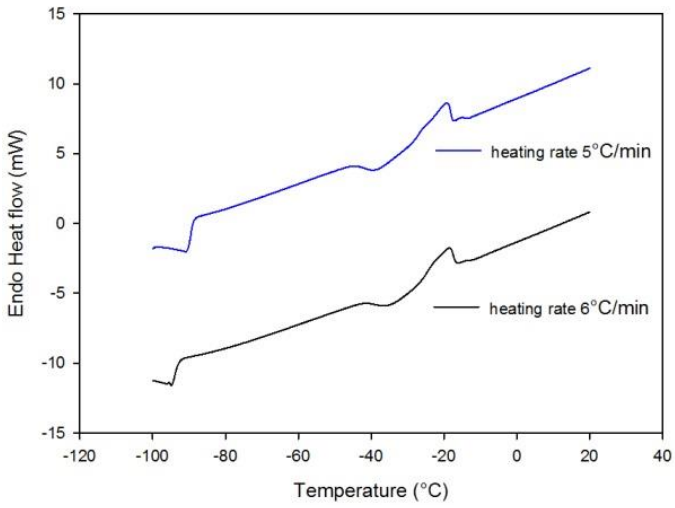

b

Figure 5-10 DSC thermograms of 70% coffee (a): cooling curves of 30°C/min and 5°C/min; (b): heating curves of 5°C/min and 6°C/min

There was no crystallisation detected during cooling at 30°C/min or 6°C/min. Endothermal melting took place immediately after the exothermal crystallisation (devitrification) during heating of the sample. As the crystallisation and melting peak interfered with each other, it is difficult to obtained the peak area thus enthalpy change of the crystallisation.

Increasing freezing rate caused delayed water crystallisation in 50% coffee: water crystallised at lower temperature and less ice crystals were formed. For 70% coffee, it was not obvious to see the difference in water crystallisation as the freezing rate increased, as it is difficult to crystallise water in both freezing rate.

5.1.3.3 Effect of annealing temperature

The difficulty of crystallising water from 70% coffee was discussed in previous context (section 5.1.1.2) and the effect of annealing to produce ice crystals in 70% coffee is investigated in this section.

As discussed in chapter 2, and shown in chapter 4 for sucrose, annealing can be used during freezing to promote water crystallisation, and is a possible way to obtain maximum ice formation (Roos and Karel 1991) (see phase diagram in section 2.1.5.2). During annealing, the sample was first frozen rapidly then heated to the annealing temperature ($T'g<T_{anneal}<T'm$) and held there for a certain period of time to allow water crsytallisation to happen (see section 2.2.2) (Ablett, Izzard *et al*. 1992, Egawa, Yonemochi *et al*. 2005). The annealing temperature should be set between T'm and T'g. When the sample is higher than T'm, ice might melt and dilute the unfrozen state; while at temperature lower than T'g, the viscosity is so high (could be at a magnitude of 10^{12}Pa s) for crystallisation to take place (10^{8}Pa s for ice formation to occur according to literature) (Luyet and Rasmussen 1967).

Several annealing temperatures between -45°C to -25°C were applied (for an annealing time of one hour) to investigate their effect on water crystallisation. Heating curves of annealed samples, together with a heating curve of a non-annealed sample, are displayed in Figure 5-11. The temperature profile used in this experiment is similar with that in Figure 4-7, section 4.1.1.4.

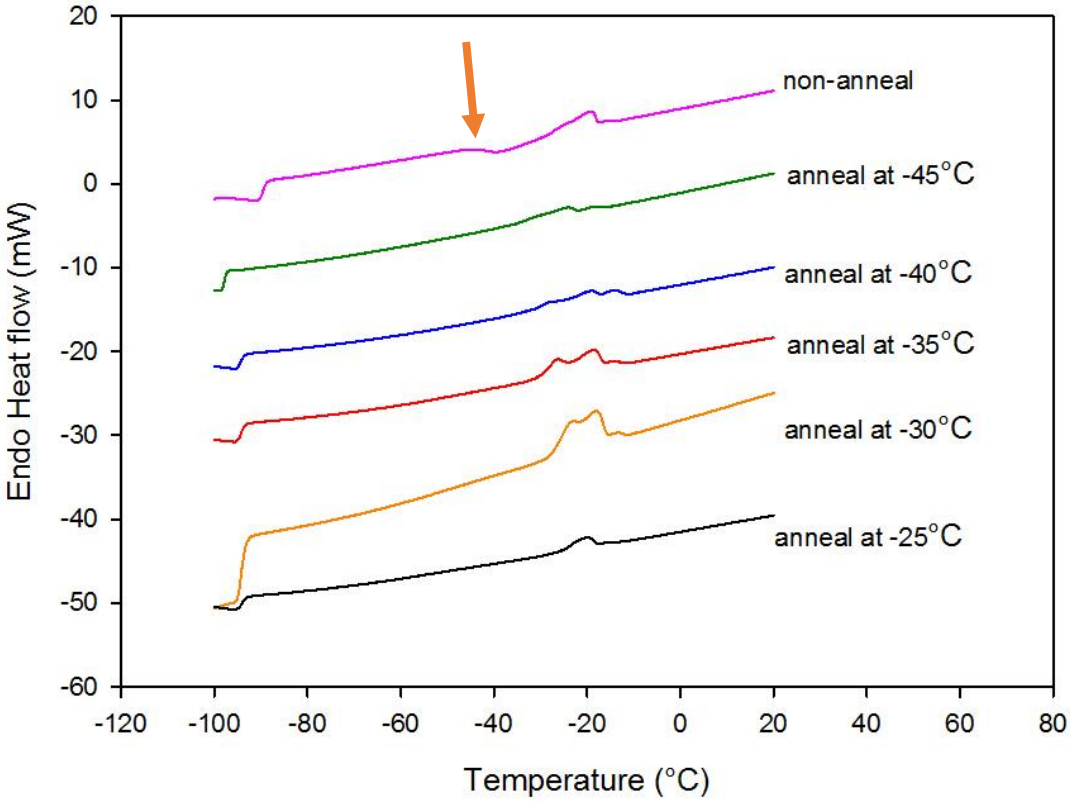

Figure 5-11 Heating curve of 70% coffee at 5°C/min after sample was annealed at different temperature for one hour. Arrow indicates devitrification peak.

Devitrification only occurred in the heating curve of the non-annealed sample at -42°C (indicated by an arrow). For the other five heating curves of annealed samples, only a

melting peak but no crystallisation peak can be seen during heating, which means water crystallisation took place before heating, probably during annealing (Roos and Karel 1991).

The area and number of melting peaks increased first when the annealing temperature increased from -45°C to -30°C (enthalpy increased from 4 to 37 J/g); however further increase in the annealing temperature to -25°C resulted in a single melting peak and smaller peak area (7 J/g enthalpy change). These results were in good agreement with reported literature that the amount of ice formation during annealing depends on the temperature difference between T_{anneal} (annealing temperature) and T'g (glass transition temperature of maximum freeze concentration). When T_{anneal} is lower than T'g, more ice will be formed as annealing temperature increases. However, further increase of annealing temperature resulted in a decrease of the ice formation (Ablett, Izzard *et al*. 1992).

Glass transition took place at -51°C in the non-annealed sample, while all the annealed samples showed glass transition temperature higher than -40°C (ranging from -35°C to -26°C). The glass transition temperature increase can be used as a sign of ice formation in the sample after annealing (Ablett, Izzard *et al*. 1992, Roos 1995). As more water crystallised into ice, the solid concentration of the unfrozen system increased, and as a result, glass transition temperature increased (Sahagian and Goff 1994).

Water crystallisation after 1 hour and 3 hour of annealing at a given temperature (-25°C) was studied and is displayed in figure 5-12.

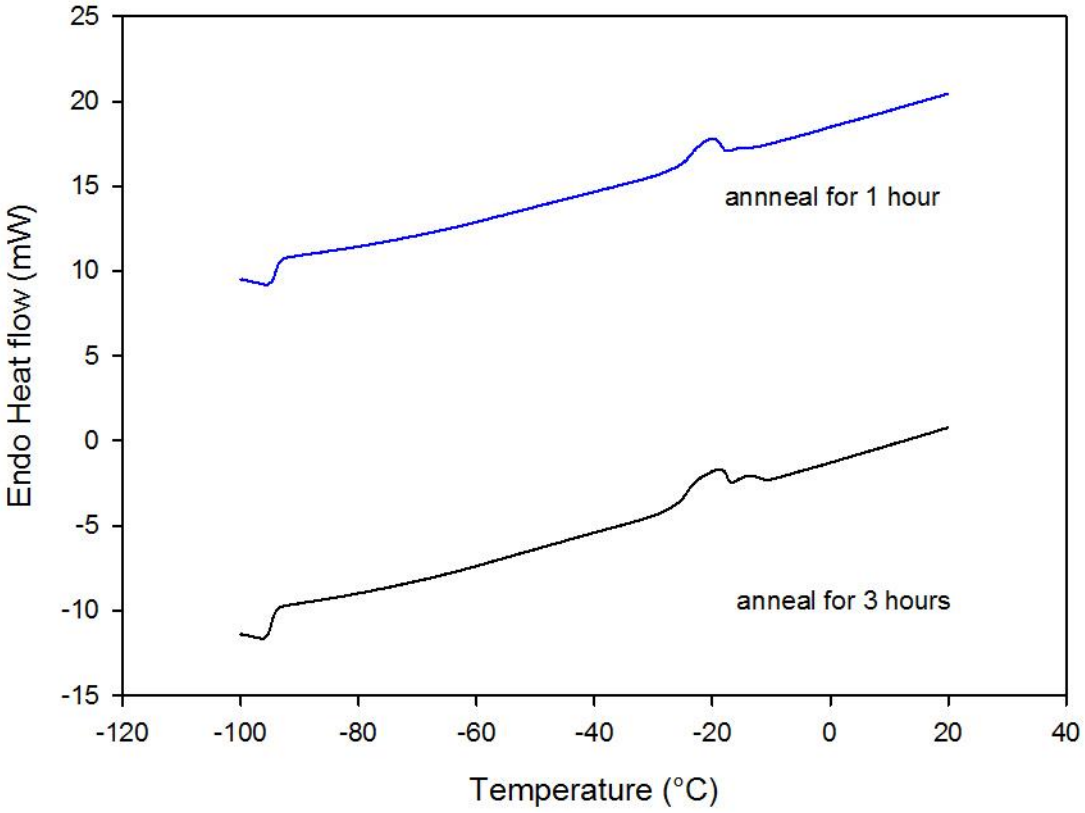

Figure 5-12 Heating curve of 70% coffee at 5°C/min after sample was annealed at -25°C for different time.

Endothermal peaks were seen during heating at approximately -24°C, identified as melting of the ice that formed during annealing. There were two peaks overlapping each other in the heating curve of sample after 3 hour annealing, and the peak area (10 J/g) was 30% larger than that for the sample after 1 hour annealing (7 J/g). It could be concluded that a longer annealing time led to larger enthalpy change, as ice formation was a time-dependant phenomenon (Roos 1995, Inoue and Suzuki 2006).

5.1.3 Visualising spontaneously formed ice crystals via cryo-ESEM

Frozen coffee sample with 30, 50 and 70% solid content were examined via cryo-SEM in this section. Details of sample preparation are displayed in section 3.5.3

5.1.3.1 30% coffee

Cryo-ESEM images of frozen 30% coffee at different magnifications are displayed in Figure 5-13.

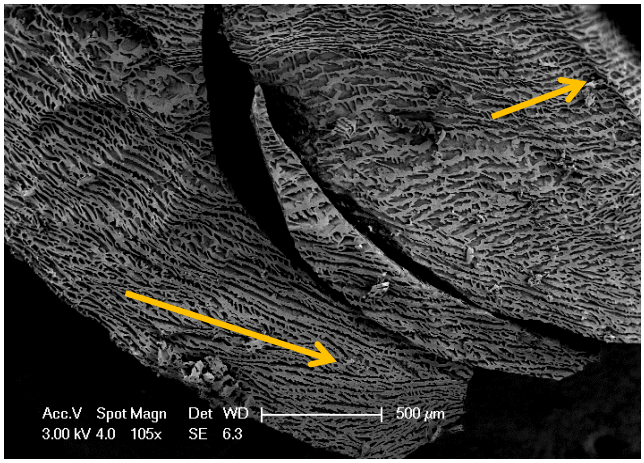

a

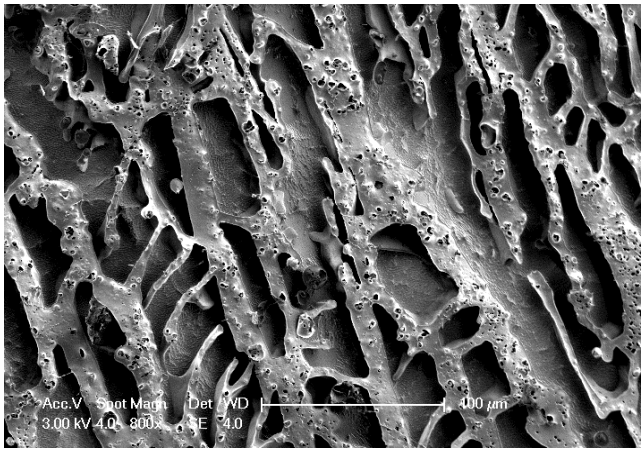

b

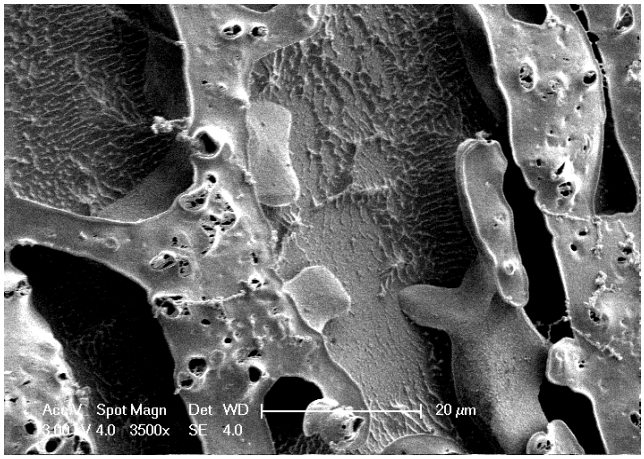

c

Figure 5-13 cryo ESEM image of frozen 30% coffee; yellow arrows in 5-13 (a) indicate the orientation of ice crystal pores

Figure 5-13 (a) shows the overall view of whole sample fracture plane. Numerous dark areas (size >20µm) can be seen in the sample, which refer to the pores left by ice sublimation.

Etching was conducted for 5mins at -95˚C (see section 3.5.3) to remove the frosted ice, which was formed during sample transfer, when the cold sample was exposed to the humid air. Frosted ice usually shows a typical 'cauliflower' shape above the sample in the cryo-SEM. The same etching conditions were used in all samples to allow the sublimation of frosted ice and visualisation of ice in sample. However, the ice crystals of this sample also sublimated. The ice crystal voids are homogenously dispersed throughout the fracture plane in Figure 5-13. In addition, it seems that ice crystals were oriented to certain directions (examples indicated by yellow arrows). This is probably due to (1) the favourable crystal growth direction (2) temperature gradient in the sample during cooling (Deville, Adrien *et al*. 2013).

A closer look at the sample is shown in Figure 5-15 (b). Dendritic voids can be seen, indicating the original dendritic ice crystal shape before sublimation. The inner surface of the voids is not smooth (Figure 5-15 c), possibly due to mechanical squeezing from ice to the solid content as water crystallised. During freezing, when water crystallises into ice, it tends to exclude solids instead of trapping it as inclusions (Hobbs 1974). Ice expands on freezing and thus the solid content become more concentrated and is rejected by ice to edge of ice crystals. (Hindmarsh, Russell *et al*. 2007). Mousavi *et al* (2007). studied the microstructure of meat and vegetables before/after freezing, and reported meat fibre shrinkage and carrot cell damage after freezing for similar reasons of ice expansion.

5.1.3.2 50% coffee

Figure 5-14 shows ESEM images of frozen 50% coffee.

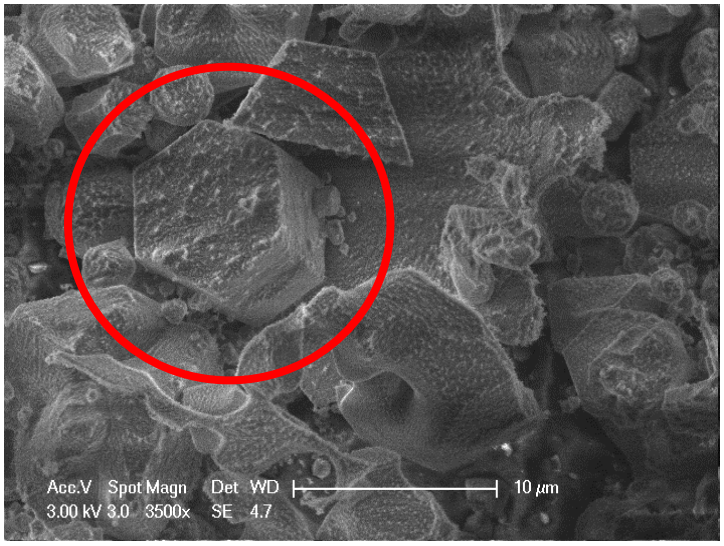

Figure 5-14 cryo ESEM image of frozen 50% coffee after 5 minute etching; circle indicates the ice crystal.

The sample was also etched for 5 minutes (at -95°C) before being examined. A hexagonal shape with a diameter of <10 µm can be seen (identified by a circle), possibly representing an ice crystal. Many ice crystals display hexagonal shape and this is linked with the hexagonal symmetry of the molecular lattice (Hobbs 1974). There is no hexagonal shape seen in 30% coffee sample in Figure 5-13, possibly because that several of them were linked together and after sublimation no hexagonal shape of single ice crystal can be identified.

The same sample was further etched for 30 minutes to remove all the ice in the sample and coated with gold for better visualisation of the solid structure. Images after ice sublimation and coating are shown in Figure 5-15.

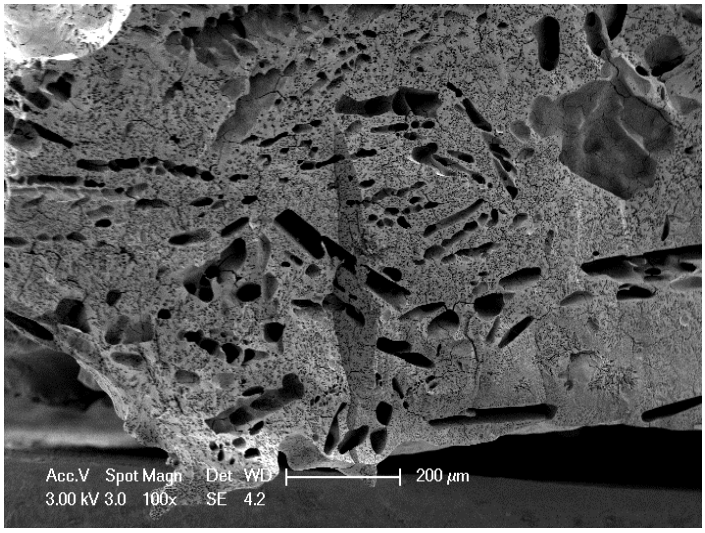

a

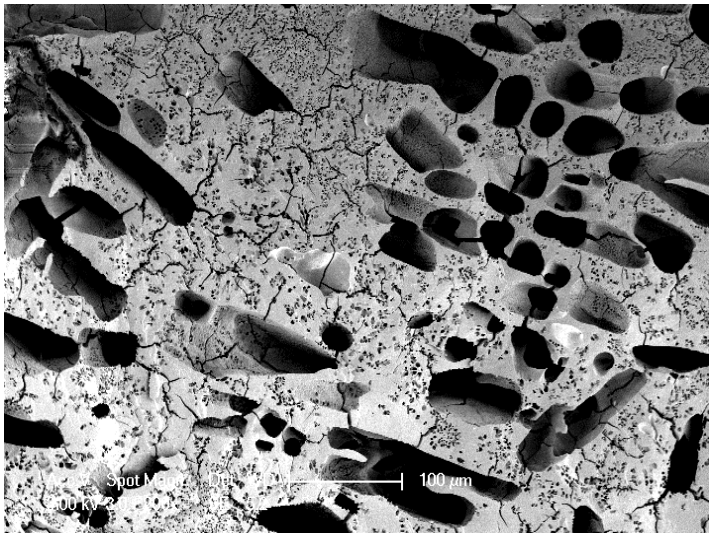

b

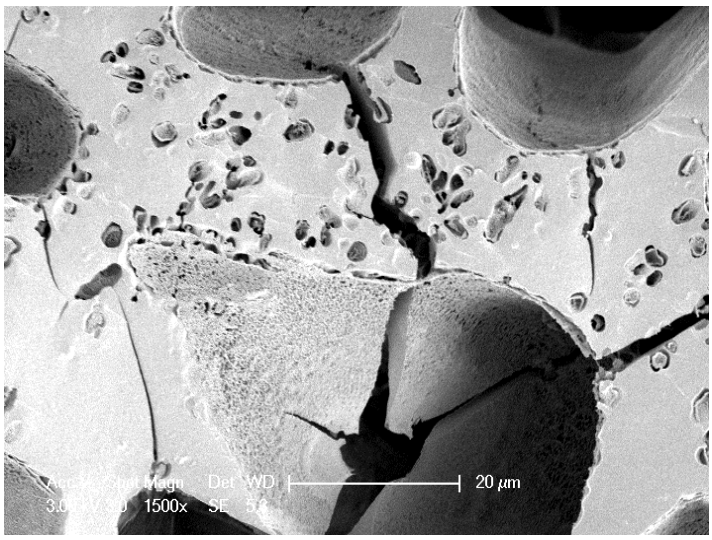

Figure 5-15 SEM image of frozen 50% coffee after all ice sublimation and coating

Figure 5-15 (a) shows an overall look at relatively low magnification of the 50% coffee after all ice had been sublimated. Numerous dark areas represent pores, which were formed by sublimation of ice crystals formed during freezing. The pores were not equal in shape/size, which indicates that the ice crystals were not homogenously formed. Magnitude of pore sizes varied from 10 to 100 μm, much bigger than the single crystal size of <10 μm seen in figure 5-14. The much bigger pore size suggests that (i) some ice crystals were linked together or (ii) during sublimation pores were connected or (iii) ice crystals of different sizes were formed as the temperature, concentration of each small area were different. The difference in ice crystal size measured in Figure 5-14 and 5-15 suggests that measuring ice crystal size by assuming they are the same as the sublimated pore size is not always accurate.

Figure 5-15 (b) shows a more detailed picture of the sample. Irregular pores are shown in the image and some of them are connected. Compared with image 5-13, the solid wall in between each pores is thicker (>20μm in Figure 5-15, and about 10μm in Figure 5-13), as the original solid concentration increased from 30% to 50%, which has also been reported in the literature (MacLeod, McKittrick *et al*. 2006).

Figure 5-15 (c) shows a small part of the sample at high magnification (1500X). A comparatively large pore is observed, around which several small caves containing small particles are seen. Those particles may be solid contents of the coffee, forced into the caves possibly due to the expansion of ice during freezing. Similar findings have been reported by Hindmarsh *et al*. (2007), who examined frozen 20% sucrose solution droplets with cryo-SEM and observed formation of a surface sucrose layer during spray freezing. They attributed the presence of this layer to the expansion of water during freezing, which forced the remaining

concentrated sucrose solution to the outside surface of the droplet (also discussed in section 5.1.3.1).

5.1.3.3 70% coffee

Frozen coffee of 70% solid content was also examined by cryo-SEM. Three selected images with hexagonal shapes are displayed in Figure 5-16.

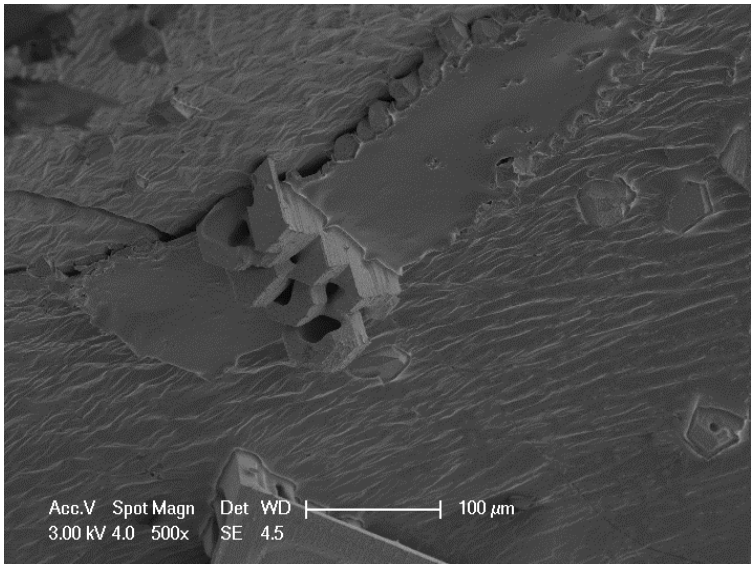

a

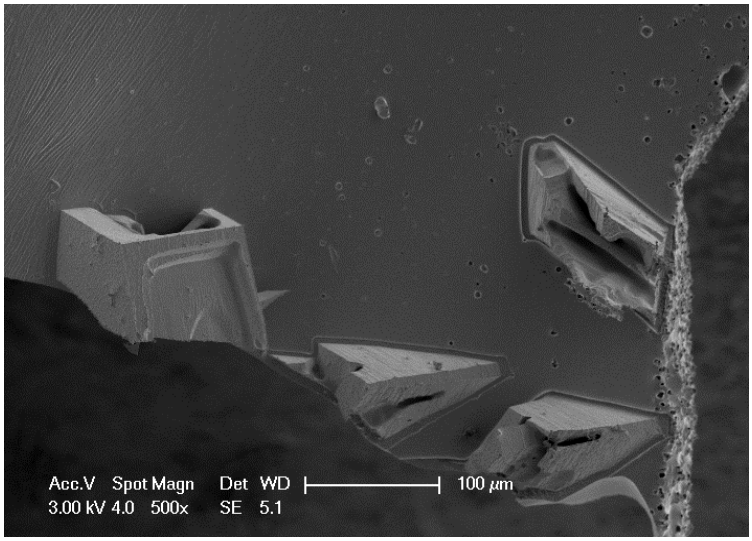

b

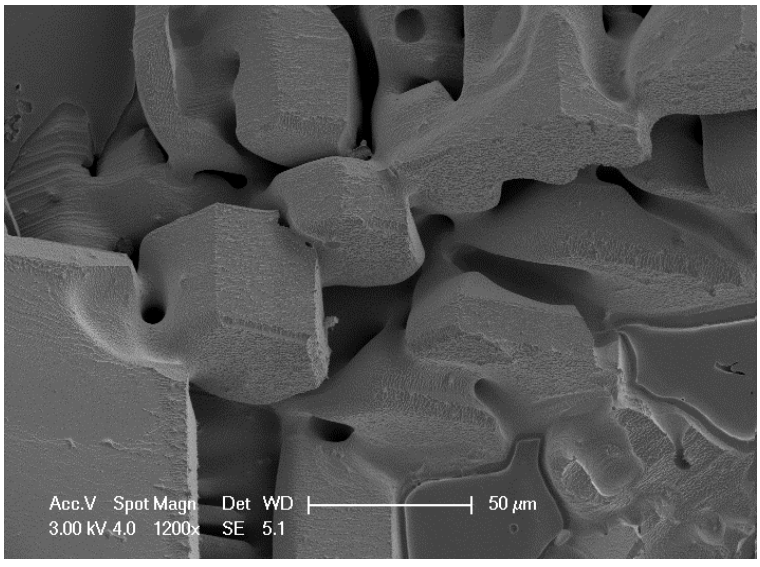

c

Figure 5-16 cryo ESEM image of frozen 70% coffee after 5-minute etching.

Figure 5-16 displays cryo SEM image of frozen 70% coffee after 5 minutes etching.

In figure 5-16 (a, b), there are several fragments of hexagonal shapes gathering together on a smooth surface. No pores can be seen, indicating that the 5 minutes of etching time (at -95°C) did not sublimate the ice crystals. It is noted that in the frozen sample, the system existed as ice crystals embedded in a glassy concentrated solution (Franks 1998). The hexagonal shapes might therefore represent ice crystals embedded in a flat surface corresponding to the concentrated amorphous solution. The size of the crystals is between 50 to 100 μm (see figure 5-16 c), which makes them larger than the size of the ice crystals in less concentrated solutions (compared with Figure 5-14, 15).

5.2 Crystal growth after ice nucleus addition

Section 5.1 discussed the spontaneous crystallisation in high concentration systems which contain air. Further study of crystal growth after ice seed addition is studied and displayed in section 5.2.

5.2.1 Aerated sucrose and cmc system

This section presents work on crystal growth kinetics, determined under a microscope after ice nucleus addition in systems containing air. Mixed sucrose and cmc were used as samples instead of pure sucrose-water system, because 60% sucrose solutions were not viscous enough to stabilise air bubbles. Air bubbles disappeared soon after the 60% sucrose was aerated.

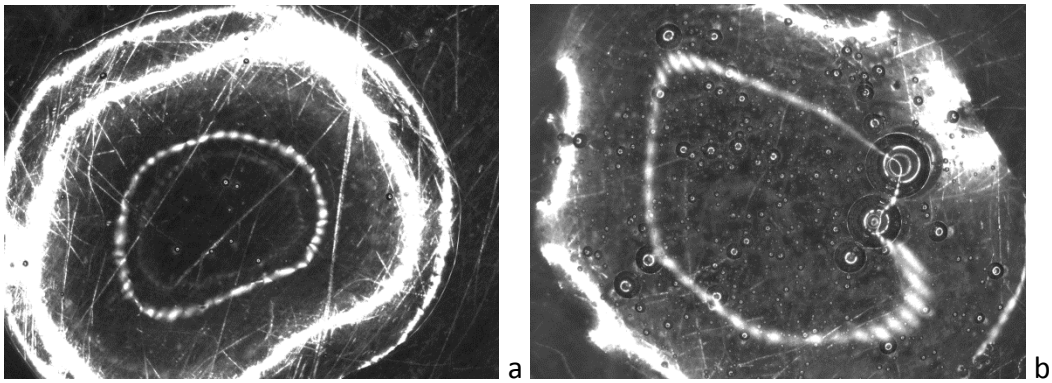

Figure 5-17 Microscope image of 59% sucrose and 1% cmc droplet (a) before aeration (b) after aeration

A solution of 59% sucrose and 1% cmc was aerated until it increased its volume by 25%. Microscope images of the droplet before and after aeration are shown in Figure 5-17. Few small air bubbles can be identified in the droplet before aeration, while the aerated droplet contains large number of air bubbles of different sizes. The method of aeration is described in section 3.3.1.

Figure 5-18 displays crystal growth rates in sucrose and cmc solution with 40% moisture content with and without air.

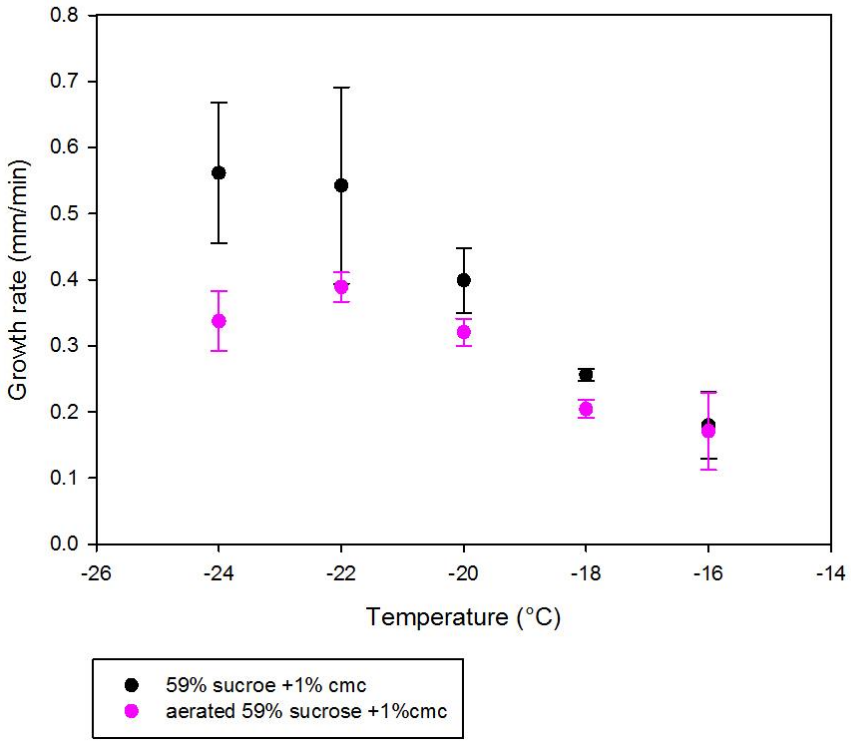

Figure 5-18 Crystal growth rate in 59% sucrose and 1% cmc system with/without air bubbles

The behaviour of sample without aeration displayed in Figure 4-23 shows that the crystal growth rate increased from 0.2mm/min to 0.55mm/min as temperature decreased from -16˚C to -24˚C.

As the temperature decreased from -16°C to -20°C, growth rate in the aerated sample increased from 0.2 mm/min to 0.3 mm/min, as there was greater supercooling. However, when the crystallising temperature fell below -20°C, crystal growth rate was fluctuating between 0.3 and 0.4 mm/min.

At each given temperature, crystal growth was slower in the system with air bubbles. This is due to the delay in heat transfer and mass transfer when air bubbles are distributed in the

solution (Sofjan and Hartel 2004, Cook and Hartel 2010). In addition, as temperature decreased, aeration showed a more significant delaying effect on crystal growth.

A detailed look at the freezing front in the aerated system is provided in Figure 5-19.

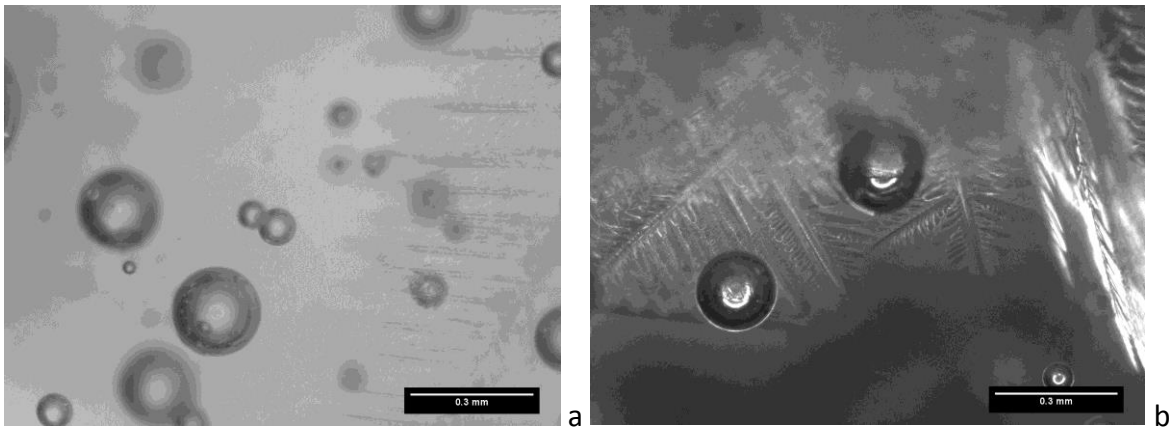

Figure 5-19 Representative zoom-in pictures of crystallising front in aerated 59% sucrose and 1% cmc solution.

Multiple air bubbles were distributed unevenly in the sample. Parallel dendritic ice structure was identified as the freezing front of crystallisation. In the experiment, it appeared that crystallisation did not affect the position of air bubbles as they crystallised (this was evident by visual observation of the crystallising sample during the experiment), and they remained at the same position/state as the solution transformed from liquid to solid.

5.2.2 Aerated gum arabic system

50% gum arabic was also used to study the effect of aeration on water crystallisation kinetics by ice nucleus addition.

In 50% gum arabic solutions, complete removal of air bubbles trapped in the sample during preparation was not possible.

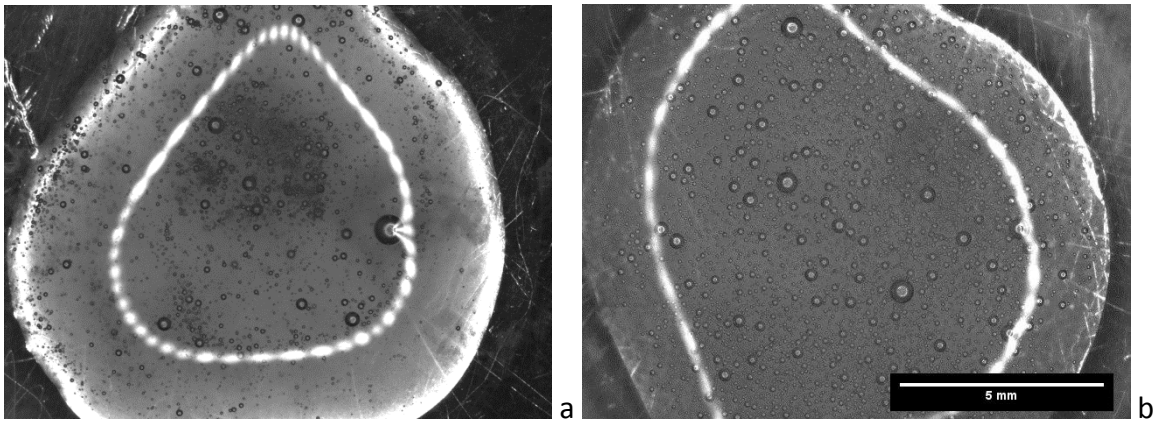

Figure 5-20 Microscope image of 50% gum arabic (a) before aeration (b) after aeration (both images have same scale).

Figure 5-20 shows images of the system before and after aeration (air added until the volume expanded by roughly 20%). The method of aeration is described in section 3.3.1. Air bubbles (with max size of about 0.5mm in diameter) are observed in both cases. After aeration the number of the air bubbles was increased, however the difference between two samples were not very significant.

The crystal growth rate in aerated and nonaerated 50% gum arabic are displayed in Figure 5-21.

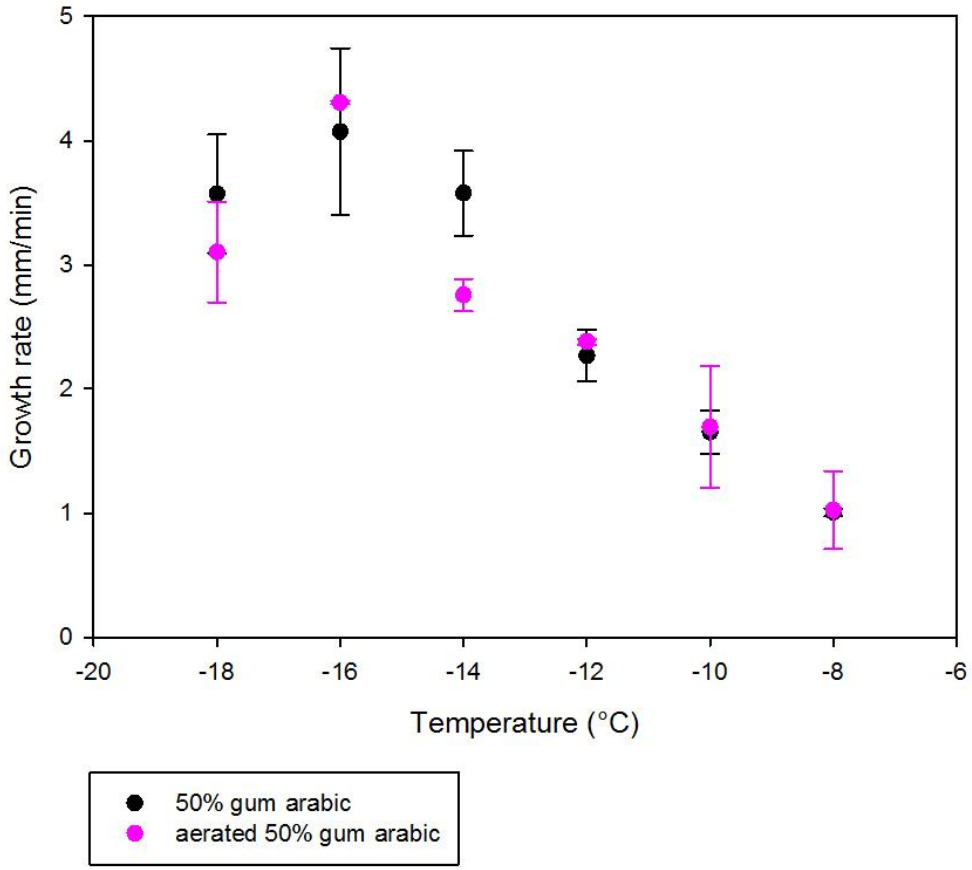

Figure 5-21 Crystal growth rate in 50% gum arabic with/without air bubbles. Experiments were triplicated and error bars show one standard deviation.

The growth rate of ice crystals in the aerated 50% gum arabic system did not show significant differences from that of the non-aerated sample. This might be due to the fact that air bubbles existed in the non-aeration sample as well (see figure 5-20), while additional aeration appeared to marginally affect air bubble distribution and crystal growth kinetics. In each sample, growth rate increased monotonically as temperature decreased from -8˚C to -20˚C then decreased after temperature dropped below 20˚C.

5.2.3 Comparison between coffee, sucrose and gum arabic

Crystal growth rates of 60% coffee are shown in Figure 5-22, which also includes growth rates of 60% sucrose and gum arabic for comparison.

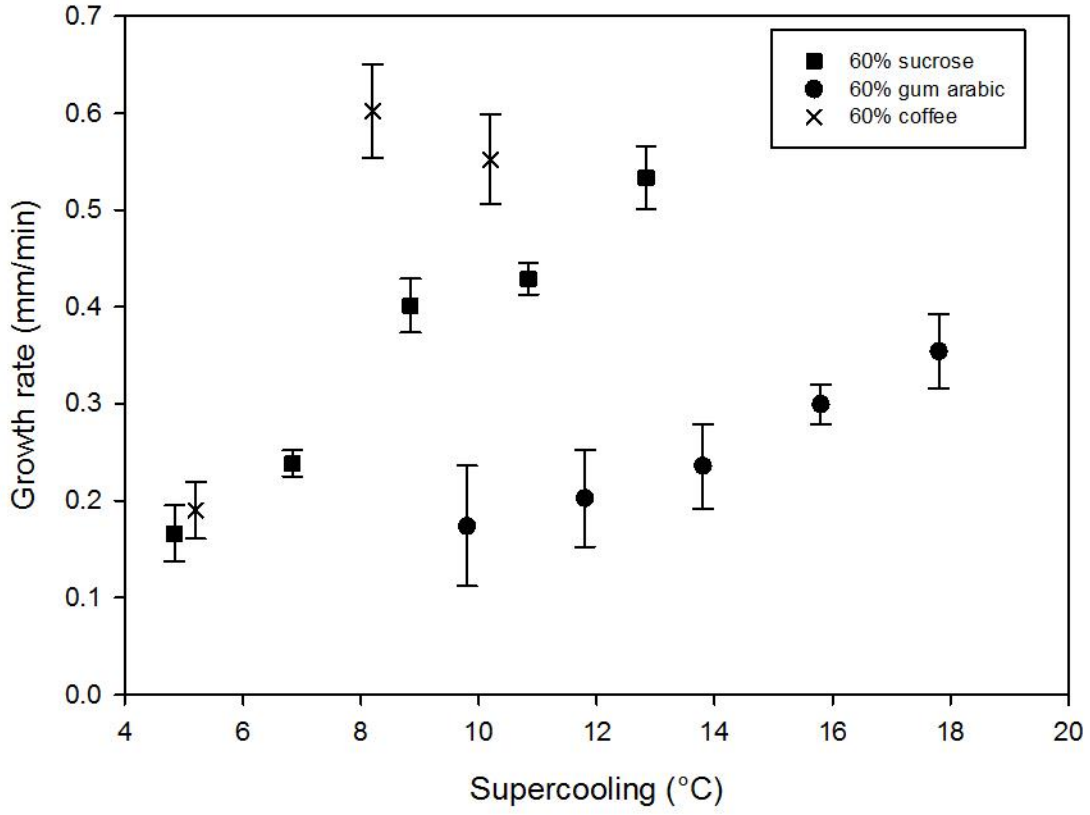

Figure 5-22 Crystal growth rate in 60% systems: coffee, sucrose and gum Arabic. Sucrose results already shown in section 4.3.1. Experiments were triplicated and error bars show one standard deviation.

The crystal growth rates of coffee were close to the rates of sucrose in the investigated conditions. At low supercooling (approximately 5°C), crystal growth rate was below 0.2 mm/min. Increasing the supercooling level to 9 or 11°C resulted in a higher growth rate at 0.6 mm/min. Image processing for the crystal growth kinetics in coffee sample proved very

challenging due to the opacity of coffee, as shown in the Figure 4-23. Only three data points were obtained for the coffee system due to the difficulties in image processing.

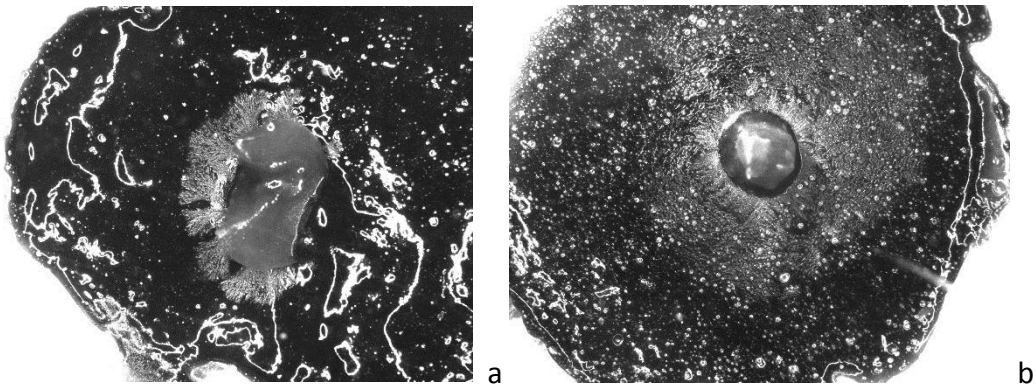

Figure 5-23 Selected microscope images of 60% coffee droplet after adding ice nucleus to show the challenge in image processing: (a) ice crystal area was easy to distinguish; (b) ice crystal area was difficult to distinguish.

In figure 5-23, two crystallising coffee samples are shown. In the first one (figure 5-23a) some colour difference can be seen in the middle of the sample, which was attributed to crystal growth after the ice nucleus was added. However, it was not always easy to tell the boundary between the crystallised area and the remaining solution, as for example can be seen in Figure 5-23 b. Efforts were made to modify lighting conditions (i.e. lighting angle, lighting intensity) and improve the image quality, but it was still difficult to quantify crystallisation area on some occasions. To obtain more detailed study of crystal growth from opaque systems, different microscope techniques need to be considered, for instance, polarised-light microscopy, which can differentiate crystalline from amorphous material (Roos 1995, Mazzobre, Aguilera *et al*. 2003).

5.2.4 Visualising ice crystals formed after ice nucleus addition

Frozen coffee samples, in which ice nuclei was introduced during freezing, were examined using the cryo-SEM technique, to investigate the morphology of induced ice crystals directly. 30% and 60% coffee samples were used in this section.

5.2.4.1 30% Coffee

Frozen 30% coffee sample with ice seed addition during freezing was examined and displayed in Figure 5-24.

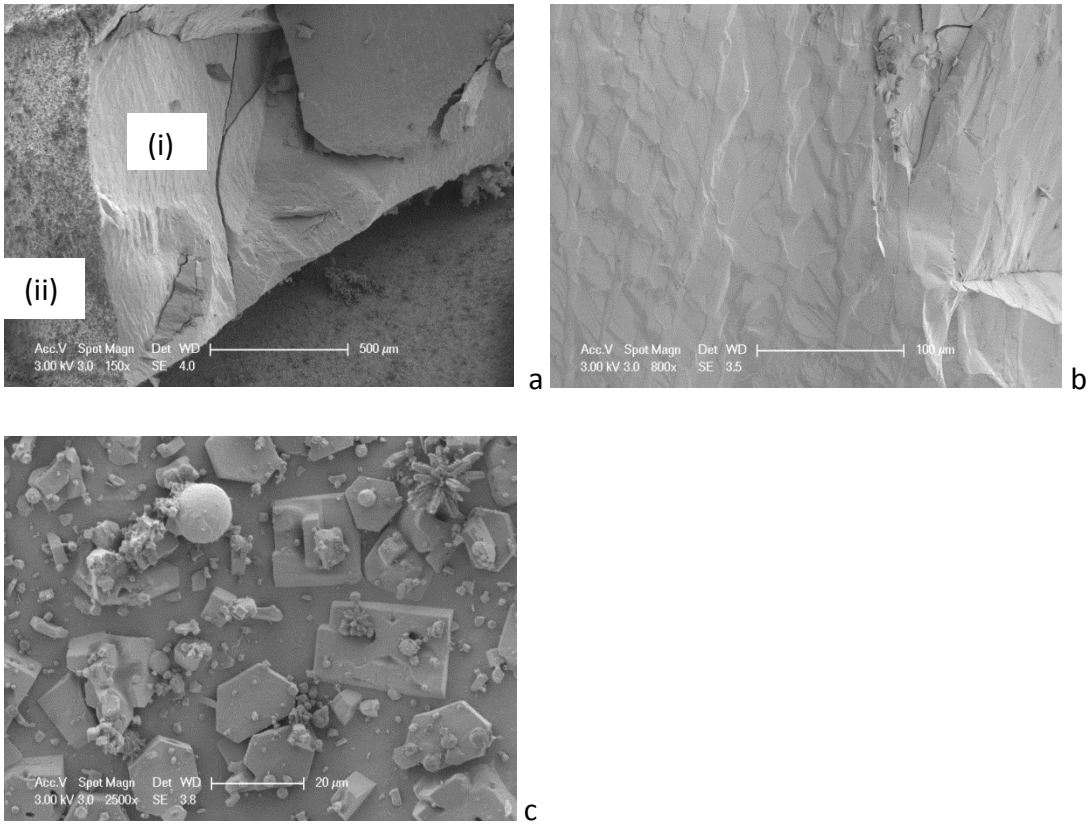

Figure 5-24 Cryo-SEM image of frozen 30% coffee after ice nuclei addition during freezing; (a) sample with two different areas i and ii ;(b) zoom-in picture of area i ;(c) zoom-in picture of area ii.

Figure 5-24 (a) shows an overall look of the frozen 30% coffee sample with two fracture surfaces (area i and area ii). No pores are observed, which indicates that the ice crystals on the system did not sublimate during etching (5min, -95˚C). A detailed look of area i (Figure 5-23 b) showed two phases: one with protuberant patterns and a flat area. Protuberant patterns might correspond to ice crystals, while the flat area is possibly the frozen concentrated solution. Zoom-in into region (ii) is shown in Figure 5-23 c, and reveals several hexagonal shapes with diameter of around 20μm. In figure 5-24c, it appears that ice crystals were developed in different forms in the frozen sample. A hexagonal shape structure indicates the existence of single ice crystals, while the continuous protuberant patterns on a surface might represent a series of crystals that are linked together.

5.2.4.2 60% coffee

Figure 5-25 (a) shows the internal structure of a frozen 60% coffee, in which an ice nucleus was added during freezing.

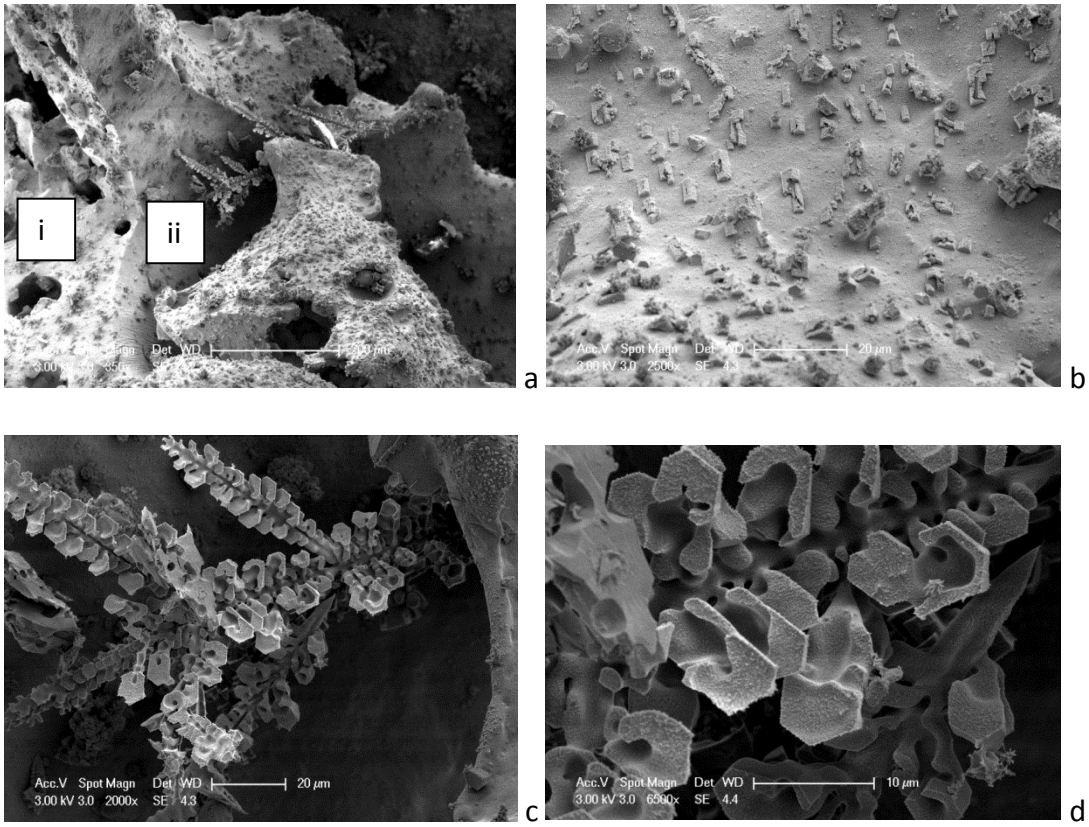

Figure 5-25 Cryo-SEM images of frozen 60% coffee after ice nuclei addition during freezing; (a) overall look of sample with area i and ii; (b) zoom-in picture of area i; (c), (d) zoom-in pictures of area ii.

Area (i) is a continuous area with some big spherical voids and small particles on the top. The big voids possibly correspond to the air bubbles trapped in the coffee during freezing. Figure 5-25 (b) provides a close look at the particles in area (i), and these particles have a certain ordered shape which might correspond to ice crystals. The size of these crystals was in <10µm.

There was a dendritic shaped structure spotted in area (ii). The zoom-in images are displayed in Figure 5-25 (c) and (d). Numerous hexagonal shapes were connected to each other and formed a chain-like tree branch, suggesting that the crystal growth was oriented from one direction to the other. The diameter of the hexagonal shapes was less than 10 µm.

5.3 Crystal growth in coffee induced by nuclei addition: scale up

Section 5.2.3 described a study on ice crystal growth from coffee solution at droplet scale (approximately 0.1mL) after addition of ice nucleus. In this section, crystallisation was studied at a larger scale (2mL). Samples of 50, 60% coffee solutions were used to study the effect of ice nuclei addition on morphology by examining the internal structure of the final freeze dried samples.

5.3.1 50% coffee

5.3.1.1 Effect of adding ice nuclei

SEM images in Figure 5-26 show the internal structure of freeze dried coffee with initial 50% solid concentration. Both samples were cooled to 10°C supercooling and held at that temperature, ice seeds were only added into sample in Figure 5-26 (b).

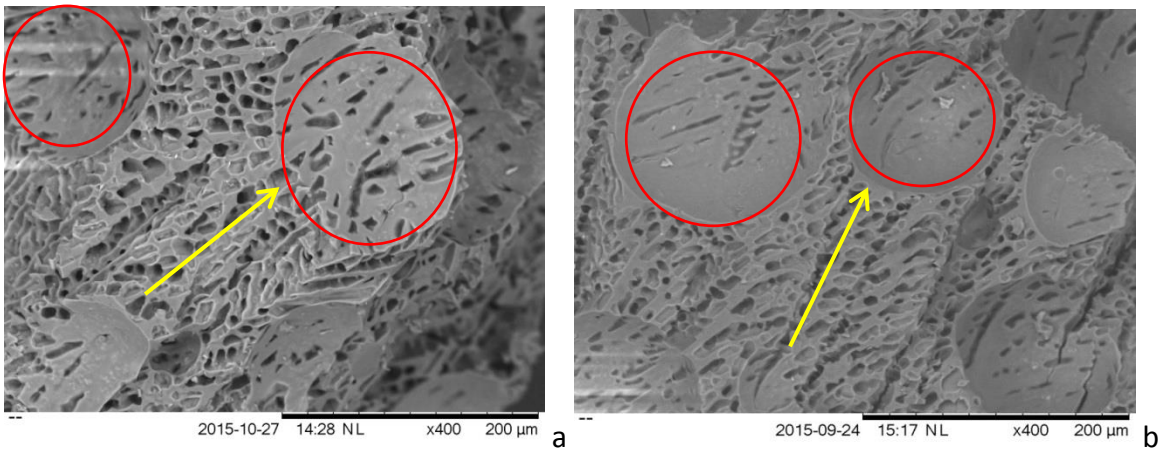

Figure 5-26 SEM images of freeze dried 50% coffee; samples were cooled to 10°C supercooling, (a) without ice nuclei addition (b) with ice nuclei addition; arrows indicate the orientation of ice crystals and circles indicate round voids.

In both images, several large round voids (>100μm) can be seen, which correspond to air bubbles (indicate by red circles), as those sample were aerated to a certain (industrially relevant) density. Large number of small pores (diameter of 10-20μm) can be seen as well, which refer to ice crystals sublimated during freezing. The distribution of ice crystals were ordered and aligned (indicated by yellow arrow in the graph). Uni-directional freezing was conducted for the sample by contacting the cooling surface from bottom of the crystallising material and insulating the sample from all other directions (details see section 3.6.2.1). It has been reported that uni-directional freezing results in parallel needled-shaped pores (Zhang and Cooper 2007) in the same direction as the temperature gradient (Mousavi, Miri *et al*. 2007).

Small pores (originating from ice crystals), were also observed on the surface of the large voids, which indicates that during freezing, when the freezing front reached an air bubble, crystal growth continued on the surface of the air bubbles This is in good agreement with the observation in optical microscope (see section 5.2.1 and Figure 5-19).

5.3.2 Effect of crystallising temperature

Effect of crystallising temperature (different supercoolings) on crystal growth and subsequently morphology of freeze dried 50% coffee was studied.

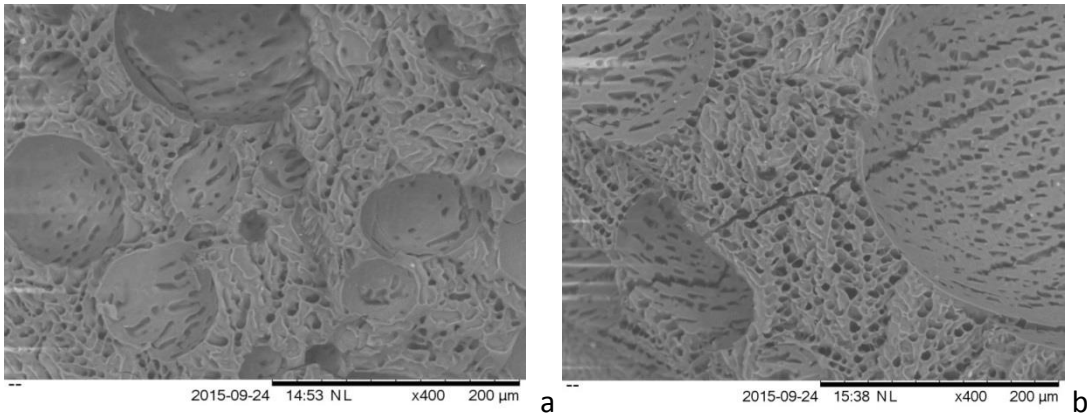

Figure 5-27 SEM images of freeze dried 50% coffee, samples were cooled to different temperatures (a: 2˚C supercooling, b: 6˚C supercooling after ice nuclei addition.

Figure 5-27 shows the structure of freeze dried 50% coffee crystallised at different temperatures (resulting in 2 and 6°C supercooling, respectively) after adding ice seeds. The inner structure in both cases appeared similar. Large round voids that represent air bubbles, and oriented small voids formed by sublimation of ice can be observed in both samples.

In all the investigated 50% freeze-dried systems, the inner structure appeared similar and not sensitive to nuclei addition or freezing temperature (over the investigated range).This is possibly due to the large amount of water available in the sample, which makes it possible to form large number of ice crystals in all the investigated conditions.

5.3.2 60% coffee

At 60% coffee concentration, there is reduced water availability and mobility (due to increased viscosity) compared to the 50% system. This led to less pores being observed in the freeze dried samples. SEM images of freeze dried 60% coffee frozen at different seeding conditions are displayed in Figure 5-28.

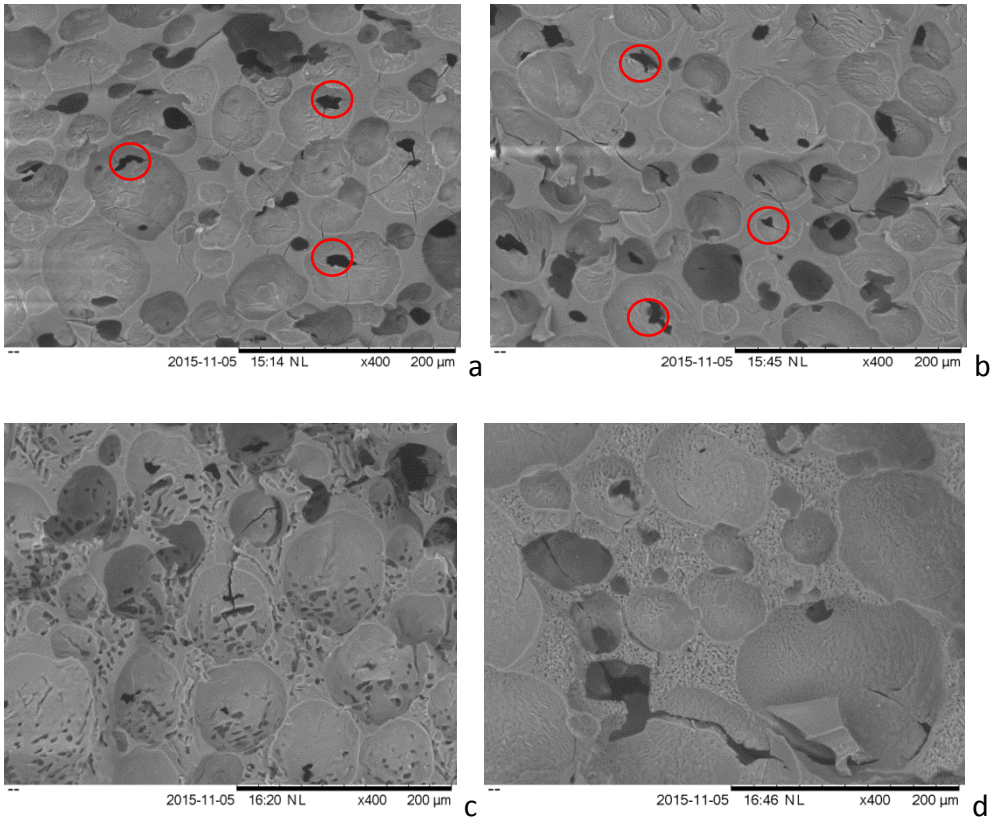

Figure 5-28 Freeze dried 60% coffee with different freezing conditions (a) crystallising at 6°C supercooling without seed addition, circles indicate collapsed area (b) crystallising at 6°C supercooling after 30µL seed addition, circles indicate collapsed area (c) crystallising at 10°C supercooling after 30µL ice seeds addition (d) Crystallising at 6°C supercooling after 50µL seed addition.

In figure 5-28 (a), the sample with no ice seed addition showed hollow areas in the structure, which correspond to air bubbles formed before freezing. Compared to the 50% coffee without seed addition (see Figure 5-26a), no small pores (related to ice sublimation) can be seen in the 60% sample. Some dark areas and wrinkled surface can be seen, possibly due to collapse during freeze drying (indicated by red circles).

As there were not enough voids (from ice sublimation) interconnecting with air bubbles to allow water molecules to exit the structure, there is a high resistance to movement of water vapor, and thus sample might get overheated and collapse (see section 2.3.3).

The sample with 30μL ice seed addition (each ice seed was 5 μL, and 6 of them were added to the sample, making it 1.5% of total volume) and cooled to 6°C supercooling resulted in similar microstructure as the no seeding sample (see Figure 5-28b).

Further increase in the supercooling level to 10°C led to structural changes (Figure 5-28 c). Apart from the voids that represent air bubbles, large number of small pores from ice sublimation can be seen as well, with a size of less than 20μm. These pores were connected with each other, which made it easier for gas to get out during drying. As a result, no structure collapse was observed.

Decreasing crystallising temperature (increasing supercooling level) accelerated crystal growth rate (Teraoka, Saito *et al*. 2002, Hindmarsh, Russell *et al*. 2005), thus more ice crystals were formed in the frozen state and subsequently a more porous structure in the freeze dried product was observed.

Another sample was added with more ice nuclei (50 μL ice seed, making 2.5% in total volume) and cooled to 6°C supercooling. Air bubbles and ice crystals pores can be identified in the Figure 5-28 d.

This section shows that freeze dried 60% coffee with different structures can be achieved by adding ice nuclei during the freezing process. The amount of ice added into the system and the crystallising temperature also affected the structure of final freeze dried product.

5.4 Characteristics of freeze dried samples

5.4.1 SEM

Several different characterisation techniques (SEM and dissolution test) were employed to understand the structure and behaviour of freeze dried products. SEM was used to visualise the structure of the sample.

5.4.1.1 30% coffee

SEM images of freeze dried 30% coffee with different magnification are shown in Figure 5-29.

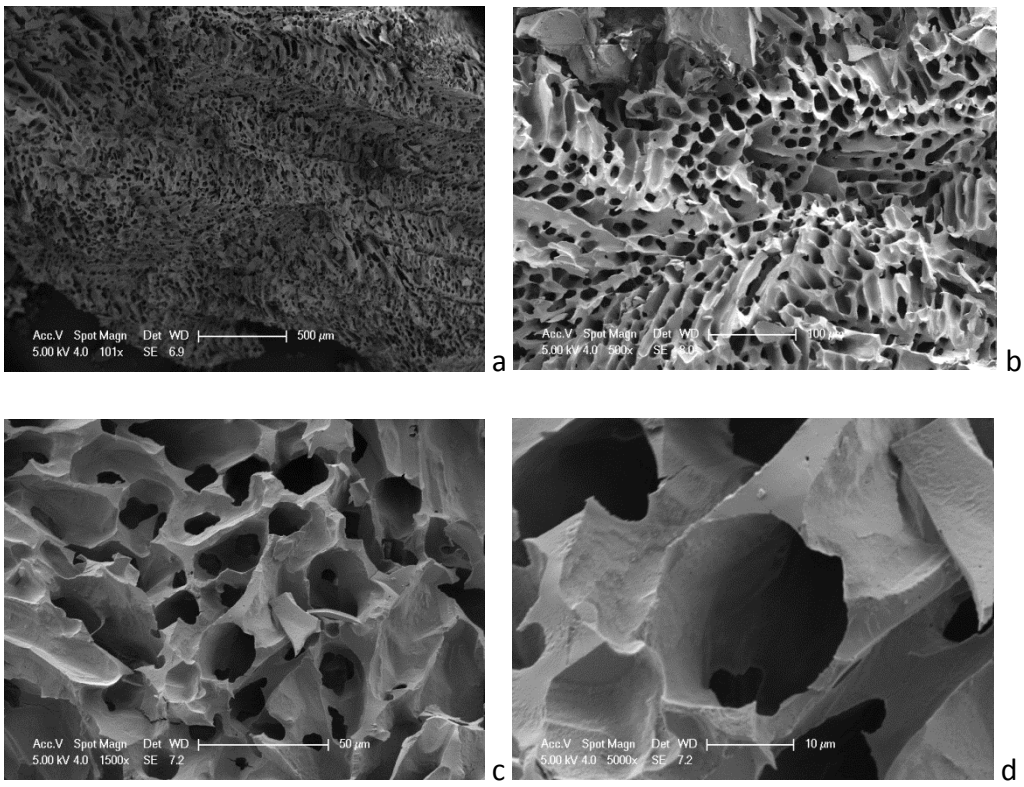

Figure 5-29 SEM images of coffee granules freeze dried from 30% solution.

Inner structure of freeze dried 30% coffee can be seen in Figure 5-29 at a range of different magnifications. No collapse or loss of structure was noticed in the solid matrix. Large number of pores can be seen in the structure, and the pores revealed the place taken by ice crystals. The size of the ice crystals was between of 10 µm to 20 µm, slightly smaller than those obtained in Figure 5-13.

5.4.1.2 70% coffee

Figure 5-30 displays the structure of freeze dried coffee with initial concentration of 70%.

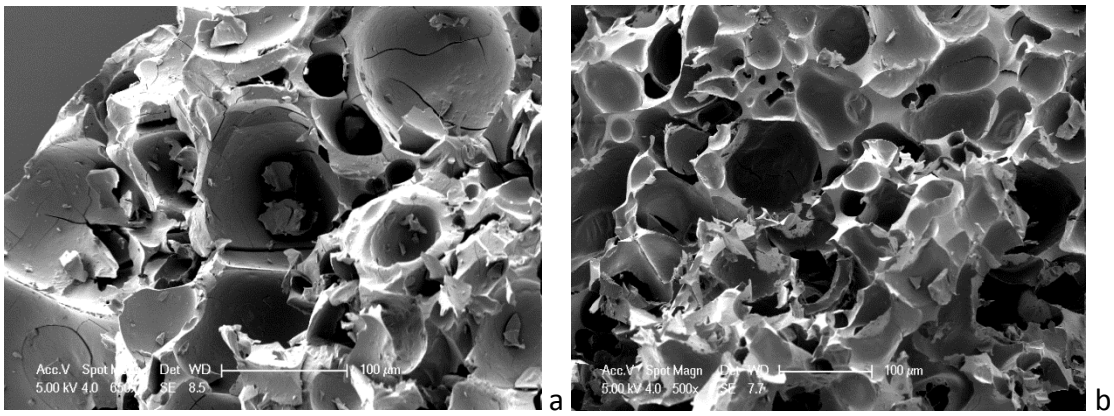

Figure 5-30 SEM images of coffee granules freeze dried from 70% solution.

Large number of pores can be seen in the structure, and the size of the pore was about 100µm, almost ten times bigger than the pore sizes observed in the 30% system in Figure 5-29. These pores might result from the air bubbles that entrapped in 70% coffee solution during freezing. However small pores created by ice crystals were not very obvious.

5.4.1.3 Commercial coffee product

The structure of commercial instant coffee granule was examined by SEM for comparison and it is shown in figure 5-31. A number of pores can be seen in the sample. Both the size and the distribution of the voids were not homogenous.

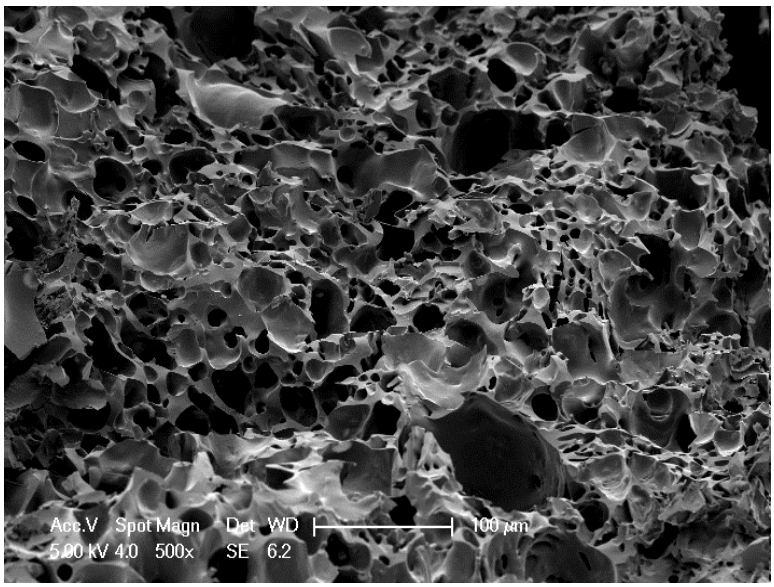

Figure 5-31 SEM images of freeze dried coffee granule from a supermarket product.

The commercial sample was less homogenous than the 30% sample obtained in this research. But the large number of pores existing and the size of the pores were closer to that in 70% coffee.

5.4.2 Dissolution

The dissolution ability of the freeze-dried samples was tested by measuring the water conductivity change as the samples were added into distilled water under controlled temperature/mixing conditions (see section 3.4.4). A collection of freeze dried samples was used in the dissolution test, and two of them are shown here, to study the relationship

between microstructure of the sample (SEM) and dissolution behaviour (conductivity measurement).

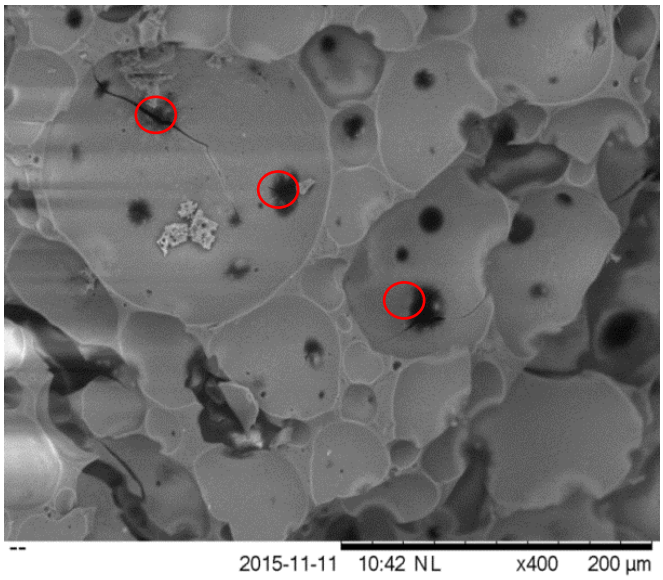

a

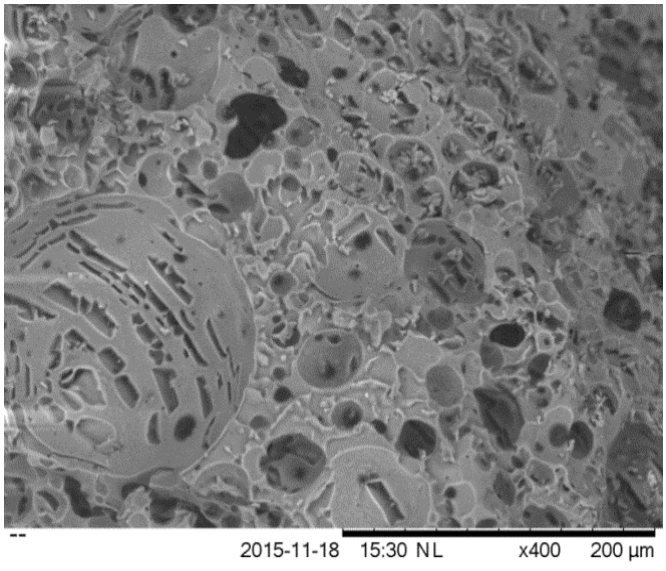

b

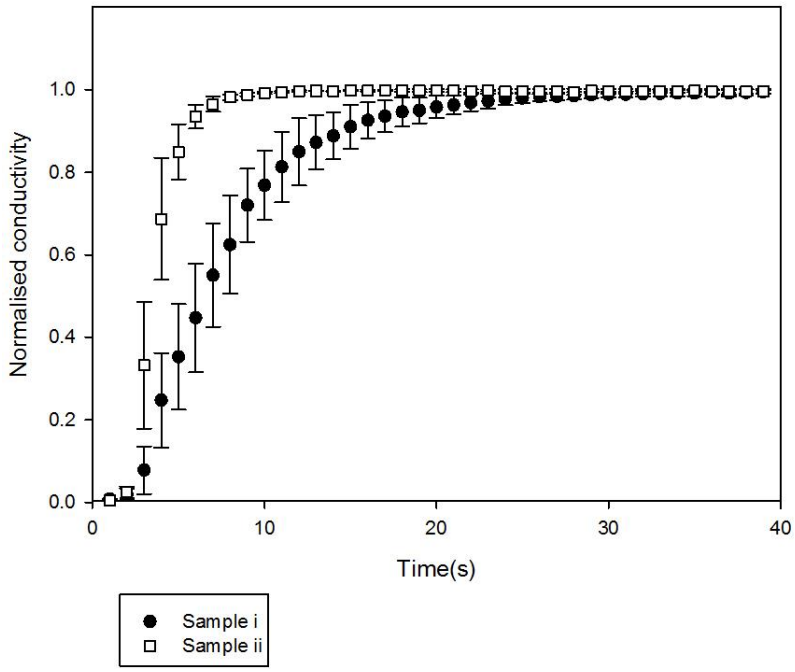

c

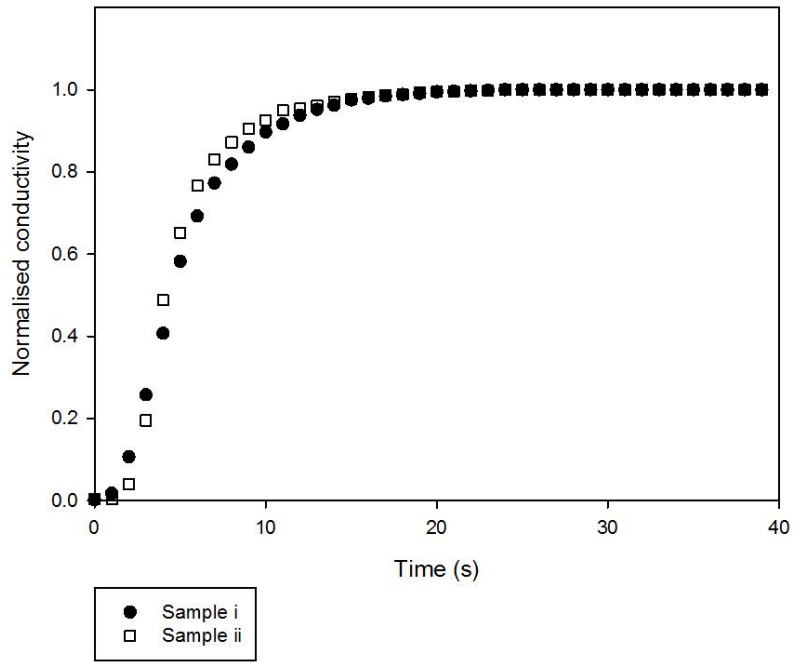

d

Figure 5-32 (a) SEM image of freeze dried sample i, circles indicate collapse (b) SEM image of freeze dried sample ii, (c) conductivity measurement during sample dissolution in 40°C water. Experiments were triplicated, and error bars represent ± one standard deviation; (d) conductivity measurements during sample dissolution in 55°C water, and experiment was conducted only once.

The two samples (i and ii) were obtained through different freezing conditions, with initial 60% solid concentration. Sample (i) resulted from fast freezing while sample (ii) was frozen at a lower rate and with ice seed addition. Figure 5-32 (a) shows large spherical voids in sample (i), which corresponded to air bubbles. Some irregular dark areas can be seen inside the voids and they suggest that collapse took place during drying (indicated by circles).

Sample (ii), however, showed a different structure (Figure 5-31 b). Large voids that correspond to air bubbles can also be seen, but no sign of collapse was indicated. Instead, large number of small pores was observed in the solid matrix, including on the inner surface of the air bubbles. This suggests the formation of ice crystals during freezing, which continued as the freezing front reached the air bubbles (also seen in Figure 5-19, 5-26).

Figure 5-32 c and d show the normalised conductivity of water after coffee samples were added into it. As the conductivity has been normalised, the maximum value of y axis is 1. When these two samples were dissolved in distilled water at 40°C (Figure 5-32 c), the normalised conductivity increased sharply to 1 within 30 seconds, showing good solubility even at this comparatively low temperature (for instant coffee). Sample (ii) dissolved faster than sample (i), as the more porous structure allowed water to enter the structure faster.

When the dissolution temperature increased to 55°C, both samples reached 100% conductivity within 20 seconds (Figure 5-32d). Both samples dissolved faster in 55°C water than in 40°C water, as the higher water temperature accelerated dissolution. At higher temperature, there is no obvious difference in dissolution rate of the two samples.

Overall, the more porous structure (sample ii) showed better dissolution as the water conductivity increased faster after the dried sample was added into water. The difference in dissolution ability between the two samples decreased at higher dissolution temperature.

5.5 Conclusions

DSC and XRD showed good agreement in studying water crystallisation in highly concentrated systems containing air. At investigated cooling rates (6°C/min, 30°C/min), water crystallised into ice in 50% coffee during freezing. However, devitrification took place in 70% coffee system, that is, water only crystallised into ice during reheating the rapidly frozen sample. Increasing the solid concentration made it more difficult for water to crystallise during freezing.

Higher scanning rate resulted in delayed crystallisation during freezing and less amount of ice crystal were formed. Annealing helped to promote more amount of ice crystallisation formation and effect of annealing also depended on temperature and time.

ESEM technique with careful etching allowed the direct visualisation of hexagonal shape ice crystals. Although sometimes the etching could also sublimate some ice crystals in the sample (for example in frozen 30% coffee sample).

Additional air bubbles showed a delayed effect on crystal growth in sucrose and cmc solution. However, the delayed effect of aeration in 50% gum Arabic was not obvious, possibly due to the already existence of air bubbles in the system during preparation.

The opacity of coffee sample caused challenges in quantifying crystal growth rate measurement. Limited data was obtained from this system and the value was close to that in sucrose solution at same concentration (60%).

Ice crystals were observed in coffee sample with ice nucleus addition in cryo-SEM in several different forms: separated hexagonal shapes, continuous protuberant patterns and oriented dendritic hexagonal shapes.

In all the investigated 50% freeze-dried coffee samples, the inner structure appeared similar and not sensitive to nuclei addition or freezing temperature. However for 60% coffee system, different structure (porous or collapsed) can be achieved by changing the ice nuclei addition (amount of ice addition, or the freezing temperature). Morphology of freeze dried samples can be studied by SEM and the dissolution ability can be tested by conductivity measurement. Porous structure sample dissolved faster than collapsed sample.

Chapter 6 Freeze drying high concentration carbohydrate solutions

The freezing process, the first step of freeze drying, has been studied as presented in Chapter 4 and 5. Water crystallisation in highly concentrated carbohydrate solutions, first a simple sucrose model system, then a more complex aerated sugar solution and eventually coffee solutions. In Chapters 4 and 5, efforts are made to show the difficulties in creating ice crystals in high solid content systems, to study the parameters which controls water crystallisation kinetics. And suggestions have been made for the modified processing conditions to freeze a carbohydrate solution, aiming to create the maximum ice formation for the subsequent ice sublimation in freeze drying step.

After water crystallises into ice, freeze drying takes place under a vacuum, that is, ice sublimates into water vapour, resulting in a dried matrix. This sublimation step is of great importance to achieve the ideal freeze dried product, and the control of sublimation in freeze drying is studied and presented in this chapter. The system investigated in this chapter is as in the previous two chapters: highly concentrated carbohydrate solutions. All the three experimental chapters in this thesis report the water crystallisation and ice sublimation (the entire process of freeze drying) of the highly concentrated carbohydrate solutions.

Studies of freeze drying highly concentrated solutions are presented in this chapter and research is carried out to investigate: (i) if freeze drying high concentration leads to a collapsed structure; (ii) the reasons that cause collapse and the factors that can control it; (iii) methods to dry high solid content systems successfully by changing the freeze drying cycle or/and freeze drying formulation.

Sucrose solutions were investigated first, and then the gum arabic solutions, and finally a mixture of gum arabic and sucrose solutions were used, to study the effect of formulation (molecular weight) on the freeze drying.

6.1 Puffing in freeze dried sucrose system

Collapse or loss of structure sometimes occurs during freeze drying, which is usually not desirable. Most of the collapse takes place in the form of volume shrinkage. However, under the existence of vacuum, volume increase (puffing) can also take place (Tsourouflis, Flink *et al*. 1976). This is less common than volume shrinkage and has not been extensively studied. However volume increase was often seen in freeze dried sucrose in this research, and puffing phenomena in freeze dried sucrose products is thus investigated. First, some images are presented in Figure 6-1 to show puffed freeze dried sucrose.

a

b

c

Figure 0-1 Photograph of 50% sucrose freeze dried in a cake tin; (b) Fracture plane of freeze dried 50% sucrose dried in a cake tin; (c) Photograph of 30, 40, 50, and 60% sucrose freeze dried in glass vials.

Figure 6-1 (a) displayed a typical puffing structure obtained from the freeze drying of sucrose. Originally a 50% sucrose solution was placed into a cake tin to fill it to a depth of 1cm. After freeze drying, the sample expanded its volume hugely; the height of the sample exceeded 6cm, which was 6 times higher than before. A cut through the sample showed the inner structure in Figure 6-1 (b), an amorphous foam structure can be seen without the typical pores created from ice sublimation during freeze drying (sublimated pores can be

seen in Figure 5-29, 5-30, 5-31). To quantify the volume expansion after freeze drying sucrose solutions, 10mL freeze drying vials were used in the following experiments as the transparent glass vial provided direct observation of the macroscale structure change of the samples. As an example, Figure 6-1 c shows typical puffed freeze dried sucrose structure in a vial: a concentrated layer can be seen at the top of the sample and inside the sample there was an irregular foam-like structure.

This puffed structure is often seen in this research and it will be discussed in the following context. Several factors (processing conditions and formulation) are investigated to study the reasons which cause puffing, and the way to avoid the puffing.

6.1.1 Effect of sample volume

Effect of the initial sample volume on freeze drying of sucrose is studied firstly and displayed in this section. Two different volumes (1mL or 3mL) were used to investigate how the initial volume of sample affected freeze drying. Two cycles are used in this section (cycle i and cycle ii, see section 3.4.3, with different primary drying shelf temperatures of -20 ˚C and -40 ˚C).

6.1.1.1 Primary drying at -40°C (cycle i)

Two sets of samples, both with concentration ranging from 10% to 60%, with two different initial filled volume of 1mL or 3mL were filled into glass vials and freeze dried. The freeze dried samples were compared, first in terms of volume change.

Sucrose solutions were dried using cycle (i), with a primary drying temperature of -40˚C.

Figure 6-2 (a) shows the volume of sucrose samples after freeze drying as a function of original concentration. Three dotted lines are also displayed in the graph, to illustrate (i)

original volume of 1mL sample, (ii) the original volume of 3mL sample, (iii) the full volume of the vial.

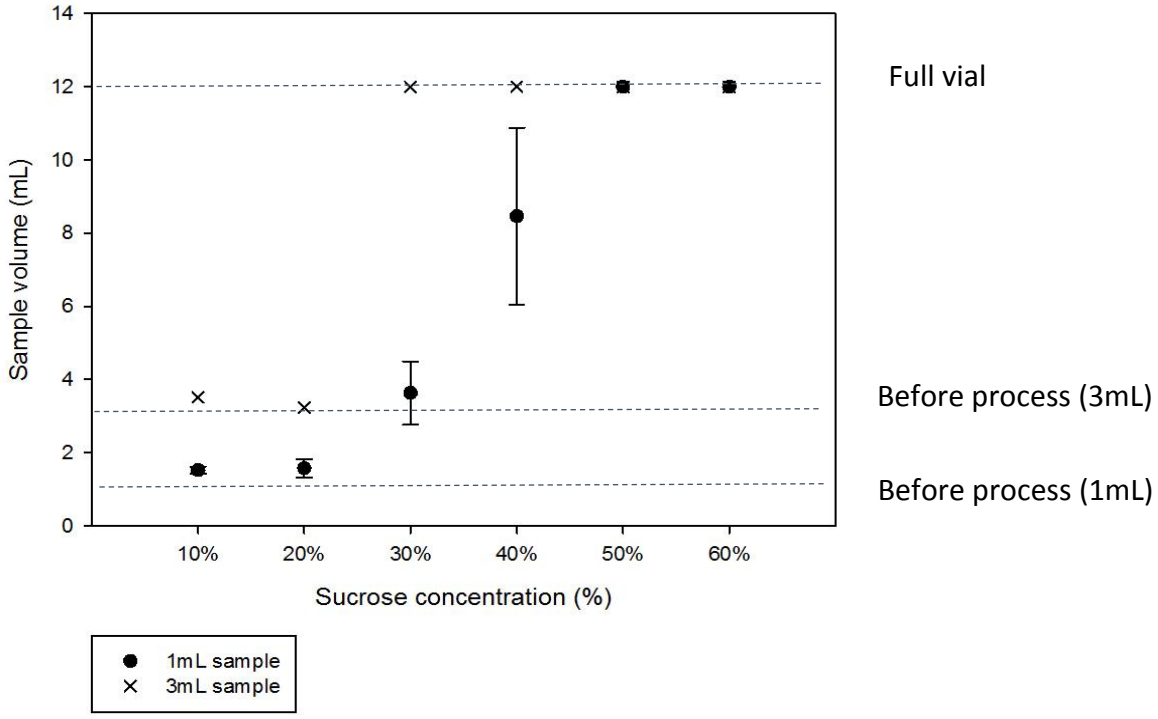

Figure 6-2 (a) Volume of freeze dried sucrose (dried in cycle i) with different original volume . Experiments of 1mL samples were triplicated, and error bars show ± one standard deviation. Experiments of 3mL samples were carried out once; (b) Photograph of freeze dried 30% sucrose (in cycle i). Left: initial 3mL sample, right: initial 1mL sample.

After freeze drying, the sample volume of 10 and 20% sucrose (both 1mL and 3mL initial volume), increased very slightly from the initial volume. The slight increase might result from the volume expansion of water when crystallised into ice.

When sample concentration increased to 30%, the volume change became more pronounced. 1mL 30% sucrose expanded its volume to 4mL after freeze drying, while 3mL 30% sucrose increased its volume to fill the whole vial (12mL). Images of these two samples are shown in Figure 6-2 (b).

Once the expansion volume reaches the top of the vial, further expansion is restricted by volume of the glass vial (12mL). As a result, when the sample volume shows 12mL, it does not show the expansion volume but the restriction from vial.

The volume expansion of freeze dried 30% sucrose can be directly seen in Figure 6-2 (b). The matrix dried from initial 3mL sample (Figure 6-2 (b) left) expanded its volume to 12mL and filled the whole vial, with a foam-like amorphous structure; while (Figure 6-2(b) right) freeze dried sucrose from initial 1mL puffed and filled 1/3 of the vial.

For concentrations of 40% and above, the volume of the freeze dried 3mL sucrose reached the maximum volume of the glass vial (12mL). While for 1mL initial volume, the puffing of the freeze dried sucrose reached the maximum at concentrations ≥50%.

Figure 6-2 (a) shows that increasing the initial sample volume resulted in more significant puffing after freeze drying of high concentrations of sucrose (≥30%). In addition to the volume change, the residual moisture content after drying was also measured (for methods to measure moisture content see section 3.4.4) and compared between two initial volumes.

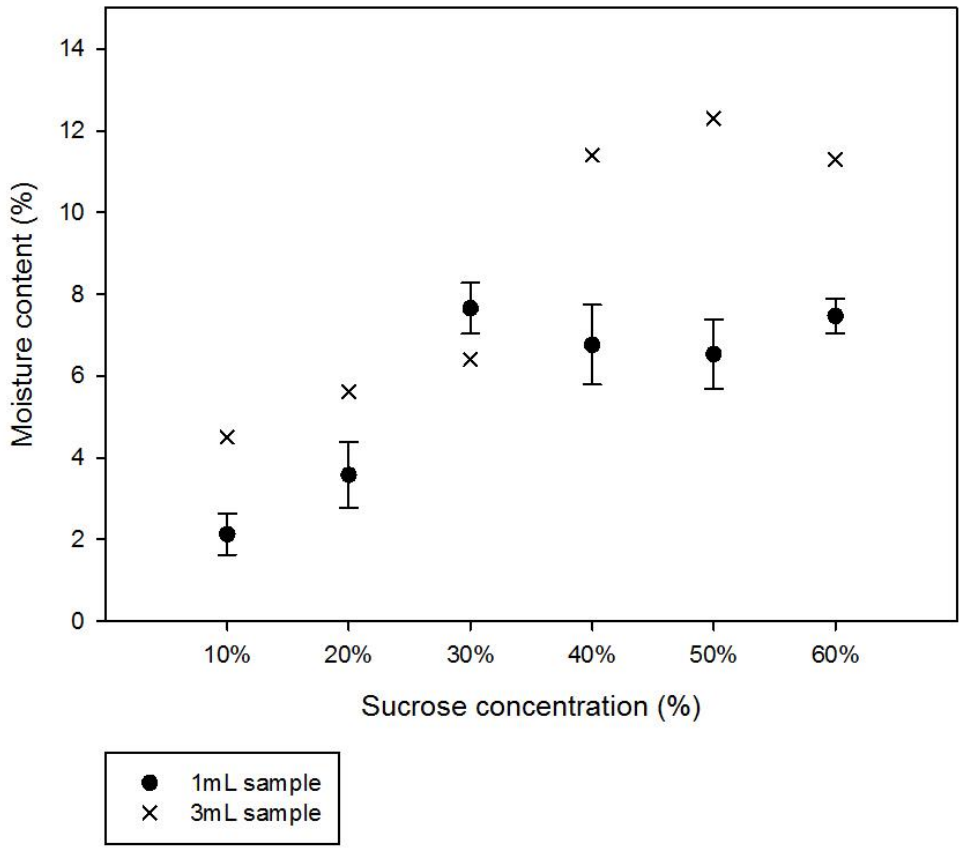

Figure 6-3 Moisture content of freeze dried sucrose samples with 1 or 3mL original volumes dried in cycle (i). Experiments of 1mL samples were triplicated and error bars show ± one standard deviation. Experiments of 3mL were carried out once.

Figure 6-3 shows the moisture content remaining in the freeze dried sucrose as a function of initial sucrose concentrations. In general the freeze dried 3mL sucrose contained more moisture than freeze dried 1mL sucrose. It can be seen that for 10 and 20% sucrose, moisture content was approximately 5% or lower for samples from both initial volumes. 30% sucrose, dried from both initial volume, contained around 6-7% moisture. Of concentration of 40% upwards, the freeze dried 3mL samples contained more than 11% moisture while 1mL samples had approximately 6-7% residual water. The large amount of

moisture in 3mL samples would not be acceptable in product as it may lead to further collapse of the sample during storage.

The experiments carried out in cycle (i) showed that when the initial sample volume increased from 1mL to 3mL, there was significant increase in both the puffed volume, and high moisture content in the remaining freeze dried sucrose matrix.

6.1.1.2 Primary drying at -20°C (cycle ii)

The effect of sample volume was also studied in another cycle (cycle (ii), with shelf temperature at -20°C during primary drying) and the sample volume after freeze drying plotted as a function of sucrose concentration with 1 or 3mL initial liquid volume (see Figure 6-4).

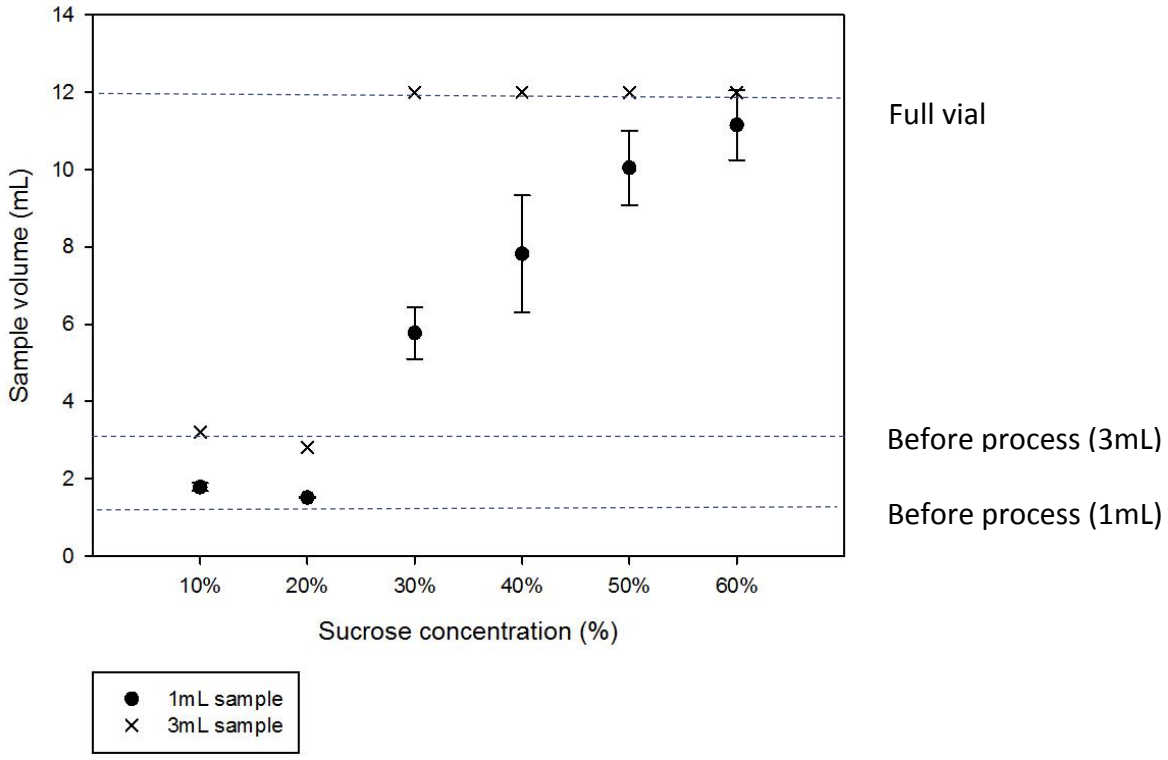

Figure 6-4 Sample height of freeze dried sucrose (drying in cycle ii) with 1 or 3 mL original volume. Triplicated experiments for 1mL samples, and error bars represent ± one standard deviation. Experiments for 3mL samples were carried out once.

Figure 6-4 shows the sample volume of freeze dried sucrose, and as for the other system, 3mL solution always resulted in larger dried sample volumes than 1mL sample. Solutions containing 10% or 20% sucrose dried without significant volume increased in both sample sizes.

At concentration above 30%, for the 1mL sample, the sample volume increased with sucrose concentration and at 60% concentration filled the whole vial. For 3mL sample, the puffed volume reached the top of vial at concentration ≥30%.

Freeze dried sucrose in this experiment can be seen in Figure 6-6, which shows images of 30% sucrose samples from freeze drying cycle (ii) with initial 1mL or 3mL liquid volume.

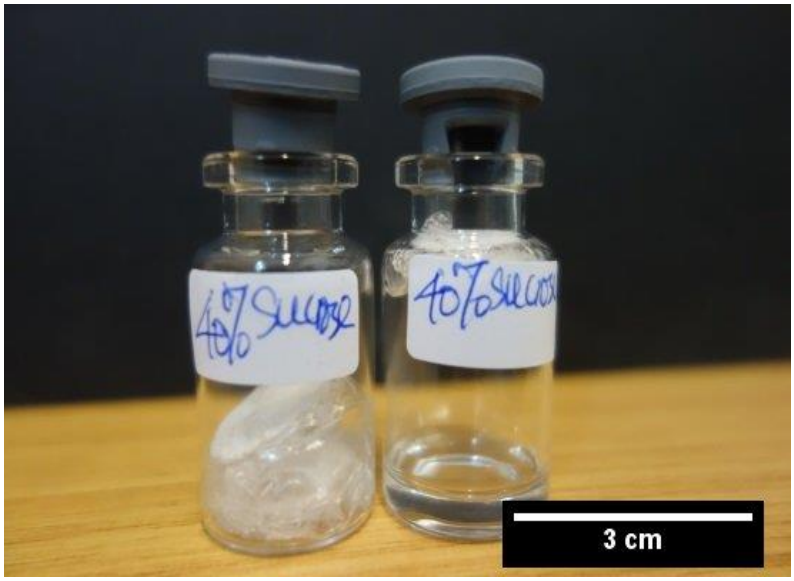

Figure 6-5 Photograph of freeze dried 40% sucrose dried in cycle ii. Left: 1mL sample, right: 3mL sample.

Figure 6-5 (left) shows the freeze drying vial containing puffed structure resulted from 1mL 40% sucrose. On the right of Figure 6-5, freeze dried 3mL 40% sucrose formed (i) a

concentrated layer at the neck of the vial (partially behind the label in the Figure) and (ii) a liquid sample left at the bottom. This suggests that during drying, puffing occurred and expanded sample reached the top of vial, as a concentrated layer was noticed at the vial neck. The existence of such a layer has been reported in the literature on the freeze drying sucrose and slowed down the rate of drying (Quast and Karel 1968, Tsourouflis, Flink *et al*. 1976). Ice sublimation may be limited due to the existence of this layer during freeze drying, so that a large amount of water remained in the sample after drying, resulting in a concentrated solution rather than a dried matrix as sucrose melt back into water. The formation of concentrated layer and the structure loss were also seen during freeze drying gelatine. When freezing gelatine solution, films were formed around ice crystals and ice sublimation was limited. As a result, the pressure and temperature inside the sample increased, causing ice melting and structure collapse during freeze drying (Kaushik and Roos 2007).

Moisture content measurement was also carried out for freeze dried sucrose from cycle (ii) and is displayed in Figure 6-6.

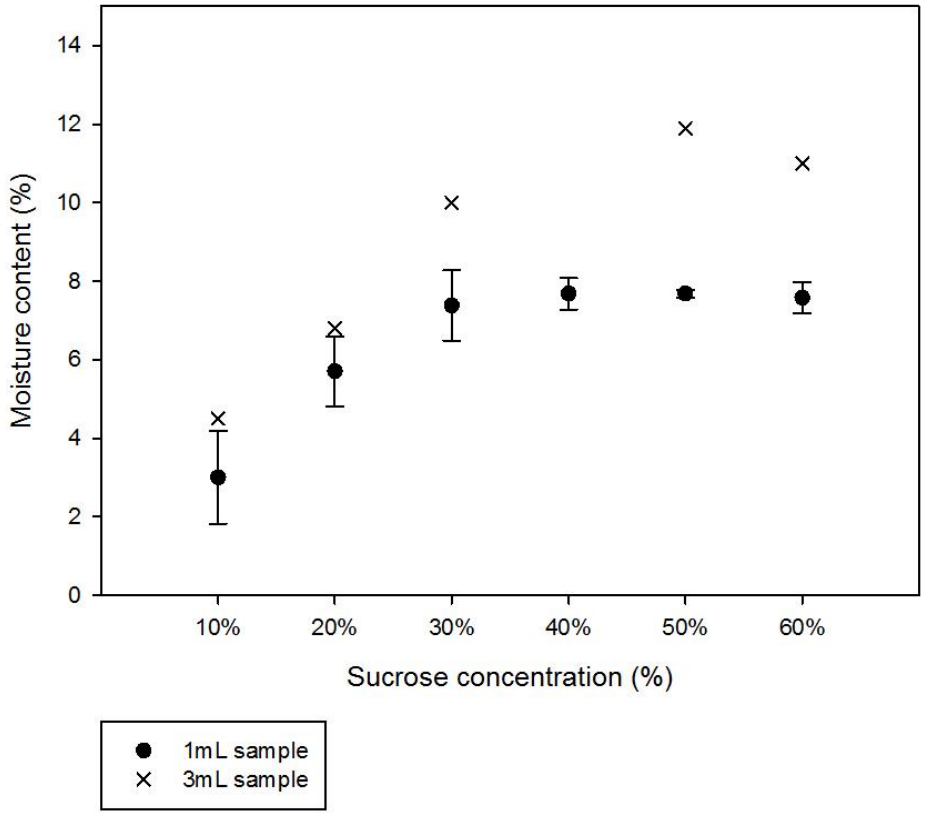

Figure 6-6 Moisture content of freeze dried sucrose samples with different original volume after freeze drying in cycle ii. Triplicated experiments for 1mL samples, and error bars represent ± one standard deviation. Experiments for 3mL samples were carried out once.

As the concentration increased, samples of both sizes contained more residual water after drying, and 3mL samples always contained more moisture than 1mL samples. For samples with 1mL volume, the moisture content was as low as 3% at 10% concentration, and increased to 8% for ≥30% sucrose concentration. Residual water in the 3mL sample was 4% at 10% sucrose then increased to around 11% at higher concentration (30%, 50% and 60%). The moisture content in 40% sucrose was 29%, much higher than the others, possibly due to the blocking effect of the concentrated layer on the top (see discussion of Figure 6-5). The

formation and inhibiting behaviour of concentrated layers may vary in each experiment even though the same formulation/freeze drying conditions were applied.

Studies carried out in section 6.1.1 shows that 3mL sample always resulted in more significantly increased volume and larger amount of residual water compared with 1mL, possibly due to the given drying time (12 hours) was not long enough to dry 3mL samples. 1mL sample was used for all the following experiments.

6.1.2 Effect of concentration

After the study of effect of sample volume on freeze drying sucrose, 1mL sample was selected for all the following experiments, as it resulted in less increased volume and less residual water. In this section, effect of concentration on freeze drying was studied in two freeze drying cycles (cycle i and cycle ii). These differed in the primary drying temperatures: one was -40°C (cycle i), and the other one was at -20°C (cycle ii). Details of the cycle parameter and temperature profile can be seen in the section 3.4.3.

6.1.2.1 Primary drying at -40°C (cycle i)

Freeze drying cycle (i) with primary drying temperature at -40°C was first used. Sucrose solutions with concentration ranging from 10% to 60% were dried, and the sample volumes and the direct observation of samples were displayed in Figure 6-7.

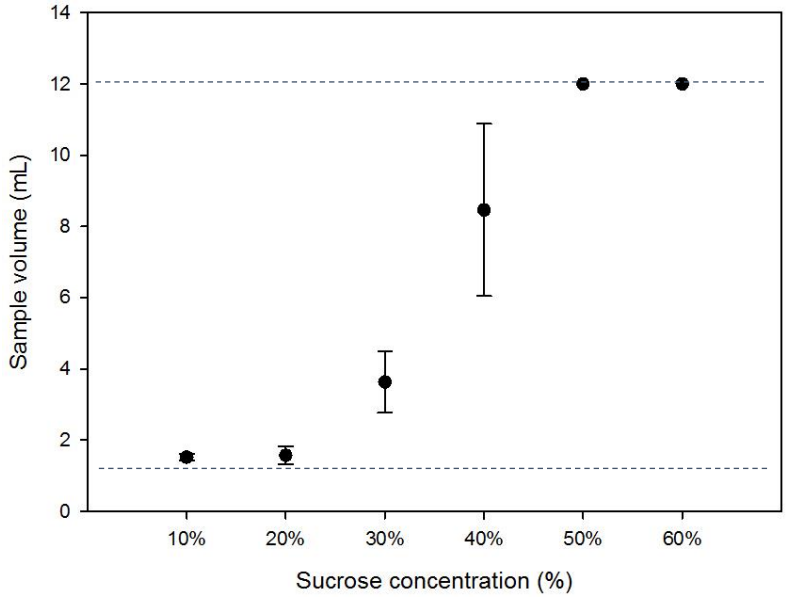

a

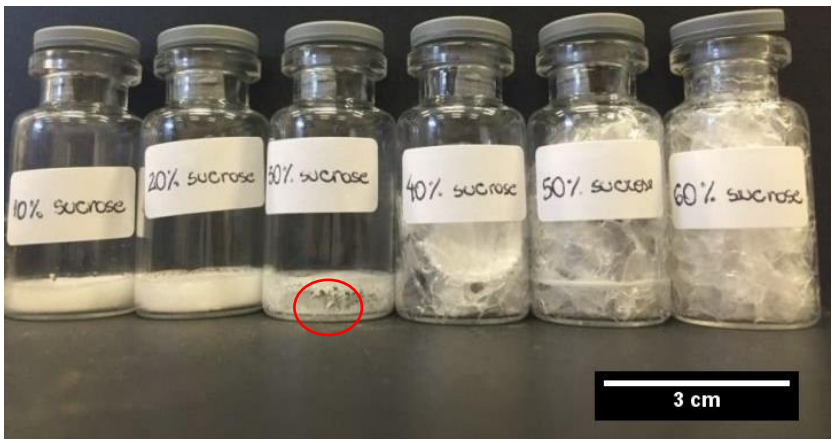

b

Figure 6-7 (a) Sample volume of freeze dried sucrose in cycle i. Experiments were triplicated and error bars represent one standard deviation; (b) Photograph of freeze dried sucrose after freeze drying in cycle I, red circle indicated the structure collapse.

Figure 6-7 (a) showed the increasing sample volume in freeze dried sucrose as the original sucrose concentration increased. Volume of 10% and 20% sucrose remained very close to the original 1mL without puffing. All concentrations of 30% and above, the sample volume increased monotonously until reaching the top of vial at 50% concentration.

A direct look at the macrostructure of the samples is provided in Figure 6-7 (b). 10 and 20% sucrose formed a cake structure without volume change after drying. The image of 30% sucrose did not show any volume increase, but some collapse in the internal structure was noticed (indicated by a circle). A concentrated layer was formed in 40% sucrose and puffing can be noticed. Significant volume expansion was seen in 50% and 60% sucrose in that the whole vial was filled with this foam-like structure. The moisture content of these samples is shown in Figure 6-8.

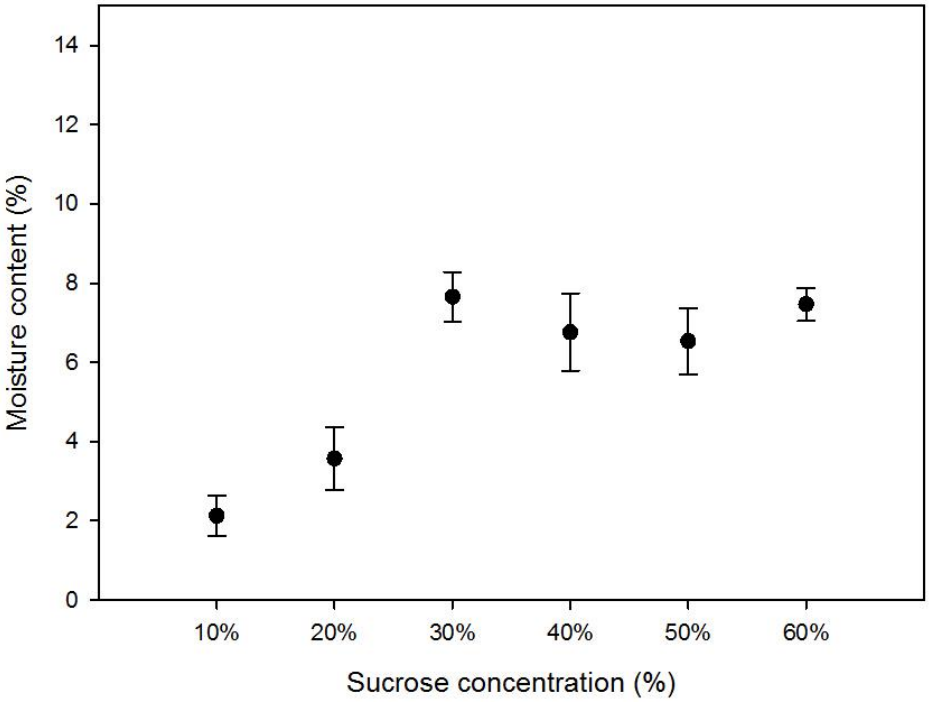

Figure 6-8 Moisture content of sucrose solutions after freeze drying with cycle i. Experiments were triplicated and error bars represent ± one standard deviation.

Figure 6-8 shows that moisture content of freeze dried sucrose increased as concentration increased. Samples that maintained the structure (see Figure 6-8), 10 and 20% sucrose,

contained less than 5% moisture. The puffed samples contained more residual moisture: between 6% and 8% for freeze dried sucrose with the initial concentration at 30% ≤c% ≤ 60%.

Increasing solid concentration resulted in more volume increase and higher residual water in the freeze dried samples, suggesting that it is more difficult to freeze dry sucrose solutions with higher concentration.

As discussed in section 2.3.3, sample temperature is a critical factor in freeze drying as overheated sample might lead to structure collapse. To understand the difficulties in the process of freeze drying high solid content sucrose system, the real time measurement of sample temperature during freeze drying was carried out. The temperature profiles of 10 to 60% sucrose during primary and secondary drying are displayed in Figure 6-9.

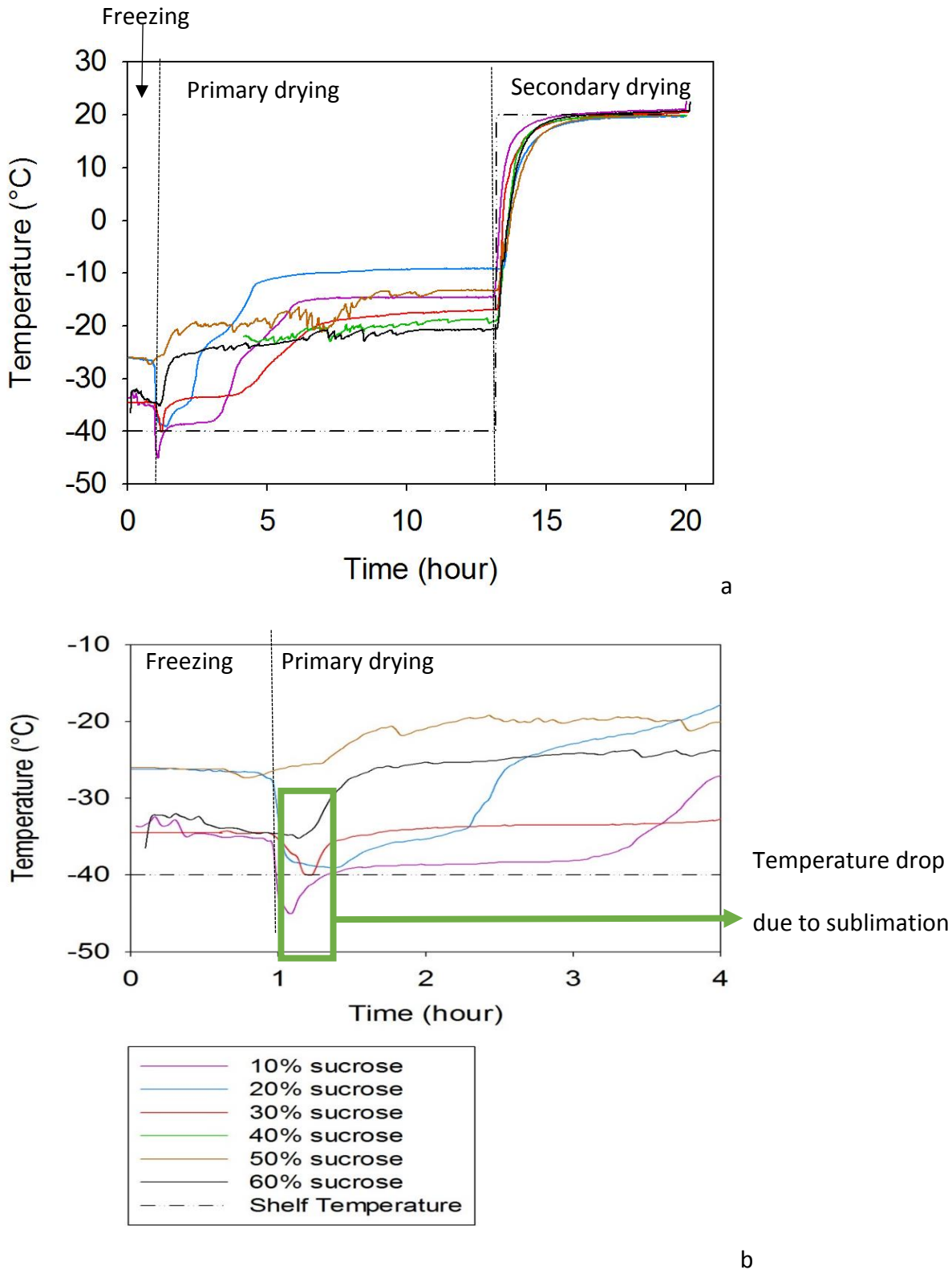

Figure 6-9 (a) Sample temperature (10-60% sucrose solutions) during freeze drying in cycle i; (b) Zoom-in of sample temperature during last one hour freezing and first three hours of primary drying. The stages of freeze drying are shown in both graphs.

Figure 6-9 shows that during a freeze drying cycle, samples started from frozen temperature, and ended up approaching the shelf temperature of secondary drying (20°C).

All sample temperatures remained lower than -20°C at the end of freezing. When vacuum was applied in the chamber (at time 1h in the profile), a sharp temperature drop can be seen (see Figure 6-10 b), due to exothermic heat transferred from the sample due to significant ice sublimation at a value of 51 kJ/mol (Ratti 2013).

The temperature drop was more significant in less concentrated systems; for example, approximately a 10°C decrease for 10% sucrose, 5°C decrease for 30% sucrose and 1°C decrease for 50% sucrose. 10% sucrose temperature was even lower than the shelf temperature, and sample temperature cannot be controlled directly, but depends on the formulation, shelf temperature, chamber pressure and heat transfer between shelf and sample (Tang and Pikal 2004, Tang, Nail *et al*. 2005) (section 2.3.2 equation 2.1). The significant temperature drop in 10% sucrose was probably due to the sublimation of large number of ice crystals.

For 10 and 20% sucrose samples, a large number of ice crystals were formed during freezing, and significant heat is transferred out of the sample when ice is sublimating, resulting in first the sample temperature drop at the beginning of primary drying and then the system remaining at low temperatures.

Collapse temperature of freeze drying has been discussed in section 2.3.3, above which sample may undergo structure loss. For sucrose system, the collapse temperature is closely linked with its T'g or T'm, which is -46°C or -34°C respectively (Roos and Karel 1991). Figure

6-9 shows that 10% and 20% sucrose temperature was lower than -34°C for at least one hour; while for 30% sucrose, the sample temperature was close but slightly higher to -34°C.

Half an hour after primary drying starts, an increase in the sample temperature can be observed. This is because there is less heat transferred out of the sample due to slower ice sublimation, as the layer resistance increases as the sublimation front moves into the sample (Tang, Nail *et al*. 2005).

This increasing temperature will not damage the structure, as the solid matrix becomes more stable with much lower water content and thus can maintain its structure at higher temperature instead of transition to liquid state (Tsourouflis, Flink *et al*. 1976).

The difference in sample temperature for various concentrations of sucrose during primary drying resulted from different sublimation rates (Franks 1998). For the high concentration samples (50% and 60%), fewer ice crystals were formed during freezing due to less available water (see discussions in Chapter 4) compared with low concentration sucrose solutions. After primary drying started, the limited amount of ice crystal sublimation did not lead to sufficient heat transfer out of the sample, resulting in a higher sample temperature for high concentration samples. As an example, one hour after primary drying starts, the temperature of 10% sucrose was -39°C (lower than T'm) while temperature of 60% sucrose was -25.5°C (higher than T'm).

The overheat (sample temperature above T'm) of the highly concentrated sucrose samples during freeze drying might cause ice melting in the sample. After ice melts into water, water evaporation might happen in the sample, instead of ice sublimation, this might cause (i) damage of previously formed porous structure; (ii) a concentrated layer formed on the top

of the sample which will further slow down mass transfer of water vapour and eventually (iii) volume expansion under the vacuum (Tsourouflis, Flink *et al*. 1976).

As mentioned in section 2.3.1, end of primary drying phase is indicated by the sharp increase in temperature. Here the temperature plateau varied between -25°C and -10°C. During secondary drying, all sample temperatures increased rapidly and approached the secondary drying temperature (20°C).

It is clear that the product quality and the processability of freeze dried sucrose depends on the initial solution concentration. Freeze dried samples with low moisture content, and without structure loss (puffing or collapse) are desired in this research. In the study of freeze drying cycle i, only the samples which temperature was lower than T'm during ice sublimation (10 and 20%) were dried without volume increase and resulted in a low moisture content (<5%). This suggested that solutions with low concentration formed large number of ice crystals during freezing, and significant heat transferred out of the sample during sublimation, maintaining sample temperature below T'm and avoiding ice melting and structure collapse during primary drying.

Apart from that, the dried cake formed from low concentration solutions has a large specific area which aids removal of absorbed water during secondary drying, resulting in low moisture content in the final freeze dried product (Tang and Pikal 2004).

6.1.2.2 Primary drying at -20°C (cycle ii)

The effect of concentration on freeze drying sucrose solutions was studied in section 6.1.2.1 using cycle (i), and shows that the result of freeze drying was closely linked with sample temperature, while sample temperature did not only depend on shelf temperature but also

on solution concentrations. As an example, the 10 and 20% sucrose sample temperature was lower than shelf temperature (-40°C) during sublimation.

In this section, the effect of concentration on freeze drying sucrose was studied in freeze drying cycle (ii) with a primary drying temperature at -20°C, to compare the effect of shelf temperature on freeze drying sucrose product quality (section 6.1.3).

Volume changes of sucrose solutions (concentration at 10, 20, 30, 40, 50 and 60%) after freeze drying at -20°C are shown in Figure 6-10.

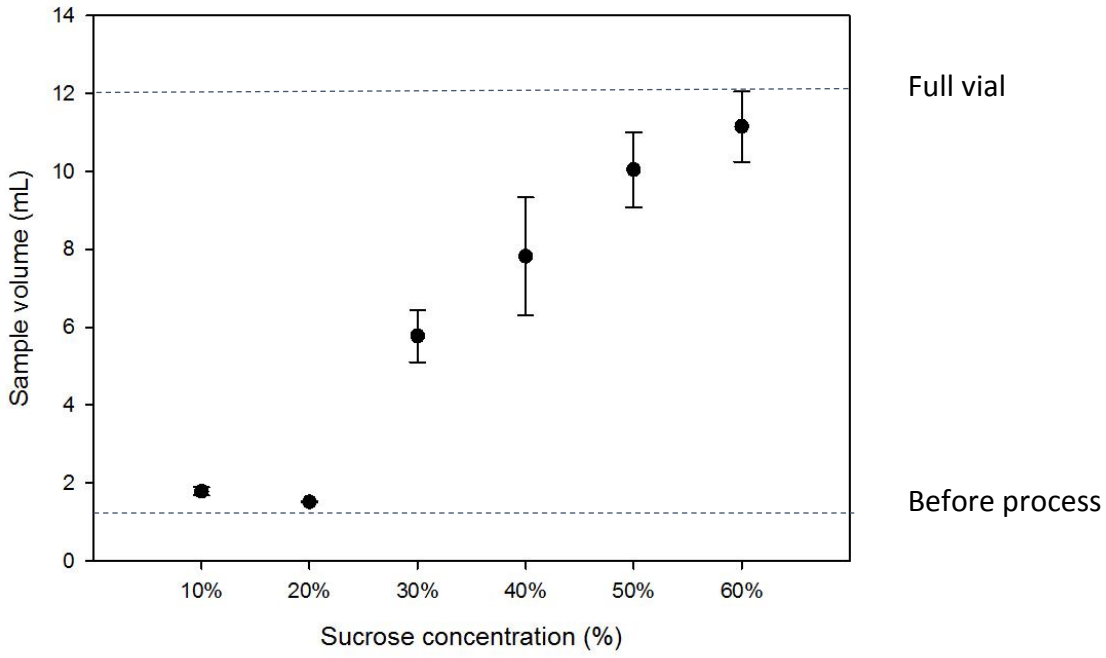

Figure 6-10 Sample volume of sucrose solutions after freeze drying in cycle ii. Experiments were triplicated and error bars show ± one standard deviation.

Samples of 10 and 20% sucrose remained at almost same volume after freeze drying in cycle (ii). While for sucrose concentration ≥30%, the dried sample volume increased

monotonously as concentration increased; e.g. volume of 30% sample was 6mL and volume of 60% sample reached the highest volume of 12 mL.

The amount of residual water in these samples is displayed in Figure 6-11.

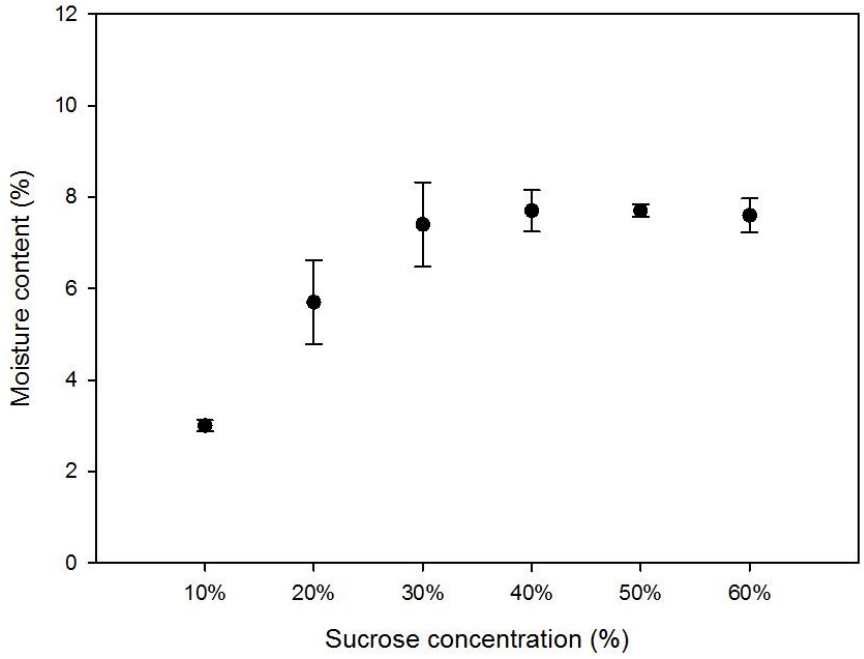

Figure 6-11 Moisture content of sucrose solutions after freeze drying in cycle ii. Experiments were triplicated and error bars show ± one standard deviation.

Sample dried from 10% sucrose was the only sample that contains less than 5% residual water, and the moisture content of the rest samples varied in the range between 6% and 8%.

6.1.3 Effect of drying temperature

Here, the behaviour of freeze dried sucrose (moisture content and sample volume) was compared between freeze drying cycle i and cycle ii (the difference in primary drying temperature, details in section 3.4.3). The sample volume is shown in Figure 6-12.

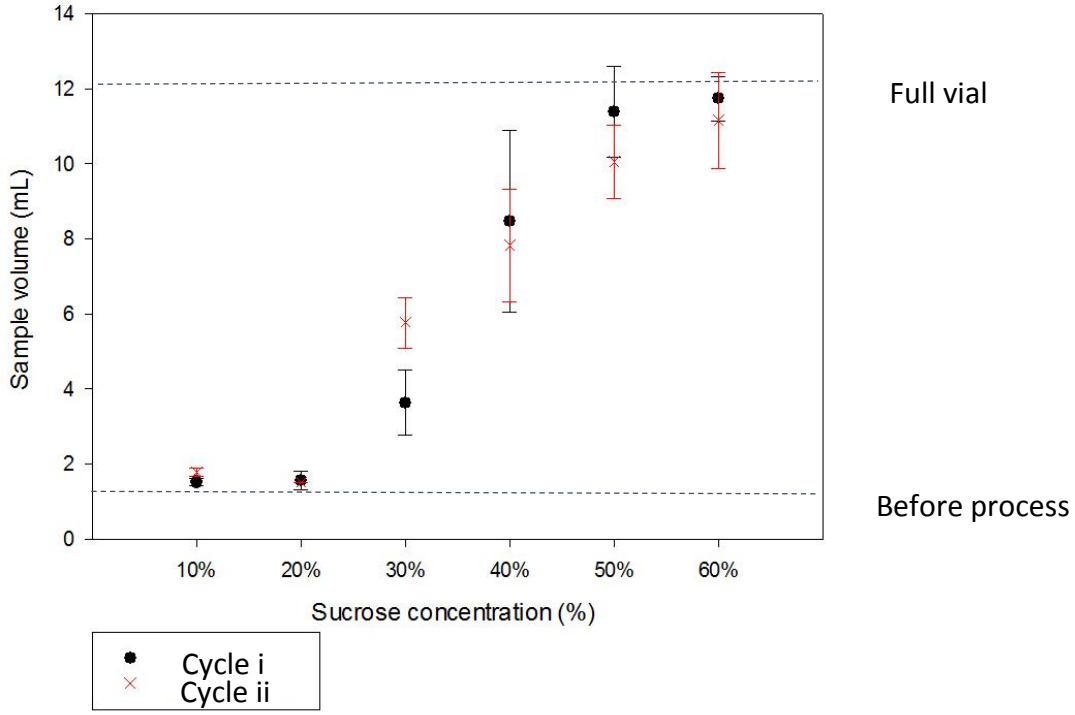

Figure 6-12 Volume of freeze dried sucrose after cycle i and ii. Experiments were triplicated and error bars show ± one standard deviation.

As discussed in section 6.1.2, sample volume increased as the original sucrose concentration increased, independent of the primary drying temperature being -20 ˚C or -40 ˚C.

For 10% and 20% sucrose system, at both drying temperatures the sample did not increase its volume after drying. While for 30% sucrose, drying at -40 ˚C (cycle i) resulted in a slight increase from 1mL to 4mL in sample volume. Increasing drying temperature to -20 ˚C (cycle ii), however, led to a more obvious increase in volume to 6mL. The difference between the

two drying temperatures became smaller at higher concentrations, as puffing became more dominating in high concentration solutions. A more straightforward visualisation can be obtained from the sample images in Figure 6-13.

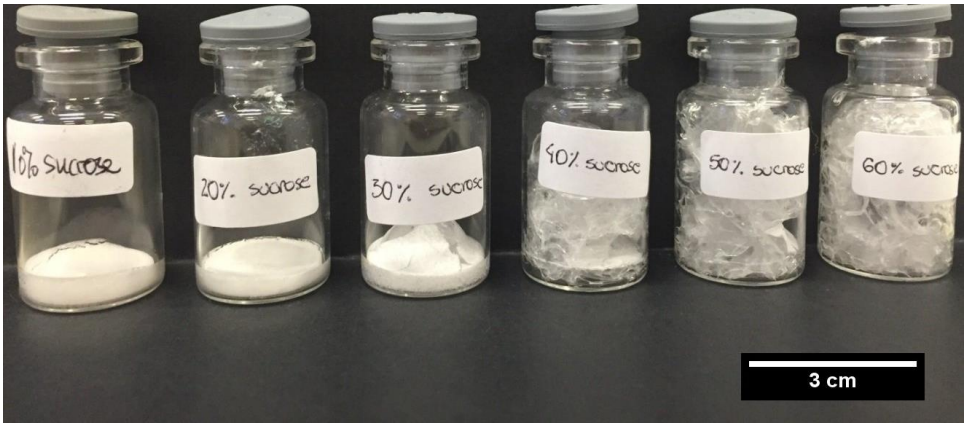

a

b

Figure 6-13 Images of freeze dried 10-60% sucrose from (a) cycle i and (b) cycle ii.

Freeze dried cakes without volume change can be seen in 10% and 20% sucrose in both conditions. For 30% sucrose freeze dried from -40 ˚C in primary drying (Figure 6-13a, cycle i), puffing took place in the middle of the sample and the rest of the sample remained at the same height. For the other 30% sucrose solution, drying at -20 ˚C resulted in more obvious

puffing with a foam-like structure being noticed in the whole sample, reaching 1 cm in height. The different behaviour of 30% sucrose with primary drying temperatures at -20 ˚C/-40 ˚C resulted from temperature history of sample during drying, as shown in Figure 6-14, together with temperature profile of 10 and 50% sucrose in both cycles.

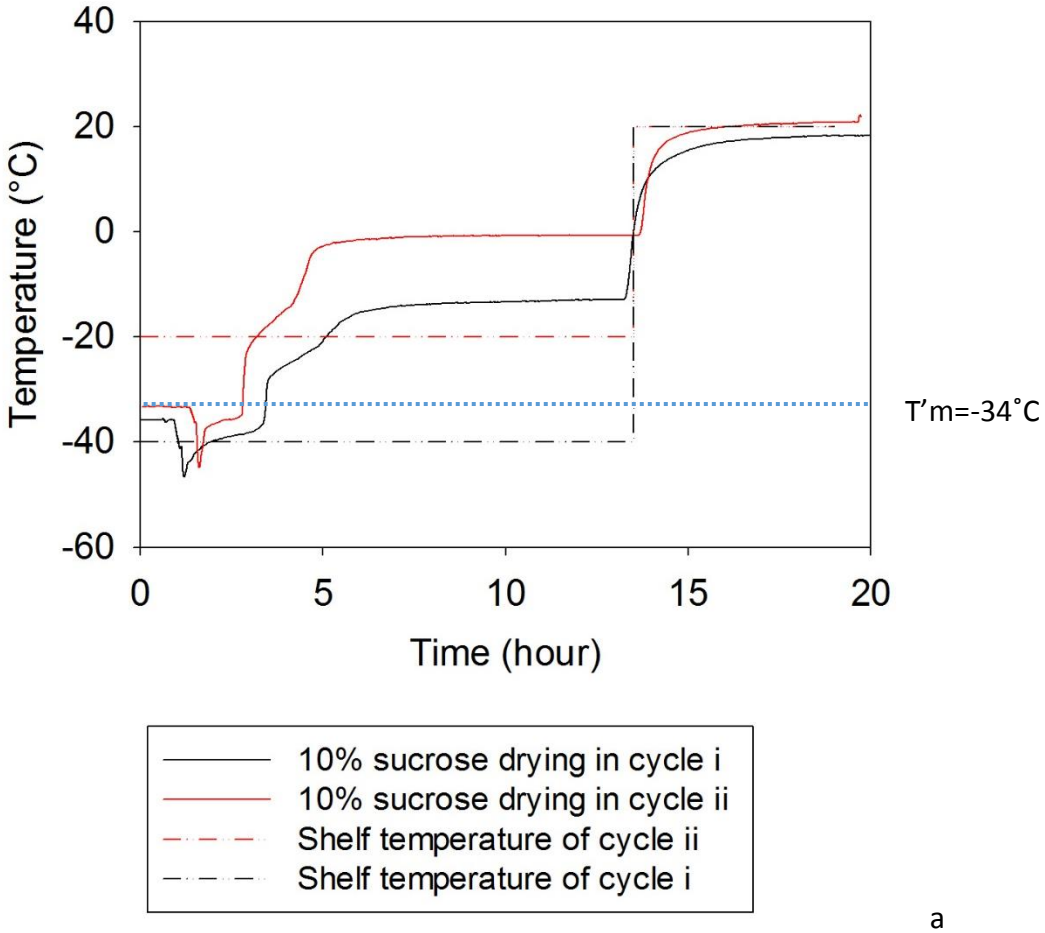

a

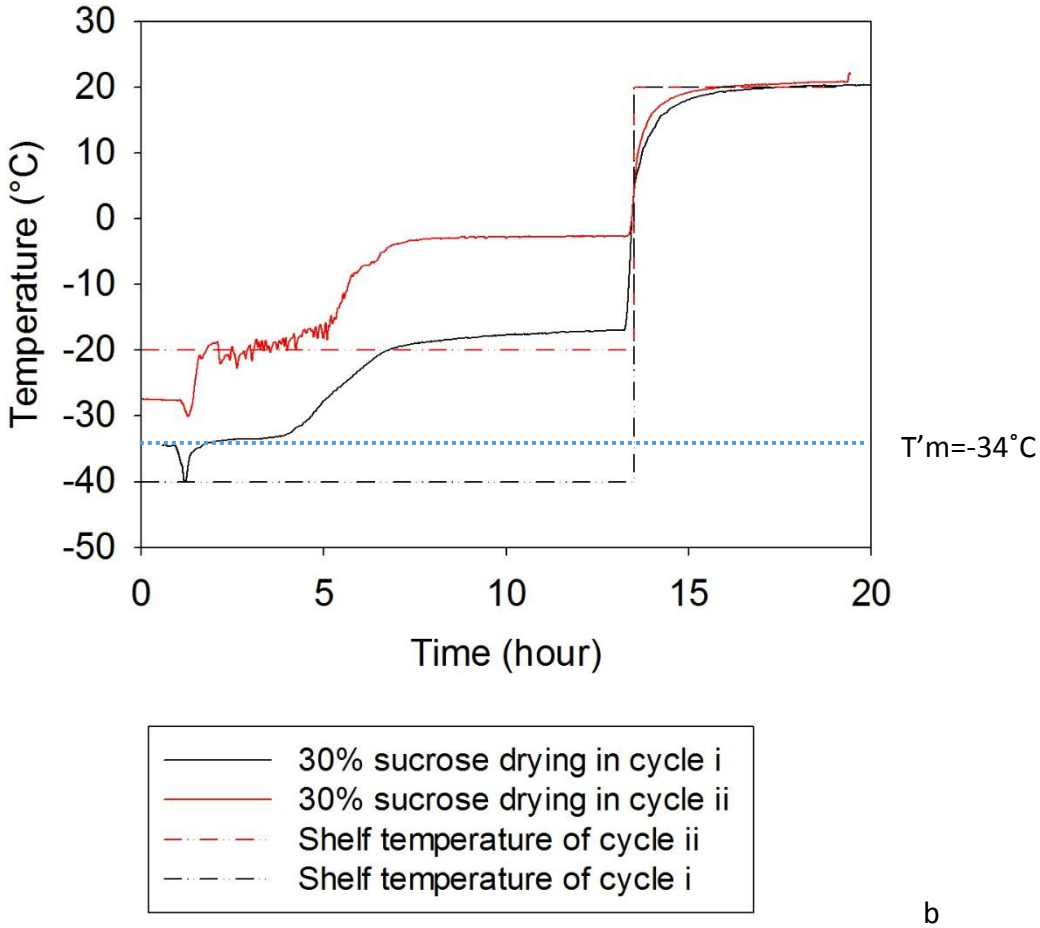
30
20
10
0
-10
-20
-30
-40
-50
Temperature (°C)
0
5
10
15
20
Time (hour)
T'm=-34˚C
30% sucrose drying in cycle i
30% sucrose drying in cycle ii
Shelf temperature of cycle ii
Shelf temperature of cycle i

b

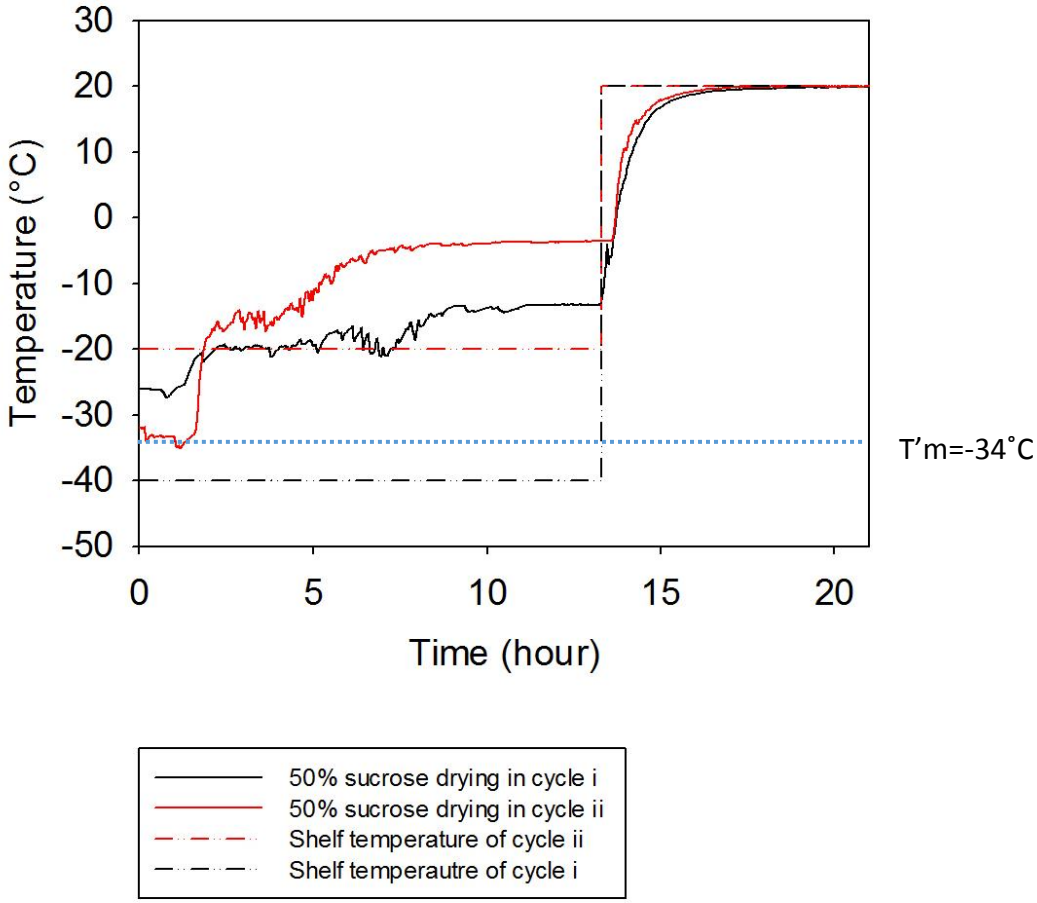

c

Figure 6-14 sample temperature during freeze drying in cycle (i) and (ii) (a) 10% sucrose (b) 30% sucrose (c) 50% sucrose. T'm of sucrose was indicated in the graphs as blue dotted lines.

Figure 6-14 (a) shows temperature profile of 10% sucrose drying at -20/-40 ˚C primary drying temperatures (cycle i and ii). Despite the difference in primary drying temperature, sample was kept below T'm (indicated by blue dotted lines) for about 2 to 3 hours, allowing time to sublimate ice crystals without ice melting. As a result, non-collapsed samples were achieved (see Figure 6-13).

From Figure 6-14 (b), the overall trend of the sample temperature for 30% sucrose drying at -20/-40 ˚C were similar: (i) the temperature experienced a sudden drop once the vacuum was applied, due to the ice sublimation; (ii) the sample temperature then increased, first

gently then sharply when most ice was sublimated; (iii) the temperature remained stable at chamber temperature (about 20 ˚C higher than shelf temperature) for the last six hours of primary drying; (iv) the sample temperature increased rapidly and approaching shelf temperature at 20 ˚C during secondary drying.

There are two differences between the two curves: (i) in cycle i sample temperature was slightly above and very close to T'm, whilst the temperature of the sample dried in cycle ii was always 20 ˚C higher than that; (ii) the temperature profile of drying at -40 ˚C was smooth while there were fluctuations in the temperature profile of drying at -20 ˚C when the temperature increased. The fluctuations suggested non-continuous ice sublimation, possibly due to the structure collapse (shown in Figure 6-13). The overheating of 30% sucrose during drying at -20 ˚C caused the collapse and puffing of the dried product.

Figure 6-14 (c) shows temperature profiles of 50% sucrose during freeze drying. Both samples which were dried at two primary drying cycles showed fluctuations during primary drying and temperatures were both above T'm, in agreements with the puffed structure obtained after drying.

Moisture content of samples dried in two cycles are displayed in Figure 6-15.

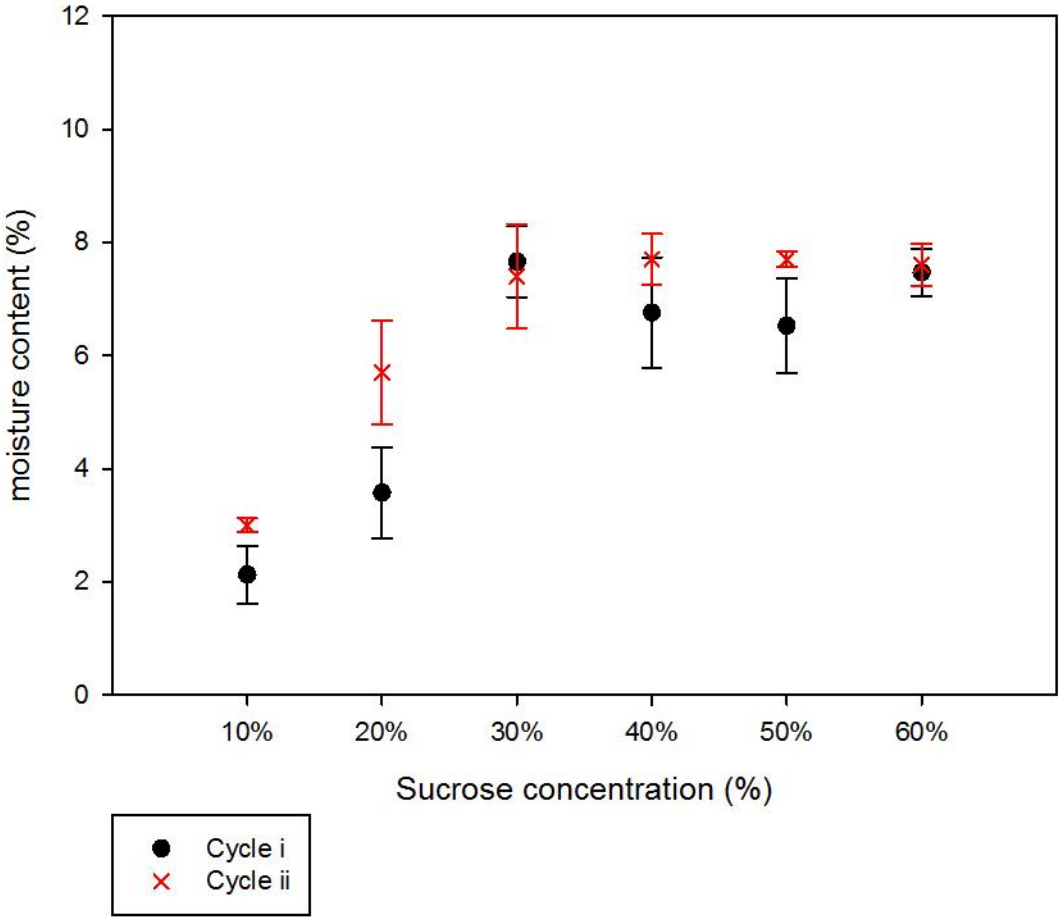

Figure 6-15 Freeze dried sucrose moisture content as a function of solution concentration after drying in cycle i and ii. Experiments were triplicated and error bars show ± one standard deviation.

For 10% and 20% sucrose, samples dried at -20˚C contained more residual water than that dried at -40 ˚C, e.g. 1% more in 10% sucrose and 2% more in 20% sucrose. In freeze dried products, less residual water is preferred as this will secure more stable sample and longer shelf life as higher moisture content might accelerate sample collapse during storage.

At concentration ranging between 30% and 60%, moisture content in the sample was around 7 to 8% for drying from both cycles.

Overall drying at lower temperature (-40 ˚C compared with -20 ˚C) can produce samples with less residual water and less volume increase, as the sample temperature was lower during primary drying. The lower temperature (-40 ˚C) was thus preferred in the experiments (e.g. in section 6.1.4).

6.1.4 Effect of heating rate on freeze drying

There is a significant temperature gap of 60 ˚C between primary drying (-40 ˚C) and secondary drying (20 ˚C) temperature in each cycle. The rate of the temperature increase between the two drying stages also plays an important role in quality of the sample.

In this section, three freeze drying cycles were used: (i), (iii), and (iv) (see section 3.4.3) to study the effect of the heating rate between primary and secondary drying. All of them employed a primary drying temperature of -40˚C and a secondary drying temperature of -20˚C. Three different heating rates were used during the transition to secondary drying:

Cycle (i); the fastest rate that the freeze drier can reach, approximately 180 ˚C/hour;

Cycle (iii); a slower heating rate of 10 ˚C/hour;

Cycle (iv); the lowest heating rate: 5 ˚C/hour.

The most straight forward way to examine the effect of heating rate on behaviour of samples is to examine samples directly. Figure 6-16 (a) has already been shown in Figure 6-13 (samples freeze dried at -40 ˚C), and is used here as a reference for the fastest heating rate (cycle i). Figure 6-16 (b and c) shows samples involved in slower heating rates during drying at 10 ˚C/hour and 5 ˚C/hour (cycle iii and iv) respectively.

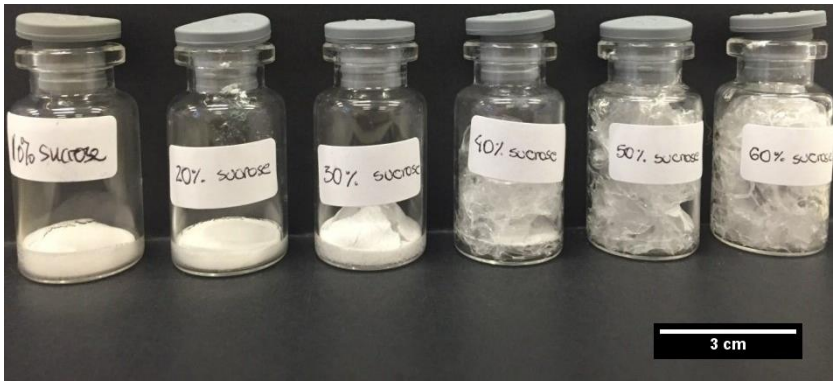

a

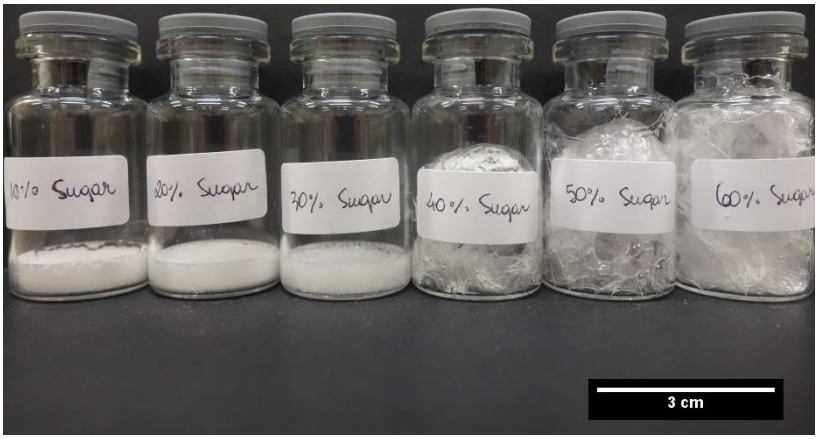

b

c

Figure 6-16 Images of freeze dried 10, 20, 30, 40, 50, and 60% sucrose after drying cycles with different heating rate (a) rapid heating of 180 ˚C/hour, Cycle i; (b) heating rate of 10 ˚C/hour, Cycle iii, (c) heating rate of 5 ˚C/hour, Cycle iv.

Structures without significant volume change can be seen for low concentration sucrose (10 and 20%), whilst puffing occurred for higher concentration systems (40, 50, and 60% sucrose) in all cycles. The most significant difference in the sample behaviour from fast/slow

heating rate was in 30% sucrose. At the slower heating rates (cycle iii and iv), no puffing can be seen in 30% sucrose, while samples dried in cycle (i) was puffed.

Volume of freeze dried sucrose using these three cycles were displayed in Figure 6-17.

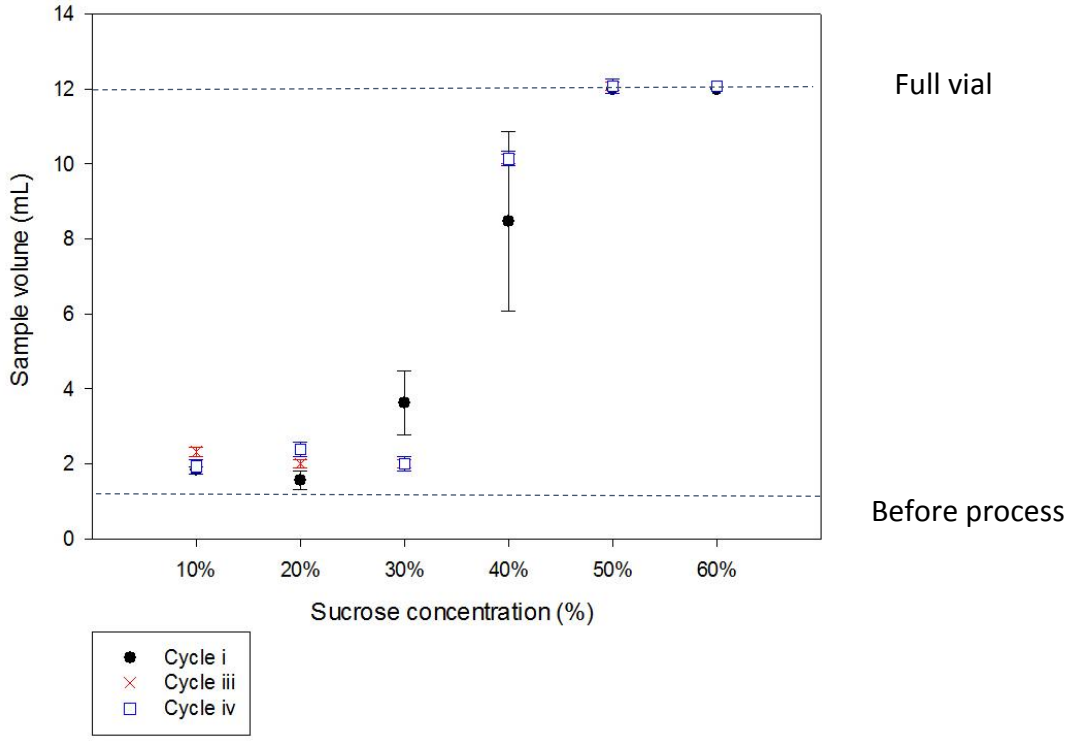

Figure 6-17 Sample volume of 10, 20, 30, 40, 50 and 60% sucrose freeze dried from three cycles (i, iii, and iv) with different heating rates. Experiments were triplicated and error bars show ± one standard deviation.

As discussed in Figure 6-16, the most significant difference in the sample volume (read from Figure 6-17) from different heating rate was in 30% sucrose samples, while the sample volume of other concentrations was not sensitive to heating rate. For 30% sucrose, after drying in cycle (i) with rapid heating, the sample increased its volume from 1mL to about 4mL. By reducing the heating rate to 10°C/hour or 5°C/hour, 30% sucrose can be dried to less than 2mL volume.

The results suggest that puffing in 30% sucrose can be reduced if the heating rate between primary and secondary drying is reduced, in agreement with the discussion in section 2.3.1.

Figure 6-18 displays the moisture content in the freeze dried sucrose matrix after different freeze drying cycles.

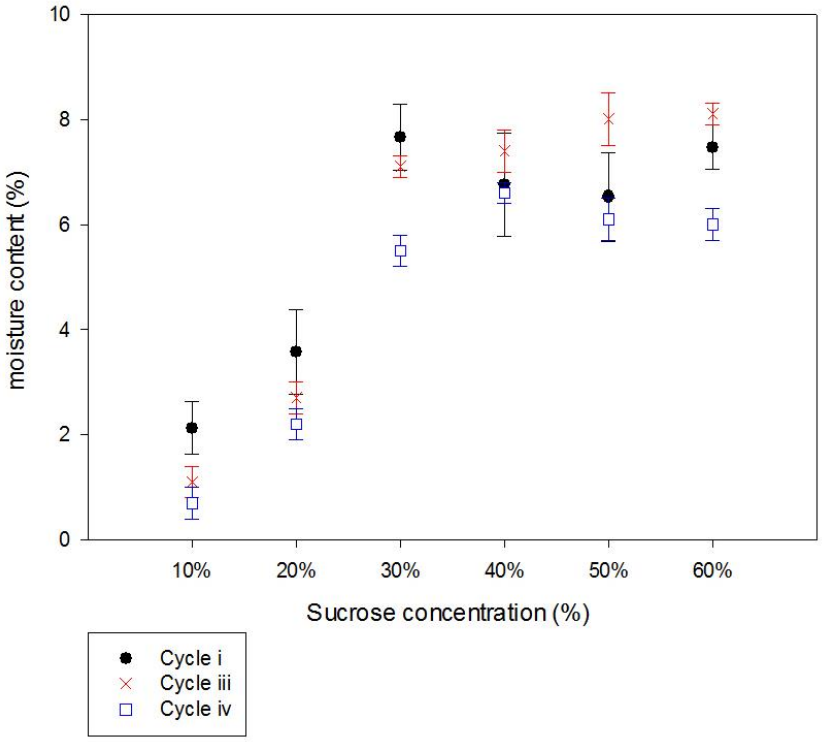

Figure 6-18 Moisture content of freeze dried sucrose (10, 20, 30, 40, 50 and 60 %) after freeze drying cycles with different heating rates. Experiments were triplicated and error bars show ± one standard deviation.

Freeze drying cycle with slower heating rate resulted in less residual water in the dried product in general; however, the decrease in the moisture content varied in each concentration. For example, there was about 1% decrease in moisture content for freeze

dried 10% sucrose using slower heating rate, and the moisture content did not show any significant difference in drying 40% sucrose.

6.2 Freeze dried gum arabic solutions

Research of freeze drying sucrose solutions was carried out in section 6.1. Here, another carbohydrate system, gum arabic, was used in the study of freeze drying high solid content system to investigate the effect of type of solid on the freeze drying. Compared with sucrose, gum arabic has much larger molecular weight (>10000), which lead to a high collapse temperature (see section 2.3.4).

6.2.1 Effect of concentration and primary drying temperature

The effect of solid concentration and primary drying temperature were investigated here using 10 to 60% gum Arabic solutions.

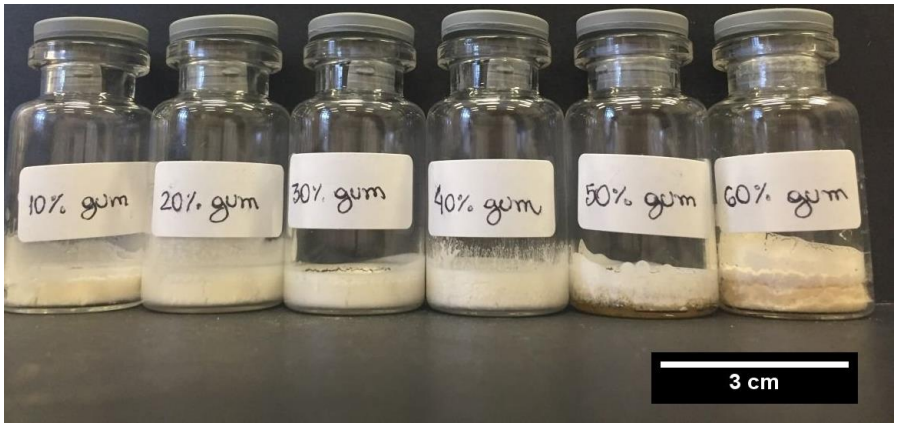

Figure 6-19 Images of freeze dried 10, 20, 30, 40, 50 and 60% gum Arabic using cycle i.

An image showing behaviour of freeze dried gum arabic (10 to 60% concentration, cycle i) is displayed in Figure 6-19. Compared to the high concentration sucrose systems, no

significant volume expansion was seen here in freeze dried gum arabic cakes. Overall, the sample maintained at the same volume as prior to freeze drying. The only exception was at 60%, where the volume increased slightly (exact value see Figure 6-20). However, in each vial, there some solids were attached to the wall of the vial as a thin layer.

Two primary drying temperatures (-40°C in cycle i/-20°C in cycle ii) were used in freeze drying gum arabic study. The volume of freeze dried gum arabic which was dried from 10-60% concentration solutions using these two drying temperatures are compared in Figure 6-20.

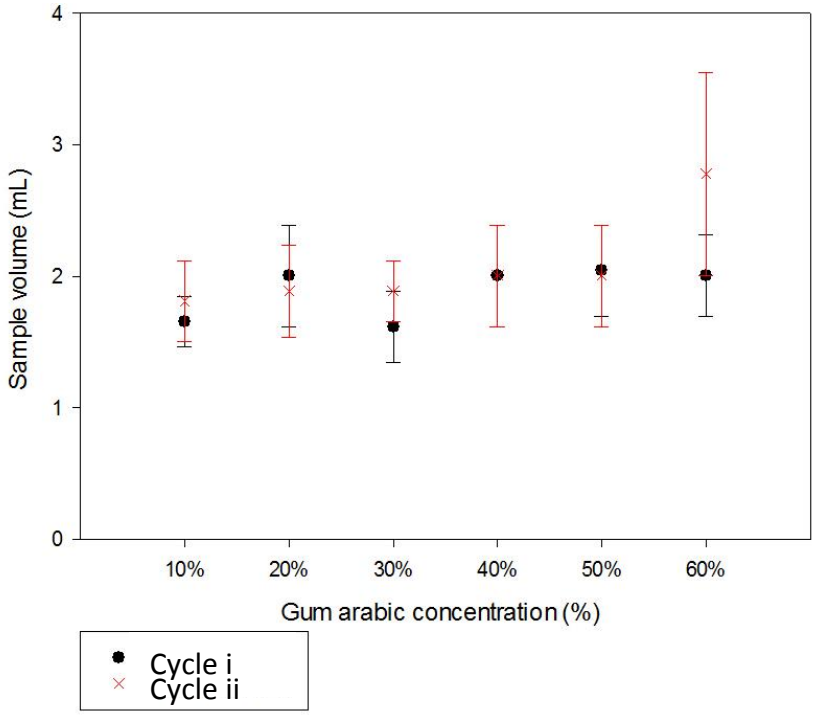

Figure 6-20 Sample volume of freeze dried gum arabic (10 to 60% initial concentration) using cycle i and cycle ii. Experiments were triplicated and error bars show ± one standard deviation.

Overall there was no significant change in gum arabic volumes before and after freeze drying. All samples, exclude 60% gum arabic, have similar volumes of less than 2mL, independent of initial gum arabic concentration or primary drying temperature. 60% gum arabic, however, increased to maximum 2.5 mL when drying temperature was at -20°C in cycle (ii).

Moisture content of freeze dried gum arabic from each concentration and drying temperatures are displayed in Figure 6-21.

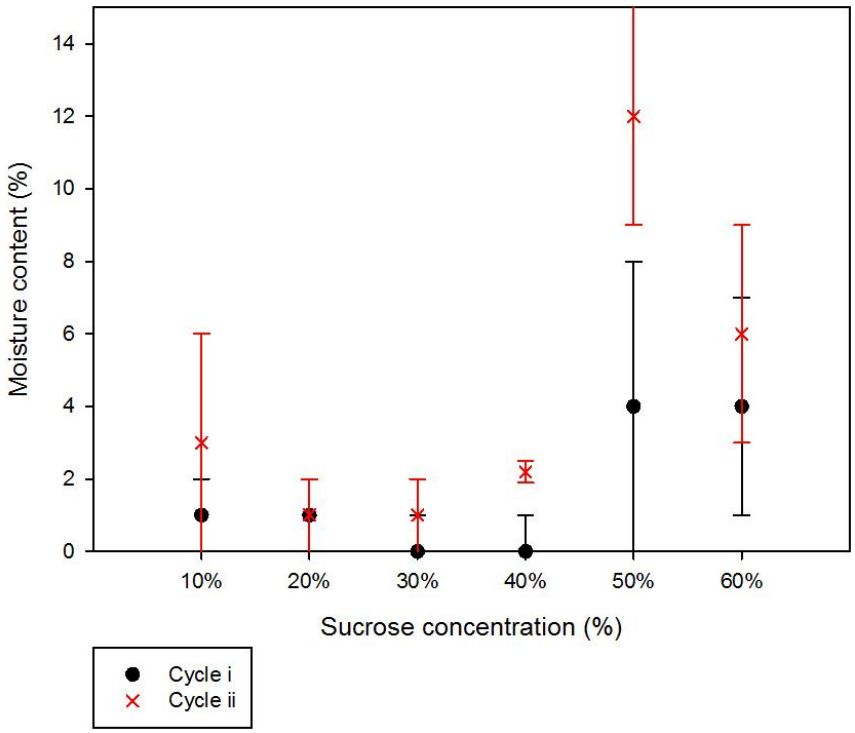

Figure 6-21 Moisture content in freeze dried gum arabic from cycle (i) and (ii). Experiments were triplicated and error bars show ± one standard deviation.

The moisture content of freeze dried gum arabic was quite low, ranging from 0 to 1% as concentration increased from 10 to 30%. When the concentration increased further to 40%, 50% and 60%, maximal of the moisture content of system was at 6%. The method to measure moisture content in gum Arabic samples see section 3.4.4.

The error bars of moisture content in freeze dried gum arabic are larger than that in freeze dried sucrose. It suggests that freeze drying gum arabic may result in samples with varied moisture content by using current drying conditions and moisture measurement method.

6.2.2 Effect of heating rate

In this section, three freeze drying cycles were used to investigate the effect of heating rate between primary and secondary drying (same cycles used in section 6.1.4: cycle i, iii, and iv) on the freeze drying of gum Arabic solutions. In Figure 6-23, sample volumes of freeze dried gum arabic are plotted as a function of initial gum arabic concentration for three freeze drying cycles with fast/slow heating rates.

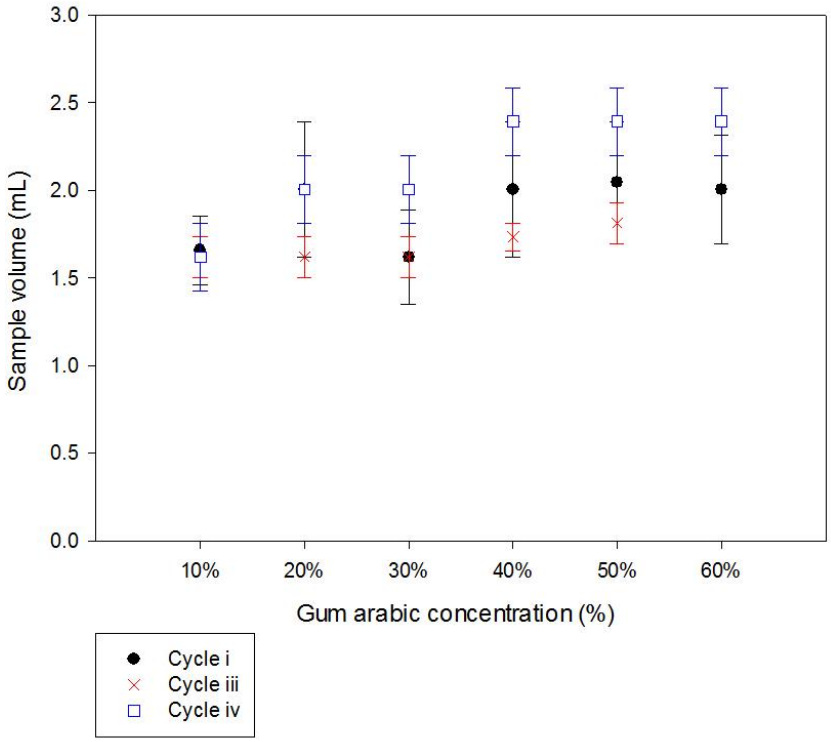

Figure 6-22 Sample height of freeze dried gum arabic after freeze drying in cycle i, iii, and iv. Experiments were triplicated and error bars show ± one standard deviation.

For each freeze drying cycle, there was a very slight increase in the average value of sample volume with concentration. However, taking into consideration the error bars and that there was no statistical analysis done, it can only be said that the samples had similar volumes with increasing gum arabic concentration.

At each given initial concentration, the heating rate marginally affected the sample volume. As all the samples heights were very close to those before freeze drying, so it could be concluded that no puffing can be seen in freeze dried gum arabic at investigated conditions.

Figure 6-23 displays moisture content of freeze dried gum arabic samples as a function of different initial concentration (10 to 60%) from three freeze drying cycles with fast/slow heating rates.

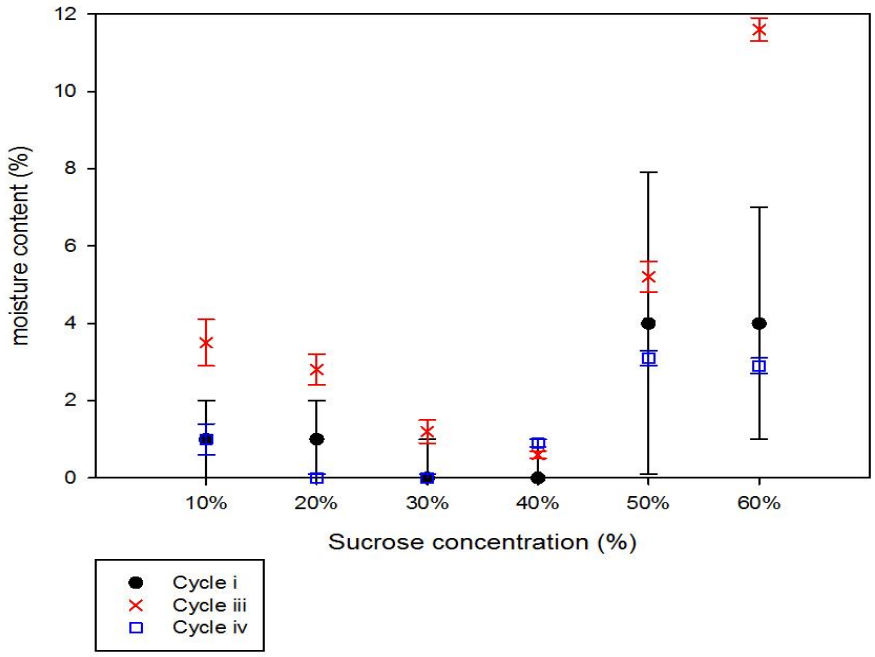

Figure 6-23 Effect of heating rate during freeze drying on moisture content of freeze dried gum arabic with different initial concentrations. Experiments were triplicated and error bars show ± one standard deviation.

Figure 6-23 shows that, moisture content of gum arabic (freeze dried from ≤40% gum arabic) was less than 4% in each freeze drying cycle. When the solid concentration increased within this range, the moisture content in the sample either stayed the same (dried in cycle i and iv) or decreased slightly (dried in cycle iii).

When gum arabic concentration increased to 50% or 60%, the moisture content in the sample increased in all freeze drying cycles. The results indicated that freeze drying gum arabic became more difficult when the original gum concentration increased to 50% or more.

The residual moisture contents of samples were around or below 5%, even rapid heating (180 °C/hour in cycle i) was employed. The only exception was the 60% gum arabic that dried in cycle (iii), which contained 12% moisture. It seemed that freeze drying 60% gum arabic dried in cycle (iii) resulted in sample with higher moisture compared than other cycles.

6.2.3 Comparison between freeze drying gum Arabic and sucrose

Results from studies on freeze drying sucrose and gum arabic are compared in this section.

First, sample volume of gum arabic and sucrose from freeze dried from cycle i are compared in Figure 6-24.

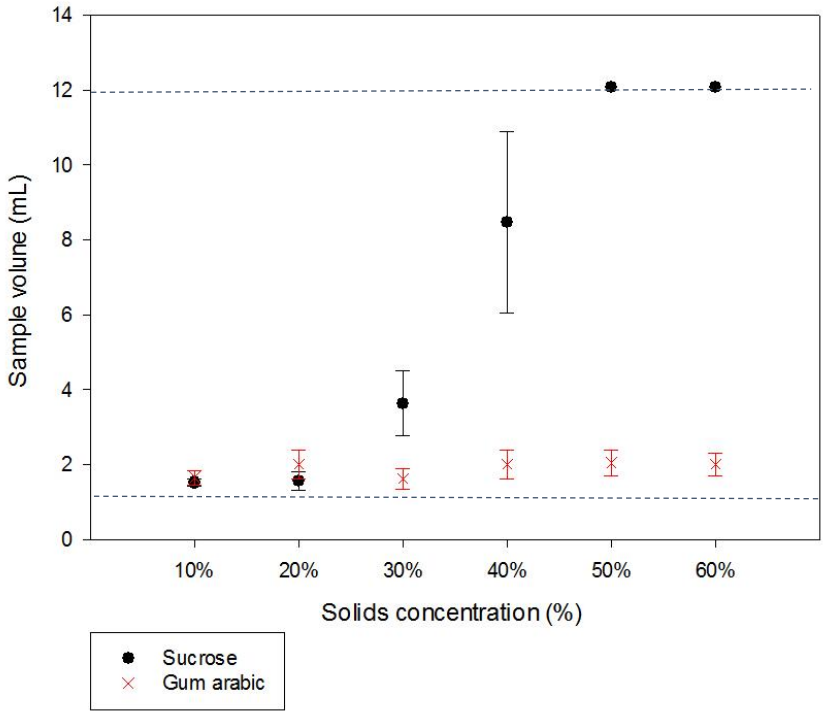

Figure 6-24 Sample volume of sucrose and gum arabic after freeze dried in cycle i; Experiments were triplicated and error bars show ± one standard deviation.

At low concentration (10 and 20%), sample volumes of freeze dried gum arabic and sucrose were similar at around 2mL. However, when the concentration increased to 30% and onwards, freeze dried sucrose expanded its volume significantly and filled the whole vial (12mL) at concentration of 50% and 60%; while gum Arabic, remained at a volume of approximately 2mL even at these high concentrations.

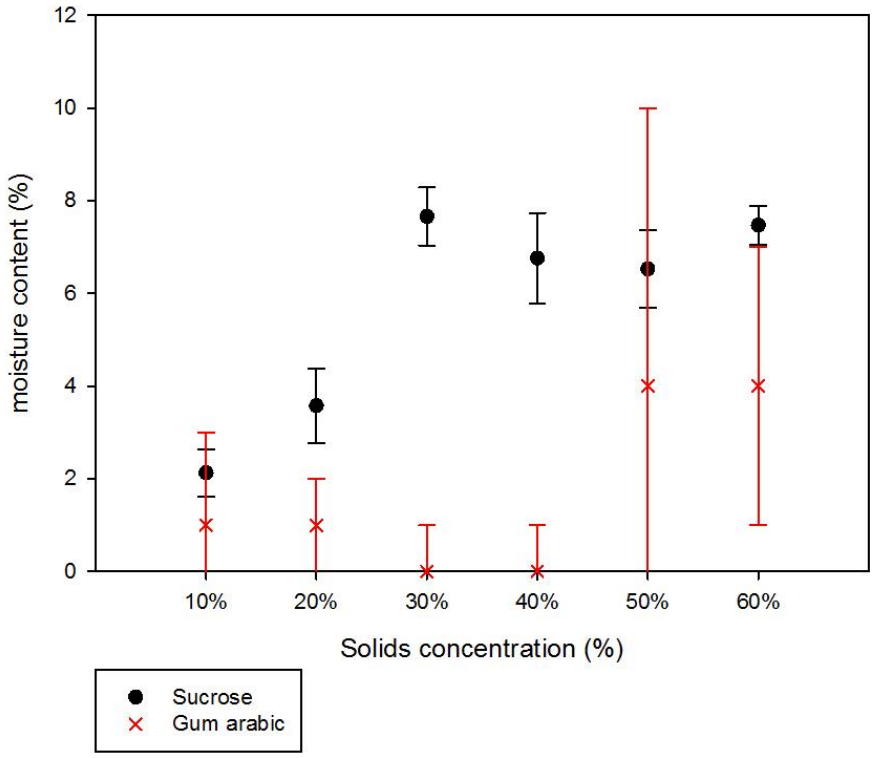

Figure 6-25 Moisture content of sucrose and gum arabic freeze dried in cycle i; Experiments were triplicated and error bars show ± one standard deviation.

The moisture contents of freeze dried 10 and 20% sucrose were lower than 4% and it increased to approximately 7% in puffed samples (initial concentration ≥30%). The collapsed structure limited ice sublimation and thus more residual water was left in the freeze dried matrix.

For gum arabic, moisture content was always lower than 5% even at freeze dried 60% concentration system, and the value was less than that in sucrose at each given concentration.

The different behaviours of these two systems after freeze drying also applied to their sample structure. Internal structure of freeze dried high concentration gum arabic and sucrose are shown in SEM images in Figure 6-26.

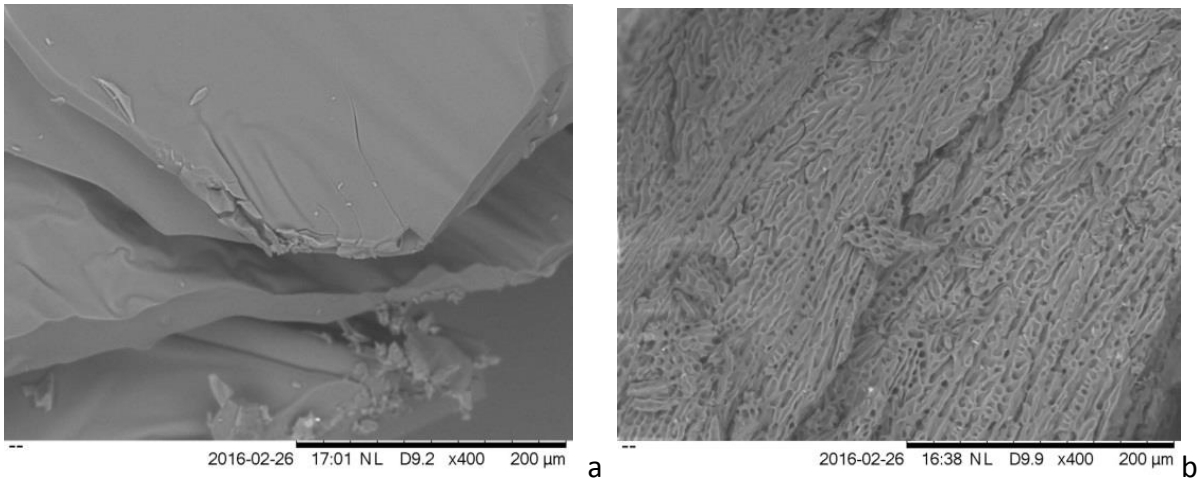

Figure 6-26 SEM images of: (a) freeze dried 60% sucrose (b) freeze dried 50% gum arabic.

Freeze dried sucrose was shown as an amorphous collapsed material with wrinkled films (see Figure 6-26 a). While gum arabic, in the other hand, showed a typical freeze dried structure (as seen in Figure 2-5): porous cake structure (Figure 6-26 b), with numerous pores resulting from ice crystals sublimation and no collapse is seen.

Results showed that gum arabic was dried with good porous structure, low residual moisture and no volume expansion in the whole concentration range (10 to 60%). While for sucrose, freeze drying resulted in collapsed structure, high residual moisture and significant puffing in high concentration (>20%).

As discussed in section 2.3.4, carbohydrate solutions with low molecular weight (e.g. sucrose) are more difficult to freeze dry compared with carbohydrate solutions with high

molecular weight (e.g. gum arabic). This was due to the fact that high molecular weight carbohydrates have higher T'm and T'g, thus a higher collapse temperature. The high viscosity of gum arabic system resulted in a high collapse temperature (Bellows and King 1972) by maintaining the system in a glassy solid state without ice melting in the sample even when the sample temperature increased. Ice crystals can thus sublimate without structure loss. For instance, gum arabic has T'm at -10°C and T'g at -15°C (Kaushik and Roos 2007), while sucrose with a much lower molecular weight (340 g/mol) (Kaushik and Roos 2007), has T'm=-34°C and T'g at -46°C.

In this section, experimental results from cycle (i) are displayed. However, gum arabic also showed better freeze dried properties in all other freeze drying cycles (iii and iv)(data not shown).

6.3 Freeze drying mixture of sucrose and gum arabic

Section 6.2.3 showed that gum Arabic can be freeze dried without structure collapse even at very high concentration, while sucrose with more than 20% concentration lead to significant volume expansion. The difference between freeze dried results of gum Arabic and sucrose may result from the fact that carbohydrates with a higher molecular weight have a higher collapse temperature in freeze drying. Here research was carried out to investigate if the quality of freeze dried sucrose can be improved by adding small amount of gum arabic into original sucrose solution before freeze drying.

6.3.1 Effect of 1% gum arabic addition

The sample volume of freeze dried sucrose with 1% gum arabic addition was compared with that of samples dried from pure sucrose at same total solids content in Figure 6-27.

Experiments results from same freeze drying cycle are displayed in same graph: Cycle i in Figure 6-27 a, cycle iii in Figure 6-27 b, and cycle iv in Figure 6-27 c.

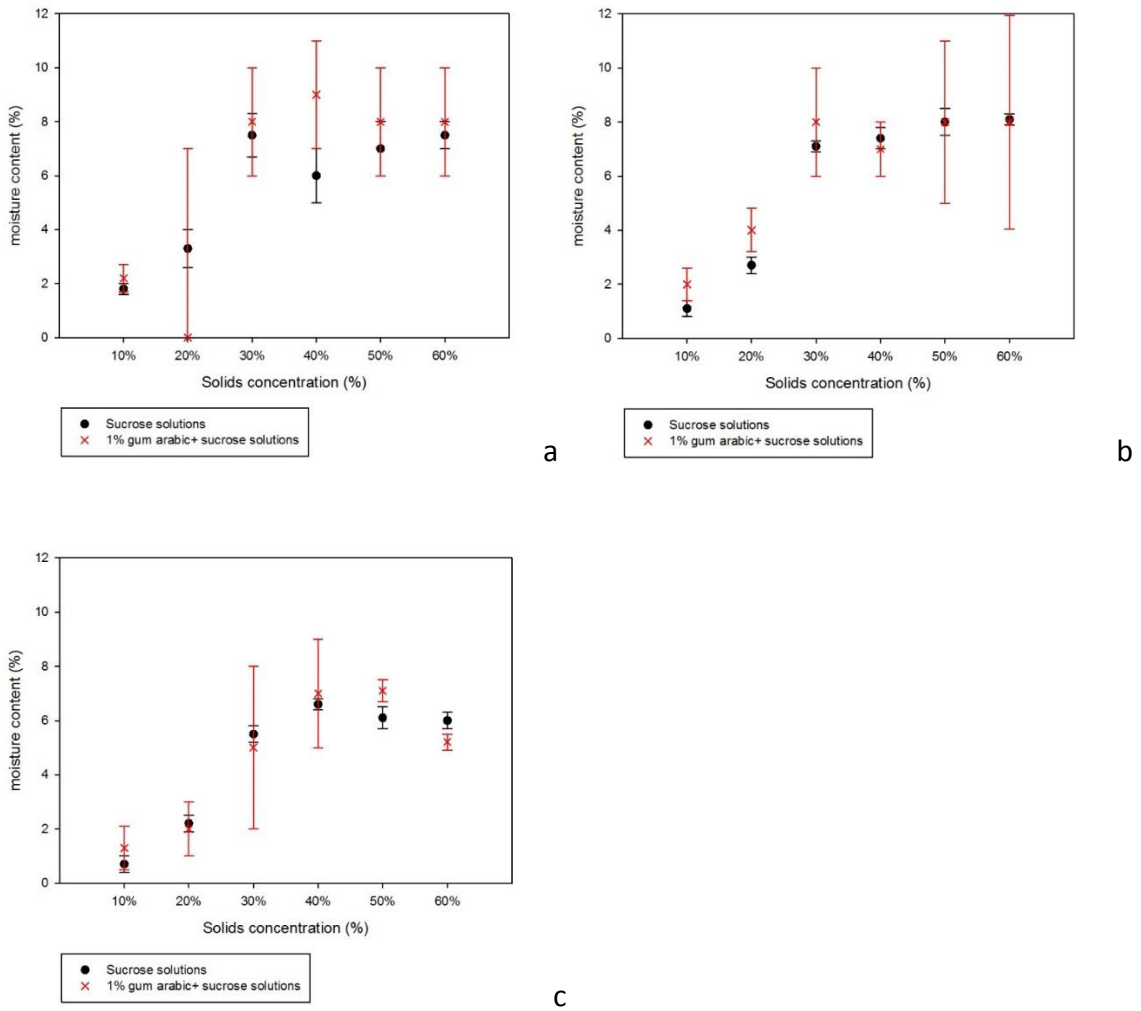

Figure 6-27 Sample volumes of freeze dried sucrose system with/without 1% gum arabic addition. Three freeze drying cycles were used (a) cycle i; (b) cycle iii; (c) cycle iv. Experiments were triplicated and error bars show ± one standard deviation.

Three different freeze drying cycles were used and Figure 6-27 (a) displays samples obtained in cycle i. The sample without addition of gum arabic showed puffing in 30% sucrose while with 1% gum arabic adding into the system, no volume increase was noticed. The addition

of 1% gum Arabic reduced the puffing in freeze drying 30% sucrose, possibly by increasing the collapse temperature. Without gum Arabic addition, the sample temperature in 30% sucrose was slightly above the collapse temperature in cycle i (see Figure 6-14b). With the addition of 1% gum arabic, the collapse temperature increased, so the sample temperature of 30% was below the collapse temperature and drying without structure loss can be achieved. 10 and 20% solids system did not show difference with/without existence of gum arabic in the sample, and neither did 50% and 60%. The former was because numerous ice crystals will lead to good freeze dried sample without volume increase. While for the high concentration systems, the ratio between gum arabic and sucrose was very small, thus the effect of addition was not obvious.

Figure 6-27 (b) plots sample volume as a function of total solids content with/without 1% gum arabic added in the system when sample was freeze dried in cycle iii. The slow heating rate during freeze drying reduced the puffing (see section 6.1.4) and thus the addition of gum arabic did not show significant difference in most of the sample volume. However it was noticed that the puffing in 40% sucrose was reduced by the addition of gum arabic.

When heating rate in freeze drying cycle further reduced to 5°C/hour in cycle iv (see Figure 6-27 c), even puffing in 40, 50 and 60% sucrose can be reduced by adding 1% gum arabic (maximal 2mL reduce in 40% solid concentration).

Figure 6-28 Photograph of freeze dried 30% system obtained from cycle (ii) (left: 30% sucrose, middle: 29% sucrose+1% gum arabic, and right: 30% gum arabic)

An image of freeze dried 30% systems showed the volume difference between three solute compositions directly. Those samples were dried in cycle (ii). Sample dried from 30% sucrose resulted in puffed volume and foam-like structure. When the total solid concentration was maintained at 30%, but 1% solids accounted for gum arabic, the sample (middle vial of Figure 6-28) maintained its structure at same volume after freeze drying, just like the 30% freeze dried gum arabic product (right in Figure 6-28).

The effect of 1% gum Arabic addition on moisture content in freeze dried sucrose is shown in Figure 6-29.

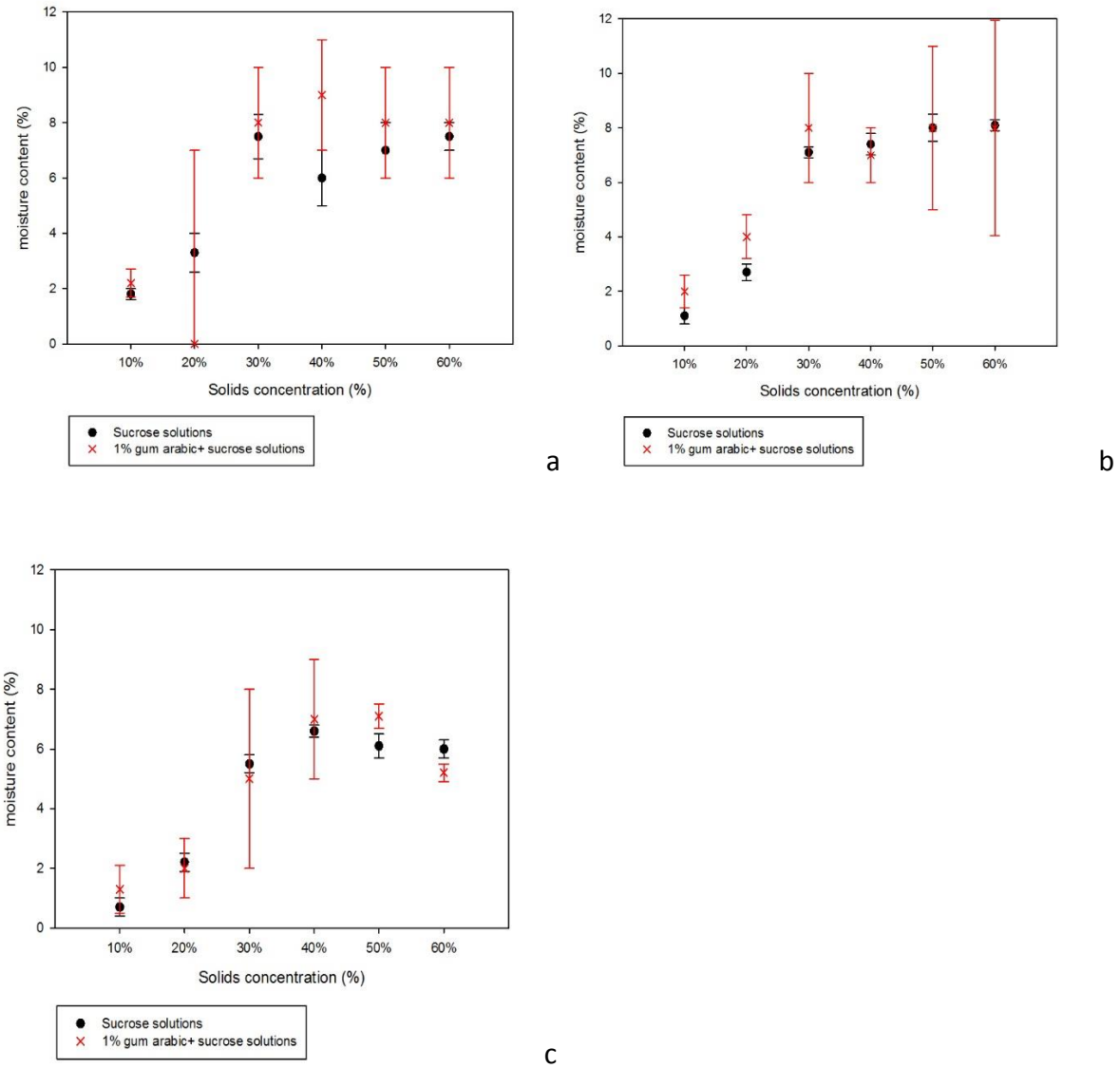

Figure 6-29 Moisture content of freeze dried sucrose system with/without 1% gum arabic addition. Three freeze drying cycles were used: (a) cycle i, (b) cycle iii, (c) cycle iv. Experiments were triplicated and error bars show ± one standard deviation.

There was no significant difference effect from gum arabic addition on moisture content of freeze dried sucrose.

6.4 Summaries

Freeze drying sucrose, gum arabic and a mixture of both were studied in this section, to investigate the freeze drying of highly concentrated systems with different molecular

weight. Sample of 1mL was filled into glass vial for each experiment. Effects of concentration, drying temperature, heating rate, and different solute type on freeze drying were investigated.

For sucrose systems, concentration affected both the processability and product quality of freeze drying. Sucrose with low concentration (10 and 20%) contained significant amount of water, which crystallises into ice crystals during freezing. The heat transferred from the the sample by ice crystals sublimation maintained the sample at the temperature below collapse temperature, making it possible for further sublimation to take place without collapse. The final products were dried without puffing and contained less than 5% residual water.

However, for high solid content sucrose systems, the limited amount of ice crystals provided insufficient sublimation and subsequently insufficient heat was transferred out of the sample, which could increase the sample temperature. Overheated products during freeze drying resulted in melting of ice, forming a concentrated layer, which may further slow down the mass transfer of water vapour.

Decreasing primary drying temperature from -20 ˚C to -40 ˚C can produce samples with less residual water and less volume increase, as the sample temperature was reduced during primary drying.

Slower heating rate lead to less volume in freeze dried sucrose, particularly 30% sucrose. By reducing the heating rate to from >100°C/hour to 5~10°C/hour, the volume of 30% sucrose can be reduced from 4mL to less than 2mL. And in general, freeze drying cycle with slower heating rate also resulted in less residual water in the dried product; however, the decrease in the moisture content varied in each concentration. For example, there was about 1%

decrease in moisture content for freeze dried 10% sucrose using slower heating rate, and the moisture content did not show any significant difference in drying 40% sucrose.

Another type of material with high molecular weight, gum arabic solutions were also used in this study, and the freeze drying was conducted successfully even at high solid concentration (60%). Samples were dried to low moisture content and sample volume expansion was not usual.

Addition of 1% gum arabic to sucrose systems helped to achieve a better quality of freeze drying to samples. The sample without addition of gum arabic showed puffing in 30% sucrose while with 1% gum arabic adding into the system, no volume increase was noticed. There was not significant difference effect from gum arabic addition on moisture content of freeze dried sucrose.

Chapter 7 Conclusions and future work

This chapter summaries the conclusions obtained from the experimental studies and suggests future work.

7.1 Summary of conclusions

The purpose of the study was to increase the initial solute concentration of solutions that are used in freezing and freeze drying processes, as an approach to reduce the energy consumption of the process. Several characteristic techniques were applied and developed to study the processes of freezing and freeze drying. The difficulties of freezing and freeze drying highly concentrated carbohydrate solutions were studied and discussed, and factors that affect water crystallisation and freeze drying were investigated. Some modifications have been suggested to improve the freezing and freeze drying processes to suit high concentration systems.

Three parts of work were conducted: (i) spontaneous crystallisation; (ii) induced crystallisation by adding ice nuclei; (iii) freeze drying. Sucrose solutions, gum arabic solutions and coffee were used. Coffee solution dehydration is a major industry process, but coffee solids are chemically and physically complex. Sucrose and gum arabic are better defined and simpler model systems.

7.1.1 Spontaneous crystallisation

- Difficulties in spontaneous crystallisation from highly concentrated systems

Water crystallisation from sucrose/coffee solutions has been studied by DSC and XRD. In agreement with reported literature, results presented in this work highlight the difficulties associated with inducing spontaneous crystallisation at low water systems, which often requires high degree of supercooling and results in a limited amount of ice crystals formation.

- Identifying ice crystal form by XRD

XRD technique was used to study of the phase transitions of water during freezing and reheating the concentrated solutions, and results from DSC and XRD showed good agreement in monitoring these phase transitions.

Physical state of the ice (amorphous, hexagonal crystal or cubic crystal) can be identified and crystal form transitions between these states can be monitored by XRD.

- Direct visualisation of ice crystals by Cryo-ESEM

It is possible to visualise ice crystals directly in frozen coffee samples by cryo-ESEM. Ice crystals show hexagonal shape in the images and ice crystal size can be obtained. Careful etching is required in these experiments, to remove the frosted ice and maintain the ice crystals in the samples.

7.1.2 Induced crystallisation by ice nuclei addition

Methods were developed to induce water crystallisation in highly concentrated systems by adding ice nucleus at two scales: droplet scale (0.1mL) and larger scale (2mL).

- Crystal growth after ice nuclei addition in droplet scale

Water crystallisation took place after ice nuclei was added into the supercooled highly concentrated droplet. The required supercooling in induced crystallisation is smaller than that in spontaneous crystallisation.

- Crystal growth study in droplet scale

This method allows the study of crystal growth in different conditions and systems, with crystal rate quantified and crystal shape captured.

Several factors slowed down the crystal growth rate: high viscosity, high solid concentration, and adding air bubbles into system. Increasing solution viscosity by adding 0.5~1% cmc could cause 40% decrease in crystal growth rate. When the solid concentration was increased from 40% to 60%, at a given supercooling (e.g. at 7°C), growth rate decreased by 95%. For a system initially without air bubbles (e.g. 59% sucrose+1% cmc), aeration showed a delayed effect on crystal growth. However, further aeration did not change the crystal growth rate in a system where air bubbles already existed (e.g 50% gum arabic).

The optical method presented in this work allows the study of crystal growth in various systems, and could be applied to study of different components, such as water, powders, or fats, offering a useful tool in crystallisation.

- Induced crystallisation in larger scale (2mL)

The effect of adding ice nuclei on water crystallisation was also studied at larger scale for 2mL of coffee samples (concentration at 50% and 60%). The morphology of the freeze dried samples were examined by SEM. Improved (dried) microstructure was obtained in 60% coffee samples with added ice seeds, suggesting that ice nuclei promoted water crystallisation during freezing.

7.1.3 Freeze drying

Highly concentrated carbohydrate solutions (up to 60% solid content) were used in the freeze drying study.

- Puffing investigated in freeze drying highly concentrated sucrose

The (rehydration and structure retention) quality of freeze dried sucrose was strongly dependant on the initial solution concentration. Sucrose solutions up to 20% could be freeze

dried without structure loss and contained less than 5% residual water. Highly concentrated sucrose solutions (30%~60%), however, resulted in significant volume increase (puffing) after freeze drying. Temperature of the puffed samples was higher than T'm during freeze drying.

- Adding higher T'm materials (gum Arabic) to improve the structure of freeze dried sucrose systems

Gum arabic, a material with high molecular weight thus higher T'm, was used in freeze drying studies as well. For this material freeze drying could be conducted successfully even at high solid concentration. Samples could be dried to low moisture content and sample volume expansion was rare.

The addition of 1% gum arabic into sucrose solution before freeze drying reduces the volume increase in freeze dried sucrose with up to 40% solid content.

7.2 Future work

Findings of this study suggest that some future work could be carried out as follows:

- Microstructure study of frozen samples by Cryo-ESEM

Efforts were made in this study to visualise ice crystals directly in frozen samples in cryo-ESEM, however, more detailed and systematic study could be carried out to have a better understanding in the microstructure of the frozen highly concentrated systems with different concentration and composition.

- Crystal growth study in droplet scale using Polarised light microscopy

In section 5.2.3, the difficulties in quantifying crystal growth rate in opaque solutions was discussed. Different techniques such as polarised light microscope can be used to modify

this method, to differentiate crystallised area in opaque systems and make it possible to study crystal growth kinetics in such system, which is very common in real food processing.

- Freeze drying experiments modification

The freeze drying experiments in this study was conducted in glass vials, and glass vials may have an effect on freeze drying, especially on the rate of heat transfer from shelf to the investigated systems. Concentrated solutions could be frozen into a cube (e.g. freeze in an ice cube mould) and then freeze dried directly on a tray, to avoid the effect from vial. The possible volume change after freeze drying can be monitored by measuring dimensions of the dried cubes.

- Gum arabic addition into sucrose systems before freeze drying

The addition of 1% gum arabic improved the structure of freeze dried sucrose with up to 40% solid content. More study on this field is suggested, to investigate the effect of gum arabic addition into sucrose solutions. DSC can be used to investigate the T'm (closely related to collapse temperature) of each formulation and the sample temperature should be monitored during freeze drying.

- Modelling development

The thesis displayed the experimental study of freezing and freeze drying processes, and mathematical models can be developed for each process, to gain a better understanding of the freezing and freeze drying processes.

List of references

1. Ablett, S., M. J. Izzard and P. J. Lillford (1992). "Differential scanning calorimetric study of frozen sucrose and glycerol solutions." Journal of the Chemical Society, Faraday Transactions 88(6): 789-794.

2. Atkins, P., J. de Paula and R. Friedman (2013). Physical Chemistry: Quanta, Matter, and Change, OUP Oxford.

3. Ayel, V., O. Lottin, M. Faucheux, D. Sallier and H. Peerhossaini (2006). "Crystallisation of undercooled aqueous solutions: Experimental study of free dendritic growth in cylindrical geometry." International Journal of Heat and Mass Transfer 49(11–12): 1876-1884.

4. Bellows, R. J. and C. J. King (1972). "Freeze-drying of aqueous solutions: Maximum allowable operating temperature." Cryobiology 9(6): 559-561.

5. Berk, Z. (2009). Chapter 22 - Dehydration. Food Process Engineering and Technology. San Diego, Academic Press: 459-510.

6. Bolliger, S., H. Wildmoser, H. D. Goff and B. W. Tharp (2000). "Relationships between ice cream mix viscoelasticity and ice crystal growth in ice cream." International Dairy Journal 10(11): 791-797.

7. Brennan, J. G. (2011). Evaporation and Dehydration. Food Processing Handbook, Wiley-VCH Verlag GmbH & Co. KGaA: 77-130.

8. Bruttini, R. and A. Liapis, I. (2006). Freeze Drying. Handbook of Industrial Drying, Third Edition, CRC Press.

9. Budiaman, E. R. and O. Fennema (1987). "Linear Rate of Water Crystallization as Influenced by Temperature of Hydrocolloid Suspensions." Journal of Dairy Science 70(3): 534-546.

10. Clarke, R. J. (1987). Coffee: Volume 2: Technology, Springer Netherlands.

11. Cook, K. L. K. and R. W. Hartel (2010). "Mechanisms of Ice Crystallization in Ice Cream Production." Comprehensive Reviews in Food Science and Food Safety 9(2): 213-222.

12. Deville, S., J. Adrien, E. Maire, M. Scheel and M. Di Michiel (2013). "Time-lapse, three-dimensional in situ imaging of ice crystal growth in a colloidal silica suspension." Acta Materialia 61(6): 2077-2086.

13. Dowell, L. G., S. W. Moline and A. P. Rinfret (1962). "A low-temperature X-ray diffraction study of ice structures formed in aqueous gelatin gels." Biochimica et Biophysica Acta 59(1): 158-167.

14. Dowell, L. G. and A. P. Rinfret (1960). "Low-temperature forms of ice as studied by X-ray diffraction." Nature 188(4757): 1144-1148.

15. Egawa, H., E. Yonemochi and K. Terada (2005). "Investigation of optimal manufacturing process for freeze-dried formulations: Observation of frozen solutions by low temperature X-ray diffraction measurements." Thermochimica Acta 431(1-2): 127-132.

16. Esfandiary, R., S. K. Gattu, J. M. Stewart and S. M. Patel (2016). "Effect of Freezing on Lyophilization Process Performance and Drug Product Cake Appearance." Journal of Pharmaceutical Sciences 105(4): 1427-1433.

17. Esquivel, P. and V. M. Jiménez (2012). "Functional properties of coffee and coffee by-products." Food Research International 46(2): 488-495.

18. Farah, A. (2012). Coffee Constituents. Coffee, Wiley-Blackwell: 21-58.

19. Featherstone, S. (2015). 8 - Ingredients used in the preparation of canned foods. A Complete Course in Canning and Related Processes (Fourteenth Edition). Oxford, Woodhead Publishing: 147-211.

20. Fellows, P. J. (2009). 23 - Freeze drying and freeze concentration. Food Processing Technology (Third edition), Woodhead Publishing: 687-699.

21. Fletcher, N. H. (1970). The Chemical Physics of Ice, Cambridge University Press.

22. Flores, A. A. and H. D. Goff (1999). "Ice Crystal Size Distributions in Dynamically Frozen Model Solutions and Ice Cream as Affected by Stabilizers." Journal of Dairy Science 82(7): 1399-1407.

23. Franks, F. (1998). "Freeze-drying of bioproducts: putting principles into practice." European Journal of Pharmaceutics and Biopharmaceutics 45(3): 221-229.

24. Franks, F. and Auffret, T (2007). Freeze-drying of Pharmaceuticals and Biopharmaceuticals, Royal Society of Chemistry.

25. Furuki, T. (2002). "Effect of molecular structure on thermodynamic properties of carbohydrates. A calorimetric study of aqueous di- and oligosaccharides at subzero temperatures." Carbohydrate Research 337(5): 441-450.

26. Garside, J., A. Mersmann and J. Nývlt (2002). Measurement of crystal growth and nucleation rates. Rugby, UK, IChemE.

27. Goff, H. D., K. B. Caldwell, D. W. Stanley and T. J. Maurice (1993). "The Influence of Polysaccharides on the Glass Transition in Frozen Sucrose Solutions and Ice Cream." Journal of Dairy Science 76(5): 1268-1277.

28. Goff, H. D., E. Verespej and D. Jermann (2003). "Glass transitions in frozen sucrose solutions are influenced by solute inclusions within ice crystals." Thermochimica Acta 399(1-2): 43-55.

29. Hagiwara, T. and R. W. Hartel (1996). "Effect of Sweetener, Stabilizer, and Storage Temperature on Ice Recrystallization in Ice Cream." Journal of Dairy Science 79(5): 735-744.

30. Hallett, J. (1964). "Experimental Studies of the Crystallization of Supercooled Water." Journal of the Atmospheric Sciences 21(6): 671-682.

31. Hartel, R. W. (1996). "Ice crystallization during the manufacture of ice cream." Trends in Food Science & Technology 7(10): 315-321.

32. Hartel, R. W. (2002). 13 - Crystallization in foods A2 - Myerson, Allan S. Handbook of Industrial Crystallization (Second Edition). Woburn, Butterworth-Heinemann: 287-304.

33. Hartel, R. W. (2008). The Crystalline State. Food Materials Science: Principles and Practice. J. M. Aguilera and P. J. Lillford. New York, NY, Springer New York: 45-65.

34. Hartel, R. W. and M. S. Chung (1993). "Contact nucleation of ice in fluid dairy products." Journal of Food Engineering 18(3): 281-296.

35. Hartel, R. W., R. Ergun and S. Vogel (2011). "Phase/State Transitions of Confectionery Sweeteners: Thermodynamic and Kinetic Aspects." Comprehensive Reviews in Food Science and Food Safety 10(1): 17-32.

36. Hartel, R. W. and D. R. Heldman (1997). Principles of Food Processing, Springer US.

37. Hindmarsh, J. P., C. Buckley, A. B. Russell, X. D. Chen, L. F. Gladden, D. I. Wilson and M. L. Johns (2004). "Imaging droplet freezing using MRI." Chemical Engineering Science 59(10): 2113-2122.

38. Hindmarsh, J. P., A. B. Russell and X. D. Chen (2005). "Measuring dendritic growth in undercooled sucrose solution droplets." Journal of Crystal Growth 285(1–2): 236-248.

39. Hindmarsh, J. P., A. B. Russell and X. D. Chen (2007). "Fundamentals of the spray freezing of foods—microstructure of frozen droplets." Journal of Food Engineering 78(1): 136-150.

40. Ho, T. M., T. Truong and B. Bhandari (2017). Chapter 5 - Spray-Drying and Non-Equilibrium States/Glass Transition. Non-Equilibrium States and Glass Transitions in Foods, Woodhead Publishing: 111-136.

41. Hobbs, P. V. (1974). Ice Physics. Oxford, Clarendon Press.

42. Huang, M. and M. Zhang (2013). 20 - Tea and coffee powders. Handbook of Food Powders, Woodhead Publishing: 513-531.

43. Icoz, D. Z. and J. L. Kokini (2008). State Diagrams of Food Materials. Food Materials Science: Principles and Practice. J. M. Aguilera and P. J. Lillford. New York, NY, Springer New York: 95-121.

44. Inoue, C. and T. Suzuki (2006). "Enthalpy relaxation of freeze concentrated sucrose–water glass." Cryobiology 52(1): 83-89.

45. Islam, A. M., G. O. Phillips, A. Sljivo, M. J. Snowden and P. A. Williams (1997). "A review of recent developments on the regulatory, structural and functional aspects of gum arabic." Food Hydrocolloids 11(4): 493-505.

46. Kallungal, J. P. and A. J. Barduhn (1977). "Growth rate of an ice crystal in subcooled pure water." AIChE Journal 23(3): 294-303.

47. Karel, M. and J. M. Flink (1973). "Influence of Frozen State Reactions on Freeze-Dried Foods." Journal of Agricultural and Food Chemistry 21(1): 16-21.

48. Kasper, J. C. and W. Friess (2011). "The freezing step in lyophilization: Physico-chemical fundamentals, freezing methods and consequences on process performance and quality attributes of biopharmaceuticals." European Journal of Pharmaceutics and Biopharmaceutics 78(2): 248-263.

49. Kaushik, V. and Y. H. Roos (2007). "Limonene encapsulation in freeze-drying of gum Arabic–sucrose–gelatin systems." LWT - Food Science and Technology 40(8): 1381-1391.

50. Kauzmann, W. (1948). "The Nature of the Glassy State and the Behavior of Liquids at Low Temperatures." Chemical Reviews 43(2): 219-256.

51. Kiefte, H., M. J. Clouter and E. Whalley (1984). "Cubic ice, snowflakes, and rare-gas solids: Surface energy, entropy, and the stability of small crystals." The Journal of Chemical Physics 81(3): 1419-1420.

52. Levenspiel, O. (1972). Chemical reaction engineering, Wiley.

53. Levine, H. and L. Slade (1986). "A polymer physico-chemical approach to the study of commercial starch hydrolysis products (SHPs)." Carbohydrate Polymers 6(3): 213-244.

54. Levine, H. and L. Slade (1988). "Thermomechanical properties of small-carbohydrate-water glasses and 'rubbers'. Kinetically metastable systems at sub-zero temperatures." Journal of the Chemical Society, Faraday Transactions 1: Physical Chemistry in Condensed Phases 84(8): 2619-2633.

55. Luyet, B. and D. Rasmussen (1967). "Study by differential thermal analysis of the temperatures of instability in rapidly cooled solutions of polyvinylpyrrolidone." Biodynamica 10(205): 137-147.

56. Luyet, B. J. (1939). "The Devitrification Temperatures of Solutions of a Carbohydrate Series." The Journal of Physical Chemistry 43(7): 881-885.

57. MacLeod, C. S., J. A. McKittrick, J. P. Hindmarsh, M. L. Johns and D. I. Wilson (2006). "Fundamentals of spray freezing of instant coffee." Journal of Food Engineering 74(4): 451-461.

58. Mahendran, T., P. A. Williams, G. O. Phillips, S. Al-Assaf and T. C. Baldwin (2008). "New Insights into the Structural Characteristics of the Arabinogalactan−Protein (AGP) Fraction of Gum Arabic." Journal of Agricultural and Food Chemistry 56(19): 9269-9276.

59. Marcolli, C., S. Gedamke, T. Peter and B. Zobrist (2007). "Efficiency of immersion mode ice nucleation on surrogates of mineral dust." Atmos. Chem. Phys. 7(19): 5081-5091.

60. Marcotte, M. and S. Grabowski (2008). 16 - Minimising energy consumption associated with drying, baking and evaporation. Handbook of Water and Energy Management in Food Processing, Woodhead Publishing: 481-522.

61. Mazzobre, M. a. F., J. M. Aguilera and M. a. P. Buera (2003). "Microscopy and calorimetry as complementary techniques to analyze sugar crystallization from amorphous systems." Carbohydrate Research 338(6): 541-548.

62. McNaught, A. D. (1997). Compendium of chemical terminology, Blackwell Science Oxford.

63. Montenegro, M. A., M. L. Boiero, L. Valle and C. D. Borsarelli (2012). Gum Arabic: More Than an Edible Emulsifier Products and Applications of Biopolymers. J. Verbeek, InTech.

64. Moreno, F. L., M. Raventós, E. Hernández and Y. Ruiz (2014). "Block freeze-concentration of coffee extract: Effect of freezing and thawing stages on solute recovery and bioactive compounds." Journal of Food Engineering 120: 158-166.

65. Mothé, C. G. and M. A. Rao (1999). "Rheological behavior of aqueous dispersions of cashew gum and gum arabic: effect of concentration and blending." Food Hydrocolloids 13(6): 501-506.

66. Mothé, C. G. and M. A. Rao (2000). "Thermal behavior of gum arabic in comparison with cashew gum." Thermochimica Acta 357–358: 9-13.

67. Mousavi, R., T. Miri, P. W. Cox and P. J. Fryer (2007). "Imaging food freezing using X-ray microtomography." International Journal of Food Science & Technology 42(6): 714-727.

68. Mullin, J. W. (2001). Crystallization. Oxford, Elsevier Science.

69. Murphy, D. (2003). "Dehydration in cold clouds is enhanced by a transition from cubic to hexagonal ice." Geophysical research letters 30(23).

70. Murray, B. J., D. A. Knopf and A. K. Bertram (2005). "The formation of cubic ice under conditions relevant to Earth's atmosphere." Nature 434(7030): 202-205.

71. Ong, L., R. R. Dagastine, S. E. Kentish and S. L. Gras (2011). "Microstructure of milk gel and cheese curd observed using cryo scanning electron microscopy and confocal microscopy." LWT - Food Science and Technology 44(5): 1291-1302.

72. Padma Ishwarya, S. and C. Anandharamakrishnan (2015). "Spray-Freeze-Drying approach for soluble coffee processing and its effect on quality characteristics." Journal of Food Engineering 149: 171-180.

73. Palzer, S., C. Dubois and A. Gianfrancesco (2012). "Generation of Product Structures During Drying of Food Products." Drying Technology 30(1): 97-105.

74. Pan, B., P. Yan, L. Zhu and X. Li (2013). "Concentration of coffee extract using nanofiltration membranes." Desalination 317: 127-131.

75. Pardo, J. M., F. Suess and K. Niranjan (2002). "An Investigation into the Relationship Between Freezing Rate and Mean Ice Crystal Size for Coffee Extracts." Food and Bioproducts Processing 80(3): 176-182.

76. Patel, S. M., C. Bhugra and M. J. Pikal (2009). "Reduced Pressure Ice Fog Technique for Controlled Ice Nucleation during Freeze-Drying." AAPS PharmSciTech 10(4): 1406-1411.

77. Patel, S. M., T. Doen and M. J. Pikal (2010). "Determination of End Point of Primary Drying in Freeze-Drying Process Control." AAPS PharmSciTech 11(1): 73-84.

78. Petzold, G. and J. M. Aguilera (2009). "Ice Morphology: Fundamentals and Technological Applications in Foods." Food Biophysics 4(4): 378-396.

79. Pikal, M. J., M. L. Roy and S. Shah (1984). "Mass and heat transfer in vial freeze-drying of pharmaceuticals: Role of the vial." Journal of Pharmaceutical Sciences 73(9): 1224-1237.

80. Pontis, H. G. (2017). Chapter 6 - Case Study: Sucrose. Methods for Analysis of Carbohydrate Metabolism in Photosynthetic Organisms. Boston, Academic Press: 79-95.

81. Pruppacher, H. R. (1967). "On the growth of ice crystals in supercooled water and aqueous solution drops." pure and applied geophysics 68(1): 186-195.

82. Pryde, J. A. and G. O. Jones (1952). "Properties of Vitreous Water." Nature 170(4330): 685-688.

83. Quast, D. G. and M. Karel (1968). "Dry Layer Permeability and Freeze-Drying Rates in Concentrated Fluid Systems." Journal of Food Science 33(2): 170-175.

84. Ramalakshmi, K., L. J. M. Rao, Y. Takano-Ishikawa and M. Goto (2009). "Bioactivities of low-grade green coffee and spent coffee in different in vitro model systems." Food Chemistry 115(1): 79-85.

85. Rambhatla, S., R. Ramot, C. Bhugra and M. J. Pikal (2004). "Heat and mass transfer scale-up issues during freeze drying: II. Control and characterization of the degree of supercooling." AAPS PharmSciTech 5(4): 54-62.

86. Ratti, C. (2001). "Hot air and freeze-drying of high-value foods: a review." Journal of Food Engineering 49(4): 311-319.

87. Ratti, C. (2013). 3 - Freeze drying for food powder production. Handbook of Food Powders, Woodhead Publishing: 57-84.

88. Renard, D., L. Lavenant-Gourgeon, M.-C. Ralet and C. Sanchez (2006). "Acacia senegal Gum: Continuum of Molecular Species Differing by Their Protein to Sugar Ratio, Molecular Weight, and Charges." Biomacromolecules 7(9): 2637-2649.

89. Rey, L. R. (1960). "THERMAL ANALYSIS OF EUTECTICS IN FREEZING SOLUTIONS." Annals of the New York Academy of Sciences 85(2): 510-534.

90. Roos, Y. (1997). "Frozen state transitions in relation to freeze drying." Journal of Thermal Analysis and Calorimetry 48(3): 535-544.

91. Roos, Y. and M. Karel (1991). "Amorphous state and delayed ice formation in sucrose solutions." International Journal of Food Science & Technology 26(6): 553-566.

92. Roos, Y. H. (1995). Phase Transitions in Foods. San Diego, Academic Press.

93. Roos, Y. H., P. J. Fryer, D. Knorr, H. P. Schuchmann, K. Schroën, M. A. I. Schutyser, G. Trystram and E. J. Windhab (2016). "Food Engineering at Multiple Scales: Case Studies, Challenges and the Future—A European Perspective." Food Engineering Reviews 8(2): 91-115.

94. Sahagian, M. E. and H. D. Goff (1994). "Effect of freezing rate on the thermal, mechanical and physical aging properties of the glassy state in frozen sucrose solutions." Thermochimica Acta 246(2): 271-283.

95. Schawe, J. E. K. (2006). "A quantitative DSC analysis of the metastable phase behavior of the sucrose–water system." Thermochimica Acta 451(1-2): 115-125.

96. Searles, J. A., J. F. Carpenter and T. W. Randolph (2001). "Annealing to optimize the primary drying rate, reduce freezing-induced drying rate heterogeneity, and determine T'g in pharmaceutical lyophilization." Journal of Pharmaceutical Sciences 90(7): 872-887.

97. Searles, J. A., J. F. Carpenter and T. W. Randolph (2001). "The ice nucleation temperature determines the primary drying rate of lyophilization for samples frozen on a temperature-controlled shelf." Journal of Pharmaceutical Sciences 90(7): 860-871.

98. Shalaev, E. Y. and F. Franks (1996). "Changes in the Physical State of Model Mixtures during Freezing and Drying: Impact on Product Quality." Cryobiology 33(1): 14-26.

99. Sofjan, R. P. and R. W. Hartel (2004). "Effects of overrun on structural and physical characteristics of ice cream." International Dairy Journal 14(3): 255-262.

100. Sperling, L. H. (2005). The Crystalline State. Introduction to Physical Polymer Science, John Wiley & Sons, Inc.: 239-323.

101. Stärtzel, P., H. Gieseler, M. Gieseler, A. M. Abdul-Fattah, M. Adler, H.-C. Mahler and P. Goldbach (2015). "Freeze-Drying of l-Arginine/Sucrose-Based Protein Formulations, Part 2: Optimization of Formulation Design and Freeze-Drying Process Conditions for an l-Arginine Chloride-Based Protein Formulation System." Journal of Pharmaceutical Sciences 104(12): 4241-4256.

102. Strumillo, C., P. L. Jones and R. Zylla (2014). Energy Aspects in Drying. Handbook of Industrial Drying, Fourth Edition, CRC Press: 1077-1100.

103. Suwelack, W. and D. Kunke (2002). Process for freeze drying coffee extract, Google Patents.

104. Takahashi, T. (1982). "On the role of cubic structure in ice nucleation." Journal of Crystal Growth 59(3): 441-449.

105. Tang, X. and M. J. Pikal (2004). "Design of Freeze-Drying Processes for Pharmaceuticals: Practical Advice." Pharmaceutical Research 21(2): 191-200.

106. Tang, X. C., S. L. Nail and M. J. Pikal (2005). "Freeze-drying process design by manometric temperature measurement: design of a smart freeze-dryer." Pharm Res 22(4): 685-700.

107. Teraoka, Y., A. Saito and S. Okawa (2002). "Ice crystal growth in supercooled solution." International Journal of Refrigeration 25(2): 218-225.

108. Thanatuksorn, P., K. Kajiwara, N. Murase and F. Franks (2008). "Freeze–thaw behaviour of aqueous glucose solutions—the crystallisation of cubic ice." Physical Chemistry Chemical Physics 10(35): 5452.

109. Tsourouflis, S., J. M. Flink and M. Karel (1976). "Loss of structure in freeze-dried carbohydrates solutions: Effect of temperature, moisture content and composition." Journal of the Science of Food and Agriculture 27(6): 509-519.

110. Uchida, T. and S. Takeya (2010). "Powder X-ray diffraction observations of ice crystals formed from disaccharide solutions." Physical Chemistry Chemical Physics 12(45): 15034-15039.

111. Vincze, I. and G. Vatai (2004). "Application of nanofiltration for coffee extract concentration." Desalination 162: 287-294.

112. White, G. W. and S. H. Cakebread (1966). "The glassy state in certain sugar-containing food products " International Journal of Food Science & Technology 1(1): 73-82.

113. Worster, M. G. and J. S. Wettlaufer (1997). "Natural Convection, Solute Trapping, and Channel Formation during Solidification of Saltwater." The Journal of Physical Chemistry B 101(32): 6132-6136.

114. Zasypkin, D. V. and T.-C. Lee (1999). "Extracellular Ice Nucleators from Pantoea Ananas: Effects on Freezing of Model Foods." Journal of Food Science 64(3): 473-478.

115. Zhang, H. and A. I. Cooper (2007). "Aligned Porous Structures by Directional Freezing." Advanced Materials 19(11): 1529-1533.

116. Zumbé, A., A. Lee and D. Storey (2001). "Polyols in confectionery: the route to sugar-free, reduced sugar and reduced calorie confectionery." British Journal of Nutrition 85(SupplementS1): S31-S45.